THE FORMATION AND DRYING OUT OF LIQUID INCLUSIONS IN CRYSTALS.

by

Edward Thomas WHITE
B.Sc.App., B.Sc. (Queensland).

A Thesis submitted for the Degree of Doctor of Philosophy in the Faculty of Engineering of the University of London.

Department of Chemical Engineering,
Imperial College,
LONDON S.W. 7.

June 1964.

SUMMARY

Consideration has been given to the mechanisms by which very regular patterns of inclusions of mother liquor form in certain crystalline solids. Experimental tests were carried out using hexamine (hexamethylene tetramine), ammonium chloride, and sodium chloride.

Two quite distinctive types of pattern were observed. In the first, the 'face' pattern, a set of inclusions was observed with one inclusion corresponding to each face of the crystal. For the dodecahedral hexamine crystals, patterns of twelve were observed; for the cubic crystals of the other materials, patterns of six. It has been shown that the formation of this type of pattern is a growth rate phenomenon. Above a certain growth rate a form of crystal growth, apparently intermediate between plane-wise and dendritic growth, is observed. In this form, the crystals grow with cavities in their faces. These may eventually seal over to form the inclusions. Measurements of the growth rate involved in this transformation have been made, and the effects of additives and differing solvents have been considered.

In the second type of inclusion pattern, the 'edge' pattern, the inclusions outline the edges of the crystal at some prior stage of growth. It has been shown that these inclusions are formed primarily through growth on rounded or irregular seed crystals.

Attempts were made to remove the included mother liquor by drying. These were generally unsuccessful. Consideration was also given to the role played by included solvent in the caking of crystals on storage.

A compilation of the properties of hexamine and its solutions is given.

A C K N O W L E D G E M E N T S

I would particularly like to thank my supervisor, Professor K.G. Denbigh, for the suggestion of this topic, and for his helpful and unfailing guidance at all stages through this thesis.

I would also like to thank the lecturing staff of this Department, in particular Dr. R.F. Strickland-Constable, Dr. G.S. Parry and Dr. H. Wilman, for their guidance, advice and the loan of equipment.

The assistance through conversation and correspondence with Mr. H.E.C. Powers of Tate and Lye Ltd., London; Dr C.W. Bunn, now of the Royal Society, London; T. Adamski, Instytut Badan Jadrourych, Warsaw; Dr. F.C. Phillips, University of Bristol; and J.D. Birchall of I.C.I., Winnington, is gratefully acknolwedged.

I an indebted to Mr. J.S. Oakley and his workshop staff for assistance in constructing and maintenancing the apparatus, to the various glassblowers who built and repaired much of the equipment and to the photographer, Mr. L. Moulder, who aided in making a prodigious number of prints, and also prepared the photographs for this thesis. I would also like to thank Mr. J. Bradnam for his cheerful and enthusiastic help at all stages during this project.

My thanks go also to Mrs. V. Phillips and Miss A. Killick who most capably typed this thesis and to Miss B. Varley who duplicated it.

By no means least of all, I would like to acknowledge the invaluable assistance of my wife who counted the sizes of more crystals than we care to remember.

Finally, I would like to record my appreciation of the award of a most generous Commonwealth Scholarship for the duration of this project, and also for the able and efficient way this Scholarship was administered by the British Council.

LIST OF CONTENTS

Page No.

Page No.

LIST OF FIGURES

(* signifies a photograph)

LIST OF TABLES

NOMENCLATURE

a	:	Volume shape factor for crystal.
A	:	Total surface area of crystal batch.
b	:	Area shape factor for crystals.
c	:	Volume shape factor for inclusions.
$f(s)$	:	Fraction of inclusions with size s.
$f(x)$	:	Fraction of crystals with size x.
$f(x_i)$	:	Fraction of those crystals with inclusion with size x_i.
m	:	Mass rate of deposition of crystals.
M	:	Mass of crystal batch.
n	:	Number of crystals in batch.
n_i	:	Number of crystals in batch with inclusions.
n'	:	Number of crystals counted in sample.
R	:	Rate of crystal growth computed from $\underline{x}$.
R'	:	Rate of crystal growth computed from $\underline{x}_i$.
R^*	:	Critical crystal growth rate.
$\underline{s}$	:	Size of inclusion.
s	:	Mean size of inclusion (volumetric basis).
$\underline{t}$	:	Thickness of crystal covering inclusion.
t	:	Mean thickness of crystal covering inclusion.
v_t	:	Total volume of included liquor
$\underline{x}$	:	Crystal size.
x	:	Mean crystal size (volumetric basis).
$\underline{x}_i$	:	Size of crystal with inclusions.
$\underline{x}_i$	:	Mean size of crystal with inclusion (volumetric basis).
$\underline{x}_i^*$	:	Critical value of $\underline{x}_i$ at which inclusions seal over ($= \underline{y}'$).
x_1	:	Mean size of largest crystals (on volumetric basis).
$\underline{y}$	:	Internal size of inclusion pattern.
y	:	Mean value of y. The Critical Crystal Size.
$\underline{y}'$	:	External size of inclusion pattern.
y'	:	Mean value of y' on a volumetric basis
α	:	Area-volume factor for distribution of x.
α_i	:	Area-volume factor for distribution of x_i.
β	:	Fraction of crystals with inclusions (number basis).
γ_A	:	Fraction of total surface area of crystals associated with crystals with inclusions.
γ_v	:	Fraction of total volume of crystal associated with those crystals with inclusions.
θ	:	Period of time after nucleation.
θ_s	:	Time when inclusions seal over.
ρ	:	Crystal density.

μ = 1 micron = 10^{-6} metre.

I. INTRODUCTION

Often small pockets of mother liquor (or other materials) can be trapped within a crystal when it is grown from a solution (or a melt). These inclusions (as they are termed) of foreign material occur commonly in many crystals of industrial importance. They are usually undesirable since they represent a source of impurity in the material. Also, their presence may be a cause of crystal caking, if the inclusion contains a solvent which can escape and evaporate from the surface.

There are many means by which inclusions may be formed and many different appearances of the inclusions resulting. Some inclusions form in patterns of great regularity; others in quite a random manner. It is the purpose of this project to study crystals with regular patterns of inclusions, since it is thought that the regularity of behaviour should be of considerable aid in understanding the mechanism of their formation. Several common materials show such regular patterns of inclusions. The material selected for especial study in this project is hexamine (hexamethylene tetramine) which crystallises as rhombic dodecahedra. These may contain regular patterns of twelve inclusions. The mechanics of the formation of these inclusions will be the major aspect of this study.

Consideration will also be given to the possibility of removing the included material from crystals already formed, for example, by drying. The role played by included solvent in the caking and agglomeration of crystals will also be investigated.

2. INCLUSIONS IN CRYSTALS - A SURVEY

2.1 PURIFICATION BY CRYSTALLIZATION

Crystallization processes are a widely used and important means of purifying and recovering solid products from impure mixtures. A large number of texts have been devoted to this subject and several are given as references [1-5].

The change in purity resulting from a single crystallization can be quite remarkable. Crystals of high purity can be grown from very impure solutions. This stems from the basic mechanics of crystal growth. As a crystal grows, molecules of the product transfer from the impure mixture to occupy more-or-less rigid positions in a crystal lattice. This lattice is extremely selective as to the molecular species which can be built into it. In most cases only the product molecules can be accepted, and a high degree of purification is achieved.

The impurities associated with most crystalline products can usually be attributed entirely to the adherent film of mother liquor on the surfaces of the crystal. However, in some cases, impurities can be contained within the crystal itself.

2.2 CLASSIFICATION OF IMPURITIES IN CRYSTALS

Some crystals can contain internal impurities, i.e. material other than the product. The means by which the impurity is held within the crystal might be used as a basis for a classification, such as that shown in Table 2-1.

The first group includes impurities which are incorporated directly

IMPURITIES IN CRYSTALS

I. Those caused by lattice mechanisms; the accommodation of single atoms, ions, or molecules in the lattice.

   A. Replacement in Lattice. 'Mixed crystals' e.g. alums, alloys.

   B. Accommodation in Interstices. 'Interstitial compounds' e.g. C in steel.

II. Those caused by surface entrapping mechanisms; the containment of discrete amounts of impurity.

   A. Parallel growth. e.g. perlite (in steel), star mica.

   B. Inclusions.

      submicroscopic, e.g. dyes in crystals, milky quartz.

      microscopic.

TABLE 2-1 CLASSIFICATION OF IMPURITIES IN CRYSTALS.

into the lattice by lattice mechanisms. An impurity molecule may directly replace a product molecule in the lattice giving rise to 'mixed crystals' such as the alums. Other examples are given by Buckley [17] pp. 588-96. Alternatively, if the impurity molecule is considerably smaller than the product molecule, it can be incorporated in the interstices of the lattice without replacement, giving rise to the 'interstitial compounds' such as carbon in iron(Buckley [17] p.396).

With these materials the impurity is incorporated unit by unit in the structure, and is dispersed on a molecular level. With the second group, the impurity is contained as discrete multimolecular conglommerates. These are usually caused by surface effects or growth irregularities in the growing crystals.

One type of growth in this second group is the alternate layer wise deposition of impurity and product, termed 'parallel growth', and is discussed in Buckley [17] pp. 402-14.

The discrete amounts of impurity are termed 'inclusions'. Some inclusions are sub-microscopic in size and may constitute only a few molecules of impurity. These can only be seen if they are coloured, e.g. dye molecules (Buckley [17] pp. 415-33), or are so numerous that they cause dispersion of light e.g. 'milky' quartz crystals. Other inclusions may be quite large and may be readily observed under the microscope, or in some cases, to the naked eye. An inclusion may contain one or several phases - gas, liquids, and solids. Examples are given by Buckley [17] pp. 433-47.

This project will be concerned only with inclusions (Group IIB of Table 2.1) and only those large enough to be seen under the microscope.

As this project is concerned only with crystallization from relatively pure solvents, the inclusion when formed will contain only a single liquid phase. However, because of the contraction of the liquid on cooling a small vapour space may sometimes be present.

2.3 TERMINOLOGY

In the literature the terms 'occlusion' and 'inclusion' have been used on various occasions to describe part or all of the classification groups shown in Table 2-1. In what follows, only the term 'inclusion' will be used, with the meaning ascribed to it above.

The term 'impurity' as used above was taken to mean material other than that considered to be the product. Impurity in this sense may not be impurity in the usual chemical sense of being undesirable or objectionable. For example, in the case of a mixed crystal such as an alum, the impurity is one of the constituents of the crystal and could equally have been considered as the product material. A crystal with water of crystallization is another example. (Refer also Buckley [17] p. 359).

In other cases the impurity may be a non-objectionable solvent. Reagent grade sodium chloride, for example, may contain an appreciable percentage of included mother liquor, yet be labelled "puriss.", since the mother liquor contains only product and water.

2.4 REASONS WHY INCLUSIONS IN CRYSTALS ARE UNDESIRABLE

The presence of inclusions in crystals may be undesirable for the following reasons.

1. The inclusion causes imperfections and non-homogeneity within the crystal. This is especially serious if the appearance of the crystal is important, or if the crystal is to be used for its optical, electrical, magnetic or other properties as, for example, the use of crystals for synthetic gemstones, lasers, radio oscillators, and semi-conductors. The effect of inclusions of gallium in germanium semi-conductor crystals has been considered by Hurle and associates [6, 7].

2. The contents of the inclusion contain impurity. The inclusion may contain materials other than the product. These materials may be undesirable with respect to the chemical purity of the material. For example, Powers [8] has shown that the coloured matter content of sugar crystals is due almost solely to the included mother liquor.

3. The subsequent behaviour of the included material may be undesirable. For example, the differential expansion behaviour of included material and crystal may stress or crack the crystal, or the escape of solvent from the inclusion may cause caking of stored crystals.

2.5 APPEARANCE OF INCLUSIONS IN CRYSTALS

The appearance of inclusions in crystals varies considerably, as illustrated by Fig. 2.1. This diagram is based on the description of various crystals given by Buckley [1] pp. 415-444, and on the classification of inclusions in sugar crystals given by Powers [8-10].

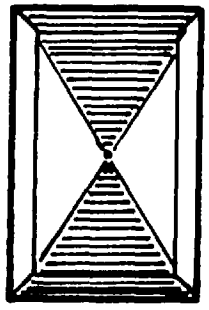

HOURGLASS

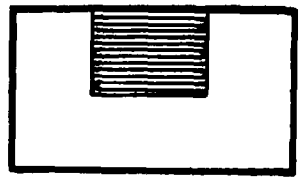

BLOCK

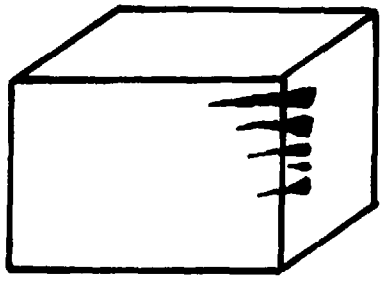

FJORD

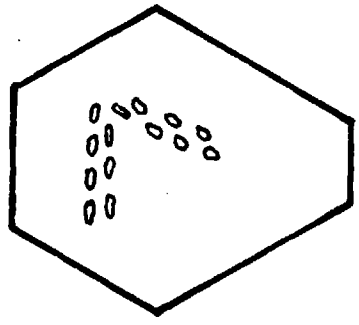

ORIENTATED

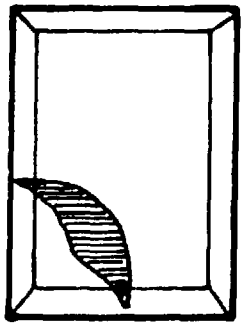

VEIL

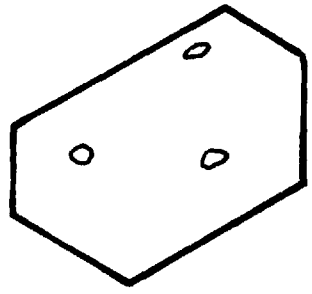

RANDOM

FIG. 2-1. SOME OF THE PATTERNS OF INCLUSIONS FOUND IN CRYSTALS.

The tendency is to classify inclusions in terms of the degree of regularity and orientation shown by the inclusion patterns. Thus the 'hourglass' appearance of Fig. 2-1, where included material (usually dye) occurs regularly with respect to certain faces of the crystal, is considered more regular than the 'random' arrangements where no order prevails.

With 'hourglass' patterns, the included materials tend to lie in the solid volumes swept out by the growth of particular faces. With 'block' patterns the included material tends to lie on what corresponded to the faces of the crystal at some previous stage of growth - often the seed crystal itself. The inclusions in 'fjord' patterns appear as tapering pipes roughly aligned to one another. In 'Orientated' patterns the tubes of inclusion tend to run parallel to the edges of the crystal. A sheet of included material gives rise to the 'veil' appearance. Where no pattern is apparent the arrangement is termed random.

This project is mainly concerned with patterns of inclusions which exhibit a regularity of appearance more pronounced than any shown in Fig 2-1. Description of these patterns will be delayed until section 2.7.

2.6 MECHANISMS OF INCLUSION FORMATION

There are several mechanisms by which inclusions might be formed. These are summarised in Table 2.2.

2.6.1. Formation in Growing Crystals

Inclusions formed in a growing crystal must depend on some

A. IN GROWING CRYSTALS (i) Adsorption processes on the surface. (ii) Initial surface irregularities. (iii) Growth of irregularities, e.g. edge or dendritic growth
B. IN FORMED CRYSTALS (i) Resealing of cracks and fractures. (ii) Local dissolution and resealing.
C. IN MELTS AND MAGMAS (i) Solidification (Inclusion Thermometry).

TABLE 2-2 MECHANISMS OF INCLUSION FORMATION

irregularity in the growth of a crystal face. This irregularity may be caused -

(i) by adsorbed impurity;

(ii) by the initial condition of the surface; or

(iii) by the non-planar growth of the surface itself.

Impurity adsorbed on a region of a growing surface might inhibit further growth on that region causing the rest of the surface to grow beyond and over the impurity entrapping it. This impurity could be a soluble or an insoluble constituent of the solution or even a gas (refer Buckley [17]. 'Hourglass' inclusions (Fig. 2-1) are probably connected with a continual form of some such surface adsorption on certain faces.

The surface irregularity may be simply the initial condition of the surface. If the surface contains pits, grooves or hollows because of prior mistreatment of the crystal or because of gross lattice defects such as dislocations and slip plane rearrangements, surface growth could seal the surface over forming inclusions. The 'block' and 'orientated' patterns might be formed in this way.

Surface irregularities may be generated by the non-planar growth of the surface itself. Growth of the edges and corners of the crystal may be at a much faster rate than the rest of the face, giving rise to hollowed faces which might later seal over forming inclusions. In some cases corner growth may become so rapid that the crystal grows as long irregular spikes in preferred directions. These spikes have a tree-like appearance and are termed dendrites. If a crystal grows dendritically, and then fills in, inclusions may be formed trapped between the original arms of the dendrites. This process of formation is described by Buckley [17] p.433. Certain 'orientated' patterns of inclusions may be formed in this way.

The gallium rich inclusions in germanium crystals described by Hurle and associates [6, 7] are formed by preferential growth at the edges of individual crystal grains. Each grain has a pit in the centre of its growing face in which the included material collects.

2.6.2. Inclusion Formation in Formed Crystals

Inclusion formation in grown crystals requires the crystal to be penetrated by some means. This may occur by local dissolution forming pits at certain spots, or by cracks and fractures formed in the crystals. The pits and cracks may fill with foreign material and seal over by

surface evaporation or further crystal growth, leaving inclusions. In these cases, unlike the mechanisms in 2.6.1., the included material need not necessarily be similar to that from which the crystal was originally grown. The sealing of crystal fissures is probably a cause of 'fjord' and 'veil' patterns of inclusions.

2.6.3. Inclusion Formation in Melts and Magmas

Melts and magmas crystallize by solidification. Impurities present in the molten material are trapped in the solidified mass. They may be within the ground mass of the solid or within individual crystals in the mass depending on the relative speed with which the impurities can be moved away from the advancing crystal front.

The presence of inclusions within naturally occurring rocks and crystals are of great interest to geologists attempting to determine the temperature at which the rocks were formed. This field of study is known as 'inclusion thermometry'. A very able review of the field is given by Smith [11], and an excellently illustrated article on the subject recently appeared in 'Scientific American' [12].

In principle the method is as follows. The majority of inclusions in rocks contain a liquid and a vapour space. It is assumed that the liquid completely filled the inclusion cavity under the temperature and pressure conditions at which the rock solidified, and that there has been no loss of inclusion contents since. Thus the vapour space is due solely to the contraction of the liquid on cooling. A thin section of the rock showing inclusions is examined on the heated stage of a microscope. The temperature at which the vapour space just disappears is noted. After a correction for pressure is applied, the resulting

temperature is taken to be the solidification temperature of the rock. There are several uncertainties associated with the procedure [11], but the method has been demonstrated to be basically correct by tests on synthetic quartz crystals [12].

2.7 CRYSTALS WITH REGULAR INCLUSION PATTERNS

This project is concerned with crystals which show very regular patterns of inclusions. The published information on such crystals is very sparse. When this project was begun the only published reference was that by Denbigh [13], and it was assumed that such patterns in crystals were a very isolated occurrence. However, it now seems that they are more abundant than was at first realised.

Denbigh [13] reported the presence of very symmetrical patterns of inclusions in crystals of cyclonite (RDX) and hexamine. In hexamine the pattern consisted of twelve inclusions regularly arranged about the centre of the crystal. This pattern has also been observed by Bunn and is described in a forthcoming book [14]. Bunn also described a regular pattern of six inclusions in cubic crystals of ammonium chloride - one inclusion corresponding to each face of the crystal. A similar pattern of six has been observed in cubes of sodium chloride by Birchall [15]. These crystals will be described in greater detail in chapters 3 and 4.

Ayerst [16] has reported the appearance of regular inclusion patterns in large crystals of ammonium perchlorate formed by rapid growth. These inclusions appear to be similar in some respects to those observed in hexamine, ammonium chloride and sodium chloride, although a detailed analysis of their arrangement and formation has not

yet been made.

Pairs of inclusions appearing in barium chromate crystals have been described by Adamski [17, 18] and are shown in Fig. 2-2. The composition of the included material is not known* although Adamski suggests that it may be products caused by radiation damage of the host material. If the inclusions did contain aqueous mother liquor they might be considered to be similar to those in the crystals described above.

These regular patterns of inclusions would seem to be formed while the crystals are growing, in which case one of the mechanisms of growth described under section 2.6.1. would be applicable.

* A request has been made for a sample of this material for moisture analysis purposes, but at the time of writing a sample had not yet arrived.

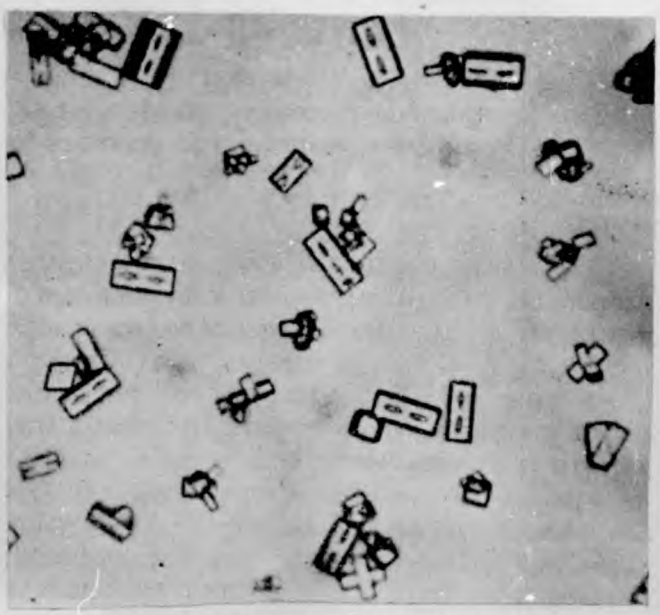

[x 400]

BARIUM CHROMATE CRYSTALS.
[Adamski, T. & Trojanowski, L. Nature, 197, 1005 (1963)]

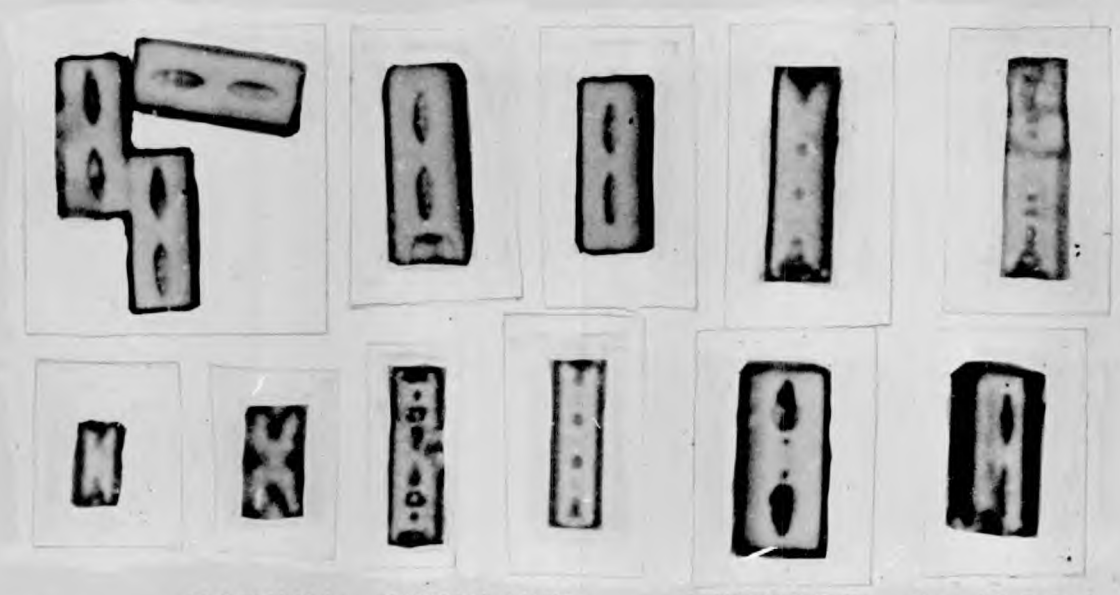

BARIUM CHROMATE CRYSTALS. [x 1200]
(Photographs supplied by T. Adamski , Poland)

FIG. 2-2. PATTERNS IN BARIUM CHROMATE CRYSTALS.

3. DESCRIPTION OF INCLUSIONS IN HEXAMINE CRYSTALS

3.1 INTRODUCTION

At the time this project was begun the only materials known to give regular patterns of inclusions were cyclonite (R.D.X.) and hexamine, as described by Denbigh [13]. Of these, hexamine, in which regular patterns of twelve inclusions had been observed, was chosen for study.

3.2 PROPERTIES OF HEXAMINE

Hexamine (hexamethylene tetramine, $C_6H_{12}N_4$) is an important industrial chemical used as an intermediate in the manufacture of formaldehyde plastics and of the explosive cyclonite (RDX). It is manufactured by the reaction between ammonia and formaldehyde in aqueous solution. The product is recovered by crystallization.

The main source of data on hexamine is a book by Walker [19]. In many respects the data there was too limited for use, so a separate compilation of the properties of hexamine and its solutions was made, and is given as a Supplement to this thesis. Some properties were not available and had to be measured. The methods used to measure these properties are given in Appendix VI. The results are incorporated directly into the Supplement.

3.3 CRYSTAL FORM

Hexamine belongs to the cubic system of crystal symmetry and crystallizes in the form of a rhombic dodecahedron, a solid figure with twelve identical $\{011\}$ faces. The crystals grow readily from most solutions. Hexamine is highly soluble in water, less so in most other solvents, and practically insoluble in hydrocarbon solvents.

Water was the main solvent used in this investigation.

3.4 OBSERVATIONAL TECHNIQUE

3.4.1. Equipment

The inclusion patterns could be seen at a suitable magnification with a low powered laboratory microscope (X10 objective, X6 eyepiece). A 35 mm. single lens reflex camera was fitted to the microscope so that photomicrographs could be made. The crystals to be observed were mounted on a recessed glass slide on the microscope stage. Further details regarding this equipment are given in Appendix I.

Because of the opaqueness and roughness of the crystal surfaces and because of the differences in refractive indices between the crystals and air, the internal structure could not be seen directly. Sectioning of the crystals (as is done with geological and biological specimens) was considered undesirable as it would cut through the patterns and inclusions. It was decided, therefore, to immerse the crystals in a fluid with the same refractive index as the crystal, in which case the surfaces of the crystal would become invisible and the internal inclusions (of different refractive index) would become plainly visible.

3.4.2. Selection of an Immersion Fluid

A suitable immersion fluid would

(i) have the same refractive index as the crystal;

(ii) have a lower density, so that the crystals would sink;

(iii) be non-viscous, so air bubbles would rise and crystals sink quickly.

(iv) wet the crystal surfaces, so that attached air would be removed.

(v) be non-reactive, non-volatile and non-toxic; and

(vi) would not dissolve the crystals to any great extent.

The refractive indices and densities of several fluids tested for hexamine crystals are shown in Table 3-1. Glycerol was first tried, but it had too low a refractive index, was too viscous, and rapidly dissolved the crystals. A mixture of clove oil and α- bromo - naphthalene had the correct refractive index but the clove oil reacted chemically with the hexamine. α-bromo-naphthalene and α-bromo-benzene were too dense and did not wet the crystals very well. Aniline proved to be quite satisfactory, although it tended to dissolve the crystals after some time, and also slowly to evaporate away. The observed appearance of hexamine cyrstals in the various fluids is shown in Appendix I.

Where the internal inclusion structure of hexamine was of interest, aniline was used exclusively as the immersion fluid. Where the surface appearance was required, paraffin or bromo-benzene was used.

3.5 APPEARANCE OF INCLUSIONS IN HEXAMINE

Many crystals of hexamine were grown. Details concerning the method of growth will be considered in later chapters. Some crystals showed numerous inclusions, others showed none. In some cases the inclusions were in quite random arrangement (Fig 3-1) with no semblance of order. However, in most crystals regular patterns of inclusions were seen. Two distinct patterns were observed, which have been termed 'FACE' and 'EDGE' patterns.

3.6 'FACE' PATTERN OF INCLUSIONS

The face pattern is a very regular arrangement of twelve inclusions

	Material	n_D 20°C	ρ 20°C
	Hexamine	1.589	1.334
a	α- bromo-naphthalene	1.658	1.48
b	clove oil	1.540	< 1.33
c	mixture of a & b	1.590	< 1.33
d	glycerol	1.473	1.26
e	bromo-benzene	1.560	1.49
f	aniline	1.586	1.02
g	paraffin(kerosene)	1.42	0.75

Data on hexamine from Supplement; other data from Lange [20]

TABLE 3 - 1 . PROPERTIES OF IMMERSION FLUIDS FOR HEXAMINE.

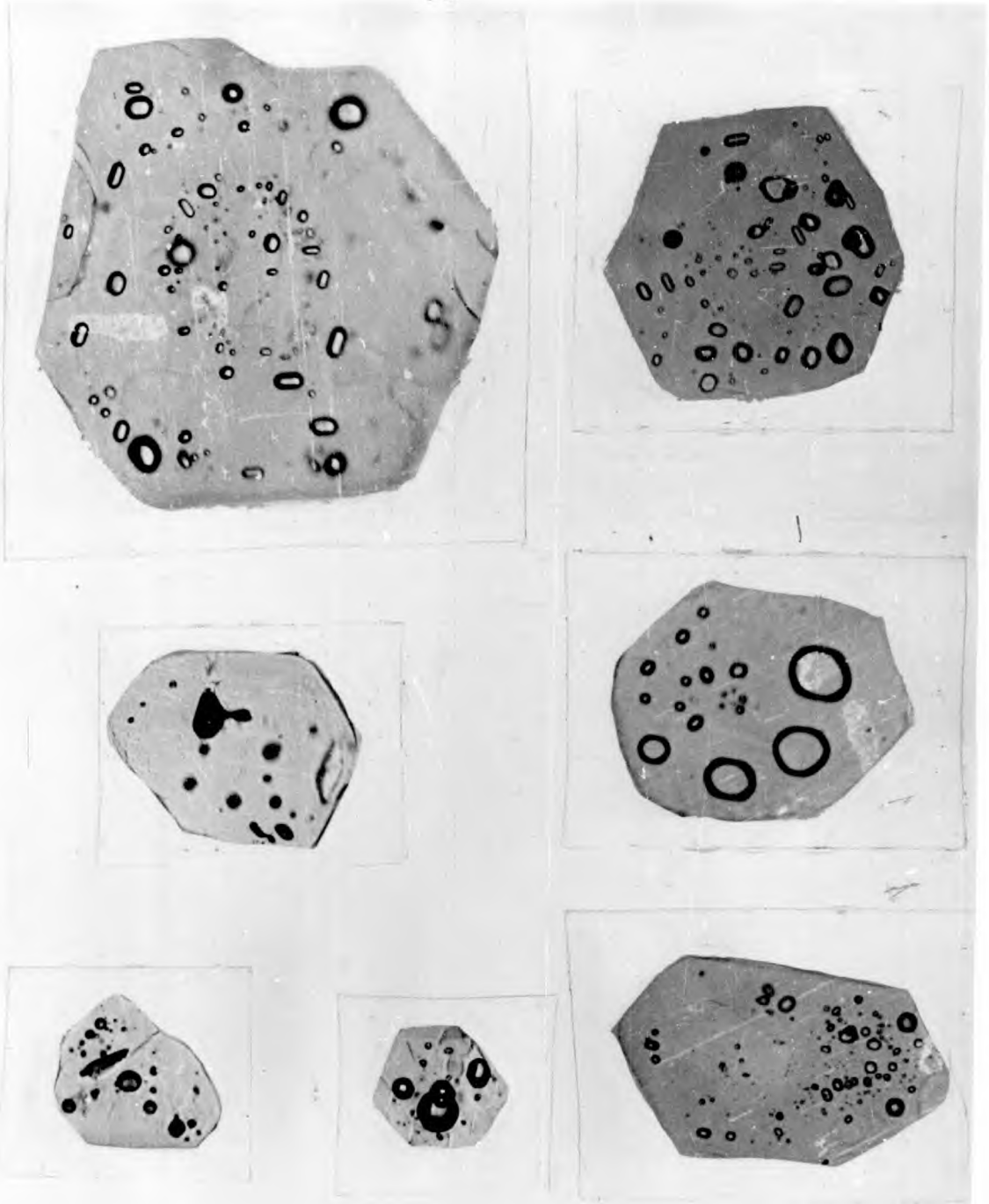

FIG. 3-1. RANDOM PATTERNS OF INCLUSIONS IN HEXAMINE CRYSTALS.
(Immersion Fluid : Aniline) [x 75]

as shown in Figs. 3-2, 3-3 and 3-4. Fig 3-2 has been published in 'Nature' [21].

In spatial arrangement the inclusions lie at positions corresponding to the centres of the faces of a rhombic dodecahedron aligned parallel to the outer crystal surfaces. In other words, if the crystal grew regularly the inclusions would lie at the centres of the faces of the crystal at some previous stage of growth.

That the inclusions have a dodecahedral pattern may be seen by comparing the photographs in Figs. 3-2, 3-3 and 3-4 with a rhombic dodecahedron constructed of 'Perspex' with marbles at the centre of each face. The different patterns, - seven membered, square, and hexagonal, shown in Fig 3-4 result merely from the different points of view taken of the three dimensional arrangement. All can be reproduced in the model.

The equivalence between the inclusion pattern and the face centres of a dodecahedron can also be demonstrated by measurements made under the microscope, one series of which is shown in Fig 3-5. The measurements in plan were made with a graduated eyepiece, those in elevation with the micrometer adjustment racking the field of view up and down. Within the accuracy of measurement, the pattern is dodecahedral.

Perhaps the most striking way of demonstrating the regular three dimensional nature of the pattern is to mount the crystal on a spike in an immersion fluid and rotate it. A movie film has been made of this, and several frames from it are shown in Fig 3-6.

This type of inclusion arrangement has been termed a 'face' pattern because the positions of the inclusions correspond to the centres of the

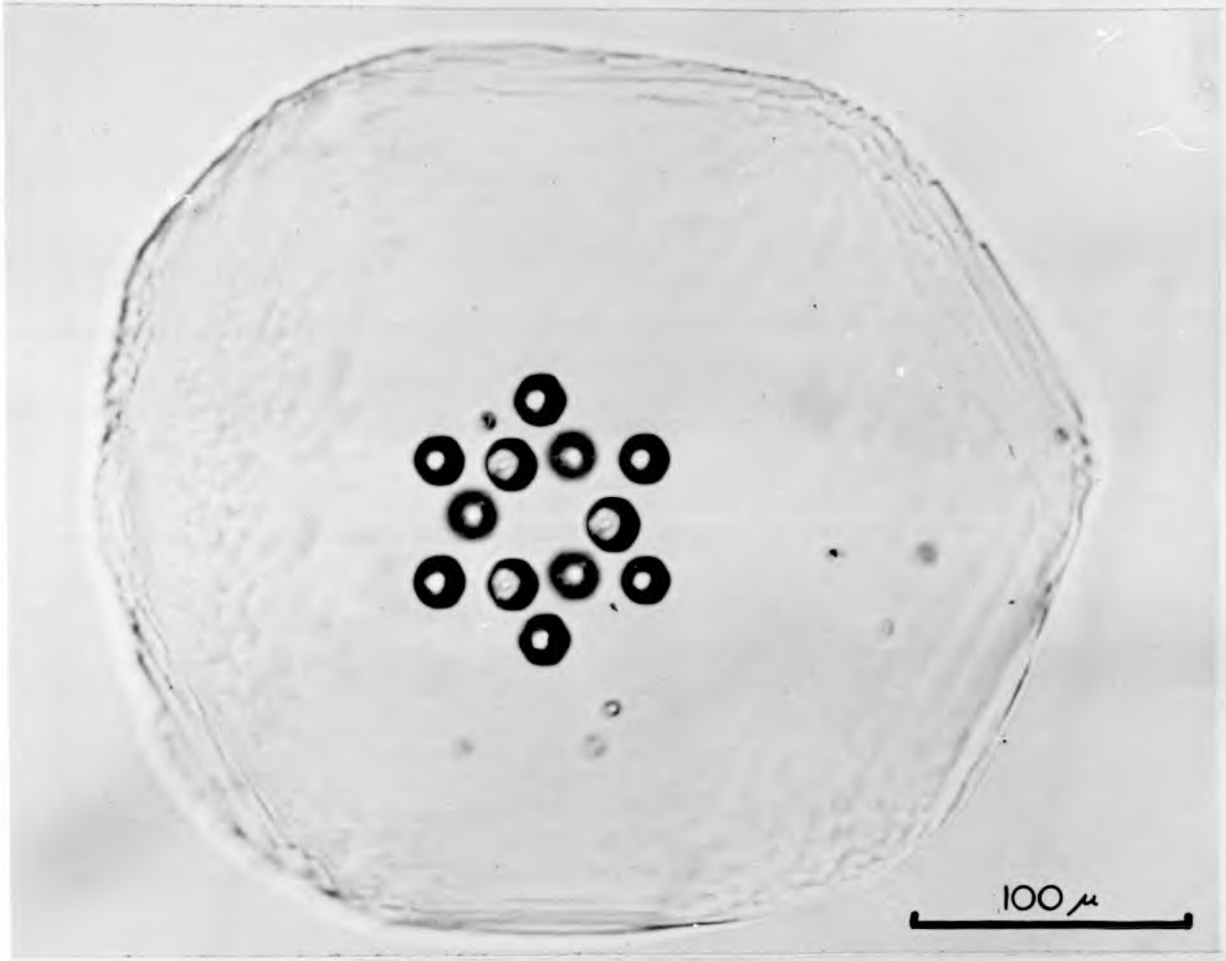

PHOTOGRAPH OF HEXAMINE CRYSTAL SHOWING INCLUSIONS [Immersion fluid :– Aniline] [x280]

PHOTOGRAPH OF PERSPEX MODEL

FIG. 3-2. COMPARISON OF ARRANGEMENT OF INCLUSIONS IN CRYSTAL WITH SPHERES IN PERSPEX MODEL.

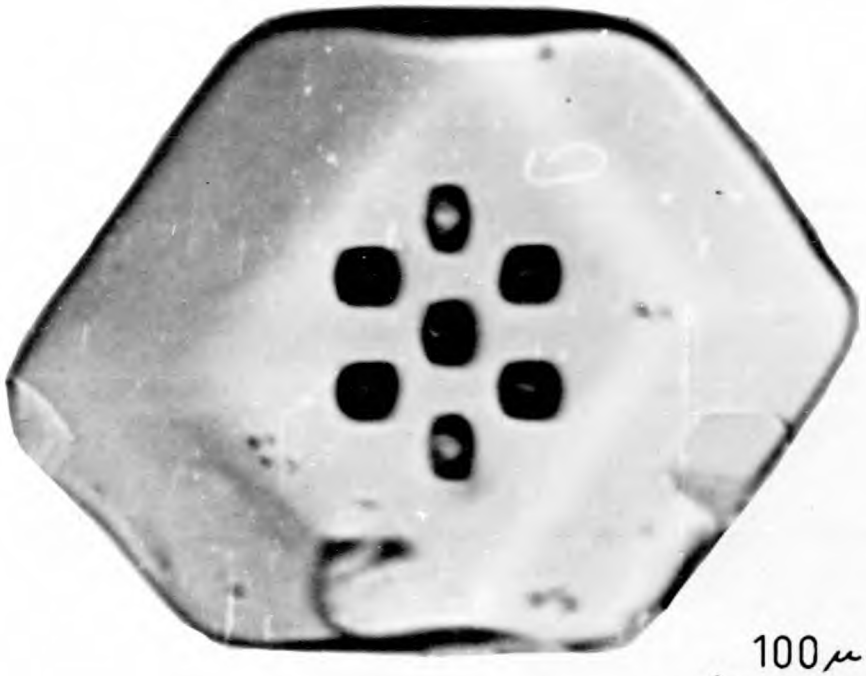

PHOTOGRAPH OF HEXAMINE CRYSTAL SHOWING INCLUSIONS. [Immersion fluid - Aniline] [x240]

PERSPEX MODEL

FIG. 3-3. COMPARISON OF ARRANGEMENT OF INCLUSIONS IN CRYSTAL WITH SPHERES IN MODEL.

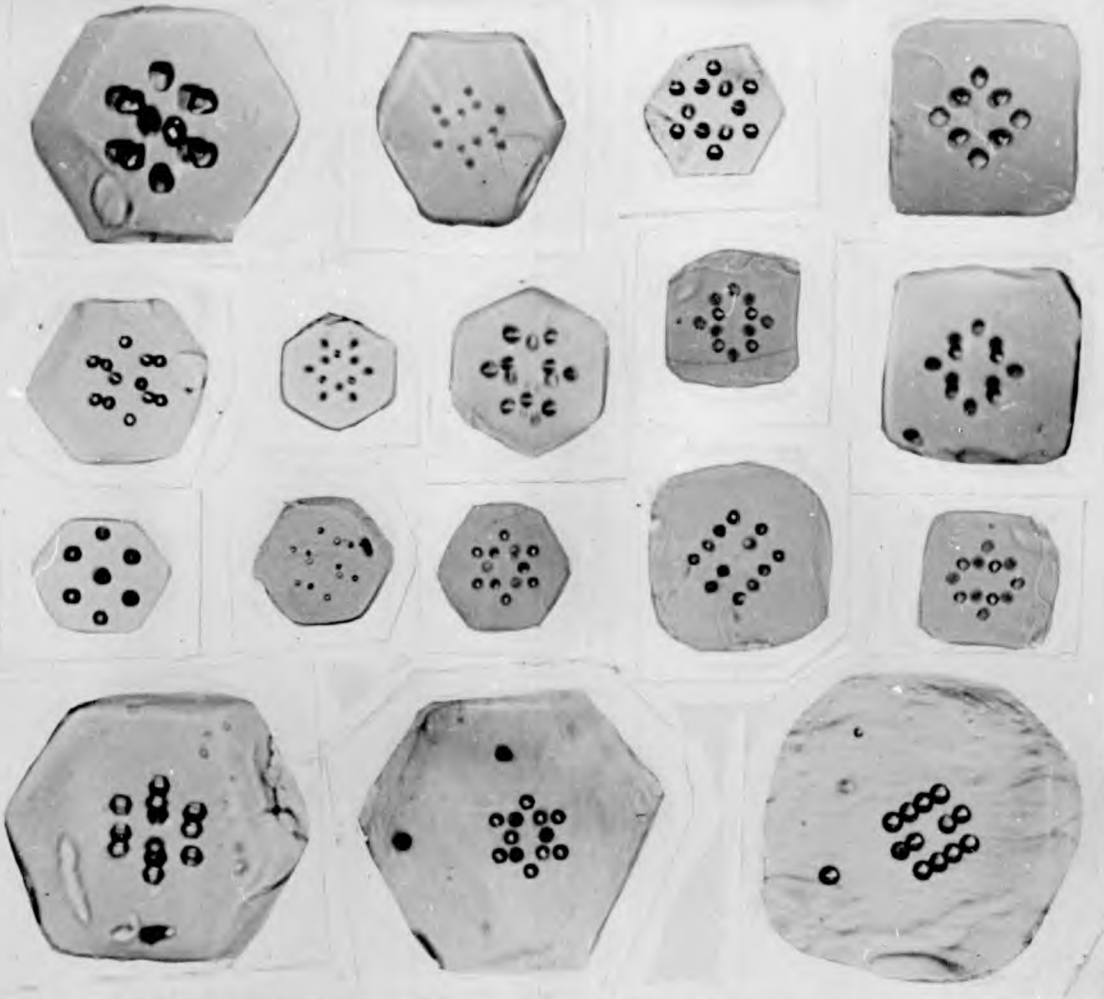

PHOTOGRAPHS OF HEXAMINE CRYSTALS SHOWING INCLUSIONS. (Immersion fluid : Aniline) [x120]

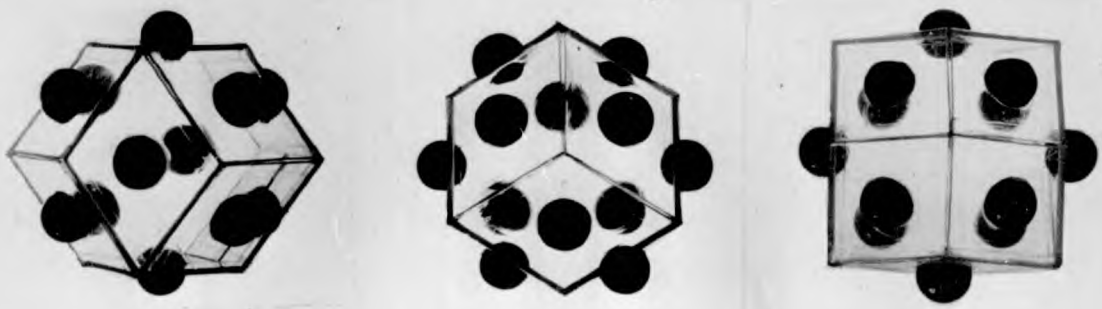

PERSPEX MODEL

FIG. 3-4. COMPARISON OF INCLUSIONS IN CRYSTAL WITH POSITION OF SPHERES IN PERSPEX MODEL.

MEASUREMENTS.

1 - 2,3 2,3 - 4,5 4,5 - 6,7 6,7 - 8,9 8,9 - 10,11 10,11 - 12	17μ ±3μ

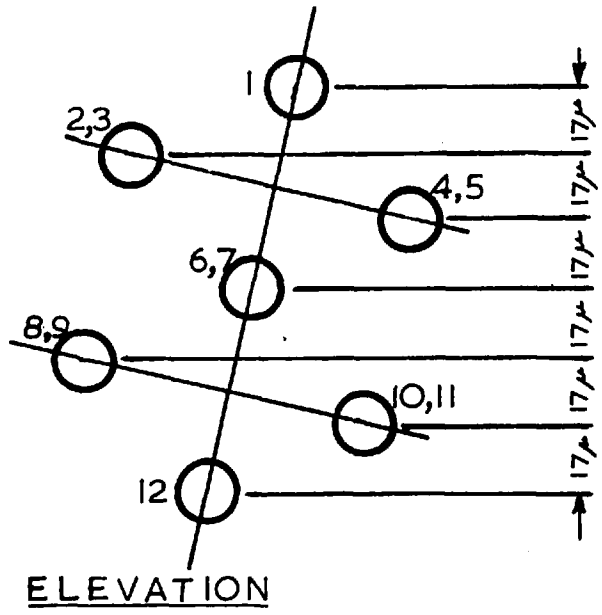

ELEVATION

SIZE OF INCLUSIONS
30μ ± 5μ.

MEASUREMENTS.

2-3, 4-5, 8-9, 10-11	50μ
3-5, 2-4, 9-11, 8-10	70μ
6-7	105μ

±5μ

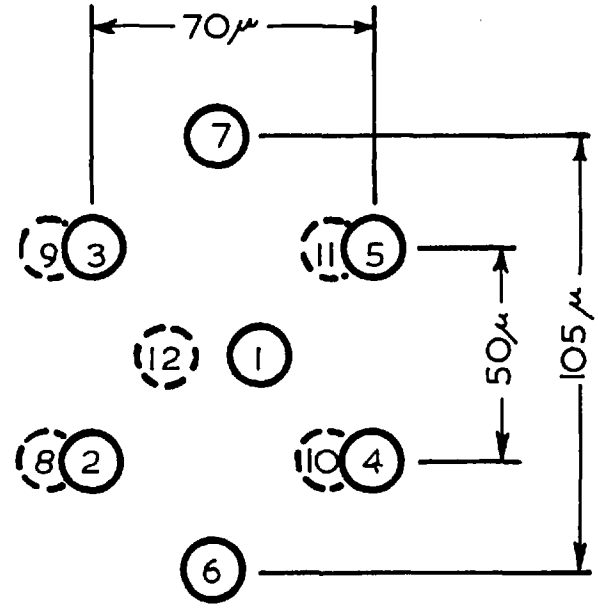

PLAN

FIG. 3-5. PATTERN MEASUREMENTS FOR INCLUSIONS IN HEXAMINE CRYSTAL.

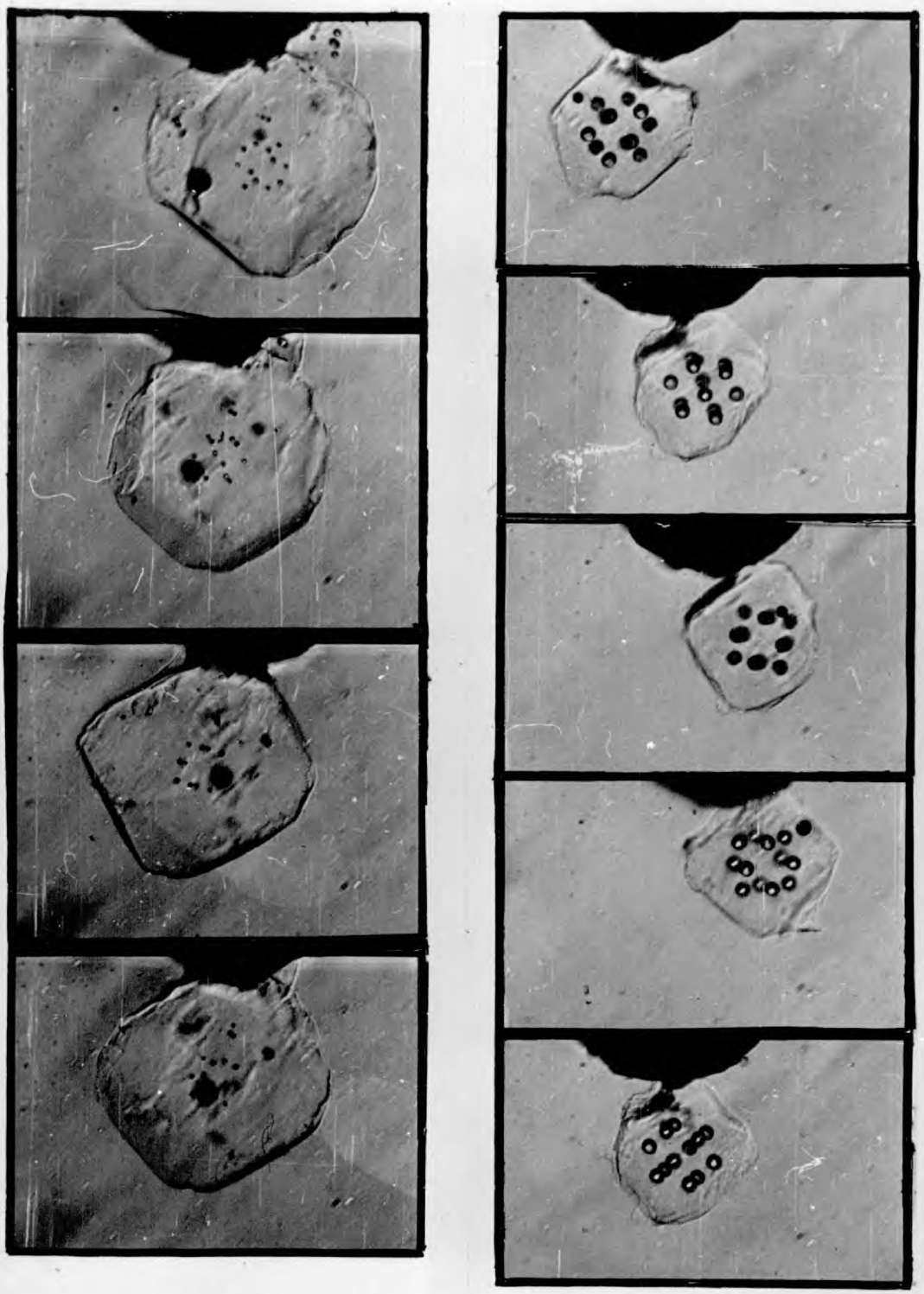

FIG. 3-6. ROTATION OF HEXAMINE CRYSTALS CONTAINING FACE INCLUSION PATTERNS.
(FROM MOVIE. IMMERSION FLUID : ANILINE.)
[x 100]

faces of the crystal..

3.7 'EDGE' PATTERN OF INCLUSIONS

In this case (Fig. 3-7) the inclusions lie along a regular pattern of lines corresponding to the edges of a rhombic dodecahedron, i.e. to the edges of the crystal at some prior stage of growth.

This may be confirmed by comparing the inclusion patterns in Figs. 3-7 and 3-8 with the edges of the crystals. In Fig 3-8, the same crystal is shown at three different depths of focus, illustrating the three dimensional nature of the pattern. The arrangement is also confirmed by rotating the crystal on a spike - (Fig. 3-9).

3.8 SHAPE AND SIZE OF INCLUSIONS

Most of the inclusions have the appearance of negative crystals, that is, they show internal faces corresponding to the external faces of the crystal. These dodecahedral faces can be seen clearly in Figs. 3-2 and 3-3, and to some extent in the other photographs. An enlargement of one inclusion is shown in Fig 3-10.

The inclusions range in size from the barely microscopic (a few microns) to a few hundred microns. Those in 'face' patterns range up to 70 μ while those in edge patterns only up to 10-20 μ .

The fraction of the total volume of the crystal that is an inclusion can range up to several percent, for some of the crystals shown in Fig. 3-4.

3.9 CONCLUSION

Hexamine crystals can exhibit two distinctly different regular patterns of mother liquor inclusions. In one, the 'face' pattern,

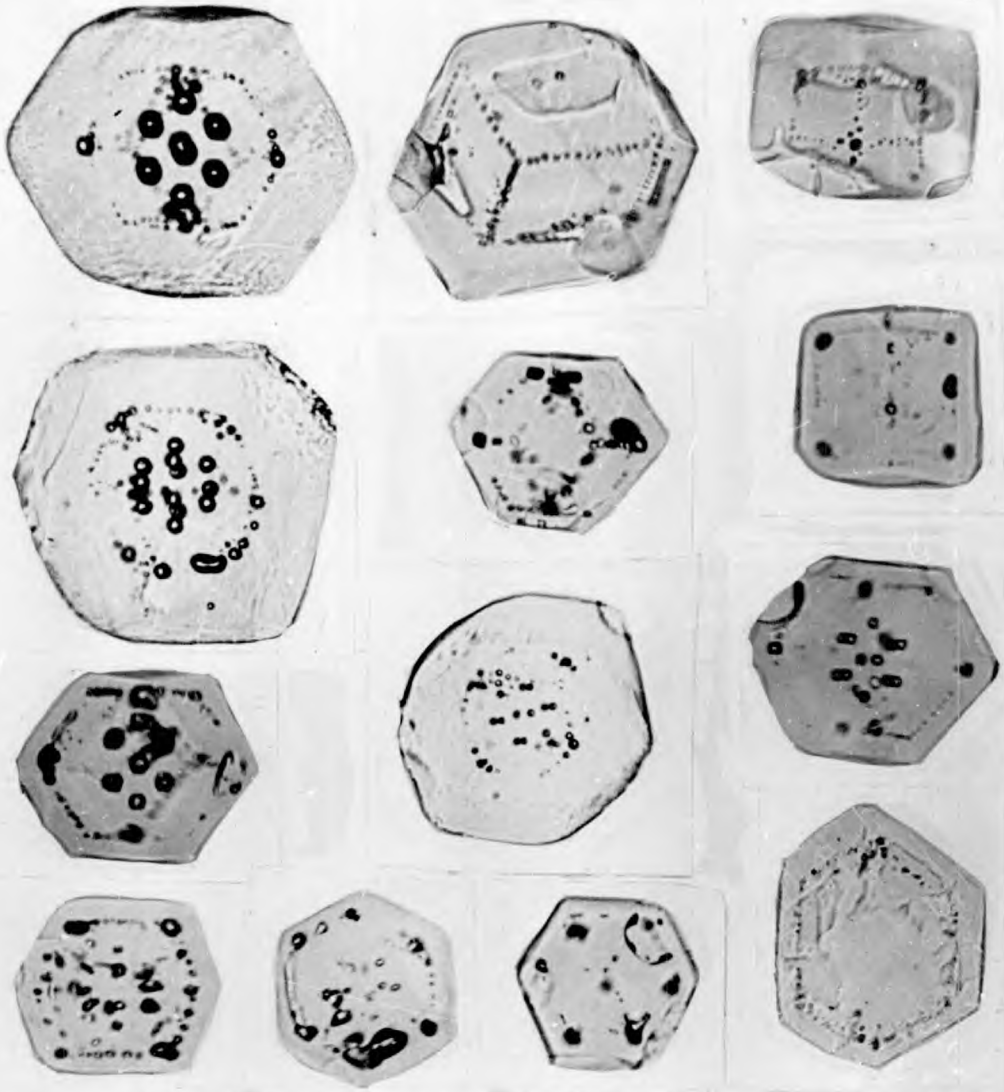

PHOTOGRAPHS OF HEXAMINE CRYSTALS SHOWING EDGE INCLUSIONS. [Immersion fluid : Aniline] [x 120]

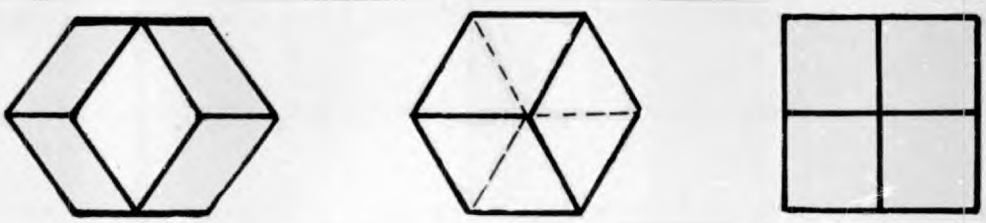

RHOMBIC DODECAHEDRON

FIG. 3-7. COMPARISON OF INCLUSIONS IN HEXAMINE CRYSTALS WITH EDGES OF DODECAHEDRON.

FOCUS NEAR BOTTOM OF CRYSTAL.

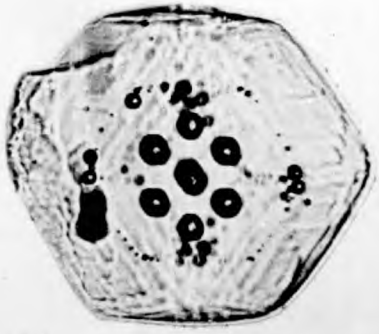

FOCUS AT MIDDLE OF CRYSTAL.

FOCUS NEAR TOP OF CRYSTAL.

FIG. 3-8. ILLUSTRATION OF THREE DIMENSIONAL NATURE OF EDGE INCLUSION PATTERN IN A HEXAMINE CRYSTAL BY FOCUSSING AT DIFFERENT LEVELS.

[x 120]

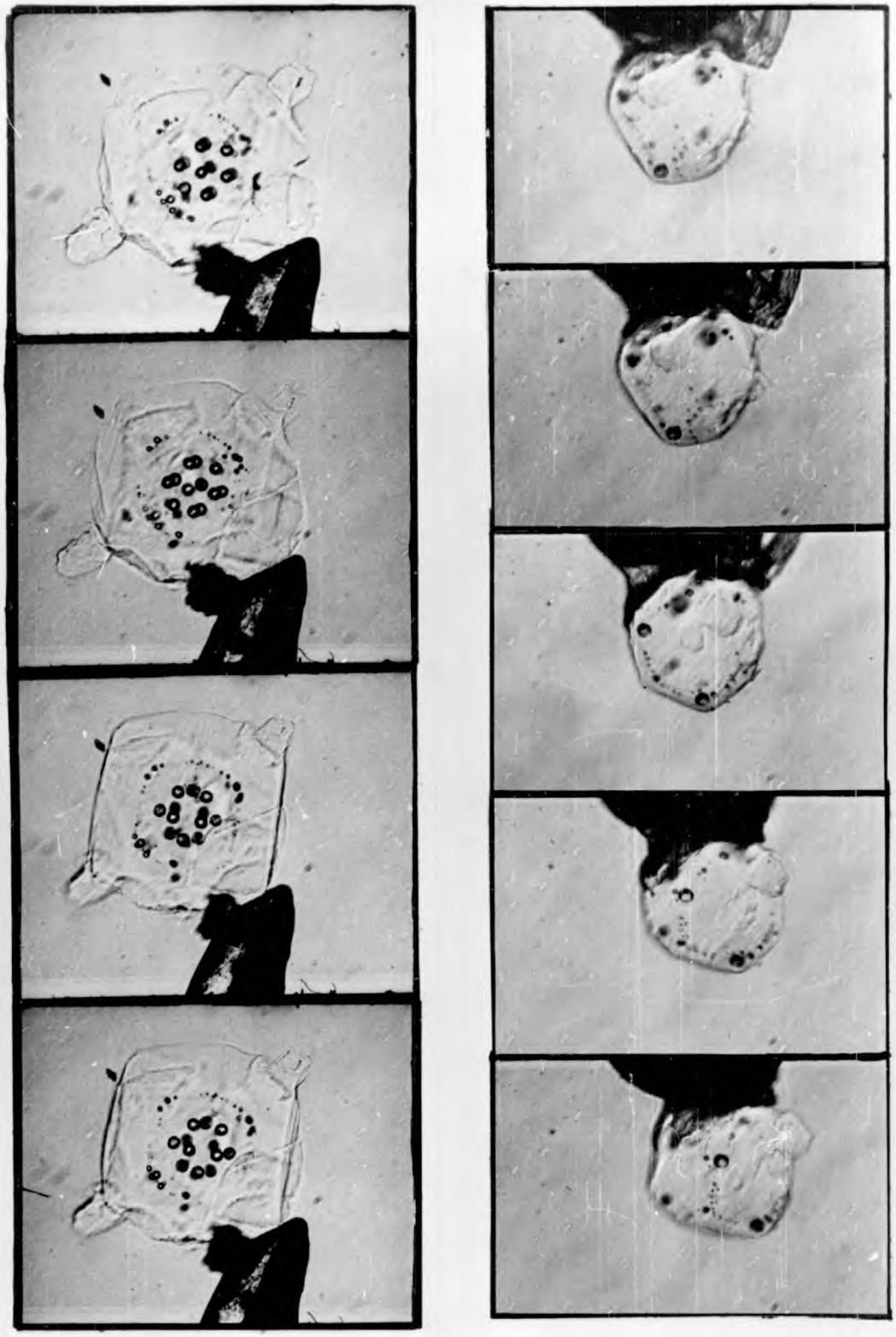

FIG. 3-9. ROTATION OF HEXAMINE CRYSTALS CONTAINING EDGE INCLUSION PATTERNS.
(FROM MOVIE. IMMERSION FLUID : ANILINE.) [x 100]

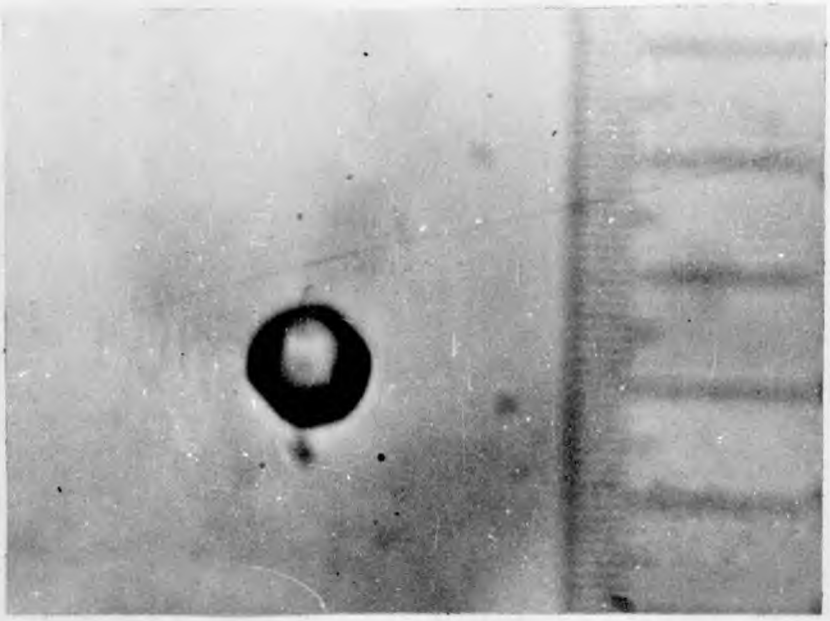

[x 70]

[x 200]

[x 300]

FIG. 3-10. DODECAHEDRAL SHAPE OF INCLUSIONS IN HEXAMINE CRYSTALS.

twelve inclusions are observed at positions corresponding to the face centres of a rhombic dodecahedron. In the other, the 'edge' pattern, lines of inclusions trace out the edges of a rhombic dodecahedron. The shape adopted by most of the inclusions is that of a negative crystal.

4. DESCRIPTION OF INCLUSIONS IN OTHER CRYSTALS

4.1 INTRODUCTION

As mentioned in Section 2.7, regular inclusion patterns have been observed in other crystals, in particular, in crystals of ammonium chloride and sodium chloride. These examples will now be examined in greater detail. The means of growing these crystals with inclusion patterns will be considered in Ch. 9. Both materials belong to the cubic system of crystal symmetry, and under suitable conditions can be crystallized as cubes.

4.2 SELECTION OF IMMERSION FLUIDS

From a knowledge of the refractive indices and densities of ammonium chloride and sodium chloride (Table 4-1) immersion liquids were chosen. For ammonium chloride, α-bromo-naphthalene was used. This material is immiscible with aqueous solution so it was necessary to dry the batches of crystals quite thoroughly before observation.

Phenol (with a small addition of water to keep it liquid at room temperatures) was used for sodium chloride crystals. After several minutes exposure to the air on the microscope slide, phenol began crystallizing, but observations were usually completed before this happened.

4.3 'FACE' PATTERN OF INCLUSIONS IN AMMONIUM CHLORIDE

The presence of patterns of six inclusions in cubes of ammonium chloride has already been noted by Bunn [14]. Each inclusion corresponds to the centre of the face of the cubic crystal at some previous stage of growth. The pattern is obviously similar in nature to the 'face' pattern in hexamine crystals. An example showing two successive sets of

MATERIAL	$n_{D_{20}}$	ρ_{20}
AMMONIUM CHLORIDE	1.64	1.53
α - bromo- naphthalene	1.658	1.48
SODIUM CHLORIDE	1.544	2.16
phenol	1.542	1.06

Data from LANGE [20]

TABLE 4 - 1. PROPERTIES OF CRYSTAL MATERIALS AND IMMERSION FLUIDS.

six inclusions is given by Bunn [14].

Examples of inclusions in crystals grown by the author are shown in Fig 4-1. The three dimensional cubic nature of the pattern is readily visible from the photographs. Also the pattern was confirmed by rotating crystals on a spike in the immersion fluid.

Some of the inclusions shown in the patterns of Fig 4-1 have an unusual shape. These crystals were photographed soon after manufacture. The shape is connected with the mechanism of growth and the high temperature coefficient of solubility of the material. This aspect will be discussed further in Section 9.2.2. After some time, these inclusions adopt the form of negative crystals i.e. each inclusion is bounded by three pairs of parallel faces mutually at right angles.

Individual inclusions in these patterns range in size up to 80μ. The amount of volume occupied by the inclusions may be up to ten percent of the total crystal. Crystals with a high percentage of included solution tend to float on the immersion fluid because of their reduced density.

4.4 'EDGE' PATTERN OF INCLUSIONS IN AMMONIUM CHLORIDE

Ammonium chloride crystals were grown which showed 'edge' patterns of inclusions (Fig. 4-2). The inclusions lie along the edges of a cube. The inclusions are quite small (up to 20μ) and constitute less than one percent of the crystal volume.

4.5 'FACE' PATTERN OF INCLUSIONS IN SODIUM CHLORIDE

Sodium chloride cyrstals can show patterns of six 'face' inclusions similar to those in ammonium chloride crystals. A photograph supplied by Birchall [15] is shown in Fig 4-3 together with photographs of crystals

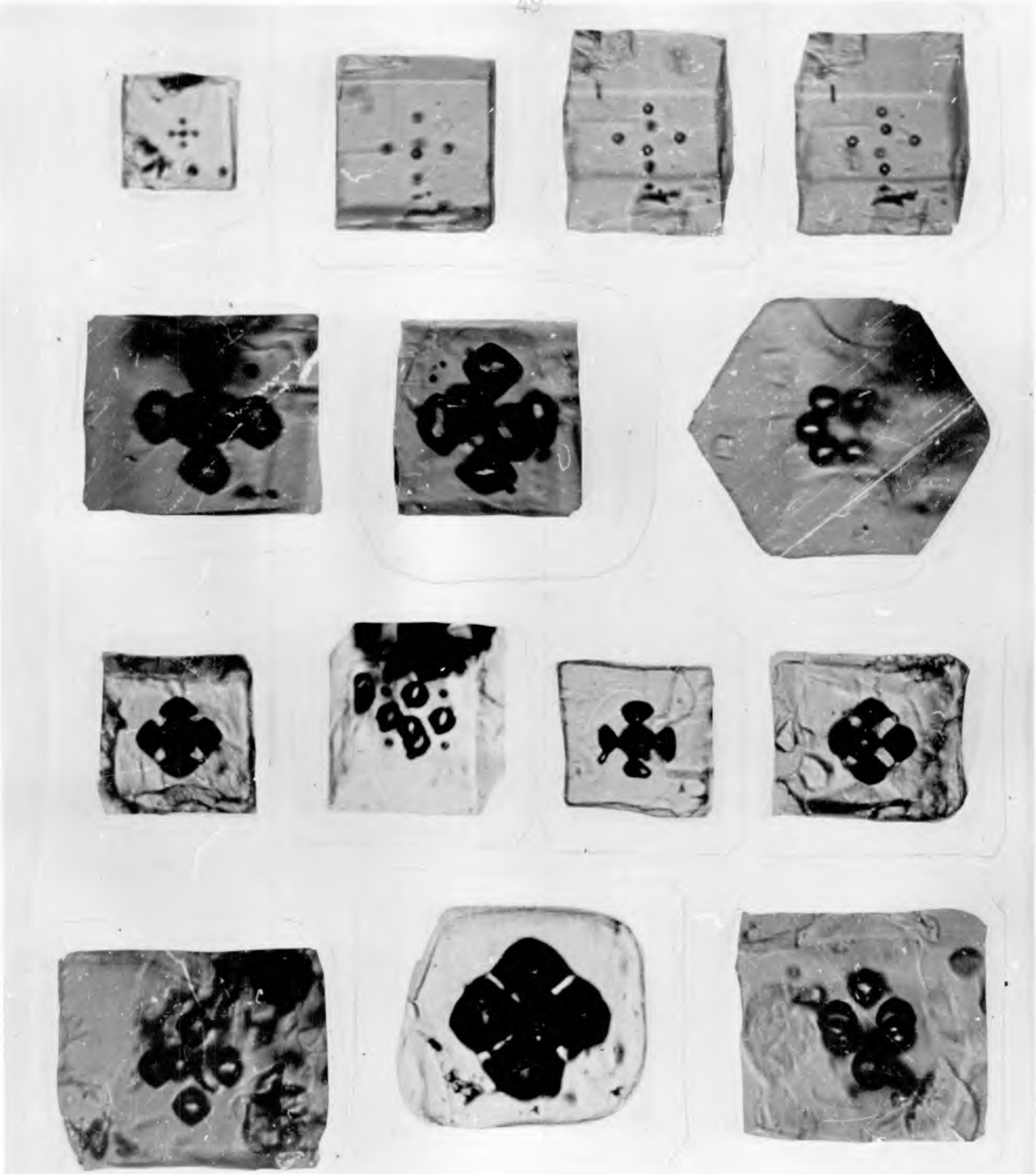

FIG. 4-1. 'FACE' PATTERN OF INCLUSIONS IN AMMONIUM CHLORIDE CRYSTALS.
(Immersion Fluid: α-Bromonaphthalene.) [x 150]

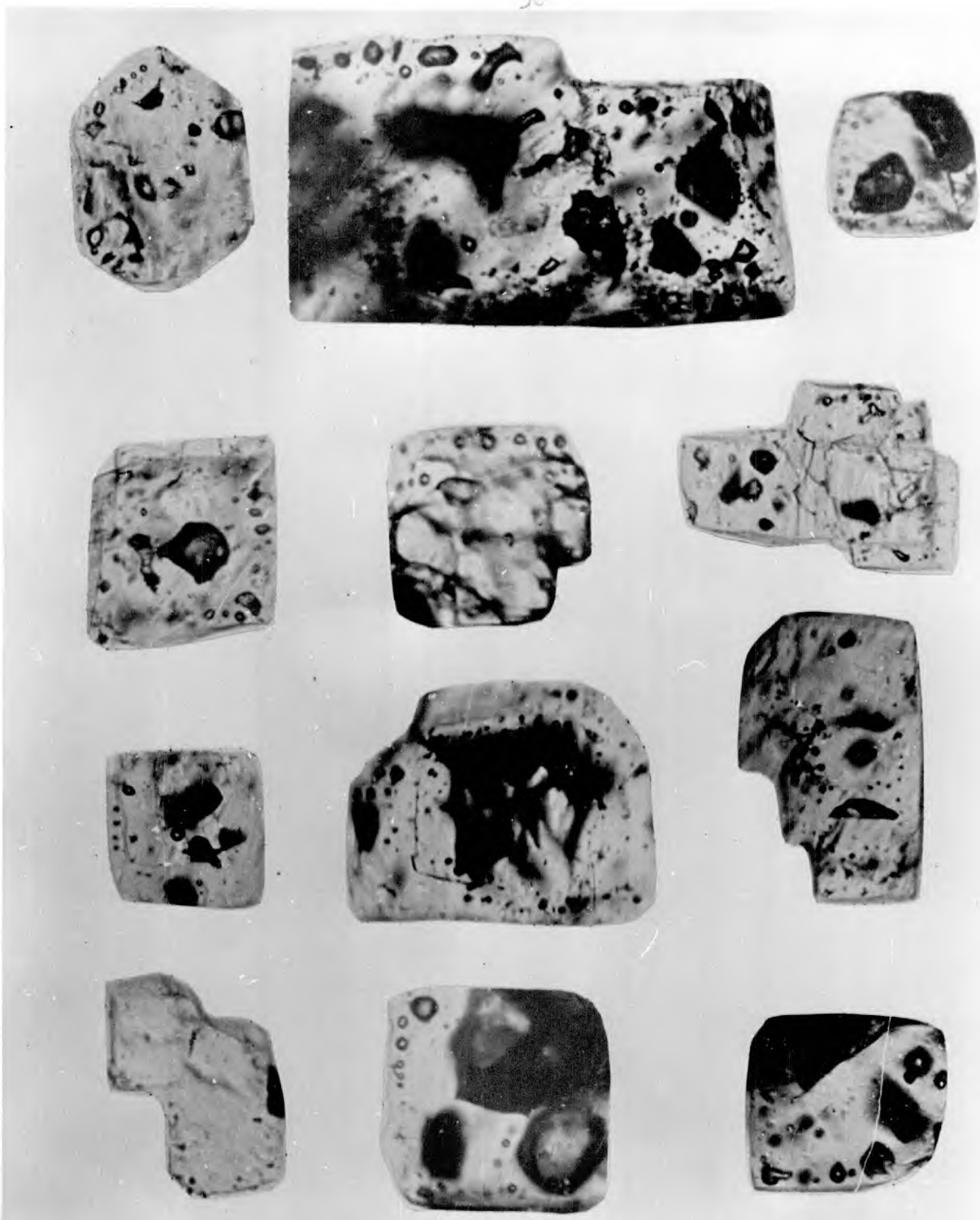

FIG. 4-2. 'EDGE' INCLUSION PATTERNS IN AMMONIUM CHLORIDE CRYSTALS [x 120]

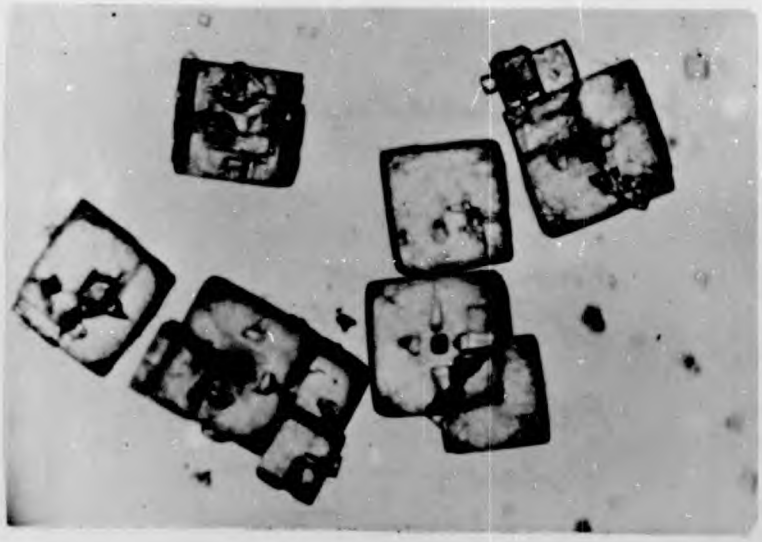

CRYSTALS PREPARED BY BIRCHALL [15].

[x 50]

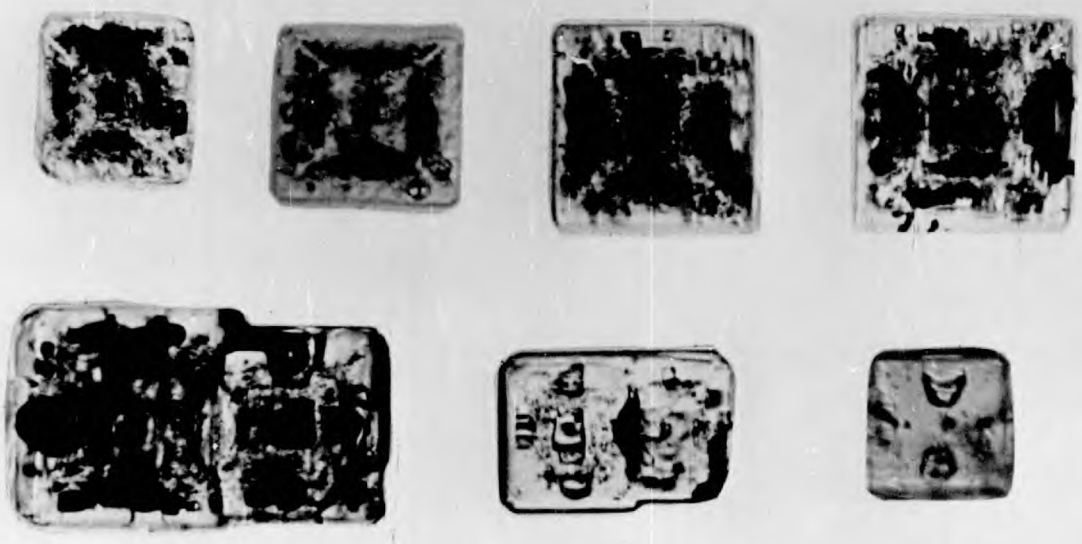

CRYSTALS GROWN BY AUTHOR.
(Immersion Fluid : Phenol)

[x 120]

FIG. 4-3. 'FACE' PATTERN OF INCLUSIONS IN SODIUM CHLORIDE.

grown by the author. Inclusions up to 60 μ have been observed in these patterns, corresponding to about five percent of the crystal volume.

4.6 'EDGE' INCLUSIONS PATTERNS IN SODIUM CHLORIDE

Patterns of 'edge' inclusions can be grown readily in crystals of sodium chloride (Fig. 4-4). The inclusions outline the edges of the cubic form of the crystals. The individual inclusions are quite small (less than 25 μ) and comprise less than one percent of the whole crystal.

4.7 REGULAR INCLUSION PATTERNS IN OTHER CRYSTALS

Regular inclusion patterns may well occur in crystalline materials other than those described above, which were the only materials considered in this project. As will be seen in the following sections of the thesis, the conditions under which these inclusions form are not so unusual. It would be very surprising if other materials did not show a similar behaviour under somewhat similar conditions. One reason why more examples may not have been reported is that it is usually the purpose of industrial operation and research investigations to prepare pure crystals. Crystals which show included impurity tend to be disregarded and discarded, and conditions which promote inclusion formation tend to be strenuously avoided.

4.8 CONCLUSION

Other crystals, in particular ammonium chloride and sodium chloride, can show 'face' and 'edge' inclusion patterns. In the case of ammonium chloride and sodium chloride the arrangements correspond to the symmetry of the cube.

FIG. 4-4. 'EDGE' PATTERN OF INCLUSIONS IN SODIUM CHLORIDE.
(Immersion Fluid : Phenol) [x 120]

5. EQUIPMENT FOR THE GROWTH OF CRYSTALS

5.1 INTRODUCTION

It was necessary to construct suitable apparatus for the growth of crystals so that the formation of inclusions could be studied. The material chosen for study was hexamine crystallizing from aqueous solution, which was known to give crystals with regular inclusions (see section 5.1).

In order to grow crystals, some means of promoting supersaturation was required. Possible means include,

(i) the use of the variation of solubility with temperature;

(ii) the removal of solvent by evaporation; and

(iii) the use of added components to 'salt out' the solute.

The solubility of hexamine does not vary greatly with temperature (Fig 5-1). So it was considered unlikely that hexamine crystals with inclusions could be grown by the first means and consideration was given to the other methods. Subsequently it was found that the first method could be used and an apparatus for growing crystals by this means is described in section 5.10.

The second means was selected as the main method for growing hexamine crystals, and an apparatus utilizing this method is described in detail in the following sections.

Consideration was also given to the attainment of supersaturation by the use of additives. Gaseous ammonia was found to be a suitable additive for aqueous solutions, while methanol, ethanol and glycerol were not (refer Supplement, section SIII). However, this means was discarded on the grounds of the practical difficulties associated with

SELECTED VALUES

T, °C	0	10	20	30	40	50	60	70	80	90	100
1000x	472	469	466	463	461	459	457	456	456	458	463

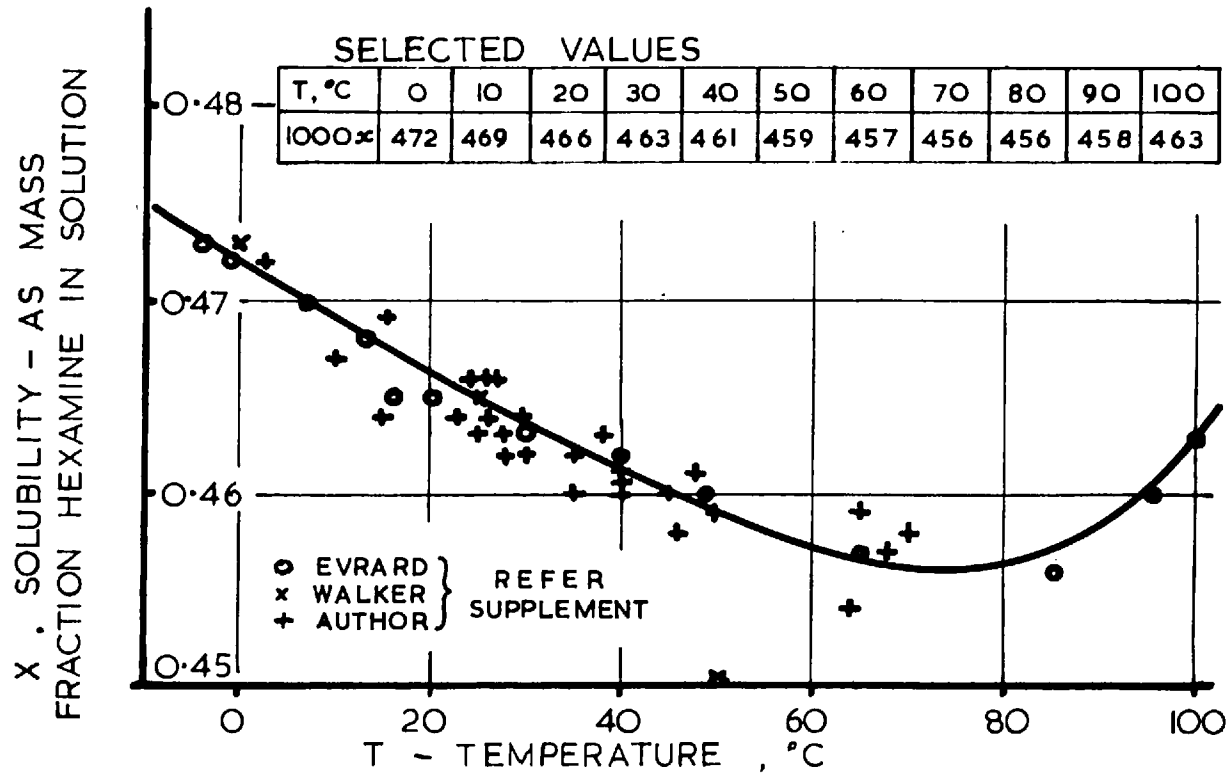

SUPERSATURATION RATIO ON HEATING A SATURATED SOLUTION FROM THE INITIAL TO THE FINAL TEMPERATURE.

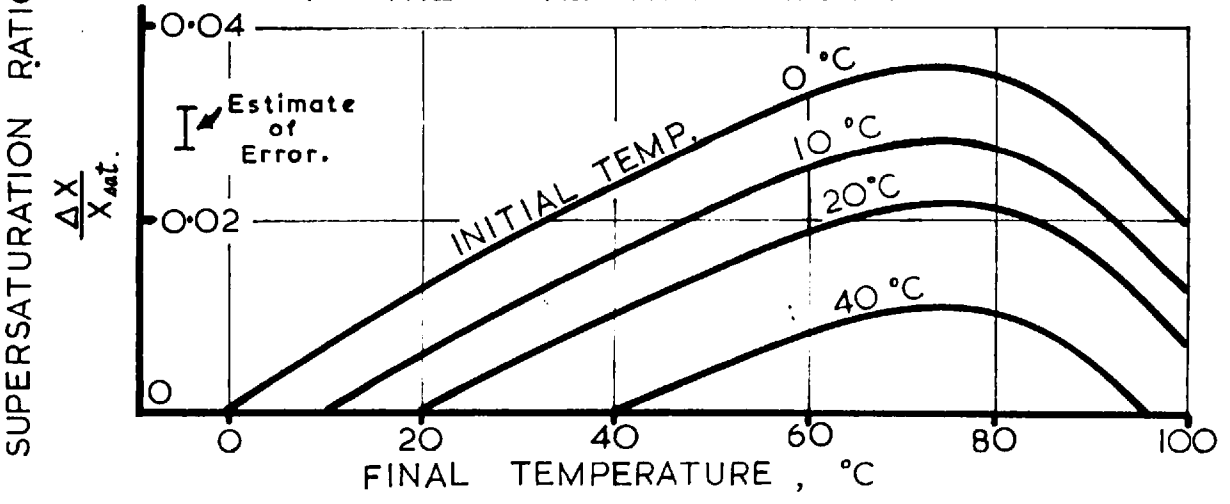

FIG. 5-1. SOLUBILITY OF HEXAMINE IN WATER, AND CORRESPONDING SUPERSATURATIONS ON HEATING SUCH SATURATED SOLUTIONS.

the controlled mixing of solution and gas, and also on the undesirability of introducing the possible complications of another 'impurity'.

5.2 DESCRIPTION OF EVAPORATIVE CRYSTALLIZER

Supersaturation was to be promoted by evaporation of the solvent, water. The product, hexamine tends to decompose in solutions above 60°C [22], so that evaporation under vacuum was necessary.

In order that crystals might be grown under known and controlled conditions it was decided to grow the crystals in a continuous crystallizer under steady state operation. The analysis of the results for growth conditions is also quite a simple matter [23-25].

Essentially the crystallizer (Fig 5-2 and 5-3) consisted of a 2-litre agitated flask (6), maintained under vacuum, and heated by an electric mantle (7). A continuous stream of saturated feed solution from a stock vessel (1) entered the flask through a flow-meter (2). The evaporated water was condensed (8) and its volume measured (9). The slurry of mother liquor and crystals overflowed through a side arm and seal vessel (10), to either a sample receiver (12) or a product store (13). Liquor and vapour temperatures, and solution conductivity could be measured.

5.3 DETAILS OF DESIGN AND CONSTRUCTION OF CRYSTALLIZER

5.3.1 Selection of Operating Conditions

A vessel of 2 litres capacity was considered to be a convenient size. The available 400W heating mantle would produce a maximum of 8g. of hexamine crystals per minute (Fig 5-4) so feed flow rates should be in the range 10-100g/min. Evaporating temperatures would be below 60°C (because of product decomposition) and above 25°C (because of the limits of condenser water temperature). Corresponding vacuums in the range 20-100 mm Hg. absolute would be required.

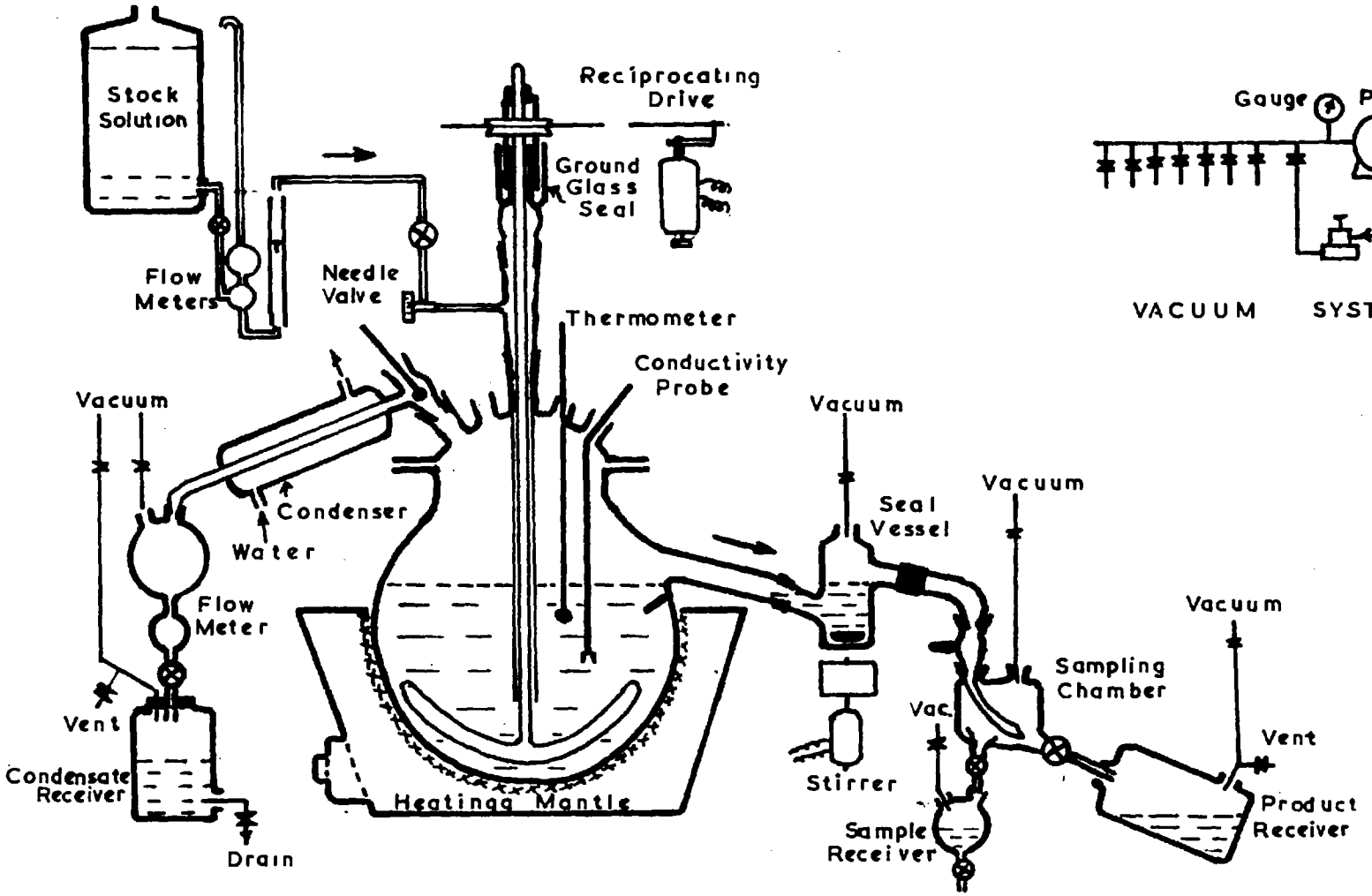

FIG. 5-2. DIAGRAM OF CONTINUOUSLY OPERATED EVAPORATIVE CRYSTALLIZER.

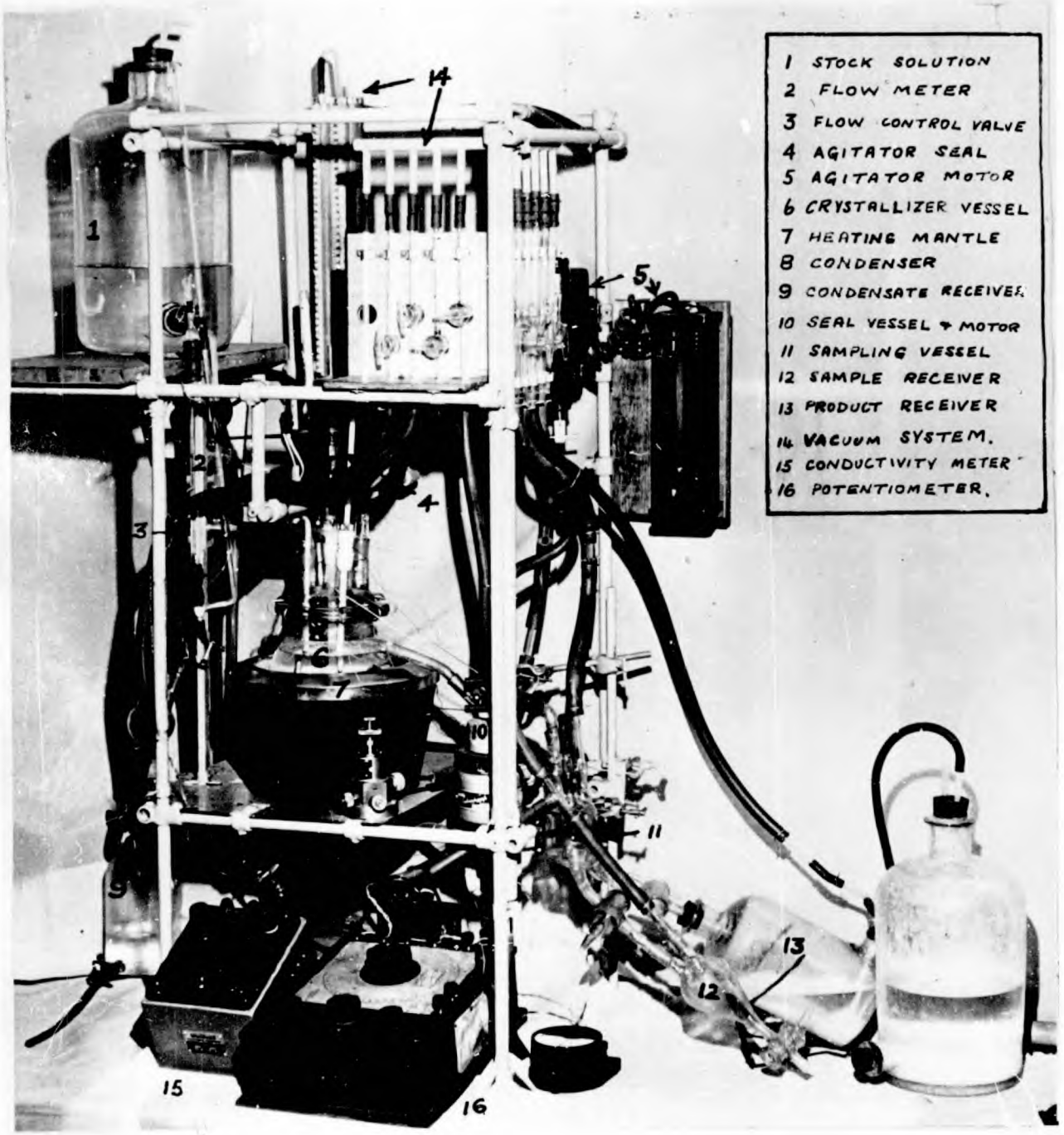

FIG. 5-3. OVERALL VIEW OF CONTINUOUSLY OPERATED EVAPORATIVE CRYSTALLIZER.

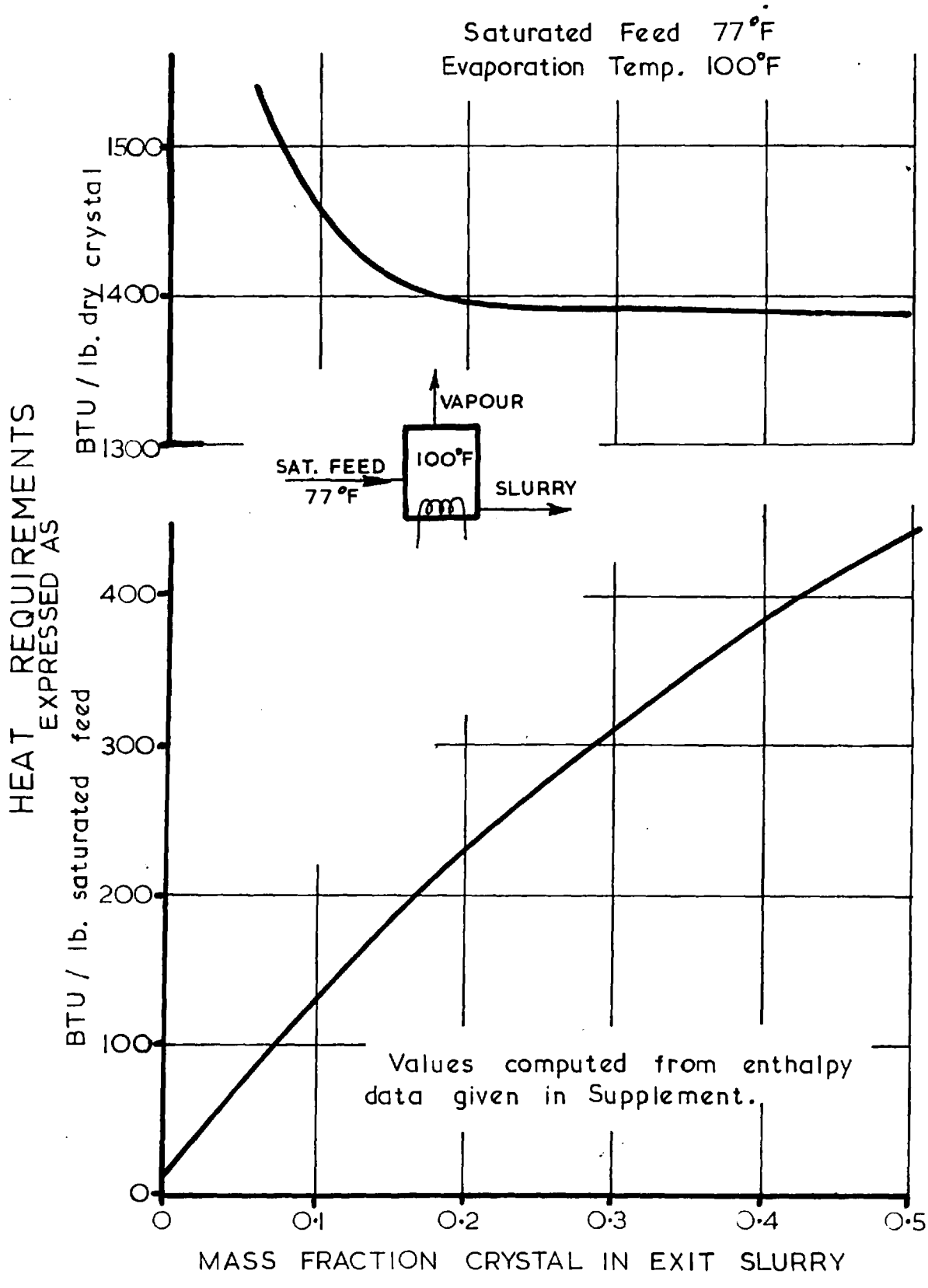

FIG. 5-4. COMPUTED HEAT REQUIREMENTS FOR CONTINUOUS CRYSTALLIZATION OF HEXAMINE.

5.3.2 Vacuum system

Suitable vacuums were produced by a single stage rotary pump (Edwards 'Speedivac' Model ISP 30) connected to the crystallizer through a trap, manifold system, and a series of vacuum tight cocks. It was necessary to maintain a very steady vacuum in the system and this was achieved by an automatic vacuum controller (Edwards V.P.C.1) acting on an air bleed. The pressure was measured by a mercury U-tube manometer.

5.3.3 Crystallizing Vessel

The crystallizing vessel (Fig 5-5 and 5-6) was a 'Quickfit' glass reaction vessel of two litre capacity fitted with a flat flange lid. The lid carried five B19 cone joints through which the stirrer, thermometer, conductivity probe, and condenser were fitted. The fifth joint was used for filling and emptying the vessel at the completion of a run. A large anchor paddle stirrer was used to achieve uniform mixing. The stirrer was supported by a stirrer guide surmounted by a ground glass vacuum tight stirrer gland. The feed entered the vessel through the stirrer guide. The stirrer gland was lubricated with glycerol. Under operating conditions there was a very slight leakage of glycerol ($\leq$ 0.1 cc/day) into the vessel. So that surfaces on which crystals could form or deposit might be reduced to a minimum, the vessel was unbaffled. A reciprocating stirrer was necessary to prevent swirl while still promoting uniform agitation. A small stainless steel baffle ($\frac{3}{4}$" x $2\frac{1}{2}$") near to the overflow outlet was found later to be necessary to prevent splash-over.

Slurry left the vessel by gravity overflow through a glass sidearm. The working capacity of the crystallizer was 1500 ml.

The flask was heated with a standard 435W 'Isomantle' heating mantle with power control.

5.3.4 Stirrer Drive

Since the crystallizing vessel was unbaffled a rotating stirrer could not be used. Instead, one using an oscillatory motion was constructed (Fig 5-7). A variable speed motor (0.1 HP) attached to a crank mechanism gave a straight reciprocating motion. This motion was transmitted by a nylon cord to a small plastic pulley mounted on the ground glass stirrer gland, to which the stirrer shaft was attached. The stroke of the reciprocating mechanism was so adjusted that each revolution of the motor corresponded to two complete revolutions of the stirrer, one clockwise and one anticlockwise. Motor speeds from 30 to 250 R.P.M. were used.

5.3.5 Condensate System

The solvent evaporated from the boiling solution was condensed in a water-cooled glass condenser (see Fig 5-6). The condensate rate was measured by the time required to fill a calibrated vessel (volume = 30.0 ml).

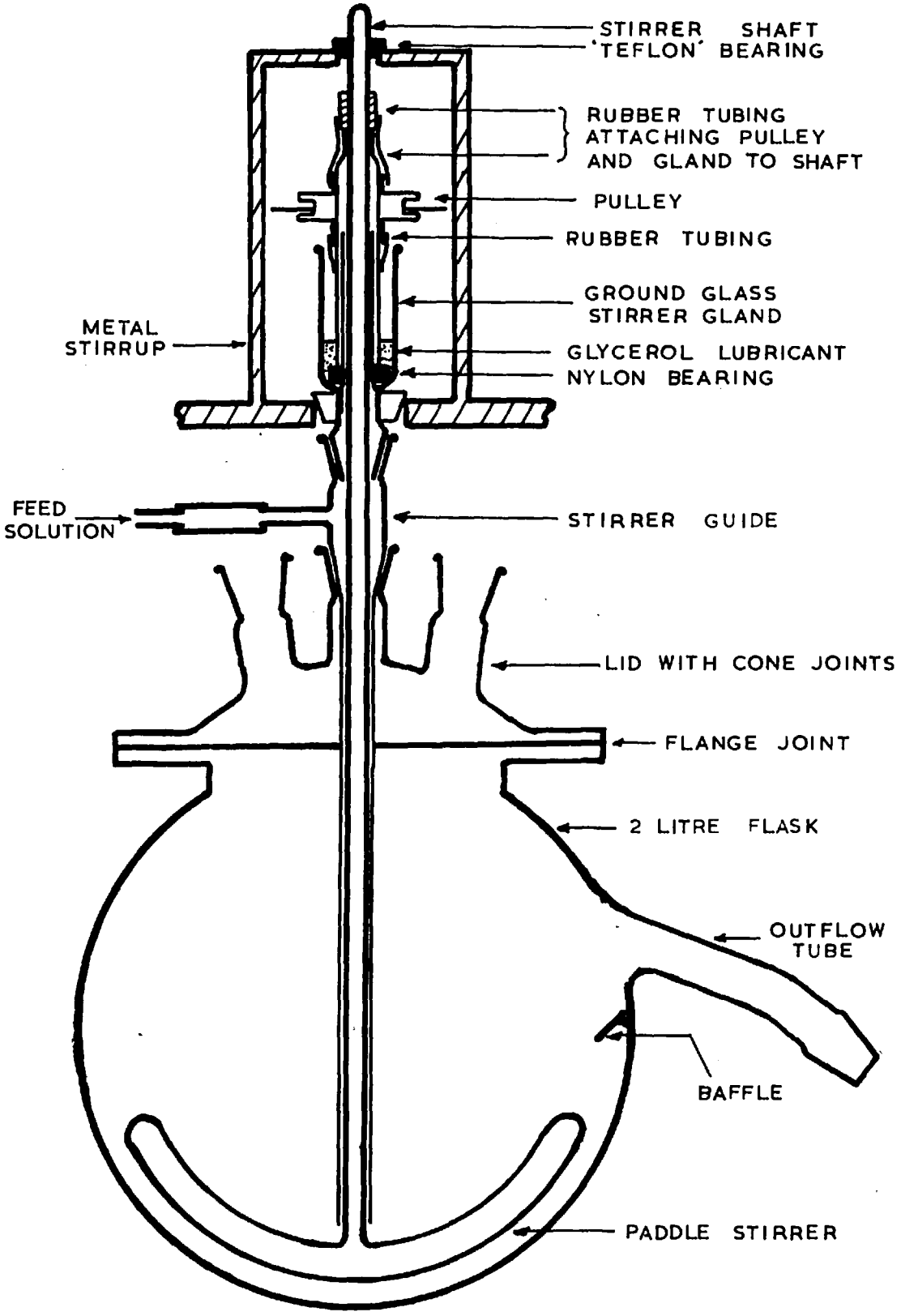

FIG. 5-5. CRYSTALLIZING VESSEL.

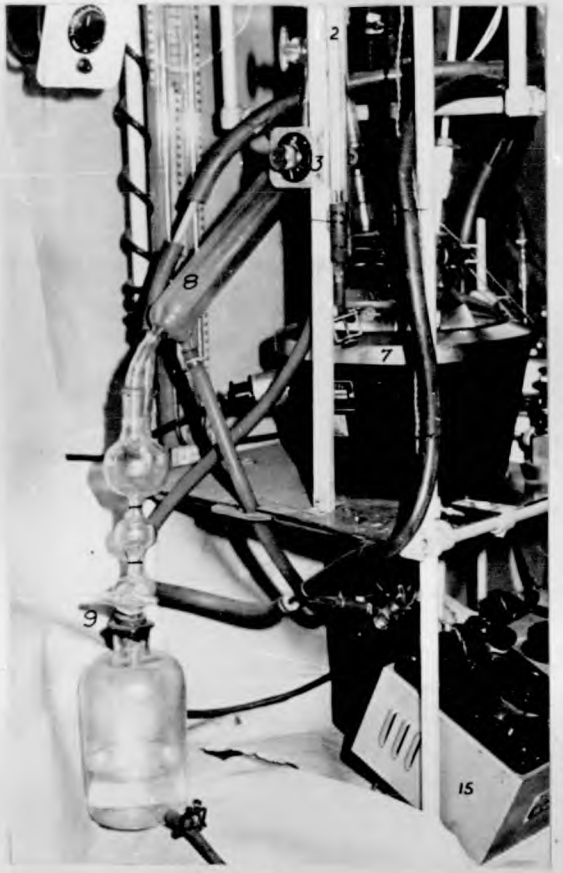

A.

B.

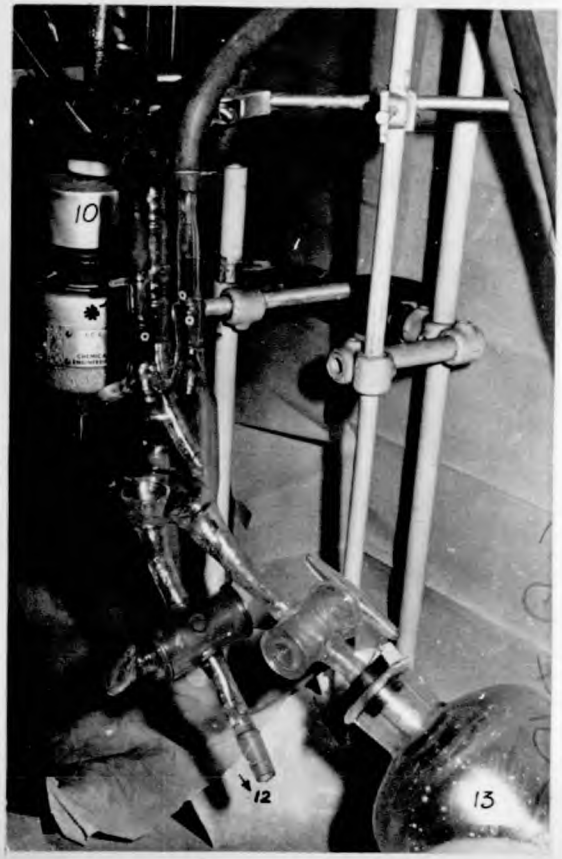

C.

FIG. 5·6 DETAILS OF CONTINUOUSLY OPERATED EVAPORATIVE CRYSTALLIZER.
A. CONDENSING SYSTEM ; B. CRYSTALLIZING VESSEL ; C. PRODUCT SAMPLING DEVICE.
(Code for numbers on Fig. 5·3).

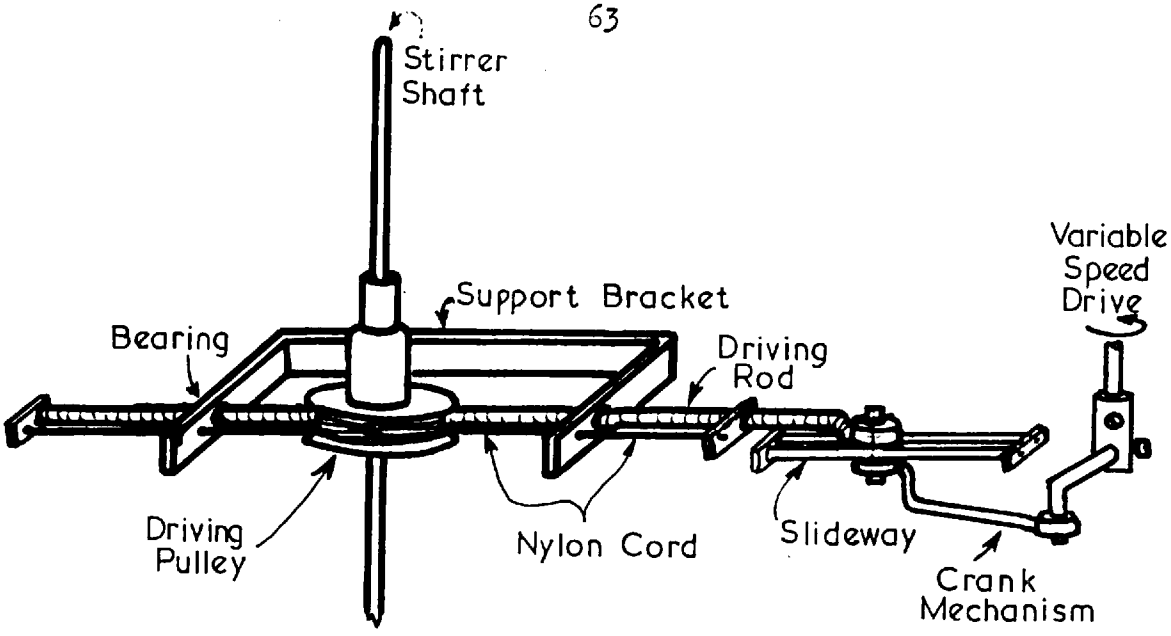

FIG. 5-7. DIAGRAM OF STIRRER DRIVE.

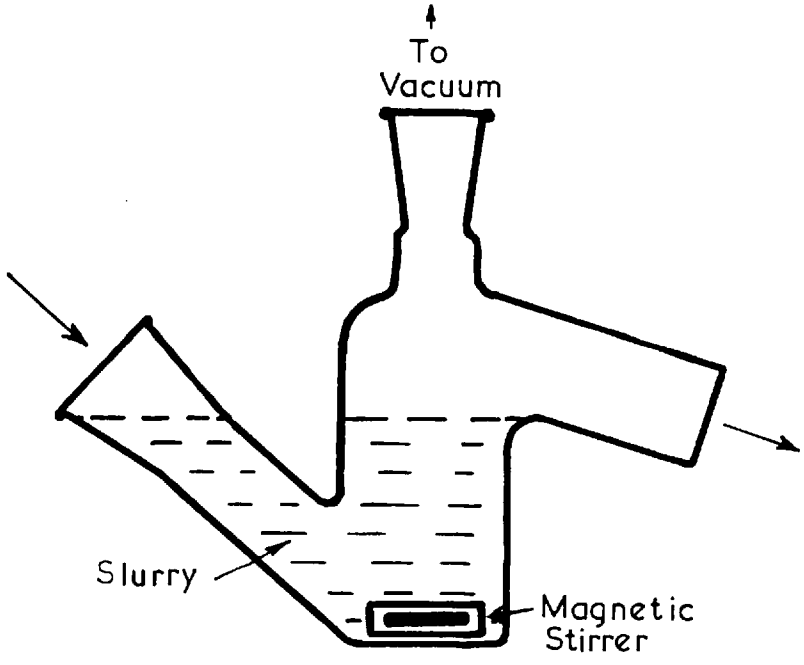

FIG. 5-8. SEAL VESSEL.

After measurement the condensate collected in a one litre receiver.

5.3.6 Feed System

The saturated feed solution was stored in a 10 litre stock bottle. It passed to the crystallizing vessel through a flow measuring device and a needle valve. The feed flow rate was measured by the time required to empty a calibrated vessel (of 103 ml volume)*. The flow was also measured by a 'Rotameter' variable area flow meter (10-100 ml/min) but this proved temperature dependent (probably because of the viscous solution) and was only used for indicating short term variations in flow rate.

5.3.7 Outflow and Product Sampling System

Slurry left the crystallizing vessel by gravity overflow into an outlet tube leading to a seal vessel. This vessel prevented vapour from by-passing the condenser and escaping through the vacuum lines from the rest of the system. Crystals were prevented from settling in the seal vessel by a magnetic stirrer. Various seal vessel designs were tried before that shown in Fig 5-8 proved satisfactory. If the depth of seal liquid was too small the seal was blown out by pressure fluctuations, if too large the magnetic stirrer was incapable of agitating the full height and the upper section of the seal vessel blocked solid.

The overflow from the seal vessel passed to the sampling chamber (Fig 5-6). The flow tube could be turned on the axis of two B19 cone joints to divert the flow to either a 250 ml sample receiver or a $2\frac{1}{2}$ litre product receiver.

Provision was made on all vessels for venting either to the vacuum system or to the atmosphere.

5.3.8 Temperature and Conductivity Measurements

The temperatures of the boiling solution and the evaporated vapour were measured by two immersion thermometers. The difference in temperature between the two was also measured to greater accuracy by a thermocouple. This difference should indicate the extent of any superheating. In all cases, once steady boiling began, no measurable superheating was observed; the temperature difference corresponded completely to the expected elevation of boiling point (see Supplement, Fig. SII-6).

A conductivity probe was inserted into the solution in an attempt to measure solution supersaturation. However, the variations of conductivity with temperature fluctuations far outweighed any change due

*This vessel was added subsequently to the taking of the photographs Fig 5-3 and 5-6 and is not shown there. The device is illustrated in Fig 5-2.

to differences in concentration. The maximum change in supersaturation one might expect would give a conductivity change less than that given by a 1°C change in temperature (refer Supplement Fig SII-21). Also the conductivity reading was affected by the amount of crystal in suspension.

5.4 CONTINUOUS CRYSTALLIZATION RESULTS

Four runs were undertaken with the continuously operated evaporative crystallizer. The results are shown in Table 5-1 and Fig 5-9.

The major point to note is that in not one case did crystals form with regular patterns of inclusions. The crystals did contain a little included moisture in the form of randomly distributed inclusions but none as regular patterns. Modifications to the method of growth were necessary and these are considered in the next section.

It might also be noted that very long periods of time were needed for the apparatus to come to a steady state as measured by the crystal content of the product (Fig 5-9). A steady value of the crystal size distribution would presumably have taken even longer still. The product crystal content also differed from the bulk and from the value computed from flow and condensate rates (Fig 5-9). This was probably caused by the baffle 'filtering out' some of the crystals from the overflow slurry. Suitable modifications, no doubt, could have been made if this method of growth had proved suitable.

5.5 MODIFICATION OF METHOD OF GROWTH

Consideration is given to the crystal shown in Fig 5-2. This crystal was one of a batch grown in a small glass flask by boiling saturated solution under vacuum for about half an hour. The size of the inclusion pattern is about one third the size of the crystal i.e. the volume of material inside the pattern is about 1/30 of the whole volume. It would seem very likely that the inclusions in this crystal were formed within the first minute or so

Run No.	1	2	3	4
Operating Temp., °C	38	48	40	53
Stirrer R.P.M. †	90	100	110	145
Condensate rate, g/min.	4.23	3.78	3.61	4.00
Feed Rate, g/min.	11.9	13.0	13.5	18.0
Product rate, g/min.	7.6	9.8	10.1	14.1
Duration of run,* min.	175	395	410	215
Slurry crystal content at end of run :				
in final sample.	0.21	0.29	0.26	0.14
in vessel	0.29	0.39	0.31	0.25
Included moisture ≠ mg/g.	2.3	1.5	3.0	1.7
Regular inclusions patterns	NONE	NONE	NONE	NONE

All runs started with saturated feed at room temperature in the vessel. All at heating rate 8 (approx. 200 W)

† As motor R.P.M. (see section 5.3.4)

* From moment of nucleation.

≠ By Karl Fischer analysis. (Appendix VI).

TABLE 5-1. RESULTS OF CONTINUOUS RUNS ON EVAPORATIVE CRYSTALLIZER.

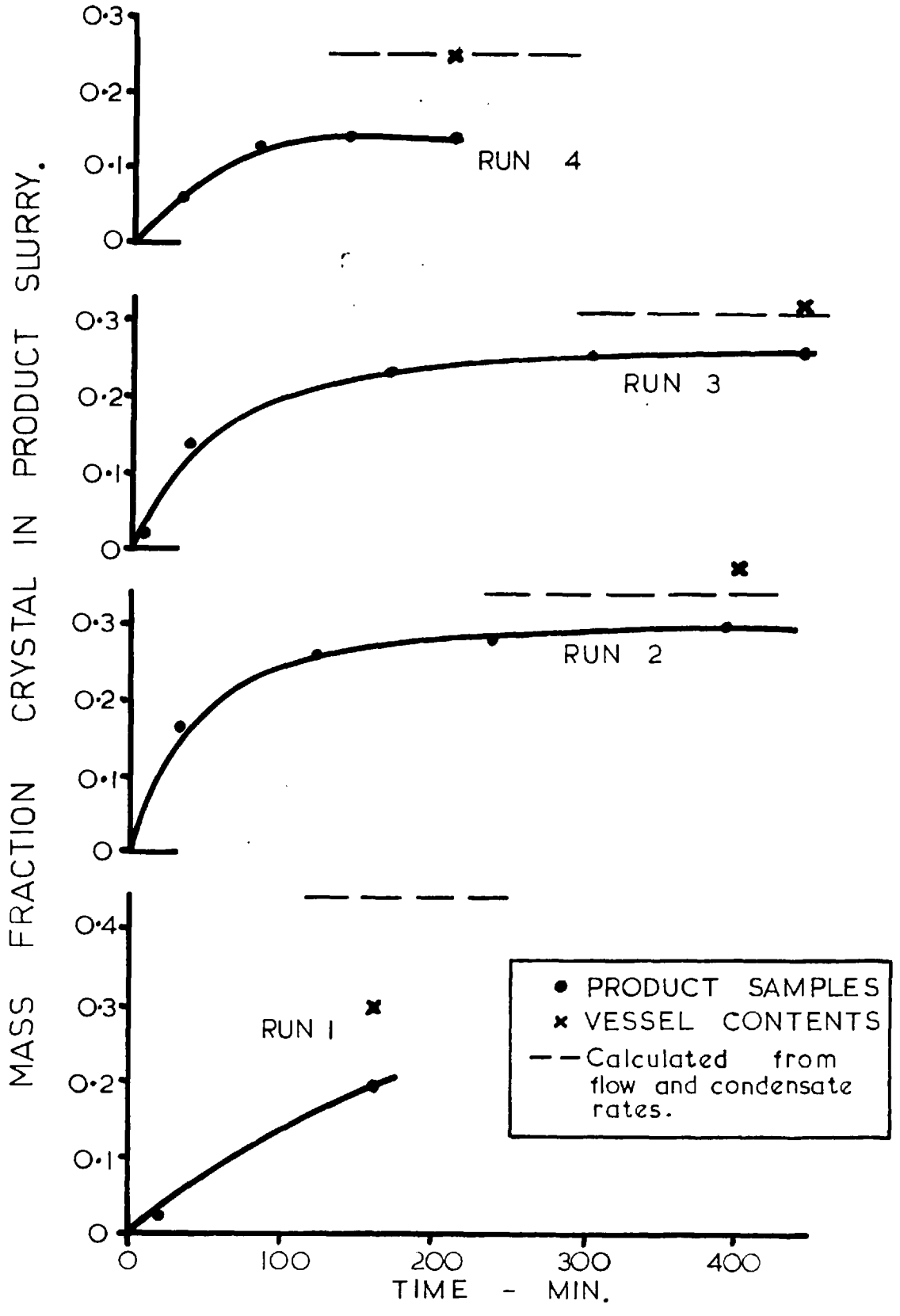

FIG. 5-9. CRYSTAL CONTENT OF SLURRY FOR CONTINUOUS CRYSTALLIZATION RUNS.

of growth of the crystal. If this were so, the initial growth after nucleation is the region of interest. An appropriate means of studying such crystal growth would be by batchwise growth of the crystal. Hence the evaporative crystallizer was modified for batchwise operation.

The analysis of results for growth conditions under batchwise (i.e. unsteady state) growth is not quite so simple as for continuous operation [26], but with certain assumptions suitable calculations can be made.

5.6 DESCRIPTION OF BATCH OPERATED EVAPORATIVE CRYSTALLIZER

The evaporative crystallizer was adapted reasonably readily from continuous to batch operation. It was necessary only to seal off the outlet tube from the crystallizing vessel, to discard the original product sampling system and to add a new sampling device (Fig 5-10).

5.6.1 Details of Modifications to Crystallizer

The glass outlet tube was effectively sealed by a rubber bung (Fig 5-10). The stainless steel baffle was no longer required and this was removed. Although parts of the feed flow system were no longer really necessary, they were retained since for each batch the vessel was filled from the stock bottle through the flow system.

The stirrer, condenser, and vacuum systems were unaltered.

5.6.2 Details of Sampling Device

The sampling device (Fig 5-10) consisted of six 20 ml sampling tubes mounted on a rotatable platform in a vacuum tight vessel. This vessel was connected to a second vacuum system maintained at a vacuum lower than that in the crystallizing vessel. A sample line ran from the crystallizing vessel to the sampling device. By opening the sampling cock on this line samples could be drawn over from the crystallizing vessel into the respective sampling tubes. A vent on the sampling line allowed the liquid leg to drain back.

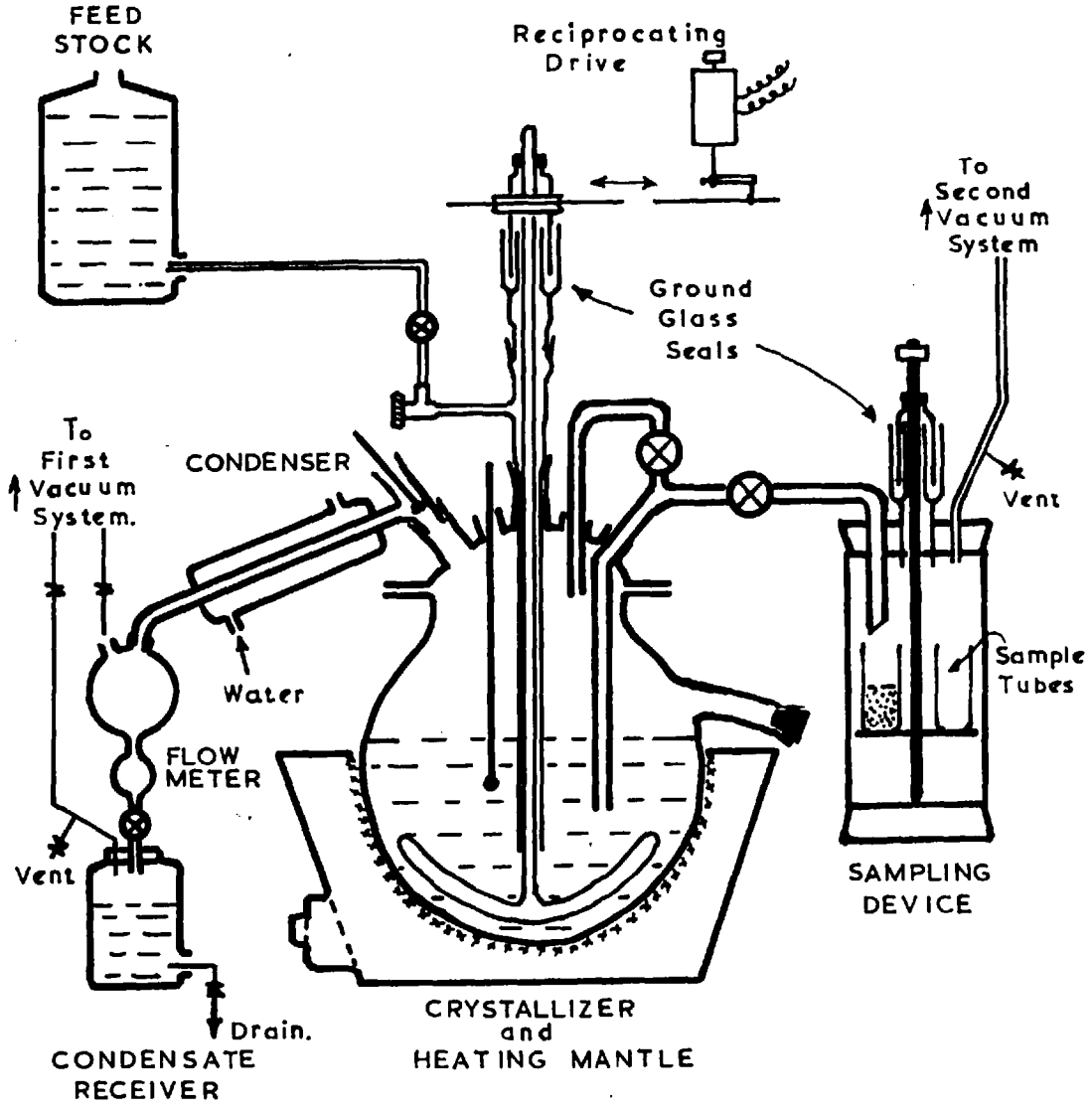

FIG. 5-10. DIAGRAM OF BATCH OPERATED EVAPORATIVE CRYSTALLIZER.

5.7 EXPERIMENTAL PROCEDURE

For each batch of crystals, the crystallizer was filled to the desired level with a slightly undersaturated solution from the feed stock bottle. Feed stocks were made from distilled water and hexamine crystals. For the initial feedstock the crystals were prepared from commercial hexamine crystals by dissolution and recrystallization. In this case the first growth of crystals was discarded as it probably contained a high percentage of the active nucleating impurities. Later feed stocks were prepared either from the filtrate of previous batches or from product crystals redissolved in distilled water. Crystals and solutions associated with any batch using added impurity were discarded.

Undersaturated feed solution was used in order to dissolve any crystal nuclei present and also to allow an interval of several minutes operation for adjustments before nucleation began. In this interval the heating rate, evaporation temperature (vacuum), and stirrer speed were adjusted to the desired values.

Time was measured from the moment of nucleation as indicated by the first cloudiness in the appearance of the boiling solution. After suitable time intervals crystal samples were taken. Condensate rate, evaporation temperature, and stirrer speed were measured during the course of the run. The stirrer speed was measured as the motor R.P.M. Each motor revolution corresponds to two complete rotations of the stirrer (see section 5.5.4).

At the end of a batch all crystal samples were filtered (while still hot), dried, and photographed. A sample from the contents of the crystallizing vessel was taken also and photographed. Four different photographs

of each sample were taken so as to obtain a representative record of the sample. Efforts were made to avoid any bias in the selection of the region of the sample to be photographed. Prints were made from each photograph and measurements were made on these prints.

5.8 EXPERIMENTAL RESULTS

Over 90 batches of hexamine crystals were grown in the evaporative crystallizer, and also about 10 batches of each of ammonium chloride and sodium chloride crystals. Some batches were concerned with the growth of 'face' inclusion patterns and others with the growth of 'edge' patterns. Details of conditions under which these batches were grown are given in Appendix III.

Representative photographs of the crystal samples are shown in following chapters. The photographs (nearly one thousand) were analysed to determine the size distribution of the crystals and the size distribution of only those crystals with inclusions. The size of the inclusions and the inclusion patterns were also measured. These data are given in Appendix III while the method of computing these quantities is shown in Appendix II.

The significance of the results will be considered in greater detail in following chapters.

5.9 DISADVANTAGE OF EVAPORATIVE CRYSTALLIZATION

Results with the evaporative crystallizer can be obtained only from samples of the crystal bulk. It is not possible to follow an individual crystal while it grows. This is a consequence of the means of generating supersaturation. The boiling of the solution would induce crystal motion even if some form of agitation were not used.

Individual crystals could be studied, if it were possible to promote suitable supersaturations by changes in temperature. Hexamine in water has a slightly negative temperature coefficient of solubility which could be used to generate small supersaturations (Fig 5-1). As it so happens, these supersaturations are sufficient to grow crystals with inclusions, and a small thermal crystallizer was built to grow crystals by this means.

5.10 DESCRIPTION OF THERMAL CRYSTALLIZER

The thermal crystallizer (Fig 5-11) was a small heated cell designed to fit on the stage of the microscope (Appendix I). The cell consisted of three glass microscope slides cemented together to form two chambers. Crystals and solutions filled the upper chamber while the lower chamber contained a heating element and heat transfer fluid. A thermocouple in the upper chamber allowed the solution temperature to be measured.

5.10.1 Details of Thermal Crystallizer

The upper chamber ($2\frac{3}{4}$" x $\frac{3}{4}$" x $\frac{1}{8}$") was formed by sealing slices of glass $\frac{1}{8}$" high between two glass slides with 'Araldite' epoxy resin . An inlet tube, an outlet tube, and a B7 socket cone were also sealed in at the ends. The cone joint could carry a 'Teflon' gland allowing a stainless steel shaft to enter the cell. When required, crystals could be grown or observed on the spike of this shaft, either while it was stationary or while it was rotated.

The lower chamber was formed from a brass wall sealed to the glass by rubber cement. A nichrome wire heating coil (10 Ω) separated from the metal wall by sheet mica passed the whole length of the chamber. Outlet and inlet tubes allowed for the flow of the heat transfer fluid (deaerated water) through the cell.

5.10.2 Details of Ancillaries

A 'Variac' auto-transformer acting through an 8:1 voltage transformer was used to control the power supply to the heating coil. The heat transfer fluid (deaerated distilled water) and the saturated feed solution were kept in stock bottles at suitable temperatures.

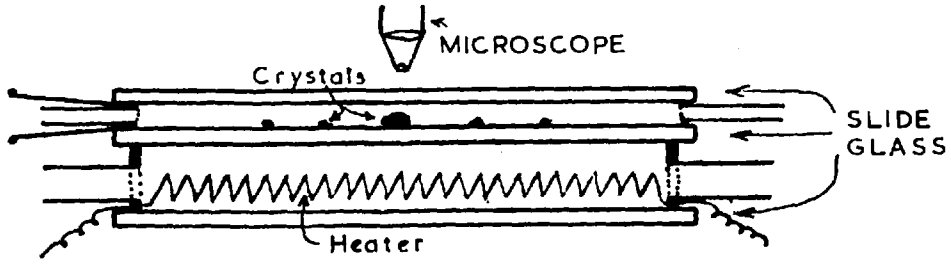

SECTION OF CELL :- Full Size

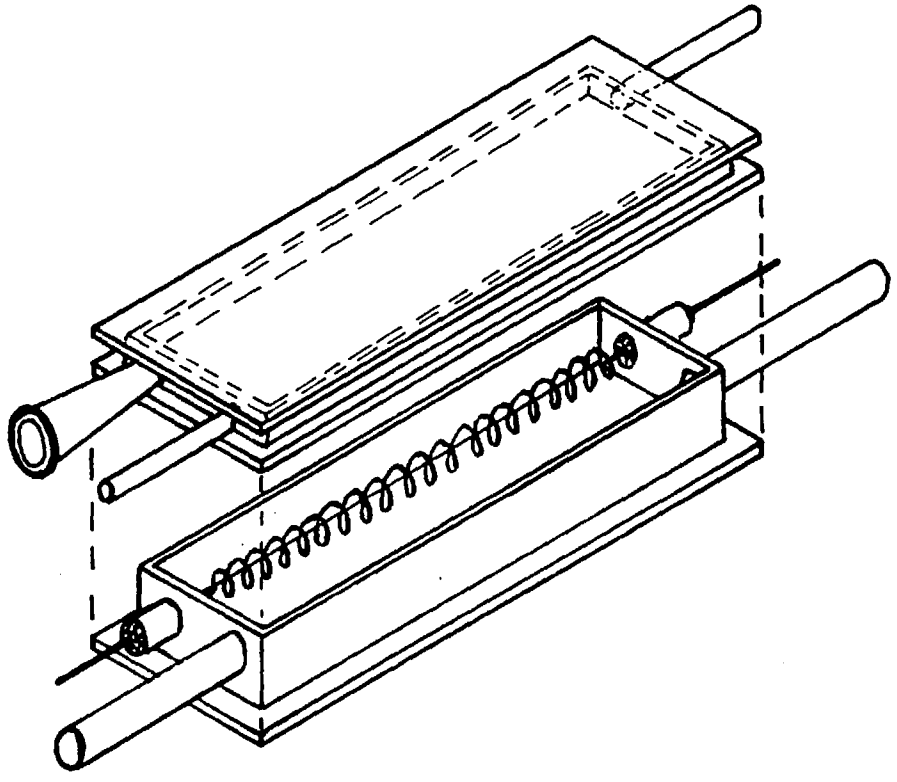

CELL - EXPLODED VIEW :- Full Size

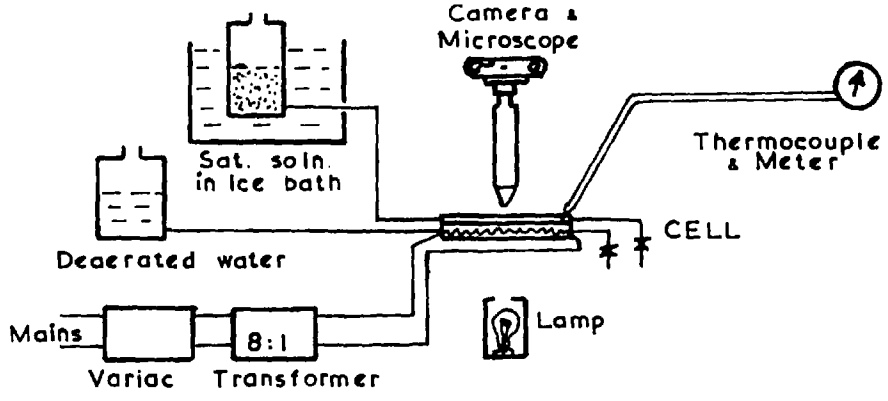

DIAGRAM OF CELL SET-UP

FIG. 5-11. CRYSTAL GROWTH CELL FOR MICROSCOPE. (THERMAL CRYSTALLIZER).

5.11 EXPERIMENTAL PROCEDURE

Some tests were conducted using a flow of solution through the cell, others using a fixed batch of solution. During a test the cell was filled with solution and the heat input adjusted. Time was measured from the moment the first crystal nucleus appeared in the field of view of the microscope. Photomicrographs were taken at selected time intervals thereafter, and the solution temperature was also measured.

The resulting photographic negatives were projected onto a screen (with a 420 times overall magnification) and the crystal sizes measured.

5.12 EXPERIMENTAL RESULTS

Examples of the photographs are shown in later chapters, together with graphical presentation of some of the results. The method of computing these values is illustrated in Appendix II. The significance of the results obtained will be discussed in more detail in the following chapters.

6. RESULTS FROM THE EVAPORATIVE CRYSTALLIZER

6.1 INTRODUCTION

It is the purpose of this chapter to relate, in an empirical manner, the size of inclusions formed in a batch to the operating conditions used in the evaporative crystallizer for that batch. Only the growth of hexamine crystals with face patterns of inclusions will be considered.

6.2 RANGE OF SIZES OF INCLUSIONS

Each crystal batch shows a range of crystal sizes and a range of sizes of the inclusions in them, (refer Fig 6-1). It can be seen that only the larger crystals have inclusions, and also that the largest inclusions are in the largest crystals. Progressively smaller inclusions are present in the progressively smaller crystals with no inclusions at all in the smallest crystals.

This is a very important observation. Quantitative evidence to support it will be given in the next chapter, where its use is critical in the understanding of the mechanism of inclusion formation.

For the purposes of this chapter it is necessary only to realize that a range of inclusion sizes is involved and that some means of specifying inclusion size is required.

6.3 SPECIFICATION OF INCLUSION SIZE

The simplest measure that can be made is the size of the largest inclusion observed in the sample. There are twelve such inclusions in the pattern in each crystal. Fig 6-2 shows the variation of this measure with the operating conditions in the batch evaporative crystallizer. The numerical data are given in Appendix III.

Similar results (Fig 6-3) are obtained if the mean inclusion size is

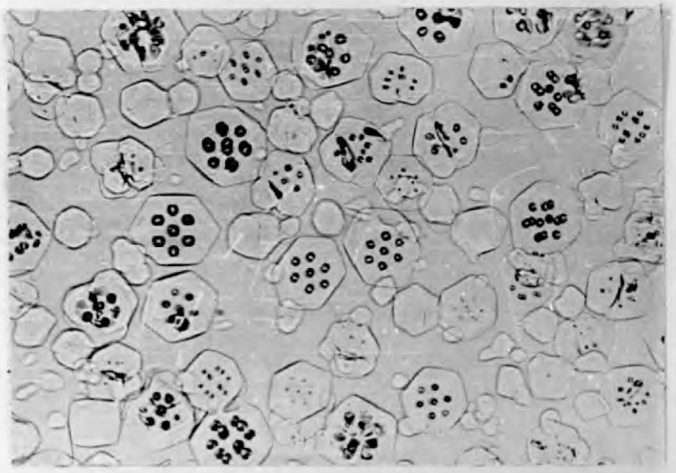

BATCH No. 34

BATCH No. 36

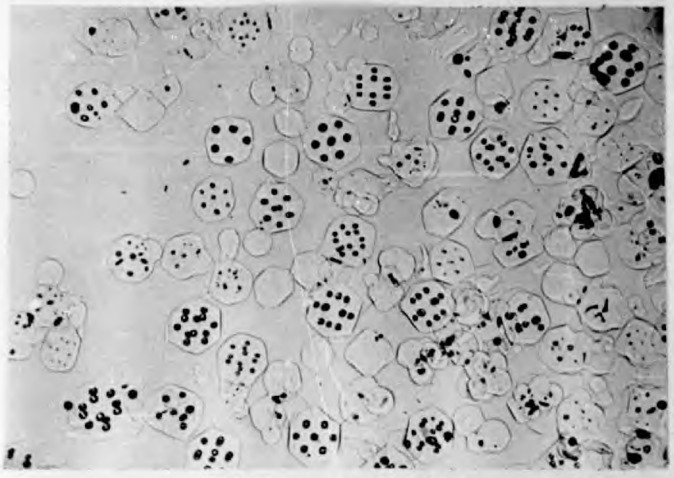

BATCH No. 38

BATCH No. 41

FIG. 6-1. TYPICAL CRYSTAL SAMPLES FROM THE BATCH EVAPORATIVE CRYSTALLIZER. [x 50]

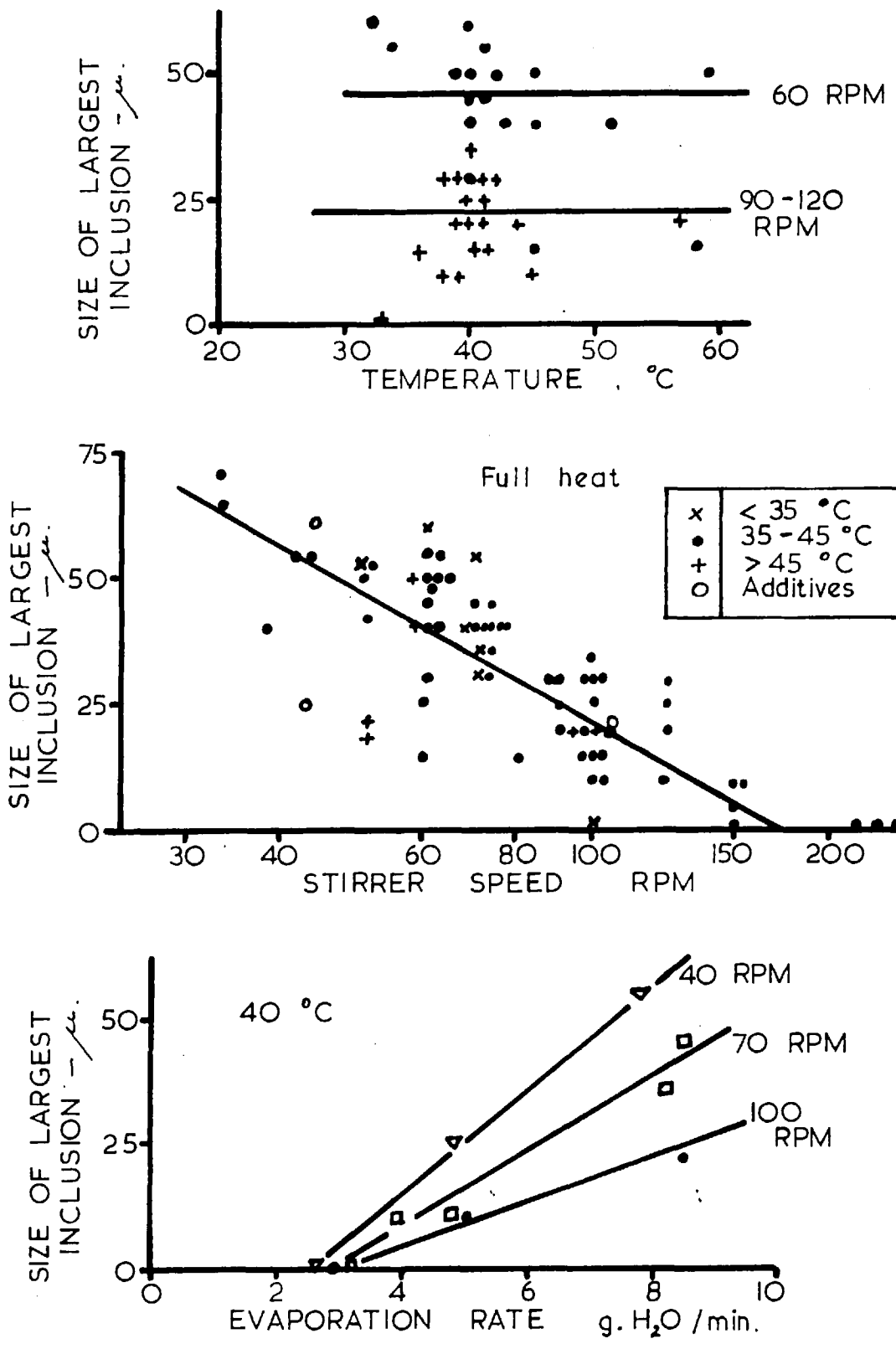

FIG. 6-2. EFFECT OF CRYSTALLIZER VARIABLES ON SIZE OF LARGEST INCLUSIONS.

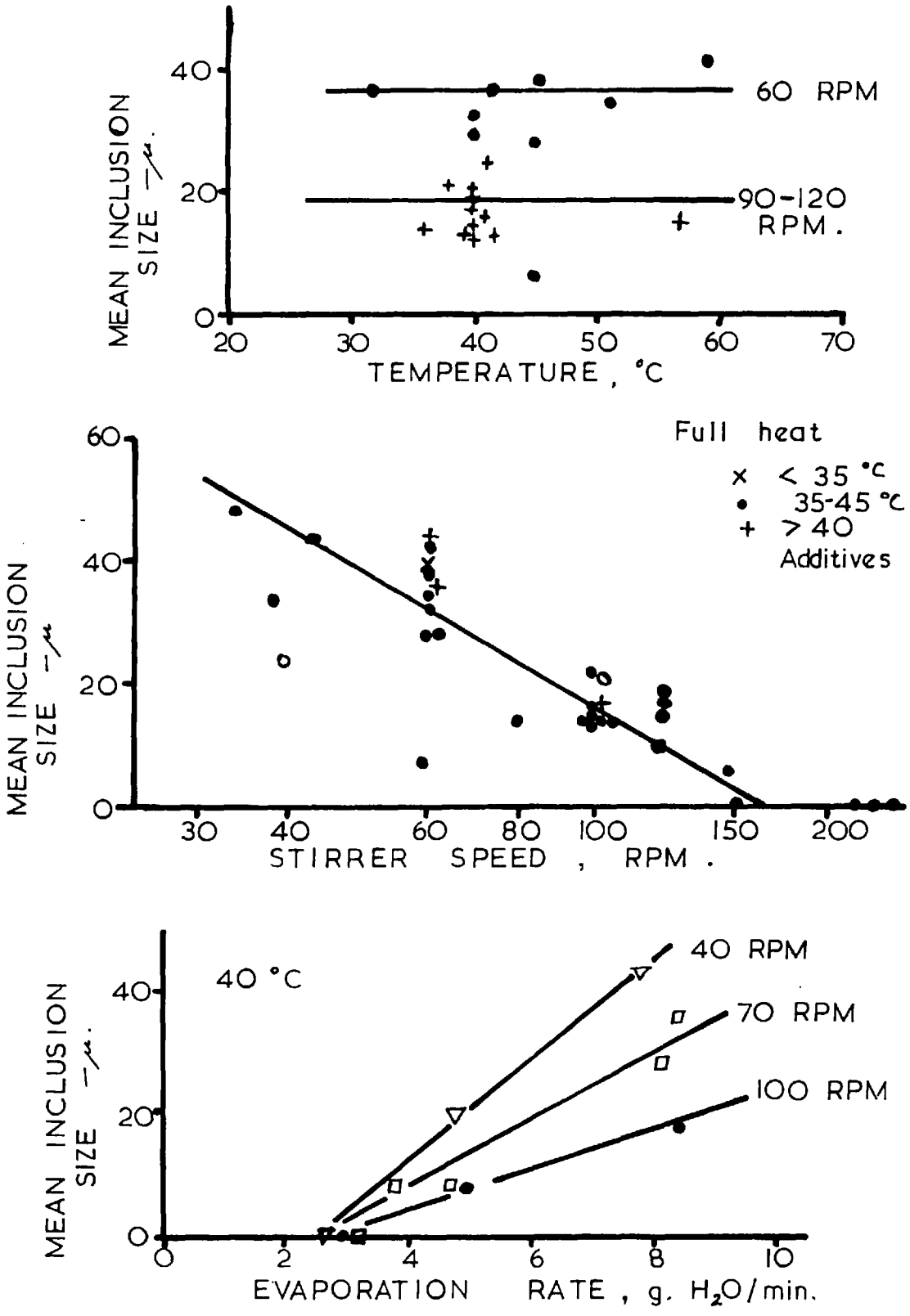

FIG. 6-3. EFFECT OF CRYSTALLIZER OPERATING VARIABLES ON MEAN SIZE OF INCLUSION FORMED.

used. The mean based on a volumetric basis can be computed from the size distribution of inclusions (refer Appendix II and Appendix III).

6.4 VARIATION OF SIZE WITH OPERATING CONDITIONS

An examination of Fig 6-2 and 6-3 would indicate the following observations :-

(i) There is a definite variation of inclusion size with agitation speed. An increased stirrer speed gives smaller inclusions in the batch.

(ii) There is a marked trend with evaporation rate. Batches with lower heating rates give smaller inclusions.

(iii) Within the scatter of the experimental results, operating temperature has no effect on the inclusion size.

(iv) Differing feed stocks used have no marked effect on the size of inclusion produced.

(v) There is considerable scatter in the data. The error in measurement would be less than $\pm$ 5μ for the mean inclusion size and $\pm$ 10 μ for the size of the largest inclusion. The scatter is greater than this.

6-5 DISCUSSION OF RESULTS

Since the scatter of the data is considerably larger than that expected from errors of measurement, some must result from variations in the crystallization process itself. Even when feeds from the same stock are used under identical conditions in consecutive runs, large variations in the size of the inclusions are observed. It will be shown later that the size of inclusion is governed by the extent of nucleation in the batch. Nucleation is an inherently variable phenomenon, and this is

undoubtedly a cause of scatter in the above results.

The results presented above are quite likely to depend on the crystallizing apparatus used. Quite different results would probably have been obtained if a different design of crystallizer or type of agitation had been used. Perhaps the same general trend of variation with batch operating conditions would exist, but without experimental confirmation this remains an assumption.

Thus the direct application of these results to full scale plant, the 'scale up' of the data, is likely to be a difficult task. An easier means of applying these results might be to consider the basic mechanism by which these inclusions form and apply the knowledge of this mechanism to other plant. If the mechanism involves nucleation and growth, at least these are phenomena about which a great body of experience and knowledge has accumulated.

Any proposed mechanism of formation must, of course, be able to interpret the results given in this chapter.

7. THE FORMATION OF 'FACE' INCLUSION PATTERNS IN HEXAMINE

7.1 INTRODUCTION

Hexamine crystals containing 'face' patterns of inclusions can be prepared by the batchwise growth of crystals. The operating conditions of the crystallizer which favour inclusion formation have been determined (Ch. 6). In this chapter consideration will be given to the mechanisms by which these inclusions form. This process will be examined first in a qualitative manner and then quantitative measurements will be described.

7.2 THE MECHANISM OF GROWTH

The formation of these inclusions is a crystal growth phenomenon, in particular, it is a phenomenon associated with rapid crystal growth. Crystals observed growing in the heated cell under the microscope demonstrate this. The fast growing crystals form inclusions, the slow growing ones do not.

Inclusions are formed under conditions of rapid growth in the following manner; at first, while very small, the hexamine crystal grows with plane faces. At a certain stage, suddenly the edges of the crystal begin to grow more rapidly than the rest and hollows are formed at the centre of each face. As this preferential growth at the edges continues, the hollows in the faces become large cavities sinking from the faces into the depths of the crystal. At a later stage the surfaces of the crystal may seal over giving plane faces again and thus trapping within the crystal the sealed cavities of included mother liquor. As crystal growth continues, the included liquor is left further and further behind in the bulk of the crystal. At formation, the inclusions have the shape of the original cavities, but after

a time the surfaces of the inclusions rearrange by dissolution and recrystallization to give the regular form of a negative crystal. When the crystal is grown under fairly uniform conditions, each face behaves similarly and a regular pattern of inclusions is obtained.

The appearance of the crystal at the stage when there is a large cavity in the centre of each face is illustrated in Fig. 7-1 to 7-3. The crystals shown were selected from samples taken at the initial stages of various batch crystallizations. In Fig. 7-1 the crystals are immersed in aniline. Patterns resulting from the alignment of the cavities are observed readily and may be compared with a plastic model with cavities on each face. The external appearance of the crystal can be seen when the crystal is immersed in paraffin (Fig 7-2).

That the cavities contained mother liquor can be seen from the crystals photographed in Fig 7-3. Mother liquor, which takes some little time to mix with the aniline, appears as dark spheres in many of the cavities. These spheres sink when released from the cavity, demonstrating that they are not gas bubbles. The shape of the cavity is clearly outlined in crystals which have just sealed over (Fig. 7-4).

The various stages in the pattern of formation of inclusions can also be seen from the series of photographs of samples taken from the evaporative crystallizer (Fig 7-13 to 7-15). These samples are to be analysed in detail later.

7.3 TERMINOLOGY

A term is required to describe the form of a crystal at the stage where preferential growth has occurred at the edges leaving cavities in the crystal faces.

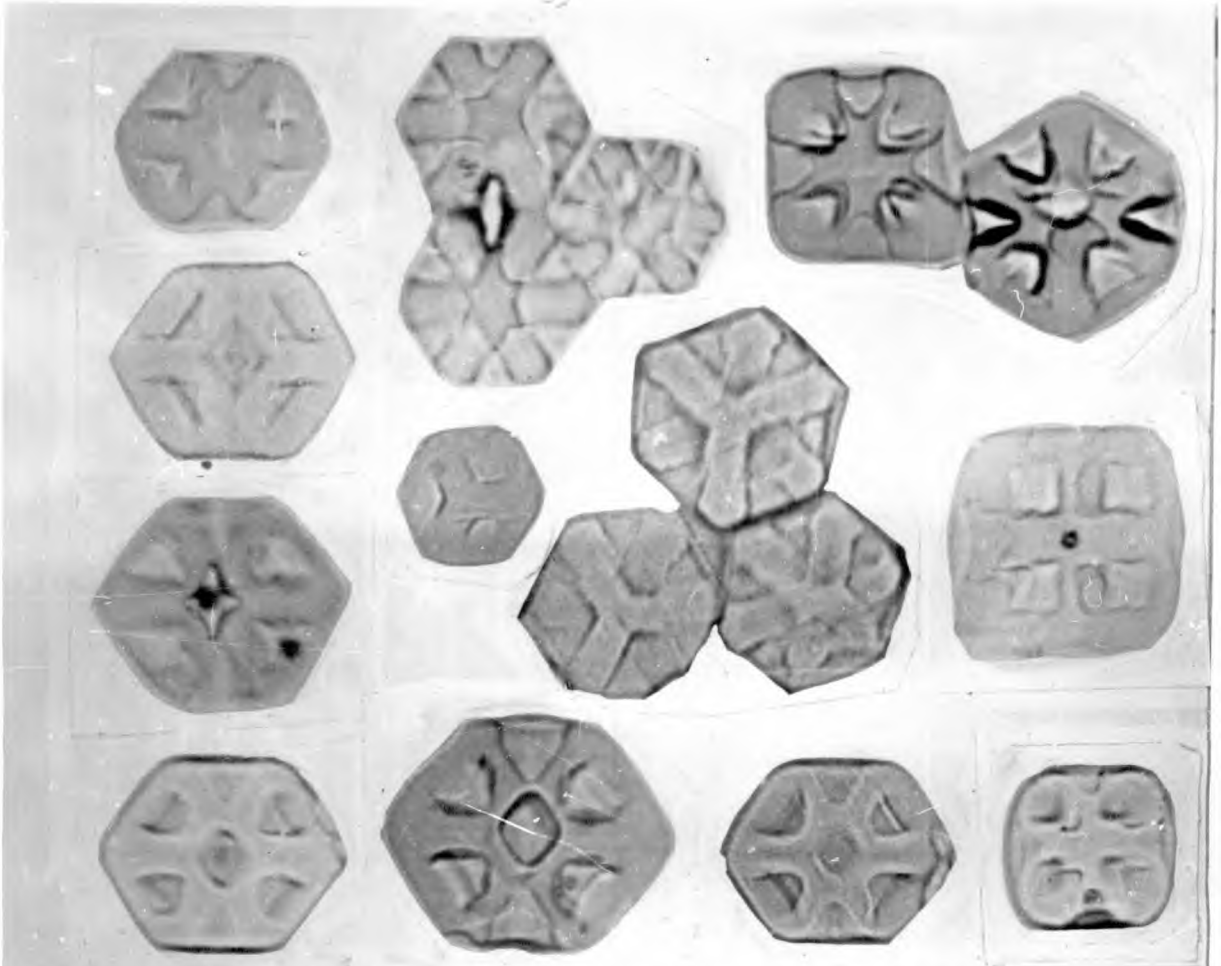

PHOTOGRAPHS OF HEXAMINE CRYSTALS AT 'FACE CAVITIES' STAGE OF GROWTH. [x 200]
[Immersion fluid :— Aniline]

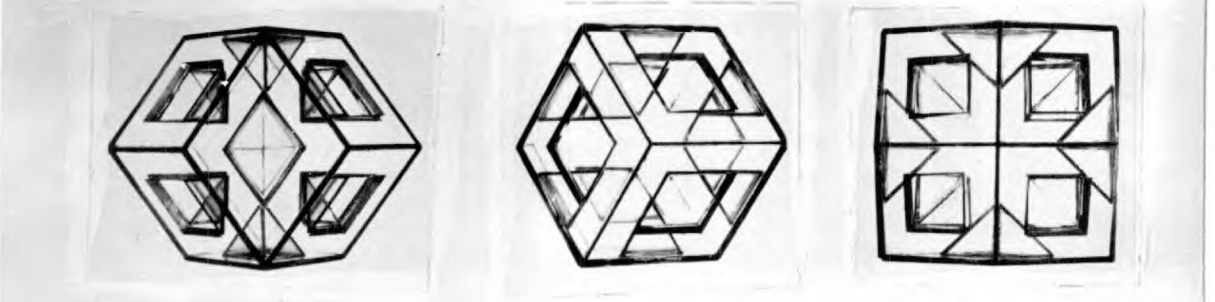

PHOTOGRAPHS OF PERSPEX MODEL

FIG. 7-1. COMPARISON OF THE PERSPEX MODEL WITH HEXAMINE CRYSTALS HAVING INCLUSION CAVITIES.

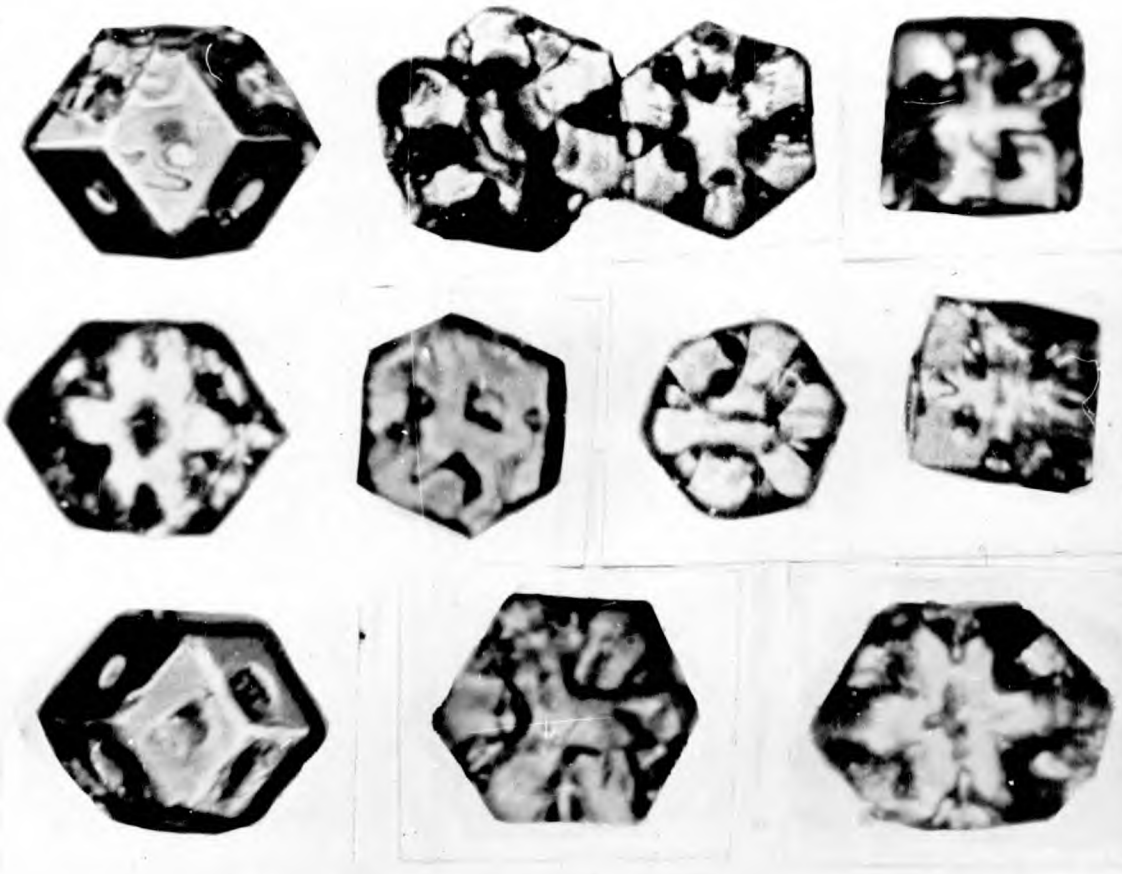

PHOTOGRAPHS OF HEXAMINE CRYSTALS AT 'FACE CAVITIES' STAGE OF GROWTH.
[Immersion fluid :- Paraffin]
[x 200]

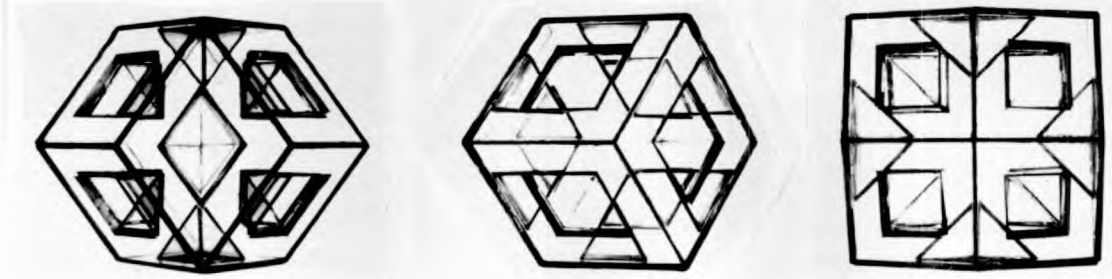

PHOTOGRAPHS OF PERSPEX MODEL.

FIG. 7-2. COMPARISON OF THE PERSPEX MODEL WITH HEXAMINE CRYSTALS HAVING INCLUSION CAVITIES.

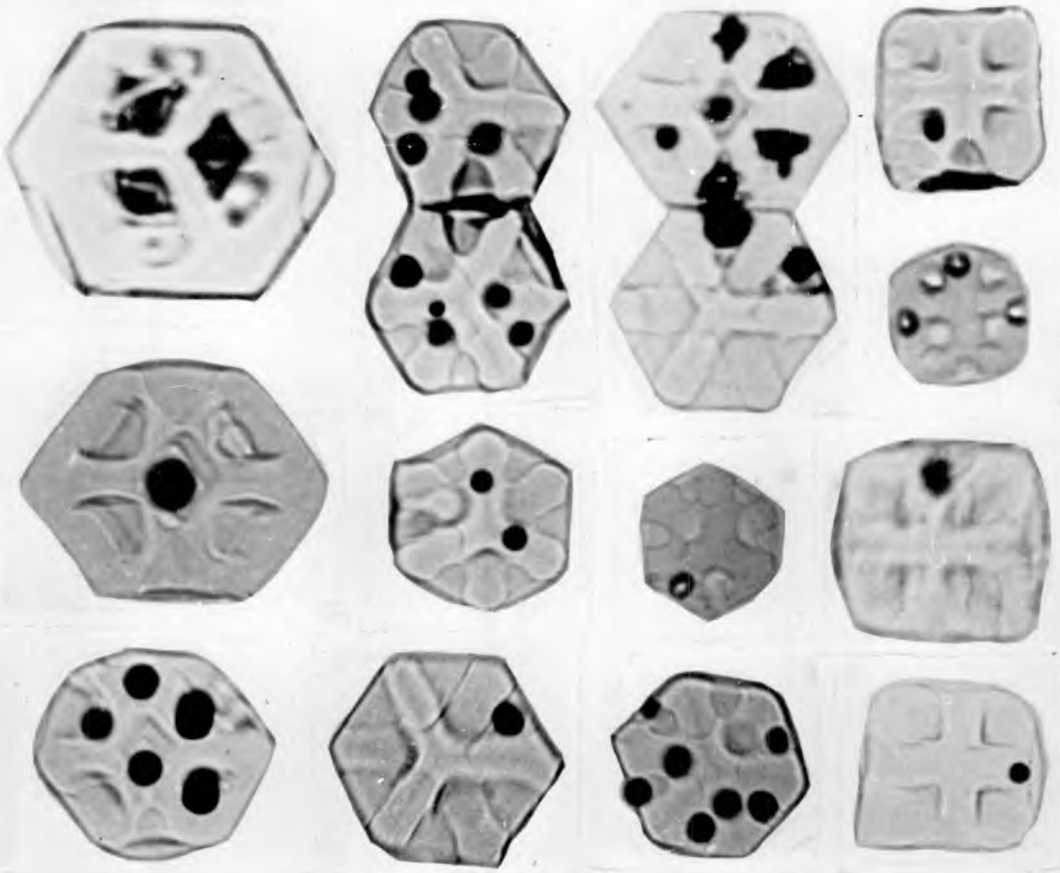

PHOTOGRAPHS OF HEXAMINE CRYSTALS AT 'FACE CAVITIES' STAGE OF GROWTH. Some mother liquor (the black spots) is still retained in the cavities.)
[Immersion fluid :— Aniline] [x 200]

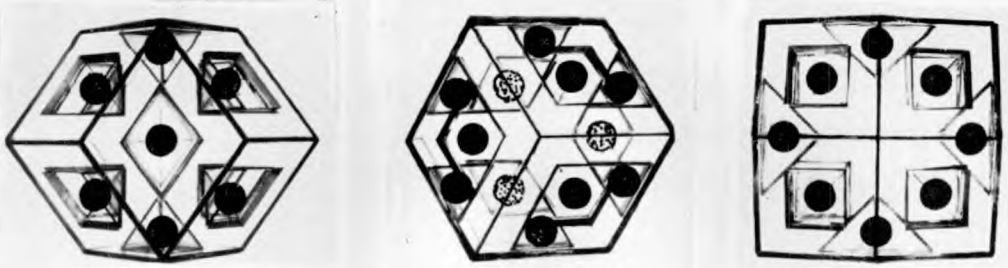

PHOTOGRAPHS OF PERSPEX MODEL

FIG. 7-3. COMPARISON OF THE PERSPEX MODEL WITH HEXAMINE CRYSTALS HAVING INCLUSION CAVITIES.

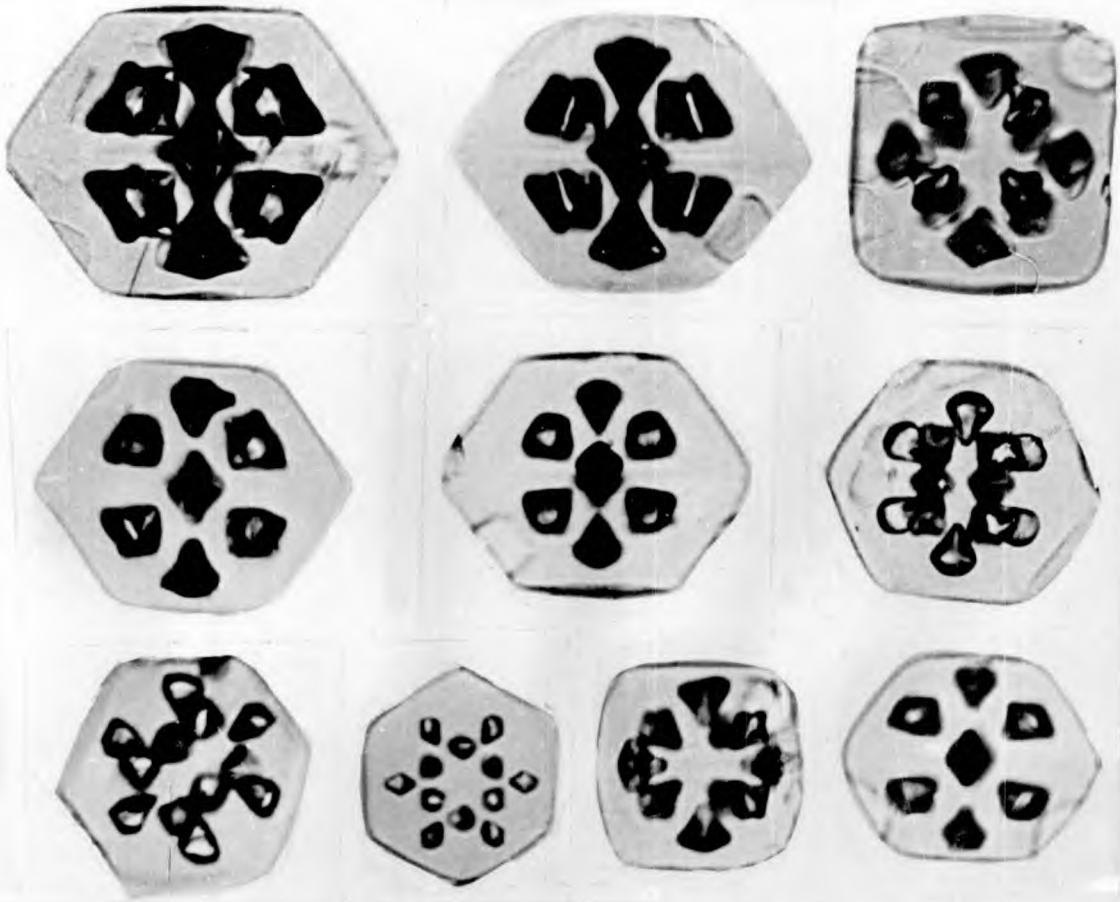

PHOTOGRAPHS OF HEXAMINE CRYSTALS HAVING INCLUSIONS. (Taken soon after formation). [x 200]
[Immersion fluid :— Aniline]

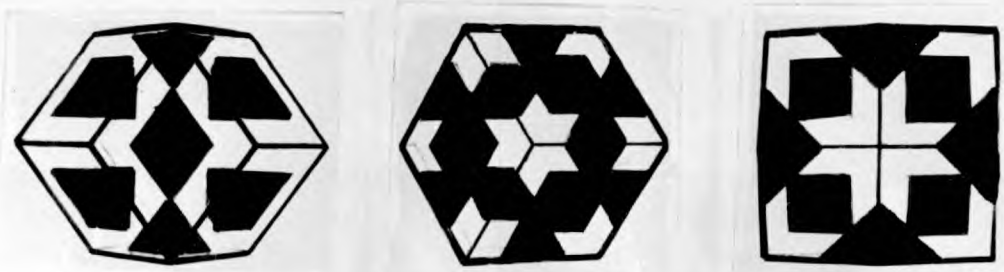

PHOTOGRAPHS OF PERSPEX MODEL.

FIG. 7-4. COMPARISON OF THE SHAPE OF THE INCLUSIONS SOON AFTER FORMATION WITH THOSE IN THE MODEL.

There are certain similarities to the dendrite, although with a dendrite, preferential growth usually occurs at the corners or in selected directions. Also, the 'firtree' appearance is missing. The appearance is very like that of the 'hopper crystal' (Fig 7-5) shown by Phillips [27]. The term 'hopper crystal' is often taken to refer to a crystal with a cavity in one face only, such as that shown in Fig 7-6. Such crystals are formed by starving one face of supersaturated solution, either by floating it face upward on the surface of the solution or by bearing the crystal face against a solid surface.

To avoid any ambiguity, the term 'cavitite' has been introduced to describe this form of crystal with cavities in all faces.

7.4 SHAPE OF CAVITIES

At the cavitite stage of growth the cavities in hexamine crystals have the shape of rhombic pyramids. That is, the cavity has tapering walls and a diamond shaped cross-section at the surface (Fig. 7-7).

This shape can be seen in Fig 7-1 to 7-4, where comparison is made with a model of a rhombic dodecahedron constructed of 'Perspex' acrylic sheet. The cavities in the model are built as rhombic pyramids tapered in such a way that the tapering faces of the cavities are parallel to dodecahedral faces (i.e. are also $\{011\}$ faces). The patterns found by rotating the model (Fig 7-1 to 7-4) reproduce the observed patterns in the crystal, indicating that this description of the shape is correct.

Because of the shape of the cavities, the width of the face remaining either side of the cavity must remain constant as the crystal and the cavity grow. That is, the edges of the crystal grow as parallel faced walls of constant thickness. This is observed to be so. Measurements

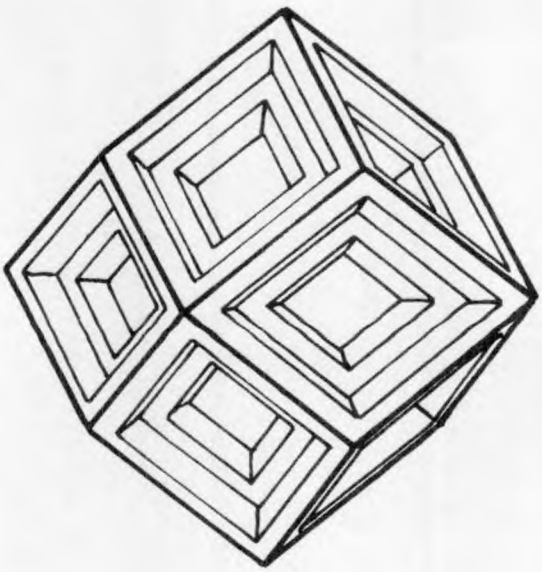

FIG. 7-5. 'HOPPER' DEVELOPMENT OF A RHOMBIC DODECAHEDRON. (Taken from PHILLIPS [27]).

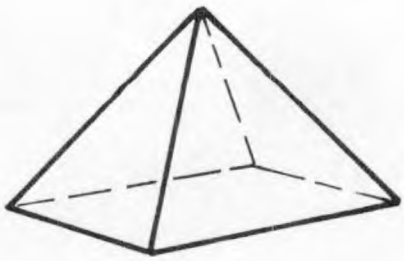

FIG. 7-7. SHAPE OF INCLUSIONS IN HEXAMINE.

FIG. 7-6. PHOTOGRAPH OF HOPPER HEXAMINE .CRYSTAL. [× 2]

show this residual face width to be between 15μ and 25μ for all crystals.

The shape of the base of the inclusion when the cavity seals over is more or less flat with a central depression. The shape depends on the means by which the plane face re-established itself.

7.5 INCLUSIONS IN LARGEST CRYSTALS

It has already been observed (section 6.2) that in batches of hexamine crystals containing inclusions, the inclusions occur only in the largest crystals. This observation is true for all the batches of crystals grown. It is confirmed by measurement of the size distributions for all the crystals in a sample, and for those with inclusions. Typical size distribution histograms are shown in Fig 7-8. It can be seen that all the crystals with inclusions lie at the largest crystal end of the histogram. Other histograms are shown later in Fig 7-16 to 7-18. The numerical data for all the batches are given in Appendix III.

7.6 RELATION BETWEEN SIZE OF INCLUSION AND CRYSTAL SIZE

That the longer size of inclusion is found in the largest crystals has already been noted (section 6.2) from a qualitative examination of the samples from the batch evaporative crystallizer. More detailed measurements will now be made.

7.6.1 Quantities Measured

For each crystal containing inclusions in a sample the following quantities were measured :

(i) The size of the crystal, x_1. In all cases the size of crystal was measured as the perpendicular distance between any pair of parallel

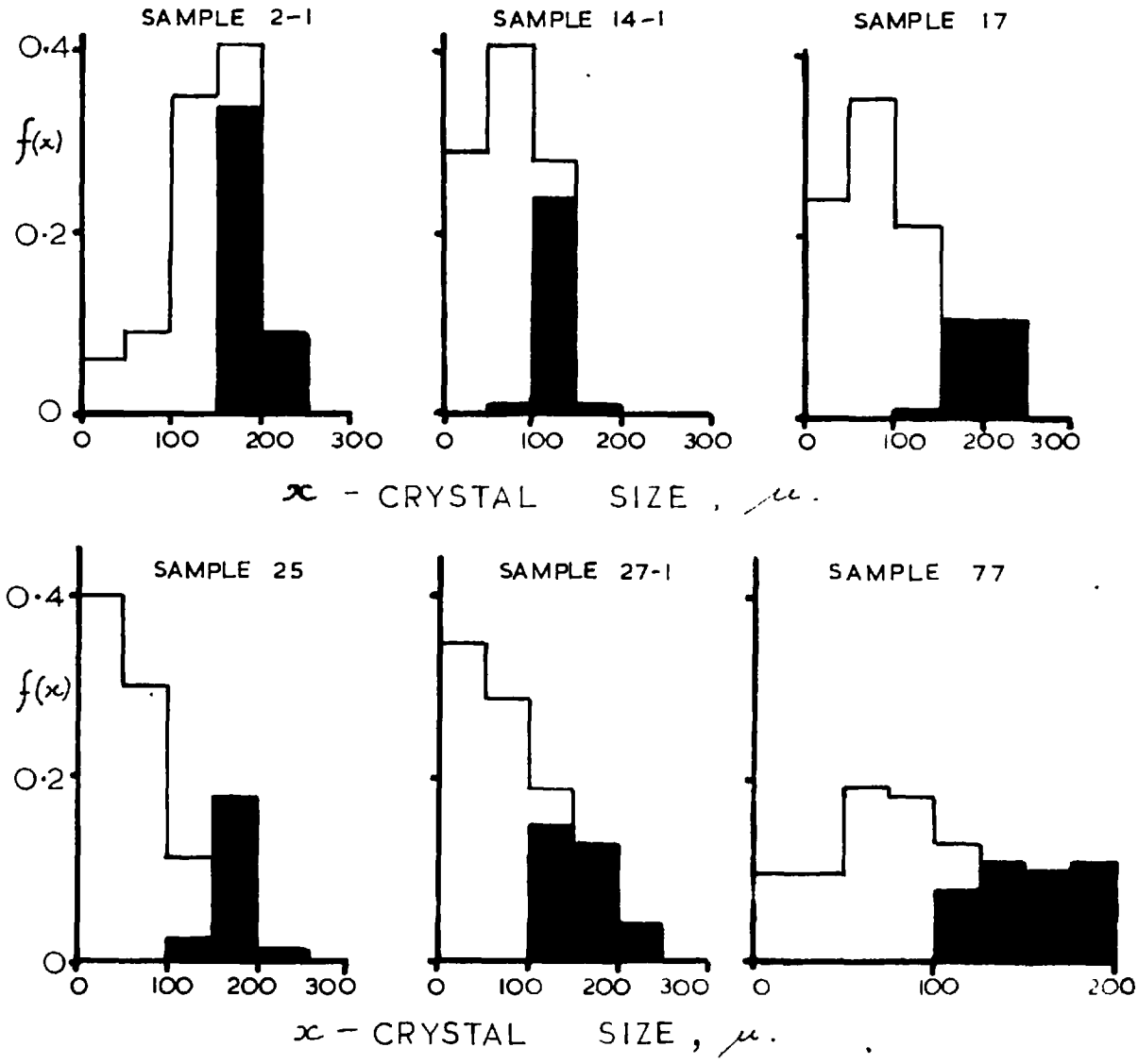

FIG. 7-8. TYPICAL CRYSTAL SIZE HISTOGRAMS.
(THE SHADED AREA REPRESENTS CRYSTALS WITH INCLUSIONS.)

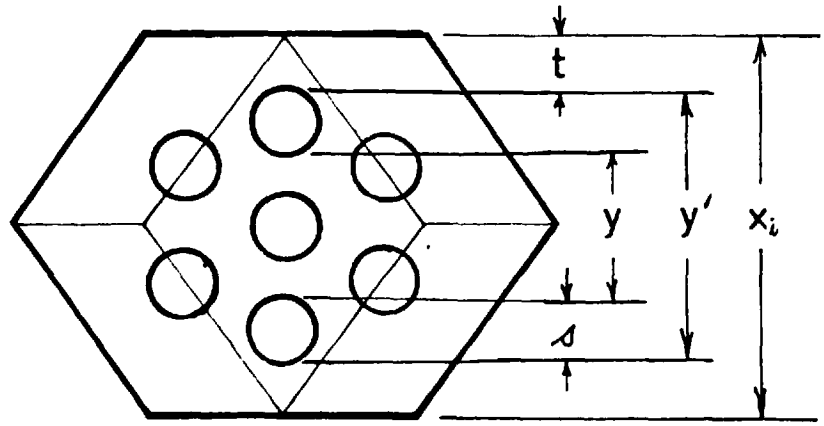

FIG. 7-9. MEASUREMENTS ON CRYSTAL.

faces. Most crystals observed lie on a face with one horizontal and four sloping faces showing, as in Fig 7-9. The two parallel faces between which measurement is made appear as the two more distant edges of the crystal.

(ii) The internal size of the pattern, y. This is the size of the crystal which just fits inside the inclusion pattern.

(iii) The outside size of the pattern, y'. This is the size of the crystal which would just contain the whole inclusion pattern.

(iv) The size of the inclusion, $s = (y'-y)/2$.

(v) The thickness of crystal covering the inclusion, $t = (x_i-y)/2$.

7.6.2 Results

Results for three samples are shown in Fig 7-10 to 7-12. These results are typical of all the samples analysed. Each figure shows a photograph of the sample analysed, an inclusion size distribution histogram, and plots of s, t, y and y' against the crystal size x_i. Analysis of these plots leads to several very important conclusions.

7.6.3 Internal Pattern Size - "Critical Crystal Size"

It can be seen that within the limits of experimental measurement, all crystals in each batch have the same internal size of inclusion pattern, y. This internal pattern size is unaffected by the size of crystal or the size of the inclusion. This is true for all the samples analysed.

Presumably, the larger and the smaller crystals have been growing for different lengths of time under different growth conditions, yet the inclusions are initiated at the same crystal size in all cases. This suggests that there is a 'critical crystal size' below which inclusions do not form. Only when crystals reach this size do inclusions have a chance of

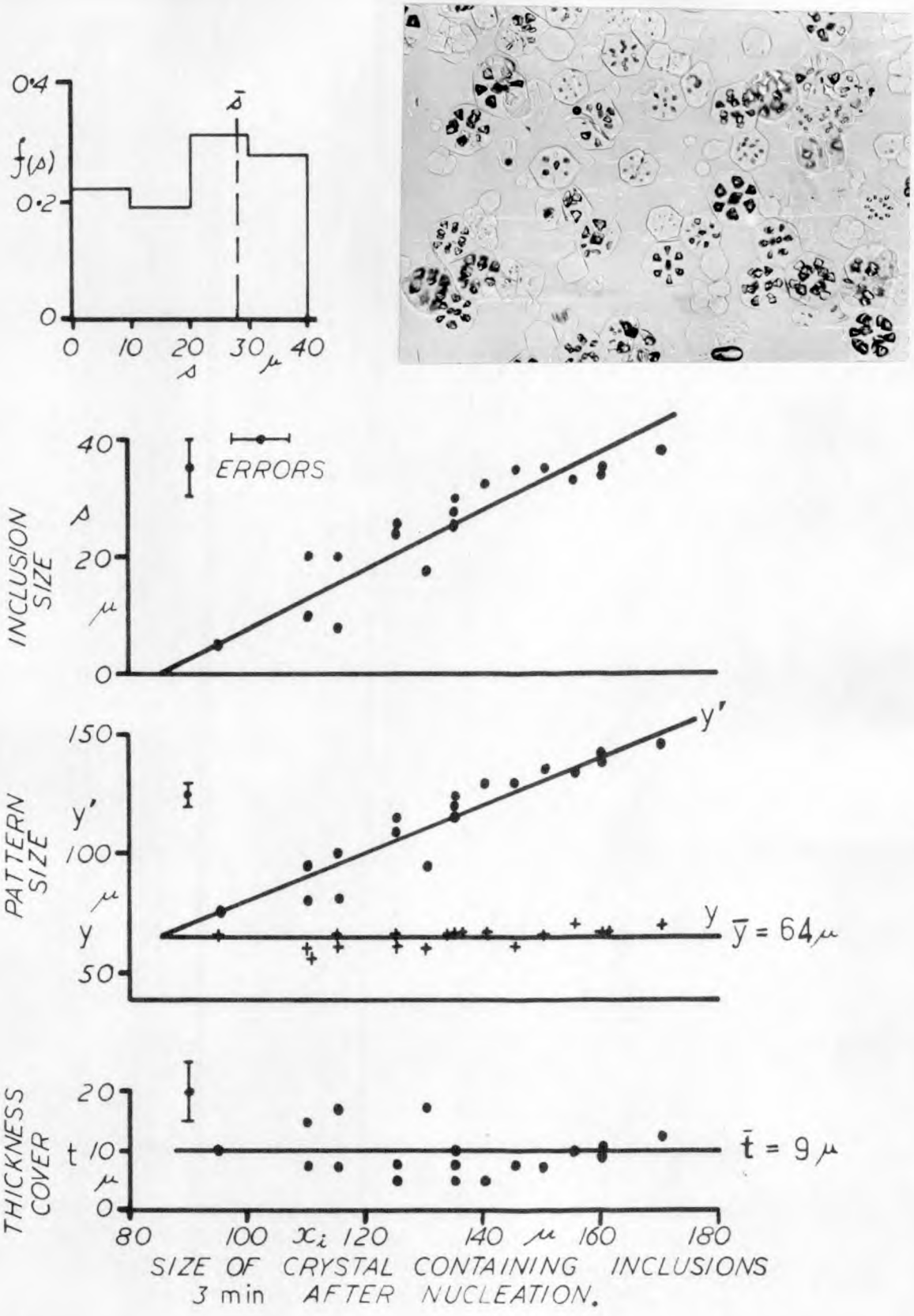

FIG. 7-10. SIZE OF INCLUSIONS AND INCLUSION PATTERNS
BATCH No 37. [60 RPM , 40 °C , Full heat.]
(Analysis of sample 3 min. after nucleation.)

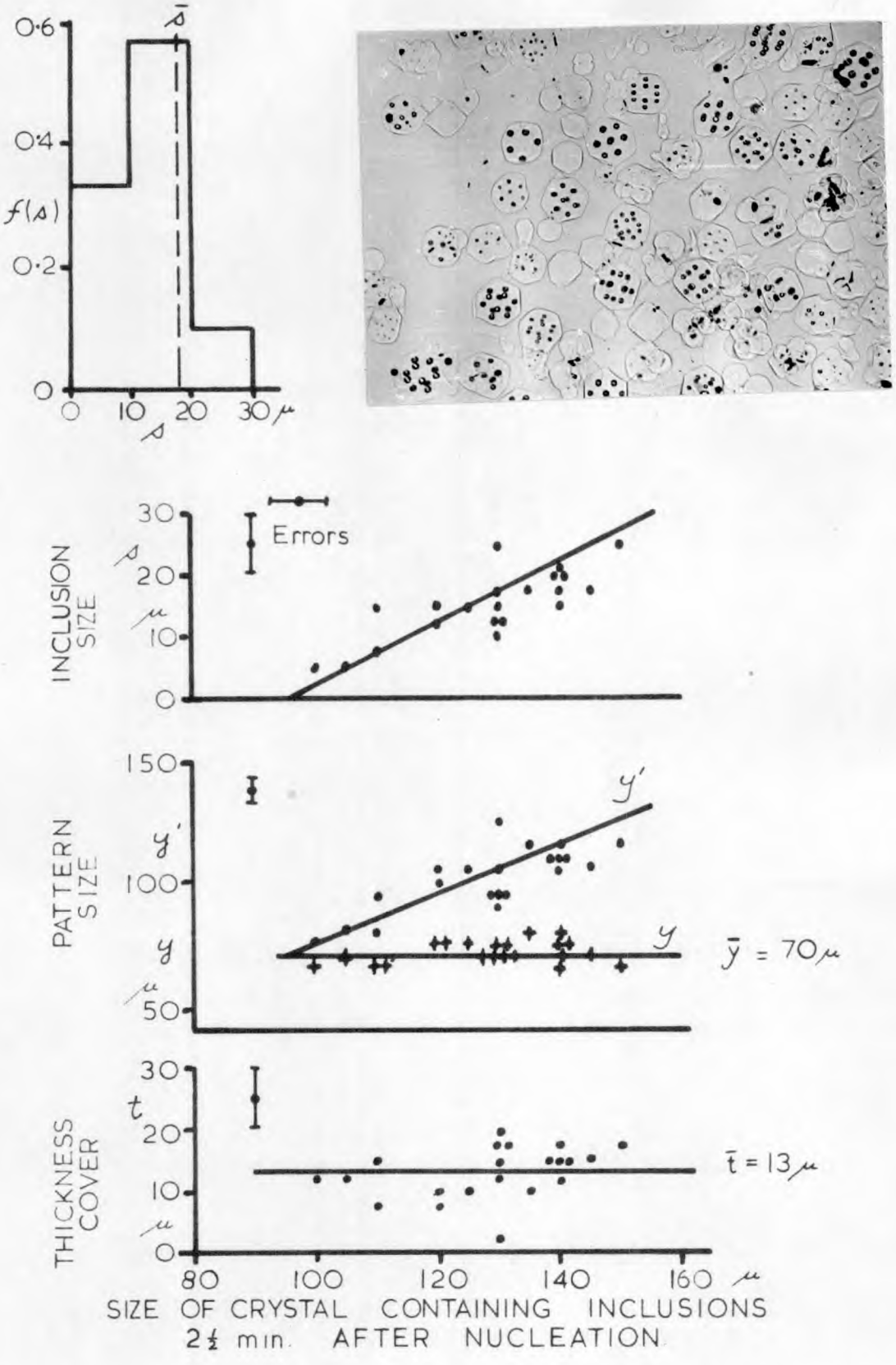

FIG. 7-11. SIZE OF INCLUSIONS AND INCLUSION PATTERNS
BATCH No. 38. [100 RPM, 40 °C, Full heat.]
(Analysis of sample 2½ min. after nucleation)

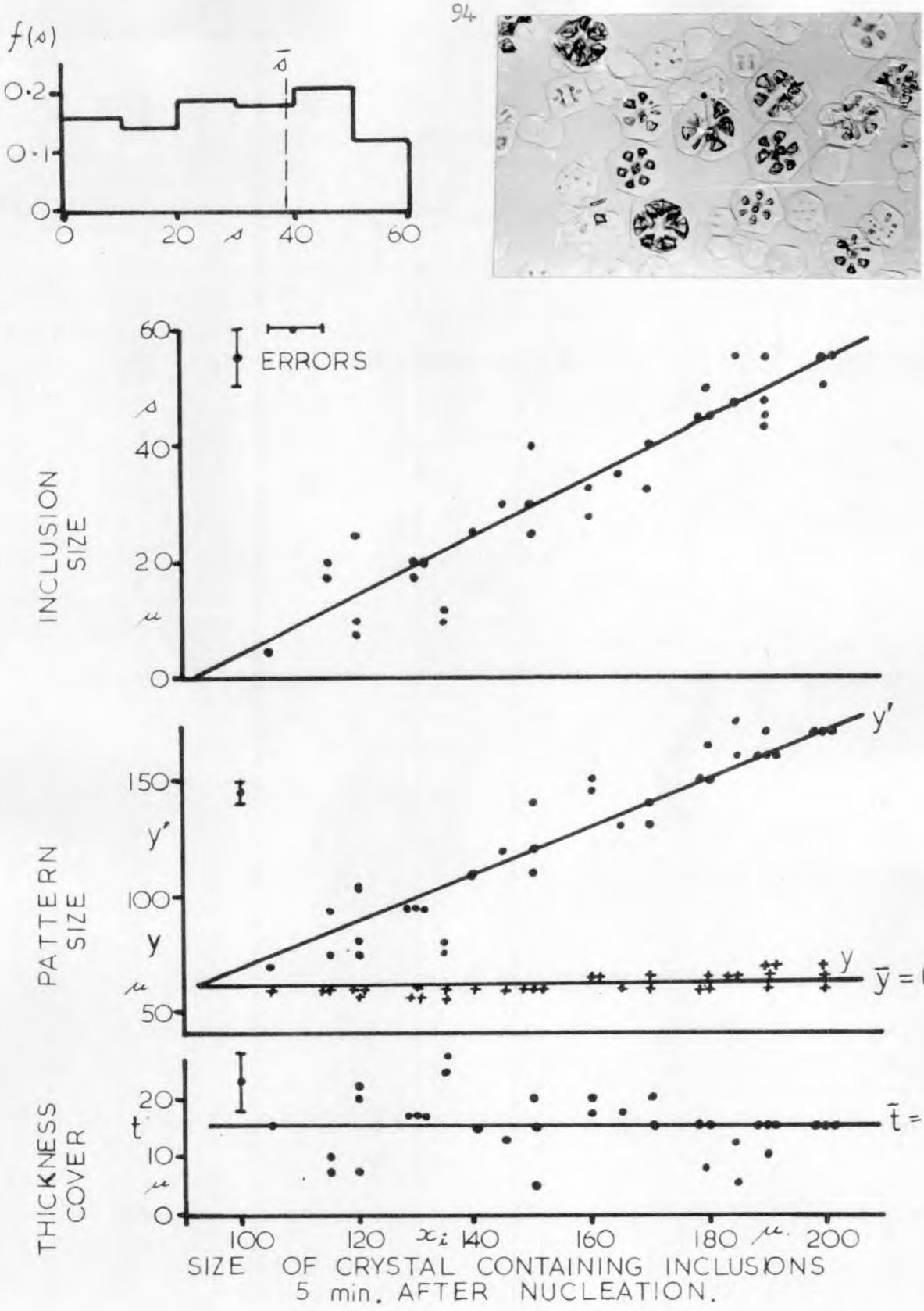

FIG. 7-12. SIZE OF INCLUSIONS AND INCLUSION PATTERNS.
BATCH No. 77. [60 RPM, 40 °C, Full heat.]
(Analysis of sample 5 min. after nucleation.)

forming.

Within the accuracy of measurement, this value is the same for all batches of hexamine crystals. The mean internal pattern size, $\bar{y}$, the 'critical crystal size', lies in the range 55 to 75μ for all batches despite the wide range of conditions and feedstocks used. (Detailed data are given in Tables IIIC in Appendix III.)

Measurements have been made of the thickness of the growing edges of cavitites (section 7.4). These values are in agreement with cavity formation on an initial crystal of this critical size.

7.6.4 Thickness of Cover - "Critical Growth Rate"

There is no measurable difference between the thickness of the cover, t, over the large and the smaller inclusions in the same sample (see Fig 7-10 to 7-12), although there is some scatter. This is true for all samples.

Thus, at the time of sampling, all inclusions have the same thickness of covering crystal. If therefore it is assumed that all the crystals in the batch grow at much the same rate at the one instant, then all the inclusions must have sealed over at the same time. That is, they all sealed over under the same critical growth conditions.

The average crystal growth rate decreases as crystallization of the batch proceeds, since the solvent is being evaporated at a constant rate while the amount of crystal surface increases. Since this quantity varies it may be convenient to specify the critical growth conditions by a 'critical growth rate'. This is the average growth rate at the moment when all inclusions seal over. Once the growth rate falls to this value inclusions will cease growing.

As well as being the critical rate at which the inclusions seal over, it is also the critical rate at which inclusions stop forming. This must be so, since inclusions do not form below this rate, yet form at all rates above. This can be seen from Fig. 7-10 to 7-12, which show a full range of inclusion sizes down to the very smallest. Thus inclusion formation must have begun at all times prior to the time of sealing, that is, at all growth rates down to the critical.

Hence the results would suggest that there is a critical growth rate for inclusion formation. Once the crystals are larger than a certain critical size, inclusions will form for all growth rates above the critical. Inclusions will stop growing once the growth rate falls below the critical.

7.6.5 Size of Inclusions

It is seen that both the internal pattern size, y, and the thickness of crystal cover, t, are constant for any sample of crystal. It therefore follows that the size of the inclusion, s, varies linearly with the crystal size x_1 by the reation

$$s = \frac{1}{2}(x_1 - y) - t$$

This relation using the mean values, $\bar{y}$ and $\bar{t}$ is shown in Fig 7-10 to 7-12. The data fit closely to it.

It also follows that the outside pattern size y' is given by $y' = x_1 - 2t$ and this is also confirmed by the plots.

7.6.6 Scatter of Results

Measurement errors, which are of the order of $\pm$ 5μ, account for some of the scatter of results. However, there are also small variations within the crystals themselves, possibly caused by variations in the growth

conditions in the crystallizer. In what follows, the mean behaviour in the usual statistical sense will be considered. Samples with large numbers of crystals will be analysed and mean quantities measured. When dealing with single crystals, allowance should be made for the slight fluctuations associated with individual crystals.

7.6.7 Details of Mechanism of Inclusion Formation

The deductions given above are vital to this thesis. If true, they allow the following explanation of the growth of face inclusions to be made.

In a batch crystallization there is an initial shower of crystal nuclei followed by further continuous nuclei formation. These nuclei grow with plane faces until each reaches the critical crystal size, when, if the growth rate is above the critical growth rate, inclusions will form. These inclusions will keep growing so long as the growth rate is maintained above the critical. Also, inclusions will keep forming as further crystals reach the critical size. Once the growth rate drops below the critical, all inclusions begin to seal over and no further inclusions are formed. Further growth just increases the thickness of crystal covering the inclusions. It should be noted that a variation of growth rate is required. The growth rate must first be above the critical value then fall below it. If the growth rate were maintained always above the critical value, an enormous cavitite with large open cavities would be obtained.

When the inclusions are growing they have the shape of rhombic pyramids, while the cavitite edges of the crystal grow as parallel walls of a constant width related to the critical size of crystal.

7.7 CRITICAL CRYSTAL SIZE AND CRITICAL GROWTH RATE

The formation of inclusions may be interpreted in terms of a critical crystal size, and certain critical growth conditions which have been represented by a critical growth rate.

It has been seen that the critical crystal size has the same value for all the batches of hexamine crystals grown. This value may be taken to be 65 $\pm$ 5u.

Whether the critical growth rate is a suitable expression for the growth conditions, and whether it varies with the operating conditions for each batch, has yet to be considered. To measure the variation of growth rate with time, a series of consecutive samples from the same batch must be analysed.

7.8 ANALYSIS OF CONSECUTIVE SAMPLES

For several of the batches, samples were taken consecutively during crystallization. An analysis of these samples will show how the growth rate, nucleation rate, and other conditions vary with the time of nucleation.

7.8.1 Quantities Measured

For each series of samples the following quantities were measured -

(i) The operating conditions of the crystallizer and the times after nucleation at which samples were taken.

(ii) The size distributions of crystals and inclusions in the samples, f (x) and f (s). These are expressed as the fraction of the total number in the indicated size range.

(iii) the fraction of the total number of crystals that contain inclusions, β.

(iv) The mean internal pattern size, $\bar{y}$ and the mean thickness of cover, $\bar{t}$, for the first sample taken after all the inclusions have sealed over.

7.8.2 Computed Quantities

From the quantities measured, the following quantities were computed. A detailed example of these computations is shown in Appendix II.

(i) The mean crystal size of all crystals, $\bar{x}$. The mean is computed on a volume (or mass) basis.

(ii) The mean crystal size, on a volume basis of only those crystals with inclusions, $\bar{x}_i$. Where the batch had no crystals containing inclusions, the mean crystal size of a certain number of the largest crystals, $\bar{x}_1$, was computed.

(iii) The total number of crystals in the batch, n. This was computed from the mean crystal size and the total mass of crystal at that time.

(iv) The number of crystals with inclusions,, $n_i = \beta n$.

(v) The total surface area of crystal, A. This was computed from the total number of crystals and the mean crystal size, with a correction, α , applied for the crystal size distribution.

(vi) The fraction of the total volume of crystal contributed by those crystals with inclusions, γ_v , and the fraction of the total surface area contributed by those crystals with inclusions, γ_A .

(vii) The mean growth rate, R. This is the linear rate of advancement of each face. It has been calculated from the known mass rate of deposition of solid, and the total surface area. An alternative measure of the growth rate (designated R') can be made from the

increase in $\bar{x}_4$ over the time interval.

(viii) The mean inclusion size (on a volume basis) $\bar{s}$.

7.8.3 Assumptions

In the computation of the above quantities the following assumptions were made. These should be noted since the significance of the results may depend upon them.

(1) The sample is assumed to be representative of the crystal population at the time of sampling. It is assumed that there is no bias in the sampling procedure or in the method of analysis of the sample, and further, that the sample does not alter (e.g. by dissolution) on storage before analysis. Every effort was made to satisfy this assumption.

(2) Each crystal is assumed to grow equi-dimensionally, there being no excessive growth on a face in any preferred direction. An examination of the samples showed this assumption to be substantially true. Presumably the agitation rates used were sufficient for uniform growth conditions to prevail around each crystal.

(3) For computations the crystals were assumed to be solid hexamine. No correction was made for the volume of solution in inclusions or in the cavities of cavitites, the crystal size of which were measured across the outer edges. This gives rise to a small but definite error, which becomes of lesser importance once the inclusions are sealed over. At the worst, this error gives an underestimate of the total number of crystals of less than 5%.

(4) It is assumed that for computing crystal quantities changes in the supersaturation of the solution may be neglected. This means that the amount of crystal at any time can be related directly to the amount of

solvent evaporated. It would be expected that the solution decreases in supersaturation as crystallization proceeds, and that the largest changes are in the initial stages of crystallization. With hexamine solutions, the supersaturations are unlikely to be large and the changes are probably minor. Unfortunately supersaturations could not be measured directly.

(5) All crystals are assumed to grow at the same average rate over a period of time. This implies that the " ΔL Law" of McCabe [28] is applicable. It follows that each crystal will grow equidimensionally (see assumption 2), and further that all crystals experience the same growth. This would be so, if conditions throughout the crystallizer were uniform, and if any growth fluctuations on individual faces or crystals were on a rapid time scale. It is observed that the largest crystals in a batch (those with inclusions) remain the largest as crystallization proceeds, with no apparent broadening of the size range. This gives some experimental support for this assumption.

7.8.4 Results

Extended series of samples were taken from thirteen batches (Batches No. 11, 26, 36-42 and 67-70). The numerical quantities measured and computed for these batches are shown in special tables in Appendix IIID.

Results for four of these batches (Batches No. 37-40) will be presented in detail. All four batches used the same feedstock and, except for different stirrer speeds, identical operating conditions (40°C, full heating rate). Three of the batches had inclusions. The fourth (Batch No. 40) with the highest stirring speed (250 R.P.M.) had none.

Representative photographs of the samples from the three batches with

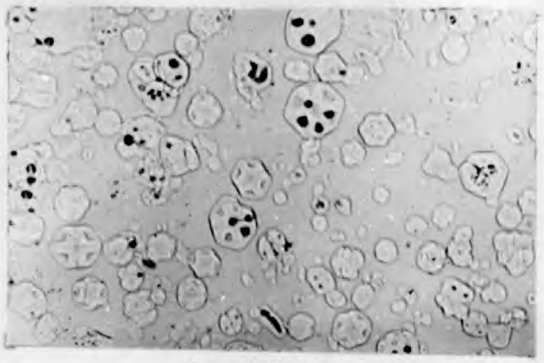

½ MIN.

4 MIN.

1 MIN.

5 MIN.

2 MIN.

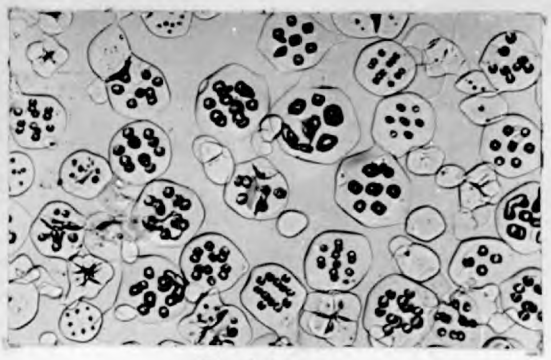

7 MIN.
(partly redissolved.)

3 MIN.

FIG. 7-13. GROWTH OF HEXAMINE CRYSTALS. BATCH No. 37
[60 RPM , 40 °C , Full heat .]

[X 50]

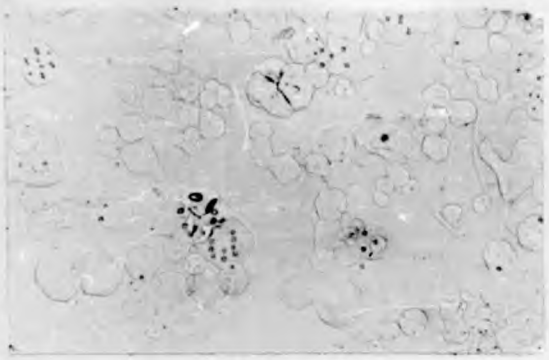

½ MIN.

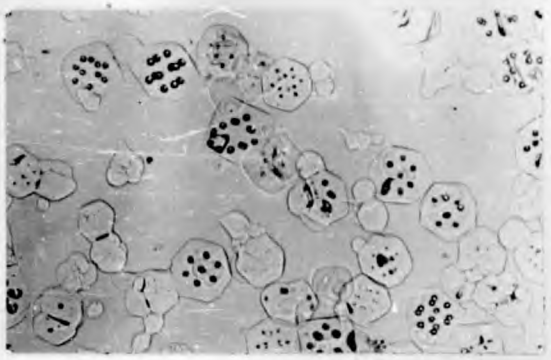

5 MIN.

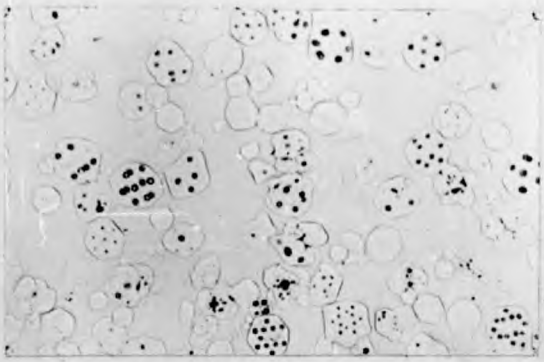

1½ MIN.

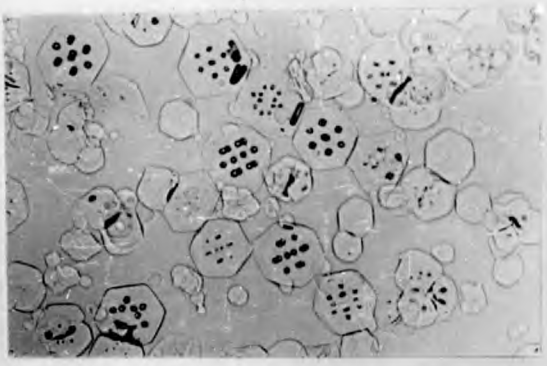

7 MIN.

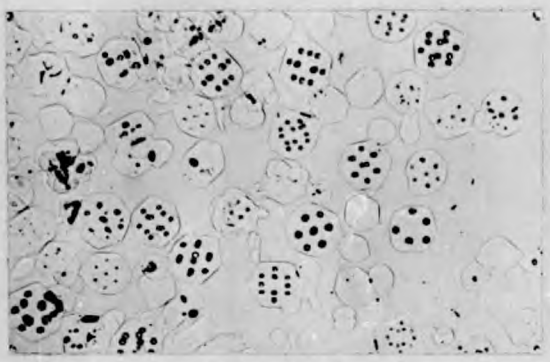

2½ MIN.

10 MIN.

3½ MIN.

FIG . 7-14.
GROWTH OF HEXAMINE CRYSTALS . BATCH No 38
[100 RPM , 40 °C , Full heat]

[x50]

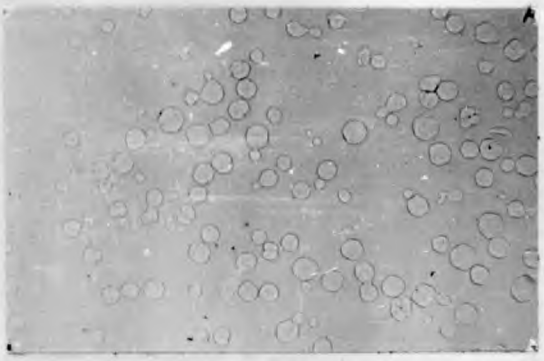

½ min.

6 min.

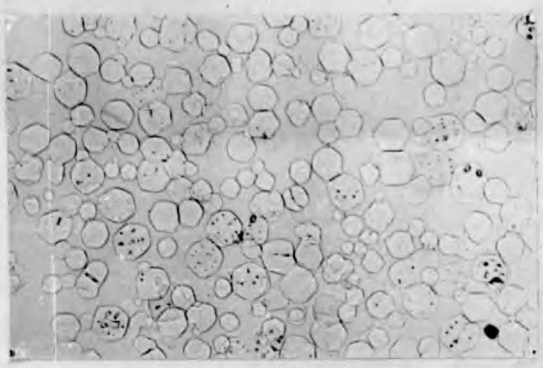

1½ min.

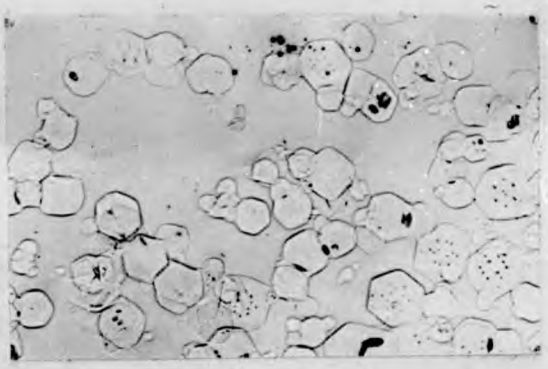

8 min.

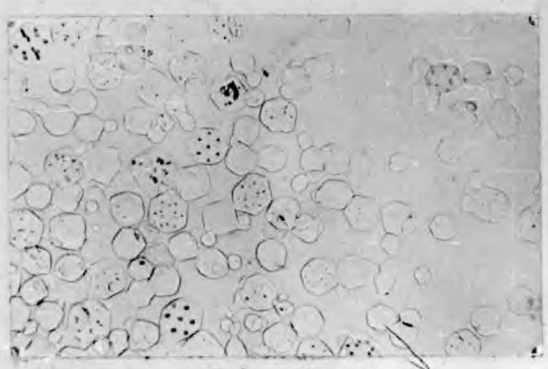

2½ min.

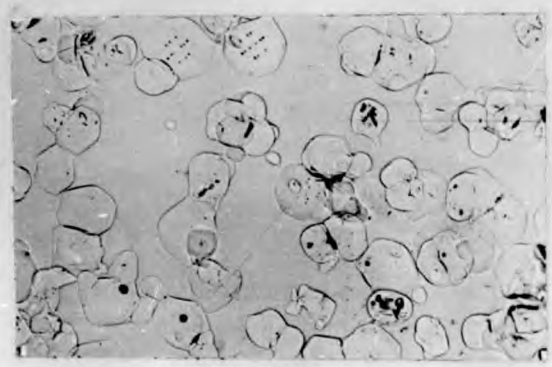

11 min.

4 min.

FIG. 7 - 15.
GROWTH OF HEXAMINE CRYSTALS.
Batch No 39
[150 RPM , 40°C , Full heat.]

[x 50]

inclusions are shown (Fig 7-13 to 7-15). The respective crystal size histograms are shown in Fig 7-16 to 7-18 while computed area and number quantities are given in Fig 7-19 to 7-21, and the growth rate values are shown in Fig 7-22 to 7-24. The corresponding quantities for the batch not giving inclusions (Batch No. 40) are shown as Fig 7-25 to 7-27.

7.8.5 Crystal Size

The various stages in the growth of crystals with inclusions can be seen from the photographs of samples (Fig 7-13 to 7-15) and may be compared to the normal growth of crystals without inclusions (Fig 7-25). The size distribution histograms (Fig. 7-16 to 7-18) give further illustration that only the larger crystals contain inclusions (refer section 7.5).

There are several sources of error in the measurement of the crystal size distribution. Some crystals lie with none of their faces perpendicular, making it difficult to measure "between parallel faces". Some, a small percentage, of the crystals appear as conglommerates. Further, it is often very difficult to see the very smallest crystals in the photographs. The number of crystals in the '< 50' range of the histograms has probably been considerably underestimated, but this does not make a very large contribution either to the total mass or the total surface area of the crystal batch, although it affects the total number of crystals.

In the duration of a batch, crystals up to several hundred microns in size were grown. Batches with higher stirring speeds generally gave smaller crystals.

If, after the initial nucleation, no further crystal nuclei were formed, the cube of the mean crystal size would vary linearly with crystallization time. The data does not follow such a relationship

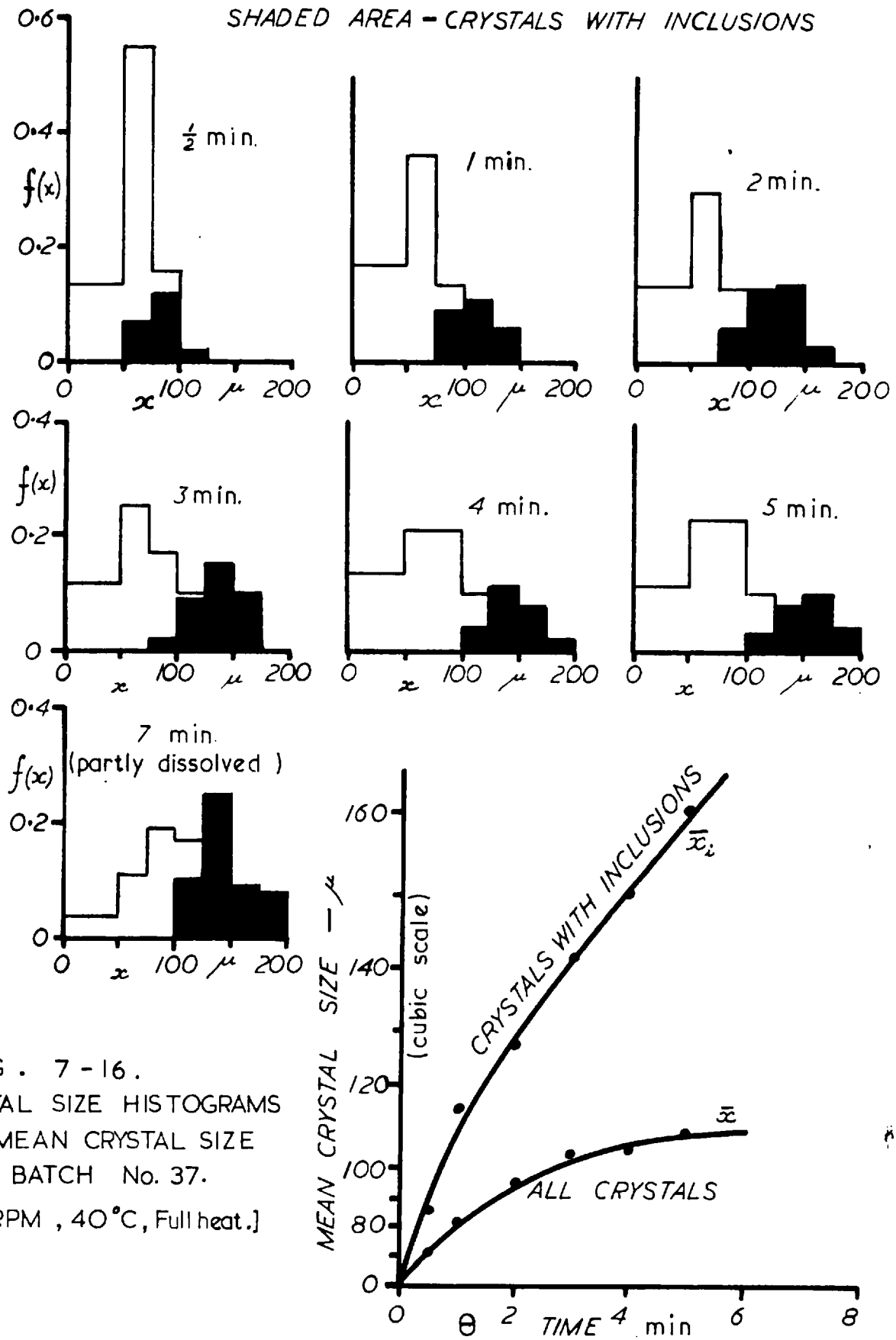

FIG. 7-16.
CRYSTAL SIZE HISTOGRAMS AND MEAN CRYSTAL SIZE FOR BATCH No. 37.
[60 RPM, 40°C, Full heat.]

SHADED AREA – CRYSTALS WITH INCLUSIONS

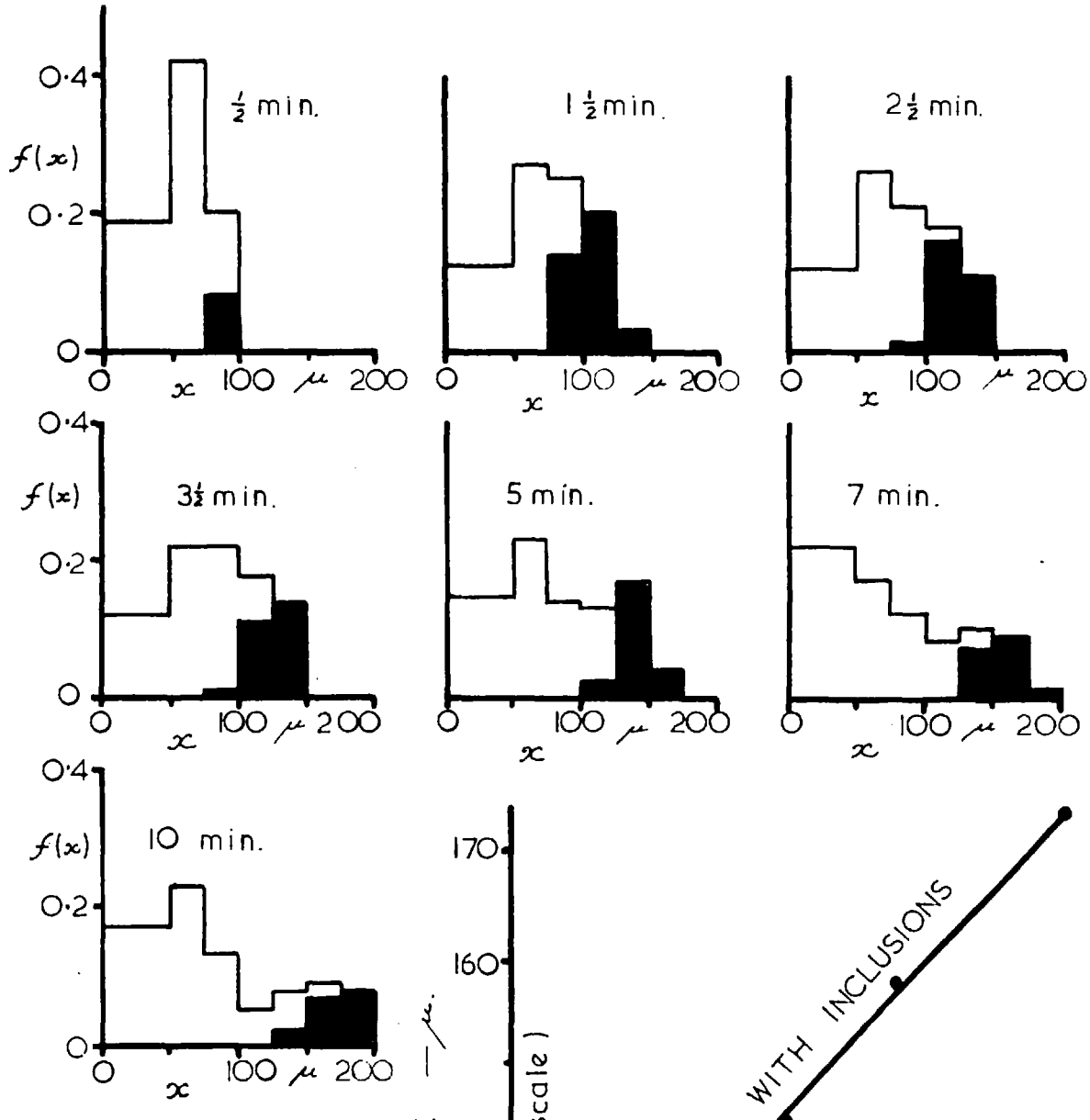

FIG. 7-17.
CRYSTAL SIZE HISTOGRAMS AND MEAN CRYSTAL SIZE
BATCH No. 38

[100 RPM, 40°C, Full heat]

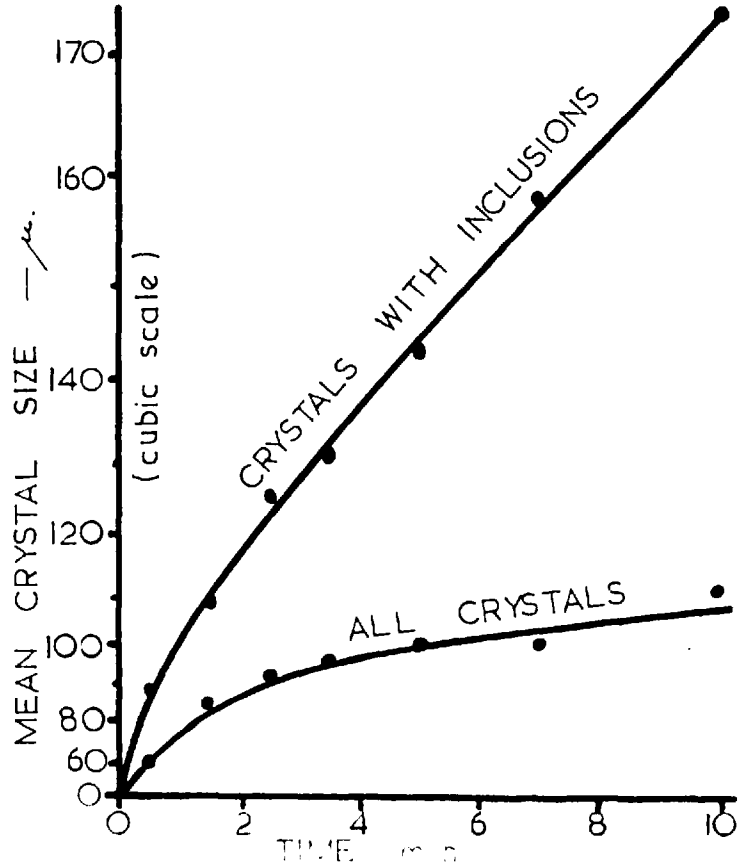

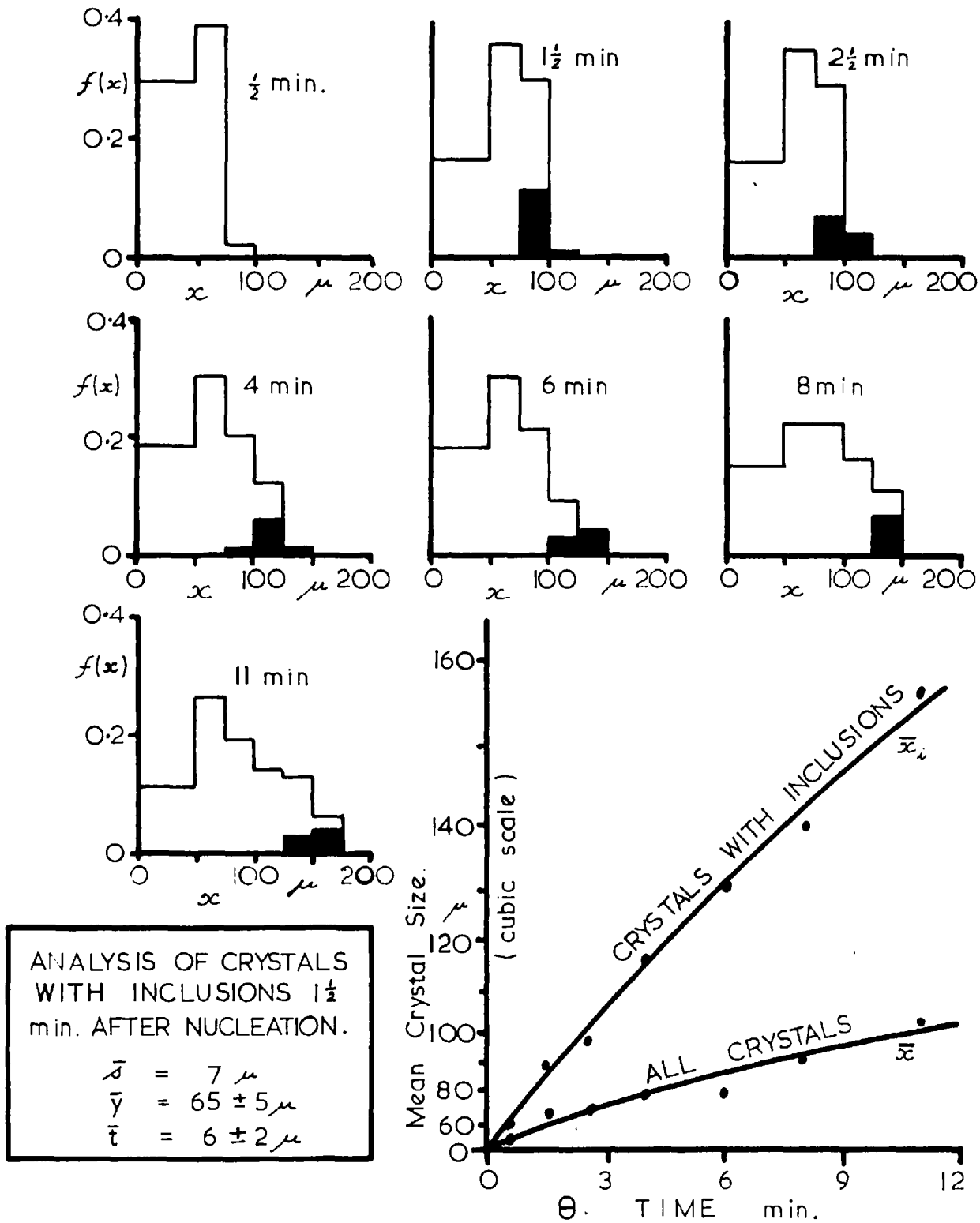

FIG.7-18. ANALYSIS OF CRYSTAL AND INCLUSION SIZE.
BATCH No. 39 [150 RPM , 40 °C , Full heat.]

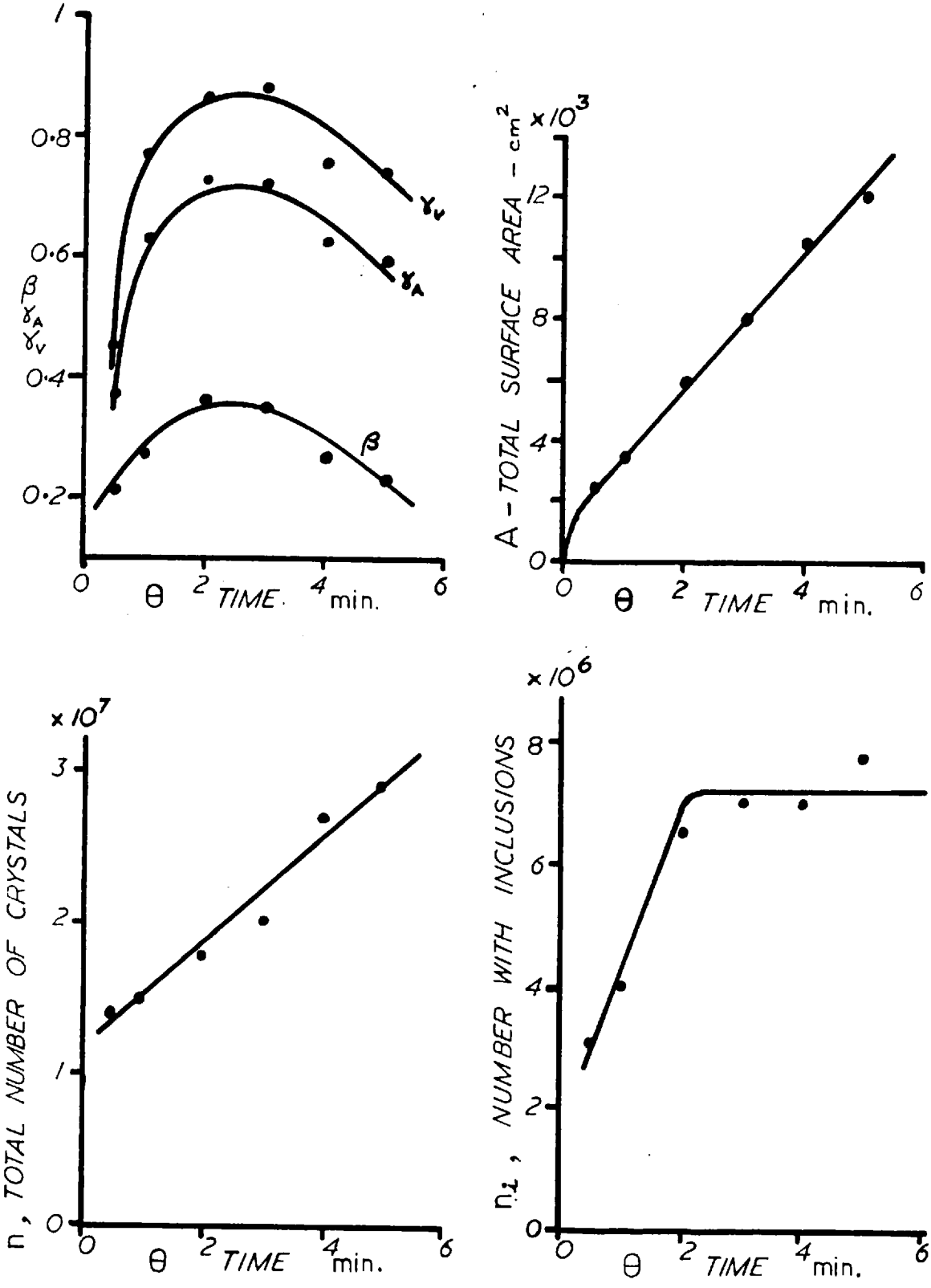

FIG. 7-19. NUMBER AND SURFACE AREA PARAMETERS
BATCH No 37 [60 RPM, 40 °C, Full heat.]

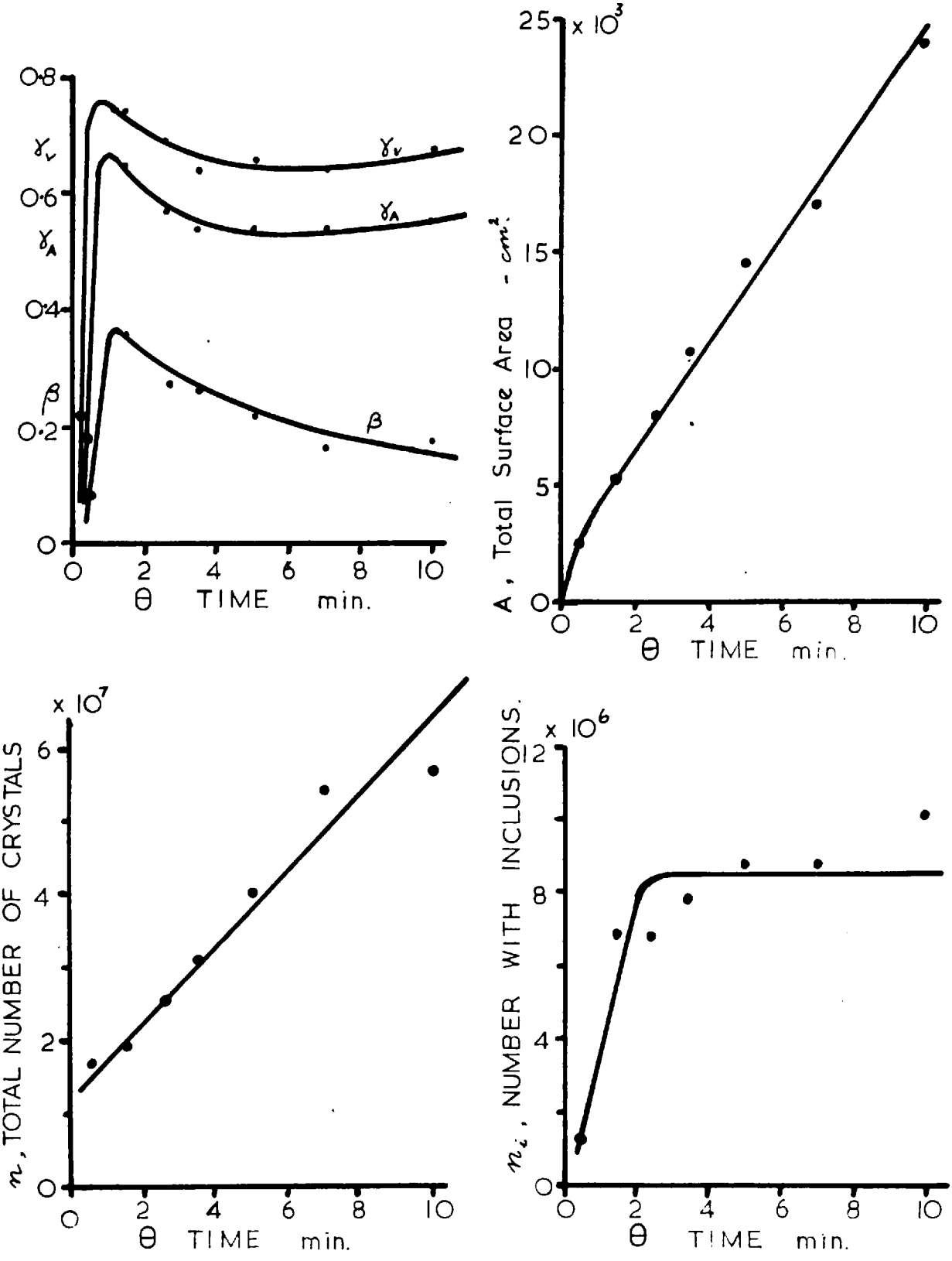

FIG. 7-20. NUMBER AND AREA PARAMETERS
BATCH No. 38. [100 RPM , 40 °C , Full heat.]

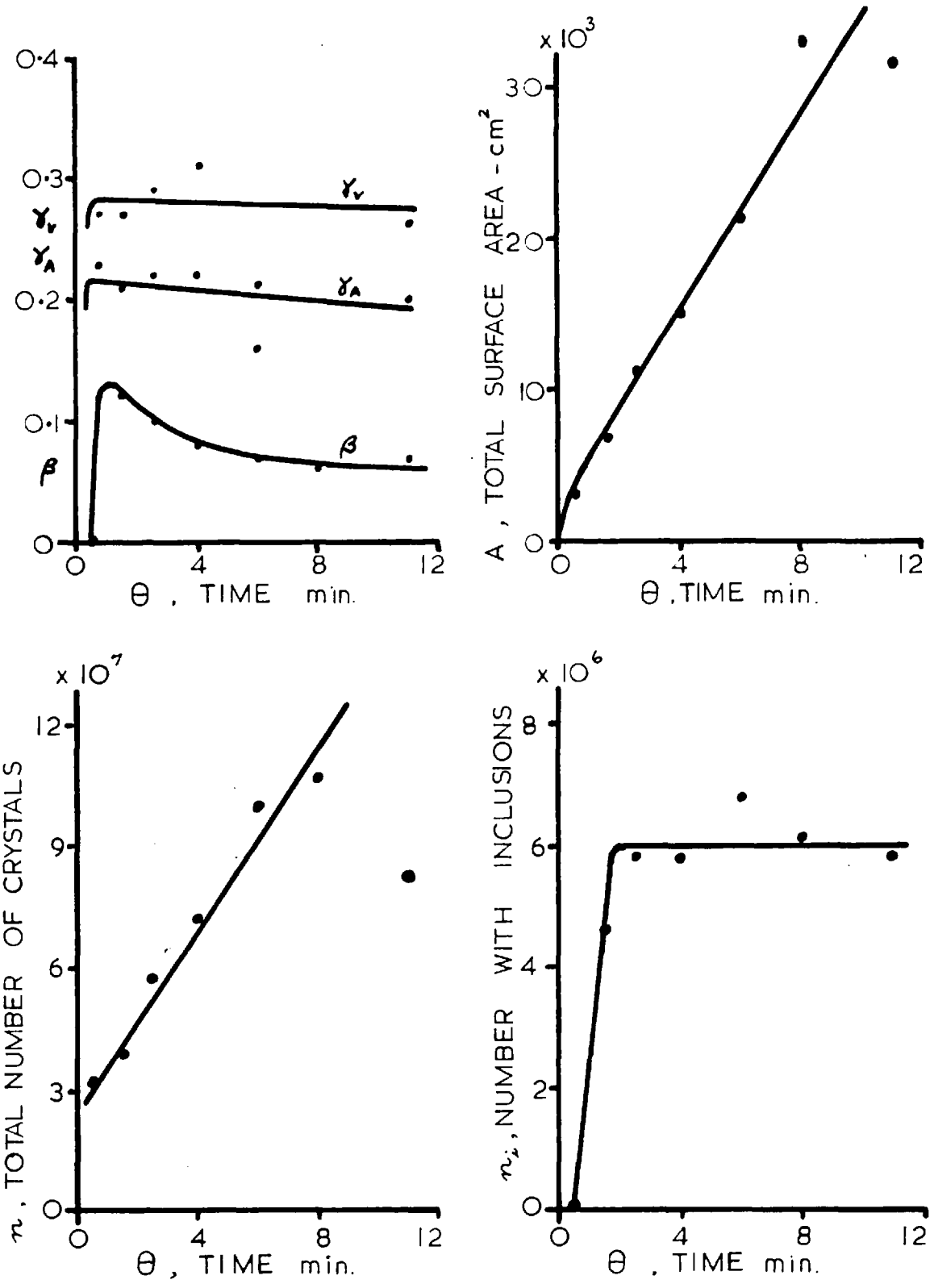

FIG. 7-21. NUMBER AND AREA PARAMETERS
BATCH No. 39. [150 RPM , 40 °C , Full heat.]

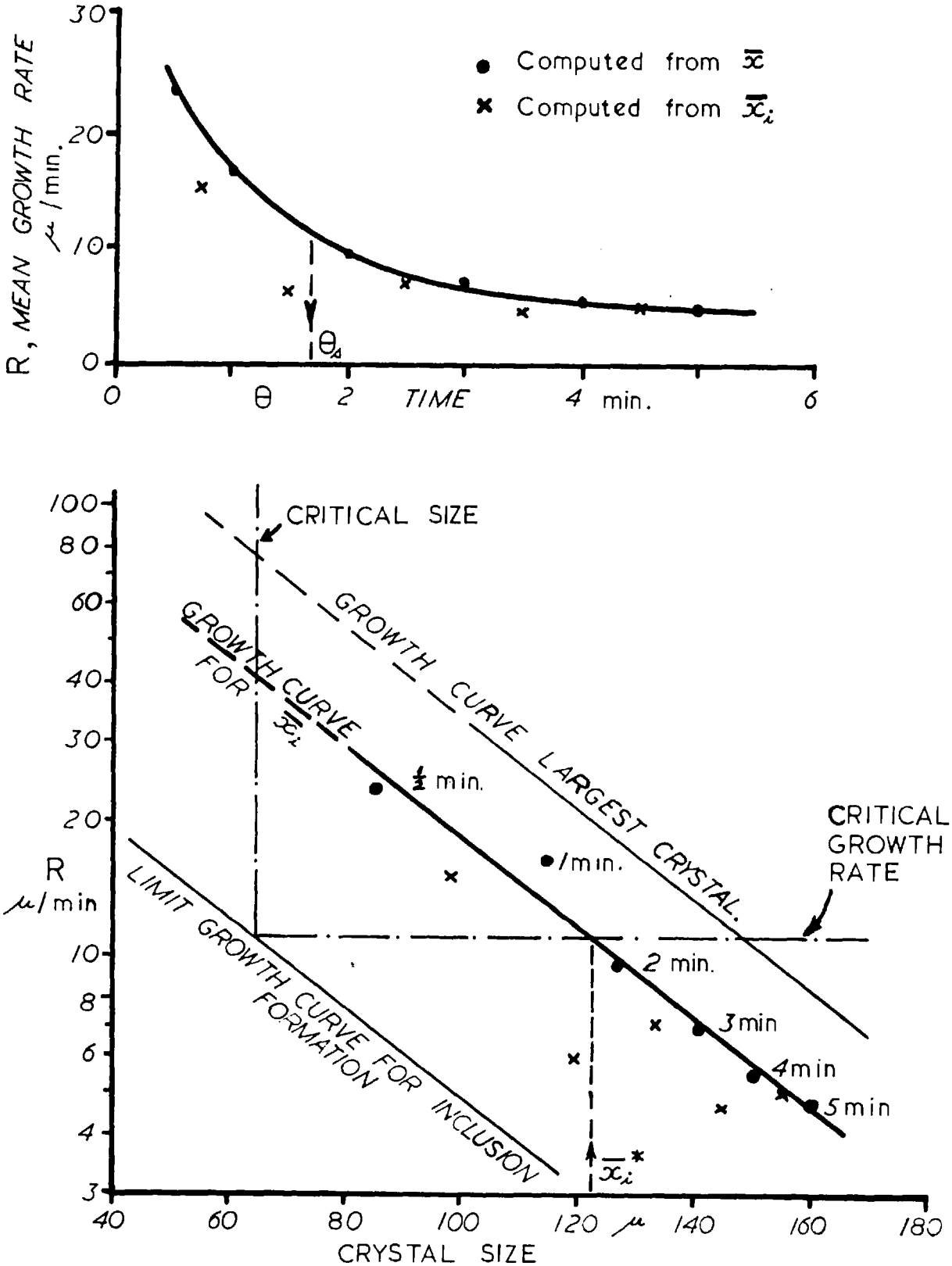

FIG. 7-22. MEAN GROWTH RATE OF CRYSTALS.
BATCH No 37. [60 RPM , 40 °C , Full heat.]

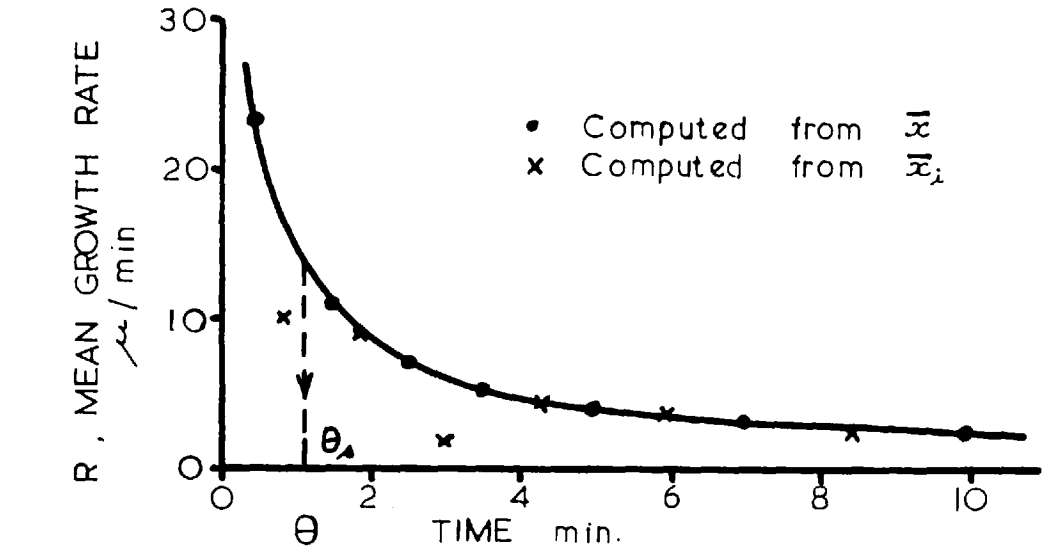

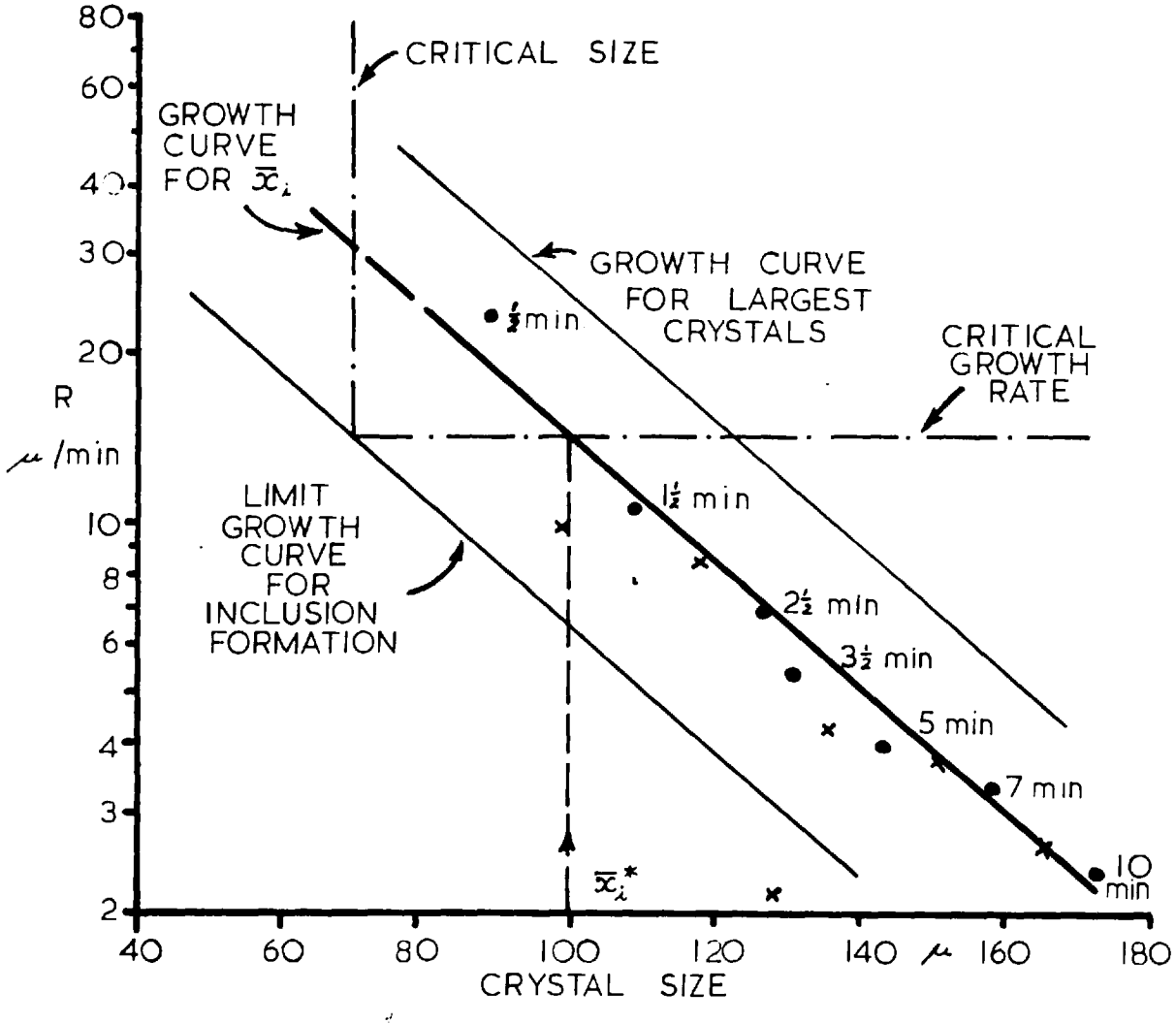

FIG. 7-23. MEAN GROWTH RATE OF CRYSTALS.
BATCH No. 38. [100 RPM 40 °C Full heat.]

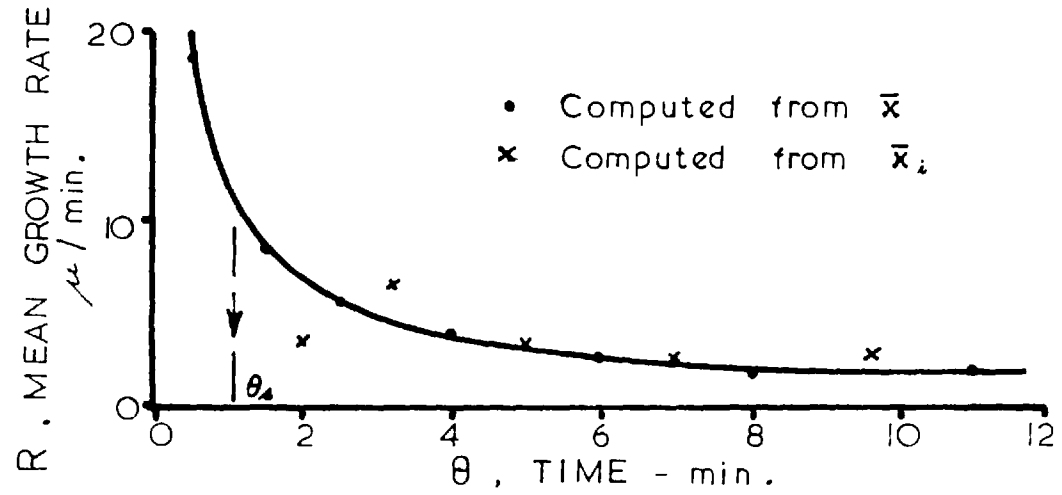

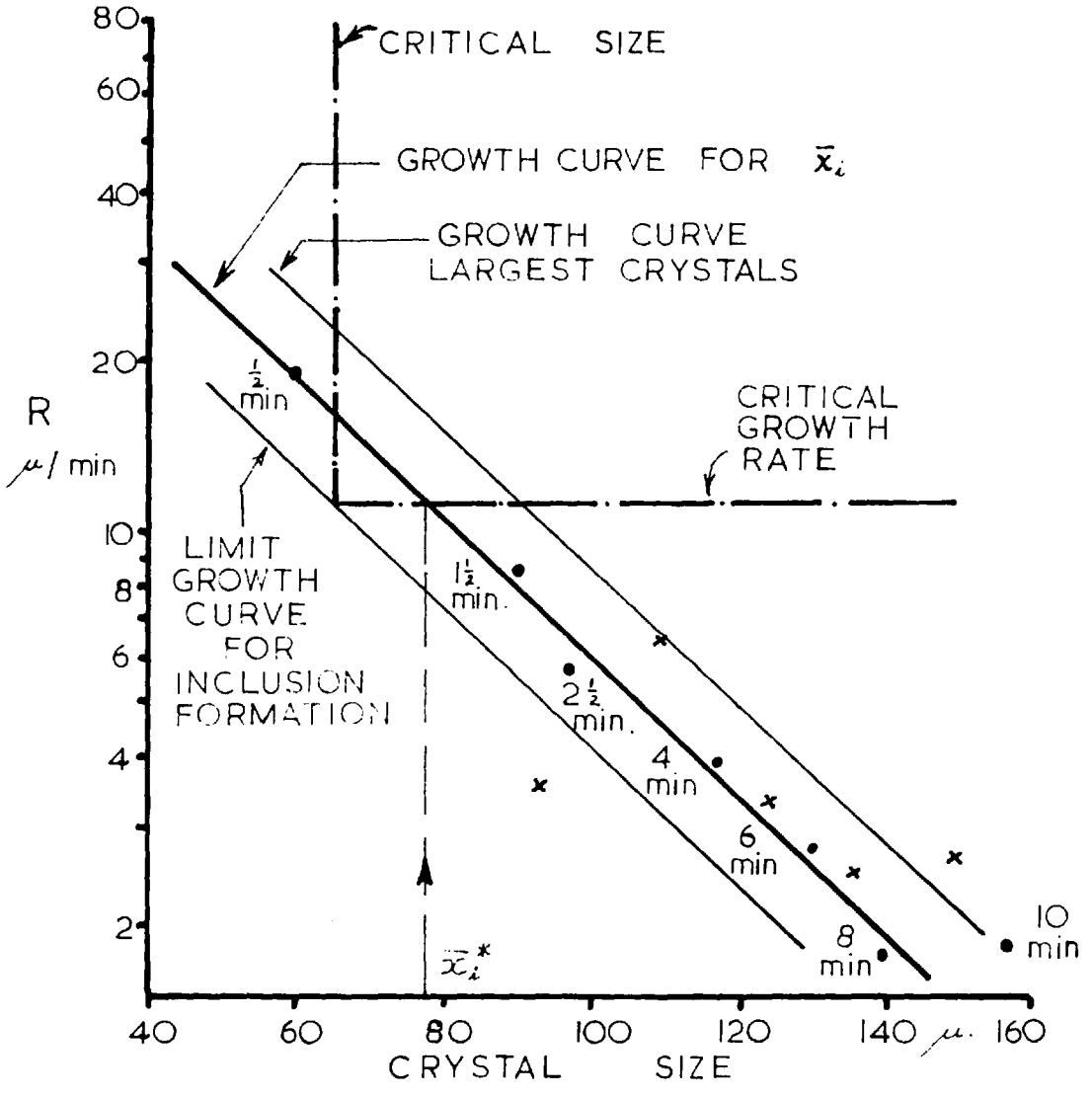

FIG . 7-24. MEAN GROWTH RATE OF CRYSTALS.
BATCH No.39. [150 RPM , 40°C , Full heat .]

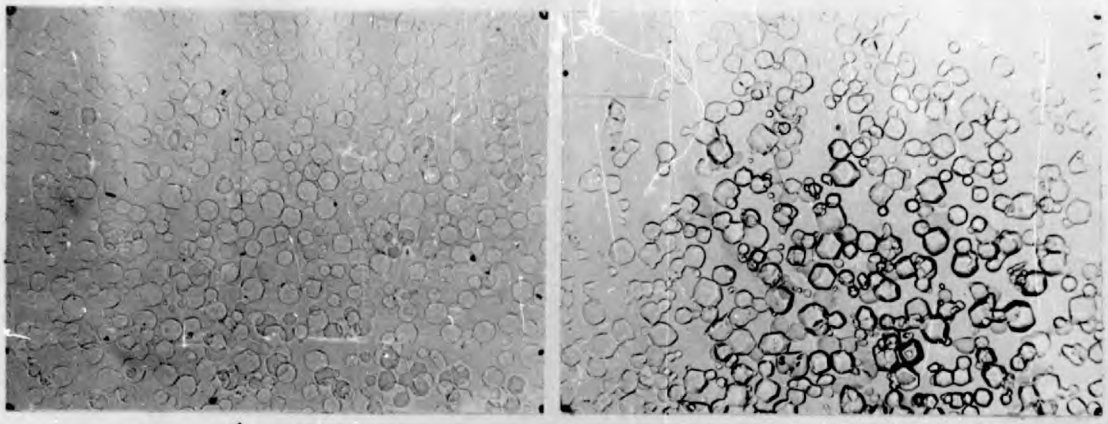

½ min.

1½ min.

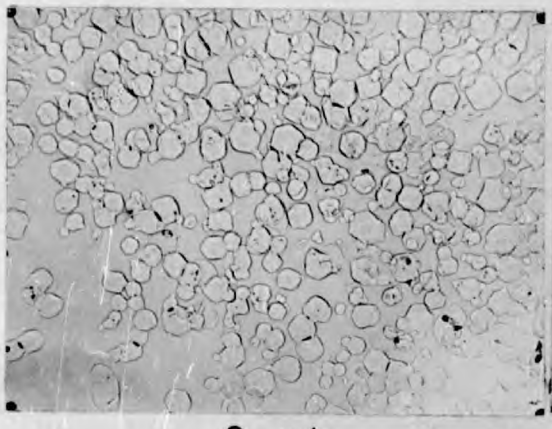

3 min.

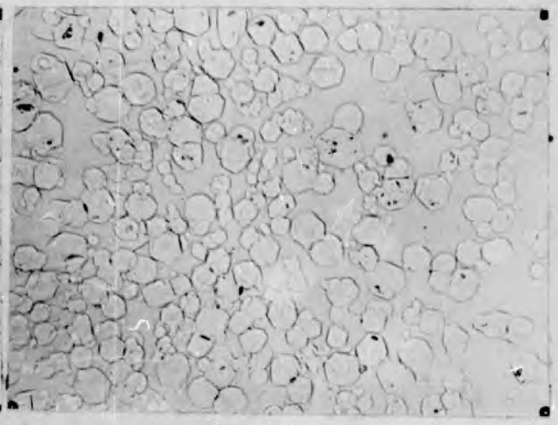

5 min.

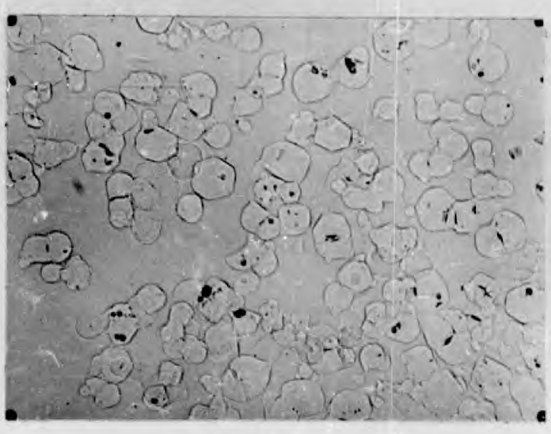

7 min.

FIG. 7-25. GROWTH OF HEXAMINE CRYSTALS.
BATCH No 40 [230 RPM , 40 °C , Full heat .]
[x 50]

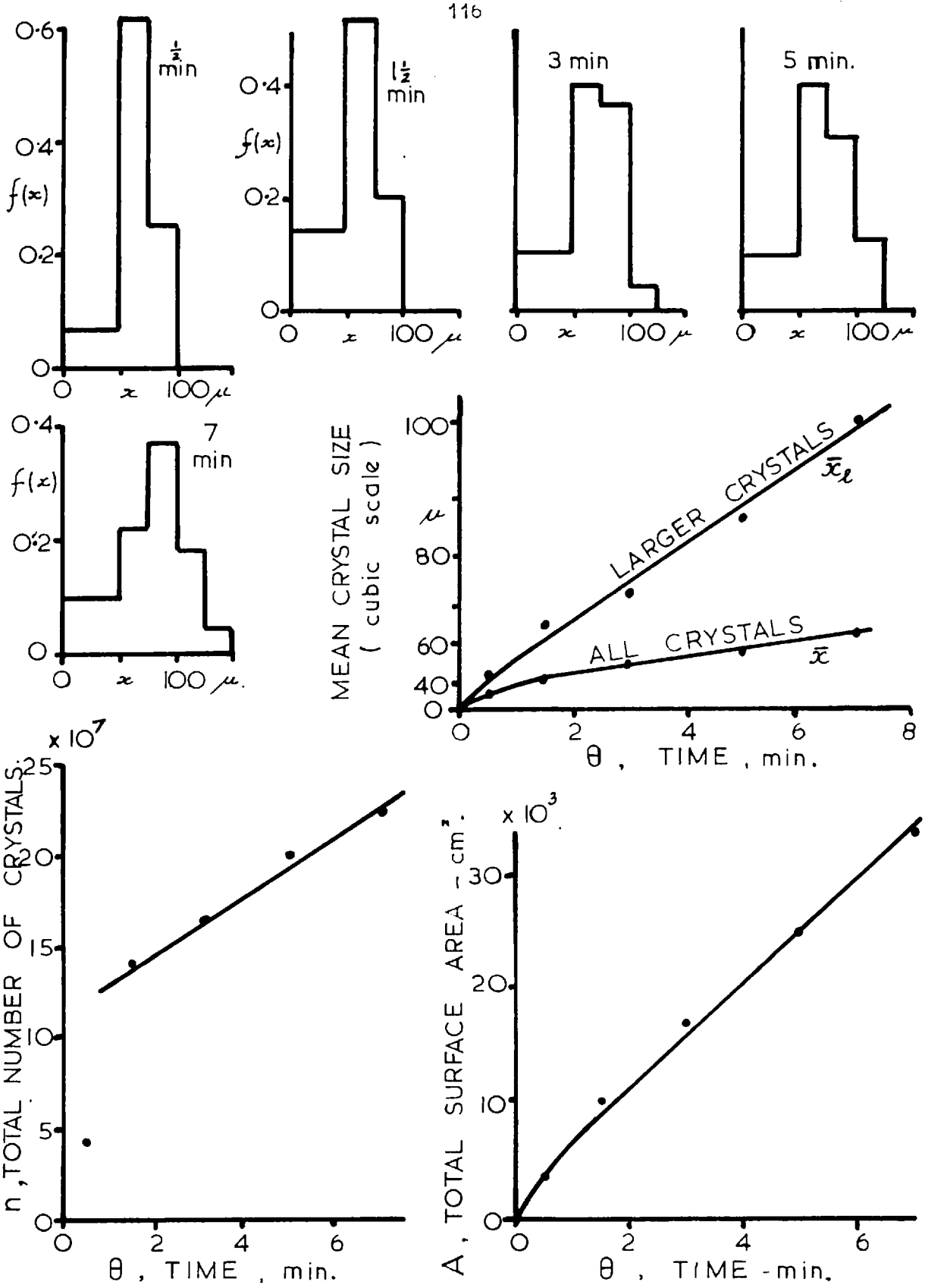

FIG. 7-26. CRYSTAL SIZE ANALYSIS.
BATCH No. 40. [230 RPM , 40°C , Full heat.]

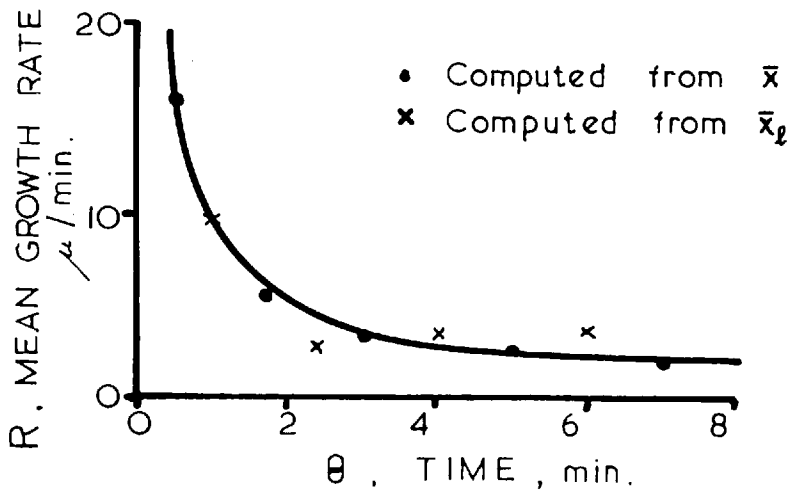

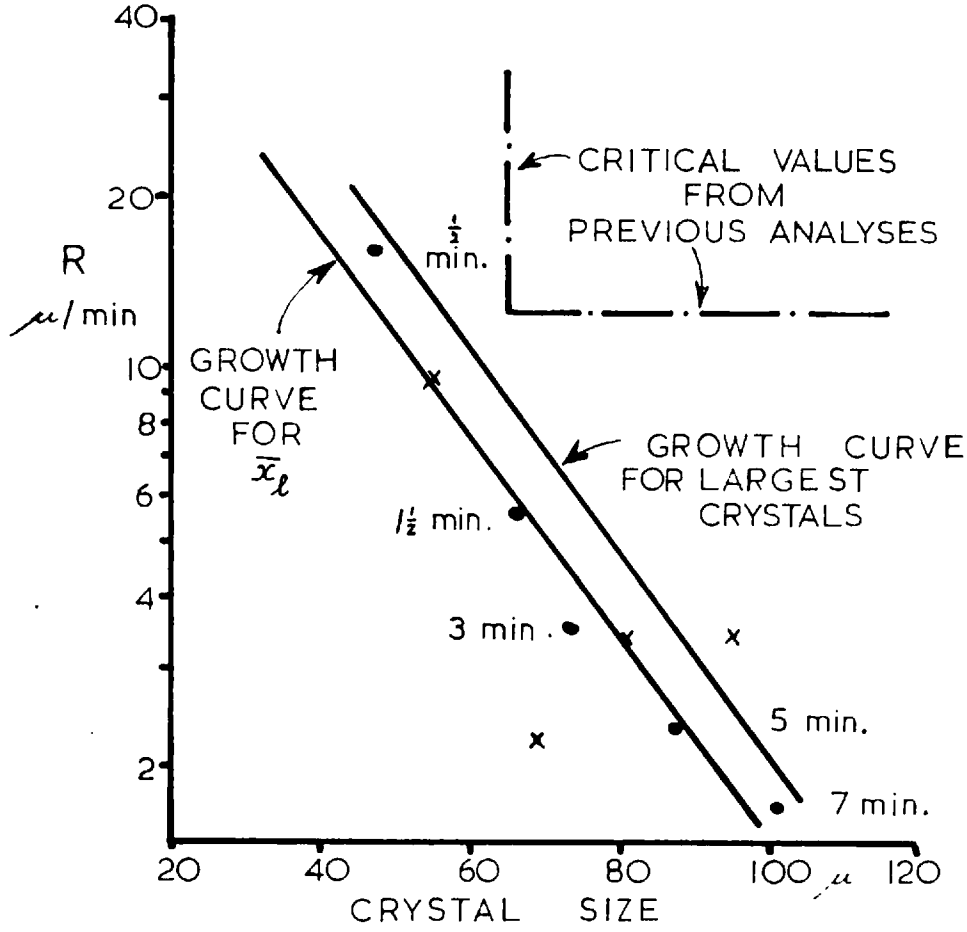

FIG. 7-27. MEAN GROWTH RATE OF CRYSTALS. BATCH No 40. [230 RPM, 40°C, Full heat.]

(Fig 7-16 to 7-18 and 7-26), indicating that the number of crystals present increased continually.

7.8.6 Number of Crystals

In the early stages of these batch crystallizations the number of crystals present is of the order of 10 to 100 million, i.e. of the order of 10^4 to 10^5 per ml. of solution.

The determination of the number of crystals is effected by the difficulties in counting the smallest crystals and thus the quantities may be underestimated by up to 20%. However, comparisons between the numbers of crystals in consecutive samples may be made to a higher accuracy since the error will be much the same from sample to sample.

The number of crystals increases continually with crystallization time (Fig 7-19 to 7-21 and 7-26) in an approximately linear manner, at least for the duration of the investigation. Thus, if required, the number of crystals in a batch could be described by an initial shower of crystals at nucleation, and a constant formation rate of further nuclei.

There is some slight suggestion in the more extended runs that nucleation may proceed in waves rather than at a steady rate. However, the data are not sufficiently accurate for any firm conclusions to be made.

Knowledge of the rates of nucleation could be used with the changes in the shape of the size histograms to check the assumption of equal growth rate on all crystals. Alternatively, using this assumption, the size histograms could be predicted. However, the computations are complex, and the accuracy of the data does not warrant their use.

The quantity, β, the fraction of the crystals showing inclusions,

rises in the initial stages of the crystallization, then falls. The actual number of crystals with inclusion patterns, n_i, also rises initially but then reaches a constant value (Fig 7-19 to 7-21). This is in accordance with the mechanism of inclusion formation already described. Under the initial conditions of rapid growth, inclusions form once the crystals reach the critical size. The 'number of crystals with inclusions' (actually cavitites), and the fraction of the total number, rise. Once the growth rate drops below the critical no further inclusions are formed, but since further crystals are being formed, the fraction with inclusions decreases.

The number of crystals with face inclusion patterns, n_i, is much the same order for all the batches analysed in detail (Refer Table 7-1 and Fig 7-30) and is about 7 million, corresponding to about 6000/ml. of solution. This point will be discussed in section 7.8.9.

7.8.7 Total Surface Area

Except for the region about the origin, the total surface area varies linearly with the time of crystallization (Fig 7-19 to 7-21 and 7-26). The continuation of the straight lines give a zero area intercept of about half a minute prior to the moment taken as the onset of nucleation. The onset of nucleation was measured as the moment when the solution changed appreciably in opaqueness, and could have been in error by nearly half a minut However, as there was no supporting evidence to confirm a linear variation of surface area with time, no alteration was made to the original time measurements.

The quantities γ_a and γ_v represent the fractions of the total surface area and total volume of crystal, respectively, associated with the crystals with inclusions. These quantities were computed to show whether crystals

with inclusions grew at the same linear rate as those without. In the absence of further nuclei formation, γ_v should increase for $\gamma_A > 0.5$, and decrease for $\gamma_A < 0.5$, if growth is the same on all crystals. However, because nucleation does occur, and because of the scatter of data these results were of limited use.

7.8.8 Growth Rates

The mean growth rate was calculated from the known constant rate of deposition of hexamine and from the total crystal surface area at each sampling time (computed from $\bar{x}$, the mean crystal size). These values were plotted against time (Fig 7-22 to 7-24) and also against $\bar{x}_i$, the corresponding mean size of the crystals with inclusions.

The quantity $\bar{x}_i$ was chosen, since once the inclusions have sealed over, it refers to a constant number of crystals (section 7.8.6). Changes in $\bar{x}_i$ are therefore a true measure of the amount of growth on each crystal. On the other hand a change in $\bar{x}$, referring to all crystals, reflects the change in the number of crystals as well as the growth on each.

Since the number of crystals with inclusions is constant, the mean growth rate can also be determined from the values of $\bar{x}_i$ directly, by the relation, $R = \frac{1}{2}\frac{d\bar{x}_i}{d\theta} \doteq \frac{1}{2}\frac{\Delta\bar{x}_i}{\Delta\theta}$

Values of R computed in this way (designated R') are plotted thus, (X), on Fig 7-22 to 7-24. Although these values are not as accurate as values of R computed from the surface area, there is substantial agreement between the two.

In these figures, the logarithm of the growth rate, R has been plotted against $\bar{x}_i$. The experimental points so plotted may be approximatedby a straight line. This line (termed a 'growth curve') represents the manner

in which the mean growth rate varies with the mean crystal size for all those crystals with inclusions. Since all crystals are assumed to grow with the same rate at the same time, crystals with size, $\bar{x}_i$ will behave identically with the mean behaviour of those crystals with inclusions. Thus the growth curve shown is also the growth curve representative of crystals with size equivalent to $\bar{x}_i$.

Other crystals of different size will have different growth curves. On the semilogarithmic plot, however, these will all be straight lines parallel to the original. This may be seen in the following way. Consider two sets of crystals, those with size $\bar{x}_i$, and those with size $\bar{x}_i + k$. At a certain time, the first set of crystals will be represented by a point (at the corresponding growth rate) on the growth curve given. The second set must have the same mean growth rate at the same time, so the point on its growth curve will merely be displaced a horizontal distance k from the other. As growth proceeds the same difference in size, k, is maintained, since all crystals grow equally. Thus a growth curve parallel to the first will be traced out.

Thus there is a growth curve associated with each set of crystals of differing size. The growth curve representing the largest crystals has been drawn (Fig 7-22 to 7-24). The position of this curve was computed from the measurement of the excess in size of the largest crystals over $\bar{x}_i$. Batch growth may be represented by an infinitude of such parallel growth curves, all lying below the curve for the largest crystals.

The growth curve of any individual crystal (if it could be measured) probably would not be a straight line on these plots, because of variations in growth conditions on the path of the crystal, and also because of growth

fluctuations on individual surfaces. The growth curves shown represent the mean behaviour of all crystals of each size.

A critical crystal size and a critical growth rate have already been proposed. These critical values would be shown on the 'growth curve' plots by two straight lines, one parallel to each axis. Together they form a region on the plot in which cavitite growth (or inclusion formation) will occur. Such growth will occur if a crystal is in this region; that is, if its growth curve passes through the region.

The critical crystal size can be plotted immediately from the measured value of $\bar{y}$ or by using the overall mean value of 65μ (section 7.7). The critical growth rate can be computed for any of the growth curves. It is most convenient to compute it for the $\bar{x}_i$ curve, i.e. for crystals of size equal to the mean of those with inclusions.

The value of $\bar{x}_i$ for which the growth rate is at its critical value, $\bar{x}_i^*$, corresponds to the mean size of all those crystals with inclusions at the moment of inclusion sealing. It was therefore computed by equating it to the volumetric mean value of y', the outer size of the inclusion pattern (section 7.6). Because of the method of computing means, estimates of $\bar{x}_i^*$ cannot be calculated from the simple relations $\bar{x}_i^* = \bar{x}_i - 2\bar{t}$ and $\bar{x}_i^* = \bar{y} + 2\bar{s}$ without serious error (see Appendix II).

By plotting the value of $\bar{x}_i^*$ on the $\bar{x}_i$ growth curve the critical value of the growth rate is determined and the region of cavitite formation is thus delineated (Fig 7-22 to 7-24). The limiting growth curve for inclusion formation, that curve that just passes through the critical region, has also been drawn. Crystals with growth curves above this will have inclusions; those below, none. The size of inclusion formed is half the horizontal distance between the critical crystal size and the intersection of the growth curve with the critical growth rate line. The size distribution of inclusions will

depend on the distribution of crystal numbers along the various growth curves. This will depend on the rate of production of nuclei after nucleation.

From the critical growth rate the time at which inclusion formation stops, θ_s , can be determined. Inclusion formation is usually compete within the first minute or two of crystallization.

There are certain uncertainties associated with the measured value of the critical growth rate. The intersection point on the growth curve lies in the region where experimental errors are the greatest. Also, up to this value the number of cavitites is continually increasing and $\bar{x}_1$ does not refer to a constant number of crystals. To compensate for this, when drawing the line of best fit to the data greater reliability was attributed to later points. An estimate of the errors associated with the critical growth rate for each batch are given, together with the measured growth rates in Table 7-1.

Within the limits of error the same critical growth rate is found for all batches, independently of the operating conditions used. This mean value is 12 ± 3 μ/min.

The constancy of this growth rate for all runs, would indicate that the growth rate is quite a suitable parameter for describing the critical growth conditions (refer section 7.6.4). Supersaturation could have been used instead, but since the critical growth rate is constant, a critical supersaturation would probably be dependant on the temperature and agitation conditions of crystallization. No measure could be made of the supersaturatio in the batch evaporative crystallizer, although estimates were made for the thermal crystallizer, (section 7.11). The values are surprisingly small for the high growth rates involved.

Batch No.	Feed Stock	Temp. °C.	Stirrer R.P.M.	$\bar{y}$ Critical Crystal Size. μ	R^* Critical Growth Race. μ/min.	$\bar{s}$ Mean inclusion size. μ	Total included volume cc.	n_1 Number of crystals with inclusions
11	3	38	100	59	8±5	22	0.61	12×10^6
26	5	42	60	65	10±5	34	1.38	7.4×10^6
36	)	40	60	64	12 ± 3	32	1.19	$7.7 \cdot 10^6$
37	)	40	60	64	11± 3	28	0.76	7.3×10^6
38	)	40	100	70	14± 3	18	0.22	8.2×10^6
39	) 7	40	150	65	11± 2	6	0.01	6.1×10^6
40*	)	40	230	-	> 9(±4)	-	-	-
41	)	57	100	69	14± 4	16	0.20	6.9×10^6
42*		33	100	-	> 12(±4)	-	-	-
67	)	32	50	60		35		
68	) 10	83	50	63		6		
69	)	58	50	72		8		
70	)	42	50	69		32		

All batches about 1400 g. solution, full heat rate(about $7\frac{1}{2}$ g. of hexamine crystallizing per min). *No inclusions.

TABLE 7 - 1. RESULTS OF BATCHES WITH CONSECUTIVE SAMPLING

For Batch No. 40, no inclusions were formed. Here the growth curve for $\bar{x}_1$ was shown (Fig 7-27). The quantity $\bar{x}_1$ is the mean size of the largest 7 million crystals in the batch. This number is approximately the same as the number of crystals with inclusions in other batches, and thus the growth curves should be comparable. The critical region as computed from the other batches is shown on Fig 7-27. It can be seen that all the growth curves for this batch lie outside of this region, so inclusions should not and did not form.

7.8.9 Effect of Crystallizer Operating Conditions

The mean values of the critical crystal size and the critical growth rate have been plotted to define the region of cavitite growth in Fig 7-28. The growth curves for Batches No. 37-40 have been replotted on this figure for comparison, while the corresponding crystal products are shown in Fig 7-29. It can be seen that the slowest stirrer speed gives the set of growth curves with the deepest penetration of the critical region and thus the largest inclusions. Faster stirrer speeds give lesser penetration and smaller inclusions.

The effect of the operating conditions on the size of inclusions formed is thus through the positioning of the sets of growth curves relative to the same critical region of growth conditions. The positioning of the growth curves in Fig 7-29 is due solely to nucleation conditions in the following manner. When the number of nuclei initially formed and the rate of further formation are low, the mean rate of growth will be high, since at any time the number of crystals and therefore the total surface area will be small. Crystals will reach the critical size rapidly while the

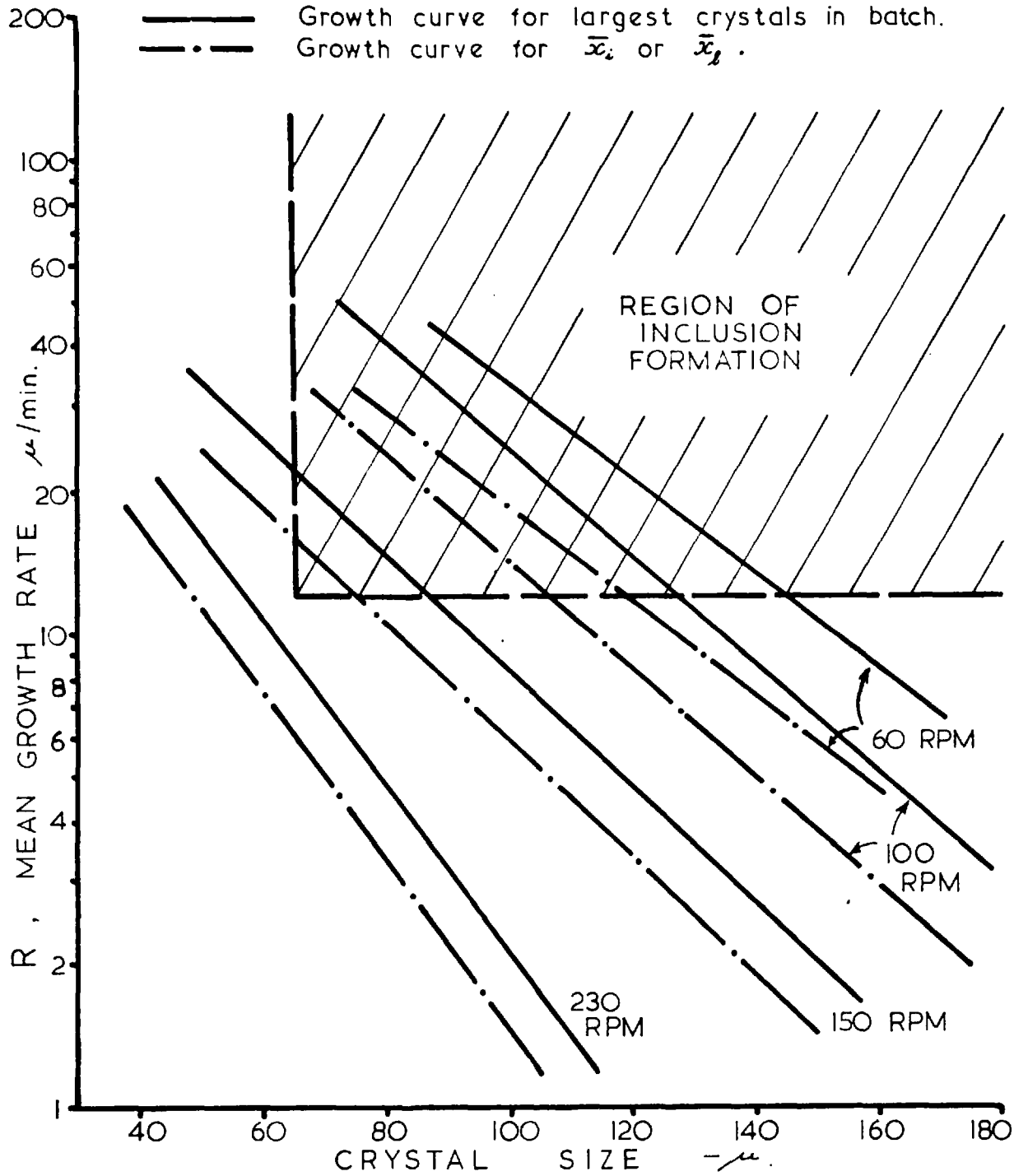

FIG.7-28. EFFECT OF STIRRER SPEED ON MEAN GROWTH CURVES. BATCHES No 37,38,39,40.
[All at 40 °C and full heat.]

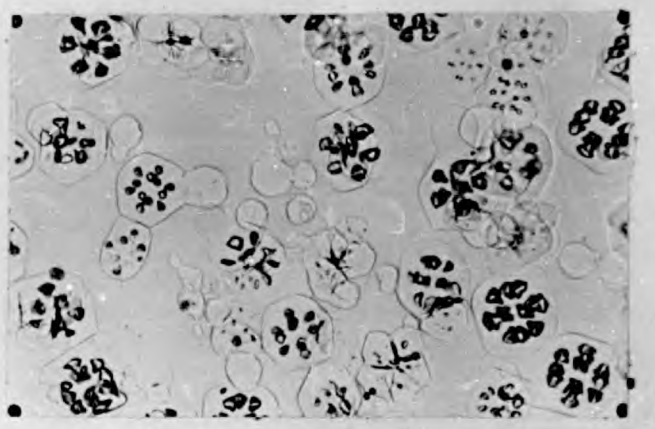

[60 RPM , 5 min.]

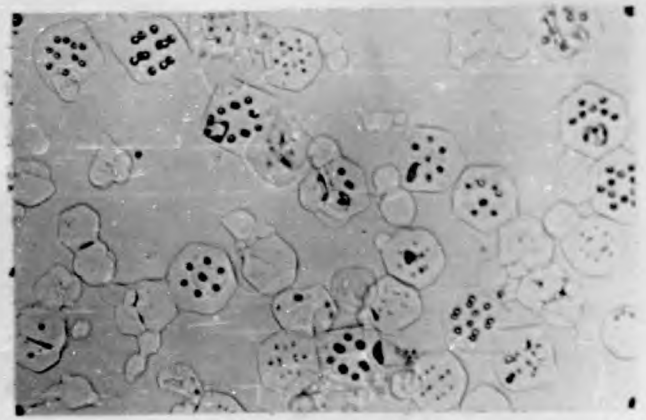

[100 RPM , 5 min]

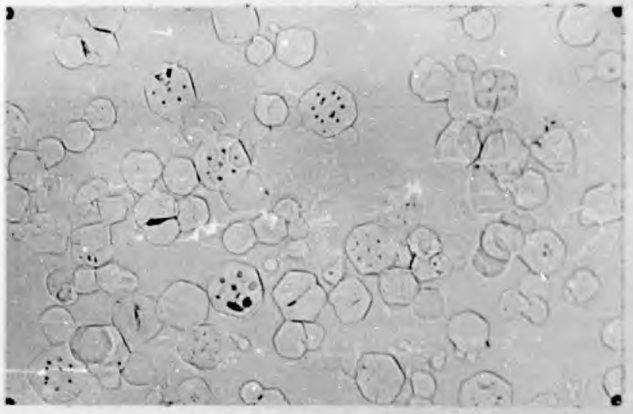

[150 RPM , 4 min]

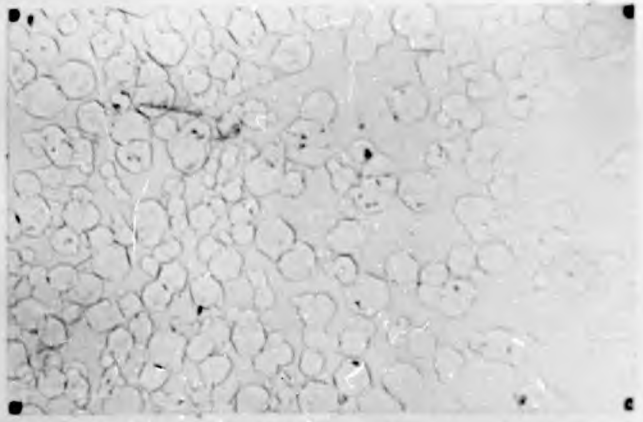

[230 RPM , 5 min]

FIG. 7-29. COMPARISON OF HEXAMINE CRYSTALS GROWN AT DIFFERENT STIRRER SPEEDS. BATCHES No 37 - 40.
[40 °C Full heat] [x 60]

growth rate is still high, and considerable growth will occur before the mean growth rate falls below the critical value. Thus the growth curves will penetrate deeply into the critical region and large inclusions will be formed.

Conversely, when the initial number of nuclei and the rate of nucleation is high, the growth rate at any time will be correspondingly much lower. By the time the first crystals reach the critical size the mean growth rate may be below the critical value and thus the growth curves will not pass through the critical region and inclusions will not be formed.

It appears, therefore, that the effect of the operating variables on the formation of inclusions will be their effect on the rates of nucleation, especially at the early stages of the batch. As might be expected, the rate of agitation has a marked effect on the formation of nuclei (Fig 7-30). The more intense the agitation the more nuclei formed. The temperature of crystallization has but small effect. Dirty solutions and the addition of foreign nuclei have marked effects. This was particularly noticed when attempts were made to use freshly dissolved solutions of commercial crystal. Inclusions were never formed. Pretreatment of the solution to remove foreign nuclei (as described in section 5.7) was necessary.

The effect of the rate of evaporation of solvent, however, does not depend on nucleation effects, but works directly by its influence on the mean growth rate (see section 7.10).

It has been noted (section 7.8.6) that the number of crystals with inclusions is approximately the same (7 million) for all batches with the full rate of heating. The number of crystals with inclusions is the result of two competing effects; the number of crystals present, and the time available for growth. If the rate of nuclei formation is low, the number of crystals reaching the critical size at any time is small, but because the growth rate is so high, the time available for inclusion formation is large.

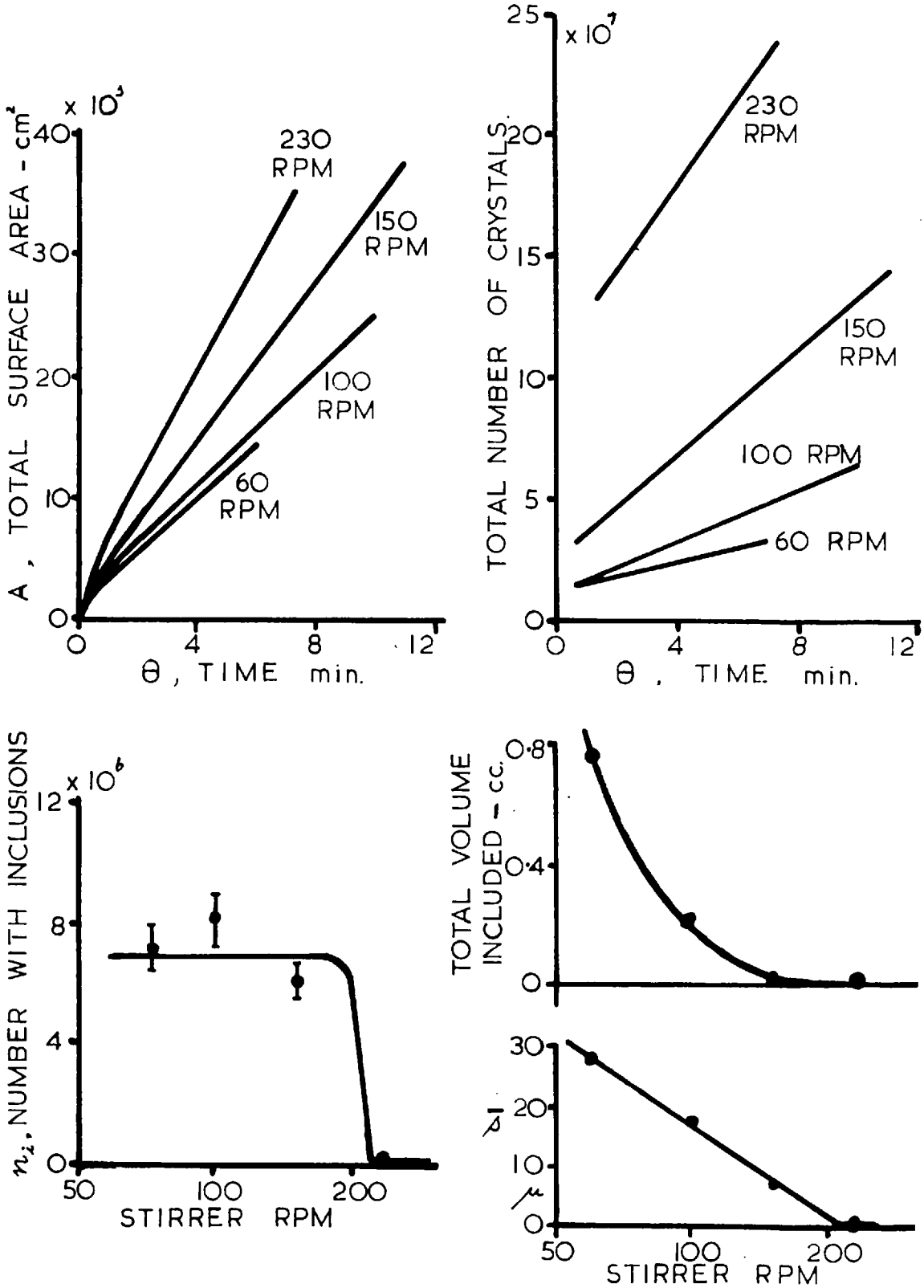

FIG. 7-30. EFFECT OF STIRRER SPEED ON NUMBER AND AREA OF CRYSTALS AND ON INCLUSION SIZE. BATCHES No 37-40 [40 °C , Full heat.]

If, on the other hand, the nucleation rate is high, the number of crystals reaching the critical size becomes large, but the time available for inclusion formation is small. The joint effect is to maintain the number of crystals with inclusions about the same.

From the mean inclusion size and the total number of crystals with inclusions, the total volume of included liquor in the batch of crystals may be calculated (Fig 7-30). Up to 2 cc. of solution may be contained in as little as 15 g. of crystal. This method of computing the volume included was compared with direct measurement on several of the samples, using the Karl Fischer analysis for water (Appendix V). The results are shown in Fig 7-31. A certain rough agreement is evident, although (i) the errors in the respective methods are large and (ii) the Karl Fischer method measures the total moisture which includes that in the regular inclusion patterns, that in random inclusions, and that adsorbed on the surface.

The large variations in inclusion size from batch to batch grown under the same conditions, presumably stems from the variations usually experienced in all nucleation phenomena.

7.9 NUMERICAL VALUES FOR CRITICAL GROWTH CONDITIONS

The formation of inclusions in crystals of hexamine has been interpreted in terms of a nucleation phenomenon and a growth phenomenon. Little of absolute value can be said about the nucleation phenomenon, as, no doubt, it depends on the type and the size of the crystallizing equipment used, as well as the operating conditions. However, qualitative estimates of the effects of changes in the operating conditions can be made on the basis of prior experience of nucleation phenomena.

CODE	SAMPLE No.
1	58
2	55
3	20
4	39-7
5	38-7
6	45
7	11-2
8	37-7
9	17
10	36-7
11	26-2

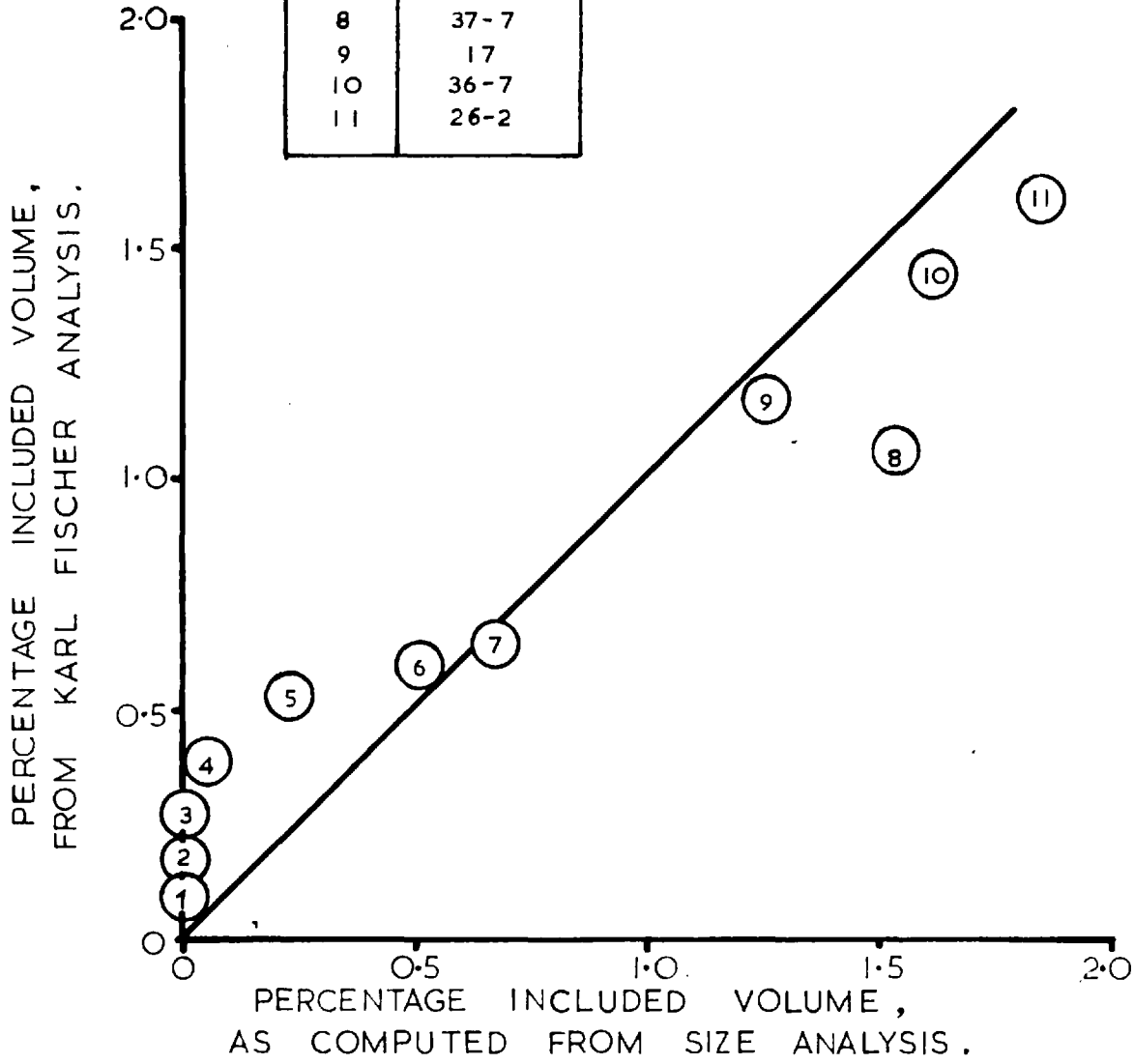

FIG. 7-31. VOLUME OF INCLUDED LIQUOR IN HEXAMINE SAMPLES — COMPARISON OF COMPUTED VALUES WITH MEASURED.

The growth phenomenon can be explained in terms of two quantities, a critical crystal size and a critical growth rate. It has been seen (section 7.7) that the critical crystal size is independent of the operating conditions used in growing the crystals. The analysis of growth rates shows that the critical growth rate also is unaffected by the operating conditions (Table 7-1). The mean values selected for these two quantities are -

Critical crystal size, $65 \pm 5\ \mu$

Critical growth rate, $12 \pm 5\ \mu$/min

7.10 INFORMATION FROM OTHER BATCHES

For the most part the results upon which the above conclusions have been made have been derived from a small number of batches, from which series of consecutive samples were taken. It is possible to get similar (though less accurate) information from those other batches for which only a single sample was taken.

Certain quantities such as the critical crystal size and the number of crystals with inclusions can be computed directly from the analysis of the single sample. However, to compute the critical growth rate some information is required about the slope of the growth curves. This cannot be computed from a single sample without some further assumption.

The assumption made in addition to the previous ones, is that the total surface area varies linearly with time with zero total surface area at zero time. This assumption is only approximately true as plots of total surface area against time (Fig 7-19 to 7-21, and 7-26) have shown. A consequence of this assumption is that the growth curve is a straight line on semi-logarithmic paper (Appendix II). The slope of this growth curve can be computed

readily from measurements made on a single sample. As $\bar{x}_i$* is measured, the critical growth rate can be computed.

As a check on this method several of the consecutive samples already analysed have been treated as if they were single samples. The values obtained (Table 7-2) are in quite reasonable agreement with previous values. The method was used to estimate critical conditions for some of the other batches and the results are shows in Table 7-3. The results confirm that the critical growth rate is independent of the batch conditions, and is approximately constant at a value of 12 μ/min. The approximate constancy of the number of crystals with inclusions is also demonstrated.

The method was also applied to those batches of crystals without inclusions. The maximum mean growth rate of the crystals at a crystal size of 65μ was computed (Table 7-4). In all cases, within the limits of error, this value was below the critical growth rate.

Several batches grown at lower heating rates have also been analysed by the method (Table 7-5). The results are in good agreement with the critical values determined previously.

It has already been shown (Fig 6-2 and 6-3) that a reduction in the heating rate decreases the size of the inclusions formed. This can also be seen from Fig 7-31A where the results for batches No. 51-55 (all at 40°C, 70 R.P.M.) have been plotted again. The same total amount of evaporation took place for each of these batches (50 g. of product formed). It can be seen that the number of crystals with inclusions, n_i, also varies with the rate of evaporation. The mean crystal size $\bar{x}$, is however much the same for all batches. This means that there is the same number of crystals in each batch and approximately the same total surface area.

SAMPLE No.	R^* † μ/min.	R^* ‡ μ/min.
37-3	10.5	
37-4	10.7	11 ± 3
37-5	10.2	
37-6	10.4	
38-2	14.2	
38-3	14.6	
38-4	12.0	14 ± 3
38-5	12.3	
38-6	11.5	
38-7	10.9	
39-2	13.5	
39-3	11.7	
39-4	14.0	11 ± 2
39-5	13.4	
39-6	16.5	
39-7	13.0	

† Computed from single sample analysis.

‡ Computed from plot of all samples (Fig 7-22 to 7-24)

TABLE 7 - 2. COMPARISON OF VALUES OF CRITICAL GROWTH RATES COMPUTED BY DIFFERENT METHODS.

SAMPLE No.	$\bar{s}$ μ	$\bar{y}$ μ	R* μ/min.	10^{-6} n_i
1	15	74	14	5.7
2-1	19	65	16	8.1
2-2	21	65	17	7.7
4	18	67	9	11.4
5	13	65	11	5.7
9	12	61	14	5.6
10	14	69	11	5.8
12	14	64	14	7.8
13	14	55	12	9.2
14	12	56	14	9.1
15	14	58	14	11.0
17	33	69	10	7.2
18	48	74	10	4.9
21	14	74	17	5.0
22	10	63	18	4.8
24	43	67	9	6.1
25	28	70	9	9.6
27	39	60	8	8.9
28	38	68	10	6.5
29	42	70	13	4.6
30	35	68	11	6.3
33	12	67	14	5.7
34	20	71	11	8.9

TABLE 7 - 3. COMPUTED QUANTITIES FOR BATCHES WITH SINGLE SAMPLES.

Batch No.	Growth Rate of Largest Crystals at 65 μ size. (μ/min)
6 *	3.5
16	4.0
20	1.8
48*	5
55*	10

* low heating rate (heat No.6)

TABLE 7 - 4. ANALYSIS OF BATCHES FOR WHICH NO INCLUSION FORMED.

Batch No.	Heat No.	$\bar{y}$ μ	R* μ/min	10^{-6} n_1	$\bar{s}$ μ
7	8	70	13	2.1	7
49	8	79	7	4.9	23
50	10	65	8	8.7	33
51	8	74	12	3.4	10
52	7	79	11	2.0	12
53	10	61	10	6.8	38
54	9	73	13	6.5	25

TABLE 7 - 5. EFFECT OF VARYING HEATING RATE.

Batch No.	Initial Contents g.	$\bar{y}$ μ	R* μ/min	10^{-6} n_1	$\bar{s}$ μ
44	680	55	10	9.8	26
45	1270	65	8	8.0	19
46	2090	74	11	9.1	18
47	1520	69	12	7.6	26

TABLE 7 - 6. EFFECT OF VARYING AMOUNT OF SOLUTION IN BATCH.

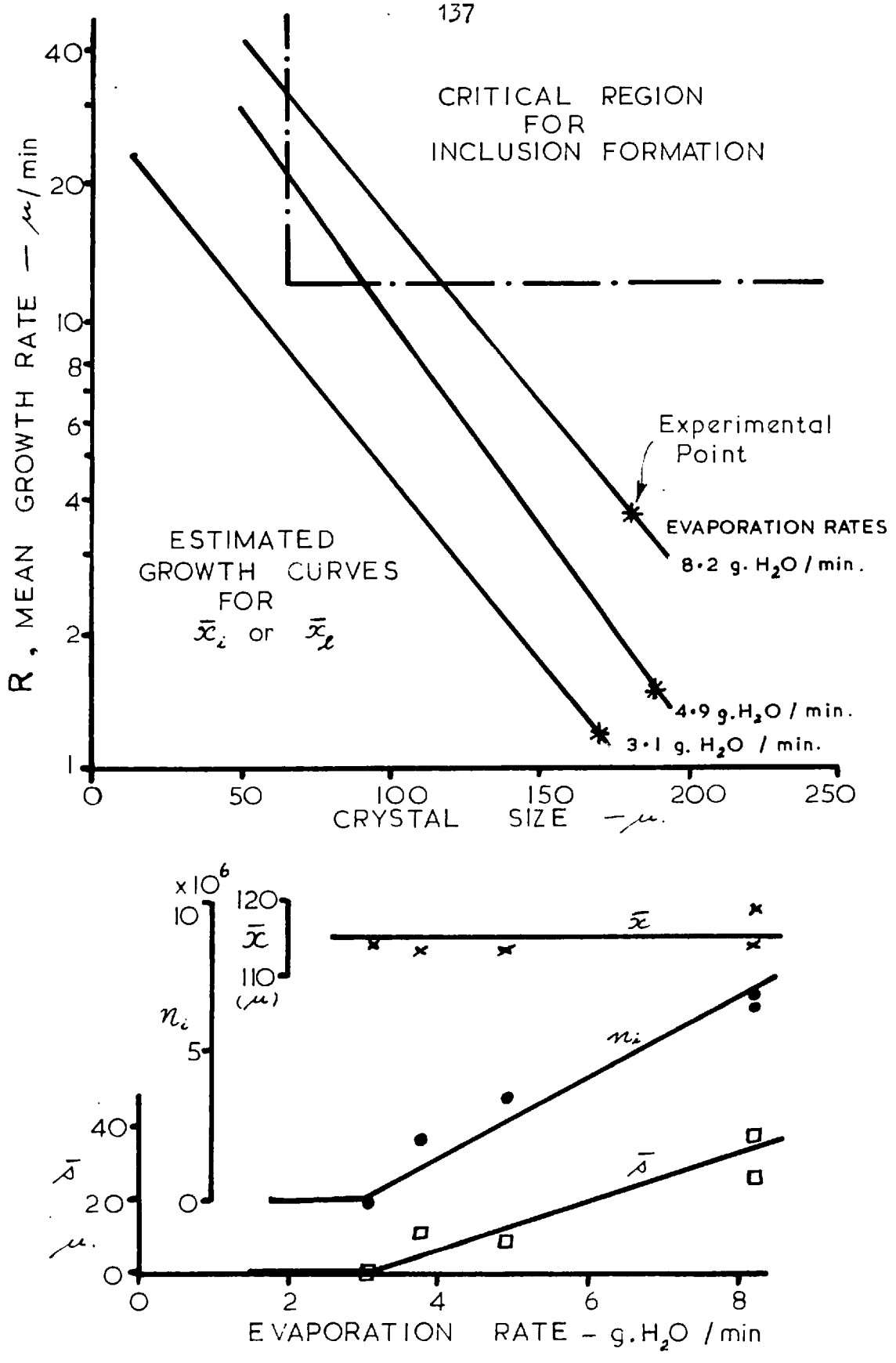

FIG. 7-31 A. EFFECT OF EVAPORATION RATE ON THE FORMATION OF INCLUSIONS IN HEXAMINE. BATCHES No 51-55. (40 °C, 70 RPM)

Thus the effect of the heating rate on inclusion formation is just its direct effect on the rate of growth. The growth curves will simply be displaced by amounts proportional to the change in heating rate (see Fig 7-31A). The amount of inclusion formation will depend on the extent of penetration of the growth curves into the critical region.

It is rather interesting that the same number of crystals is formed in each of these batches, while such different times of crystallization were used at the same stirrer speed. This suggests that the rate of crystallization is not governed by stirrer speed alone, but must be influenced by the evaporation rate or the amount of crystal in suspension.

Other batches of crystal were grown with differing amounts of solution present (Table 7-6). The amount of solution had no noticeable effect on any of the quantities measured.

7.11 RESULTS WITH THERMAL CRYSTALLIZER

In the thermal crystallizer (the heated cell) the growth of individual crystals can be followed.

7.11.1 Mechanism of Inclusion Formation

The growth of several crystals under the microscope is shown in Fig 7-32. Two examples are shown of crystals growing without inclusion formation, and two of crystals in which inclusions form.

The mechanism of inclusion formation is exactly the same as that already described. The various stages in the growth of inclusions - plane growth, cavitite formation, inclusion sealing, and further plane growth can be seen in the photographs. Because the crystal sits on a solid surface, it does not

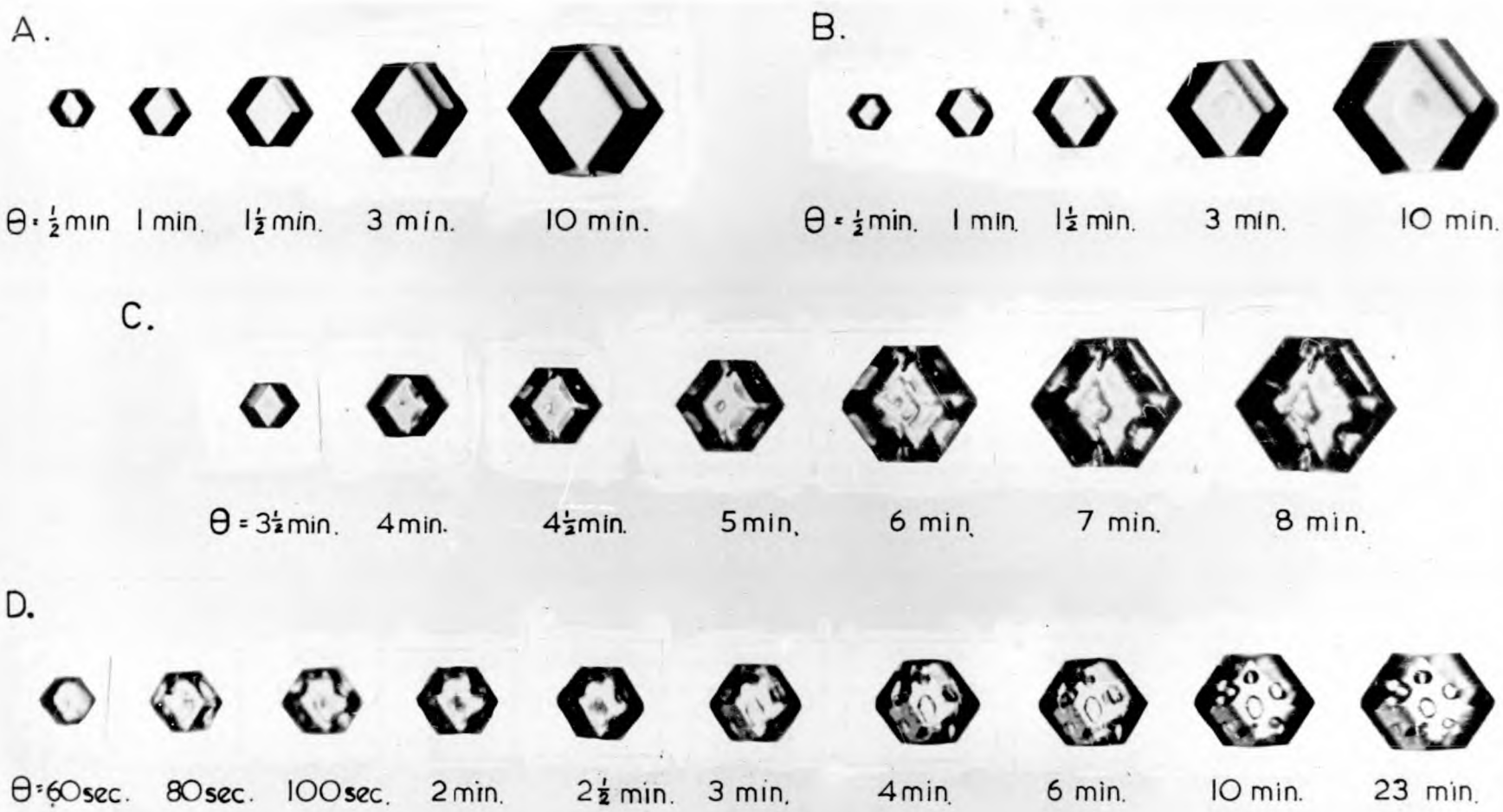

FIG. 7-32. GROWTH OF HEXAMINE CRYSTALS FROM AQUEOUS SOLUTION.
A,B : Without inclusions ; C,D : With inclusions . [x 120]
[A,B Test 28 Crystals 22,23 ; C, Test 38 Crystal 11 ; D, Test 12 Crystal 9 .]

grow equidimensionally in all directions (see Fig 7-33). The pattern of inclusions observed, therefore, is quite distorted and not as symmetrical as those obtained from the evaporative crystallizer.

7.11.2 Growth of Inclusions on Large Crystals

Placing an unblemished seed crystal in the crystallizing cell, and increasing the solution supersaturation quickly, will cause inclusion cavities to start forming on the once plane crystal faces (Fig 7-34). This will occur irrespective of the size of the initial seed crystal (provided it is over 65μ). The same effect can be obtained in the evaporative crystallizer by using large plane faced seed crystals. Several examples of crystals grown in this way are shown in Fig 7-35.

The cavities appear as large, flat, approximately diamond-shaped depressions in the centre of each face. The thickness of the growing face either side of the depression is of the same order as that measured previously for the cavitites (section 7.4). This means that the shape of the cavity corresponds to the truncated continuation of the rhombic pyramidal shape previously described. With large crystals the supersaturation is rapidly depleted, and the crystals seal over after little growth, forming very thin plate like inclusions.

7.11.3 Measurement of Growth Rates

The size of each crystal after various intervals of time can be measured from the photographs taken. The average growth rate of each face over each interval of time can then be determined from the increase in size.

Because the crystal sits on one face in a very poorly agitated solution, it does not grow equidimensionally. For example, the change in shape and size

FIG. 7-33. INCLUSIONS IN HEXAMINE CRYSTALS GROWN IN HEATED CELL.

[x 100]

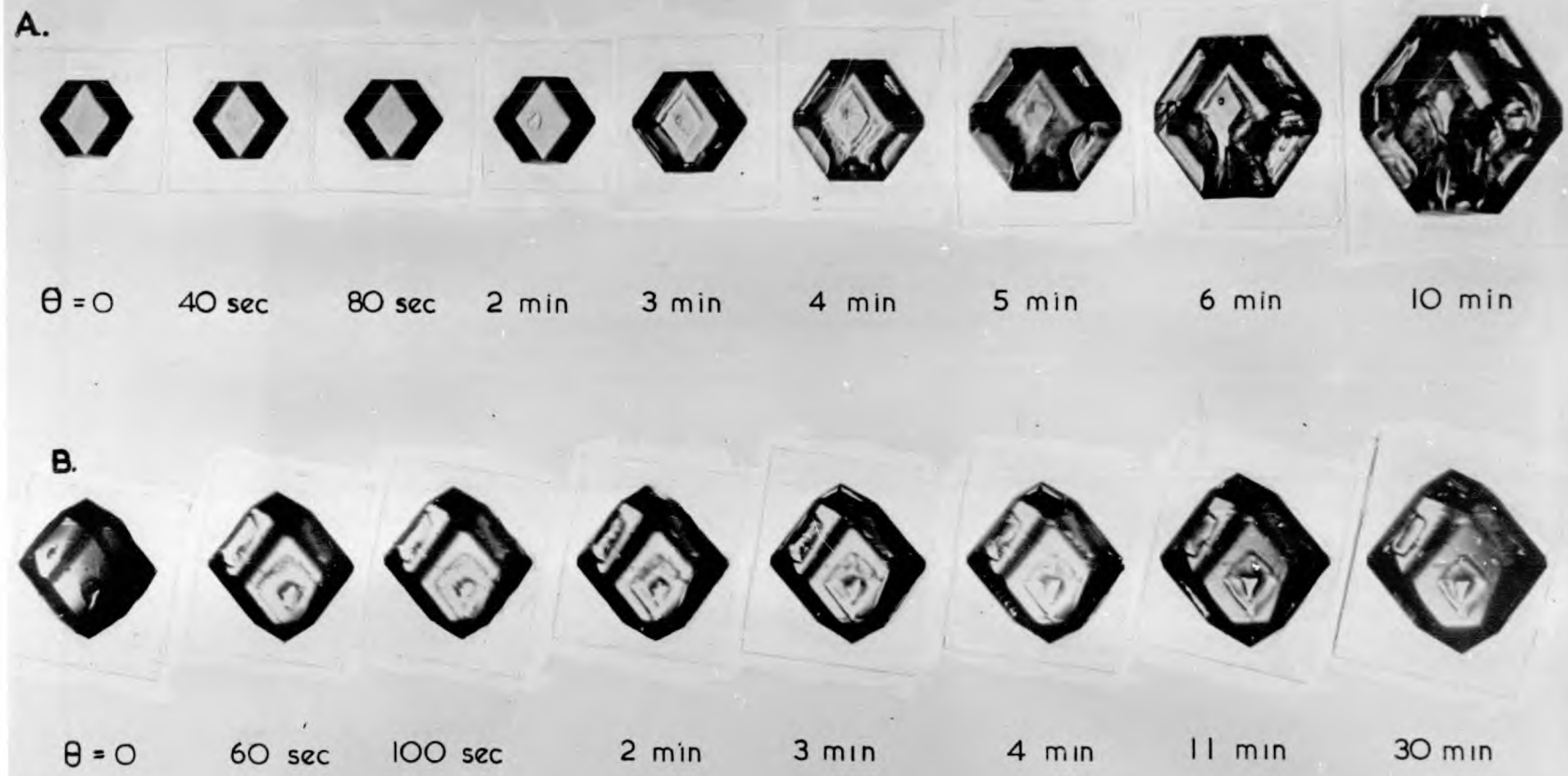

FIG. 7-34. GROWTH OF FACE INCLUSIONS ON LARGE SEED CRYSTALS
[A. - Test 32, crystal I ; B. - Test 20, crystal 16 .] [x 75]

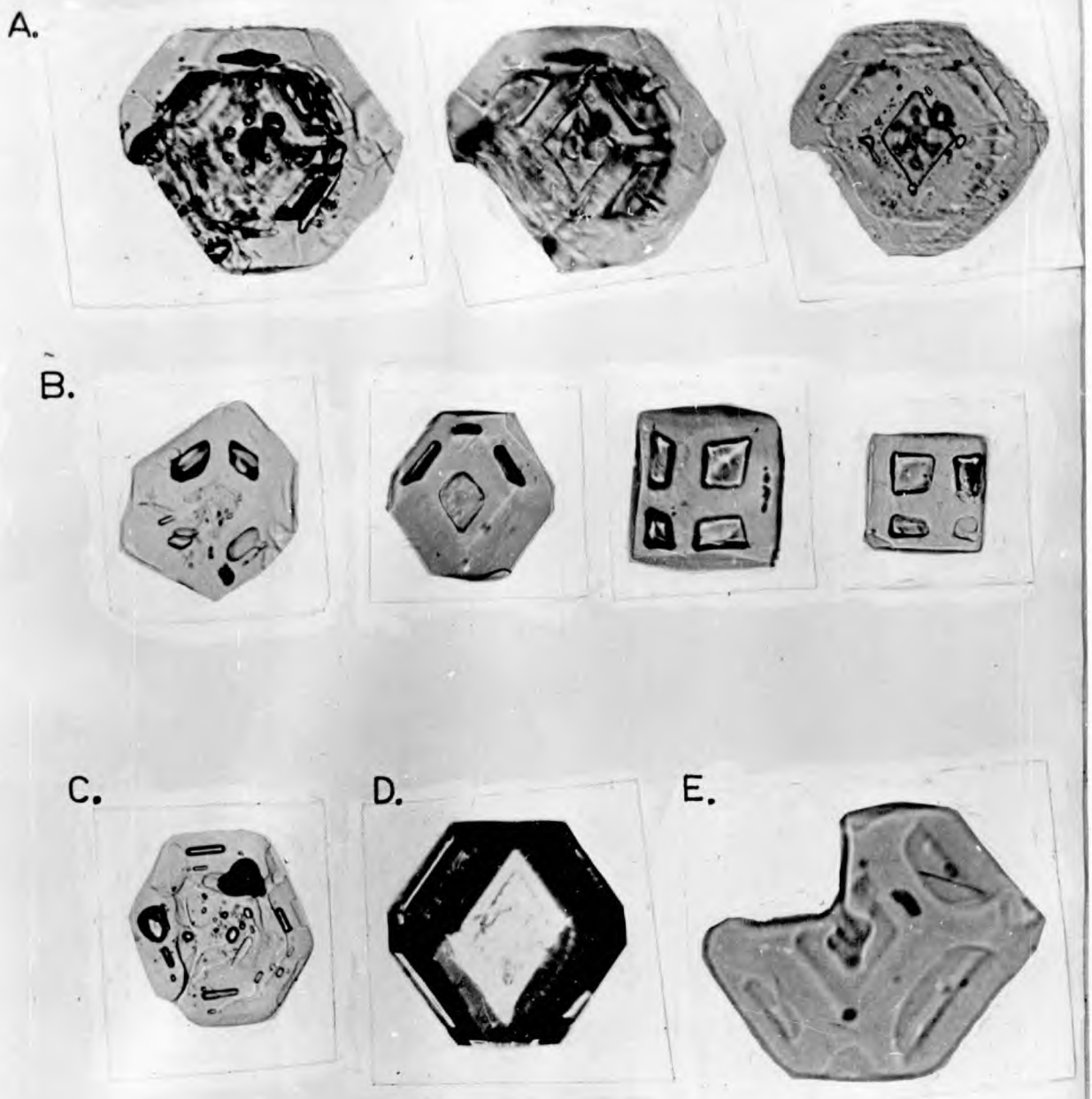

FIG. 7-35. SHAPE OF INCLUSIONS GROWN ON HEXAMINE SEED CRYSTALS.

A. Batch crystal. Photographs at different depths of field and different stages of dissolution. [Aniline ; x 75].

B. Crystals grown on slide. [Aniline ; x 75].

C. Batch crystal. [Aniline ; x 75].

D. Crystal grown on slide. [Aqueous solution ; x 75].

E. Batch crystal. [Aniline ; x 200].

with time for one of the crystals shown in Fig 7-34 is illustrated in Fig 7-36. Crystal growth occurred on a regular seed crystal initially showing the usual dodecahedral {011} faces. It can be seen that growth occurred at different rates on different faces, with the consequent change in shape. It can also be seen that cubic {001} faces developed as well initially, then started to diminish. This means that at first (at high supersaturations) the rate of growth on the cubic faces is less than that on the dodecahedral, and the cubic develop at the expense of the others. After a time the preference is reversed (Fig 7-36). Cubic faces may have developed likewise on crystals grown in the evaporative crystallizer, but because of the examination of samples immersed in aniline, they could easily have passed unobserved.

Since the crystal grows non-equidimensionally, it is necessary to be quite careful in designating the faces on which measurements are made. The majority of the crystals observed lay on a face as shown in Fig 7-36. The distance x was measured. This corresponds to the growth of the pair of perpendicular faces. The computed growth rate was the average for the two faces. The crystal size and growth rate for the crystal of Fig 7-36 are shown in Fig. 7-37.

Since the face observed is generally a perpendicular one, it is difficult to estimate the moments when cavity formation begins and ends. It will not necessarily be the same as for the upper flat faces where the change can be readily detected. However estimates of the range of conditions over which these changes took place were made.

The fit of the experimental data to this growth rate plot (Fig 7-37) is rather better than for most of the other crystals measured, mainly because

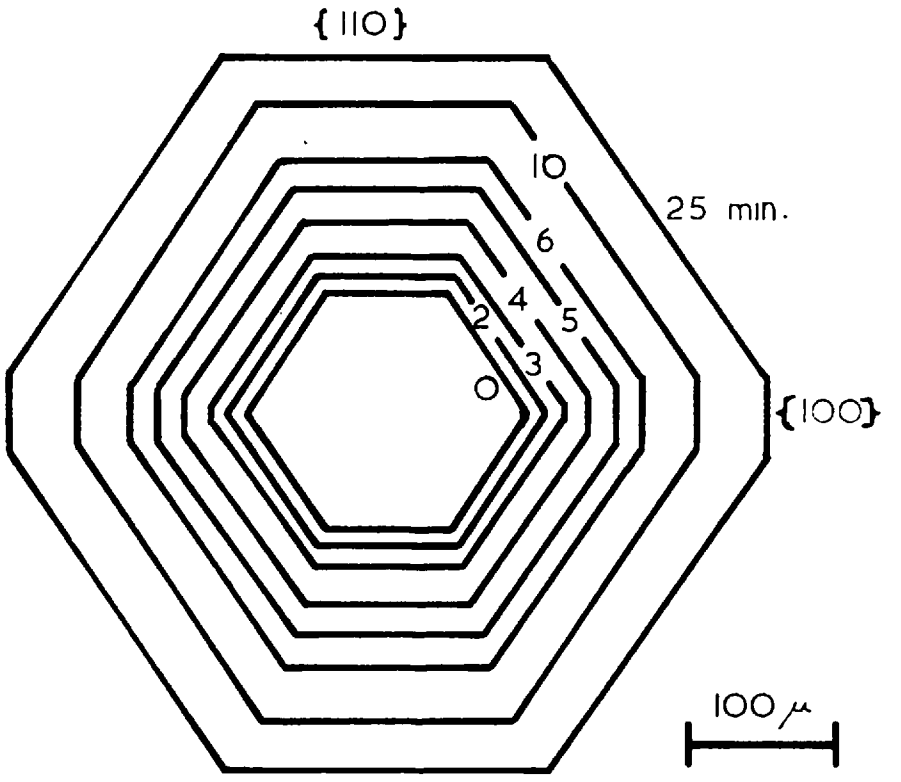

SIZE OF CRYSTAL AFTER VARIOUS TIMES.

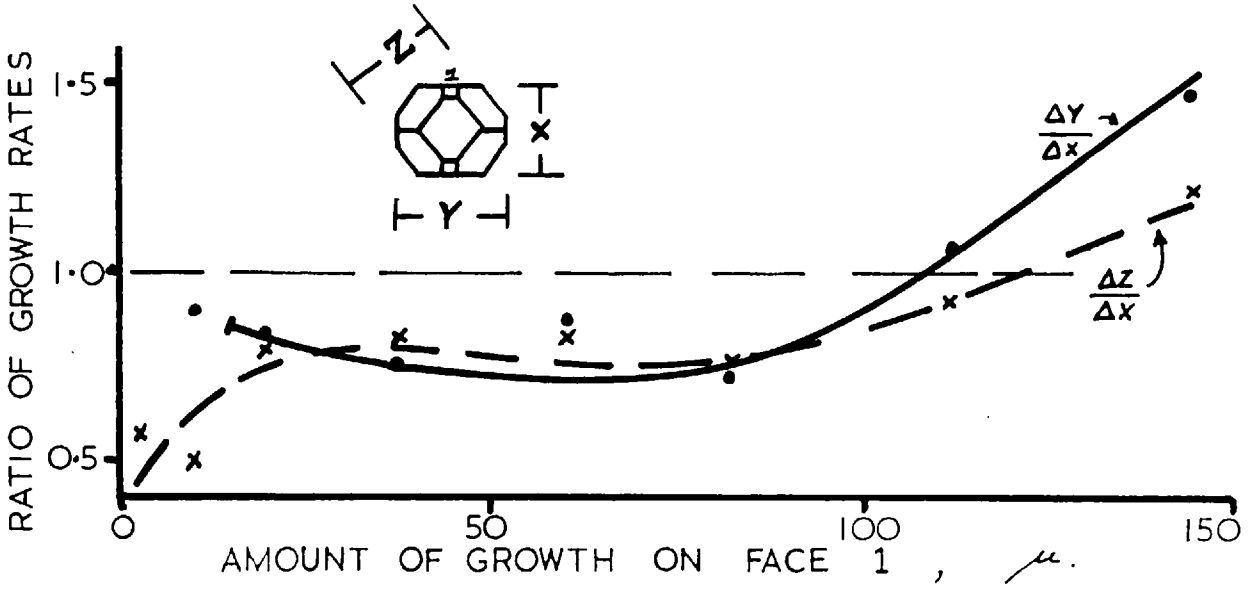

FIG. 7-36. GROWTH OF CRYSTAL , TEST No 32.

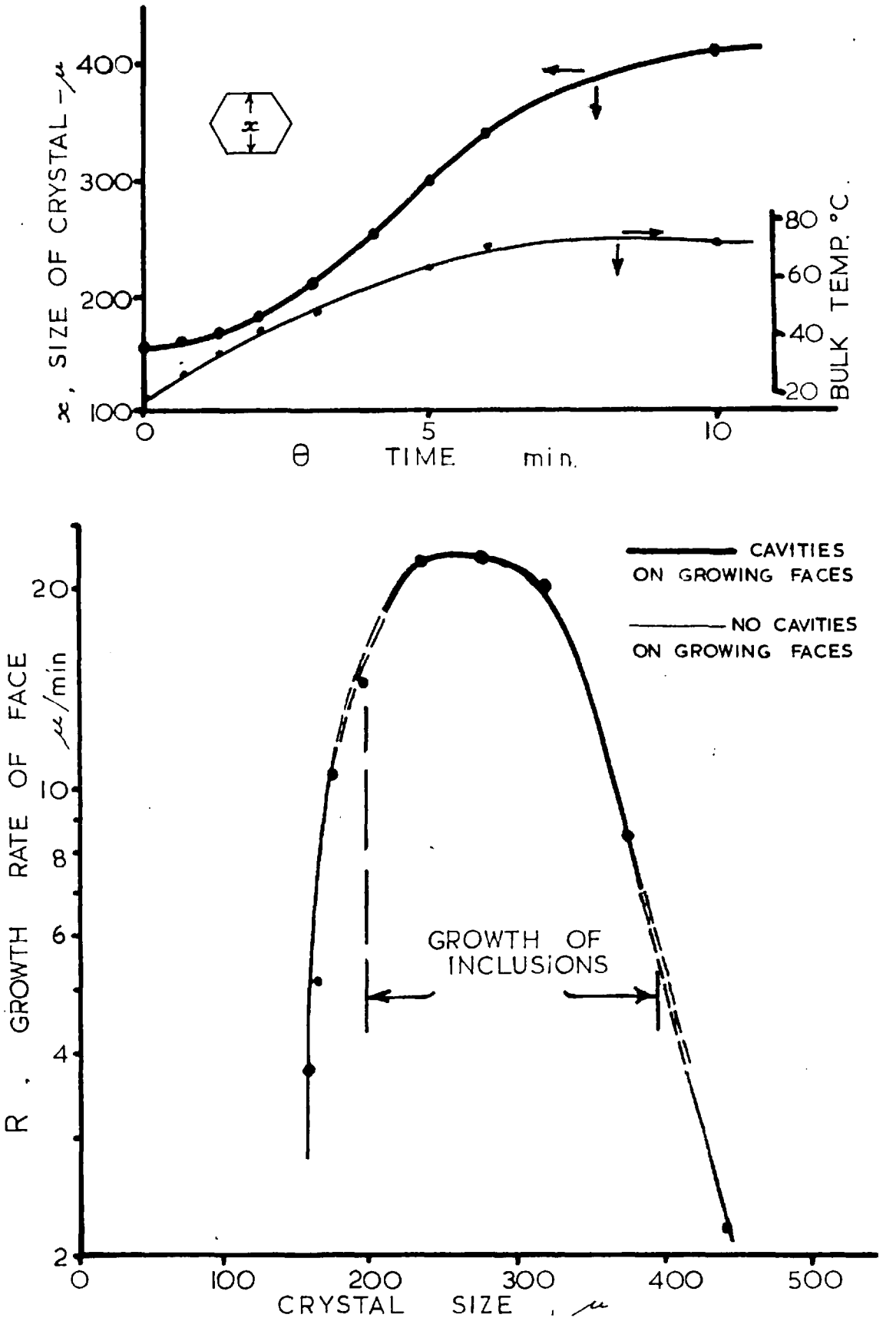

FIG. 7-37. GROWTH OF CRYSTAL. TEST No 32.

this crystal grew quite considerably. Certain inaccuracies are present in the method of computing growth rates. If too small a time interval is chosen, errors in measuring the small changes in size give rise to enormous fluctuations in the computed growth rate. If too large a time interval is chosen, actual variations in the growth rate are averaged out. This can be particularly serious about a maximum in the growth rate.

7.11.4 Comparison with Critical Growth Conditions

The growth rate curves (growth curves) of crystals observed in the heated cell may be compared with the results obtained from the evaporative crystallizer. In Fig 7-38 the growth curves for several of the crystals which nucleated and formed inclusions are compared with the critical growth region determined previously. In Fig 7-39, are shown the curves for several of those crystals which grew from nuclei but did not form inclusions. It was not possible to follow the early stages of growth of many of the crystals shown in Fig 7-38 and 7-39 because of the time required initially to focus the microscope and manipulate the camera. Fig 7-40 shows the growth curves for crystals which formed inclusions when grown from seed crystals. The corresponding curves for the growth on seed crystals where inclusions did not form are shown with the other curves on Fig 7-39.

As a whole, these typical growth curves are in substantial agreement with the defined critical region. Most of the inclusion formation takes place when the growth curves are inside this critical region and little when they are outside it. There is some variation with individual growth curves. This may be due mainly to errors in measurement. However, it should be noted that individual crystals, with their inherent variation are being measured, whereas

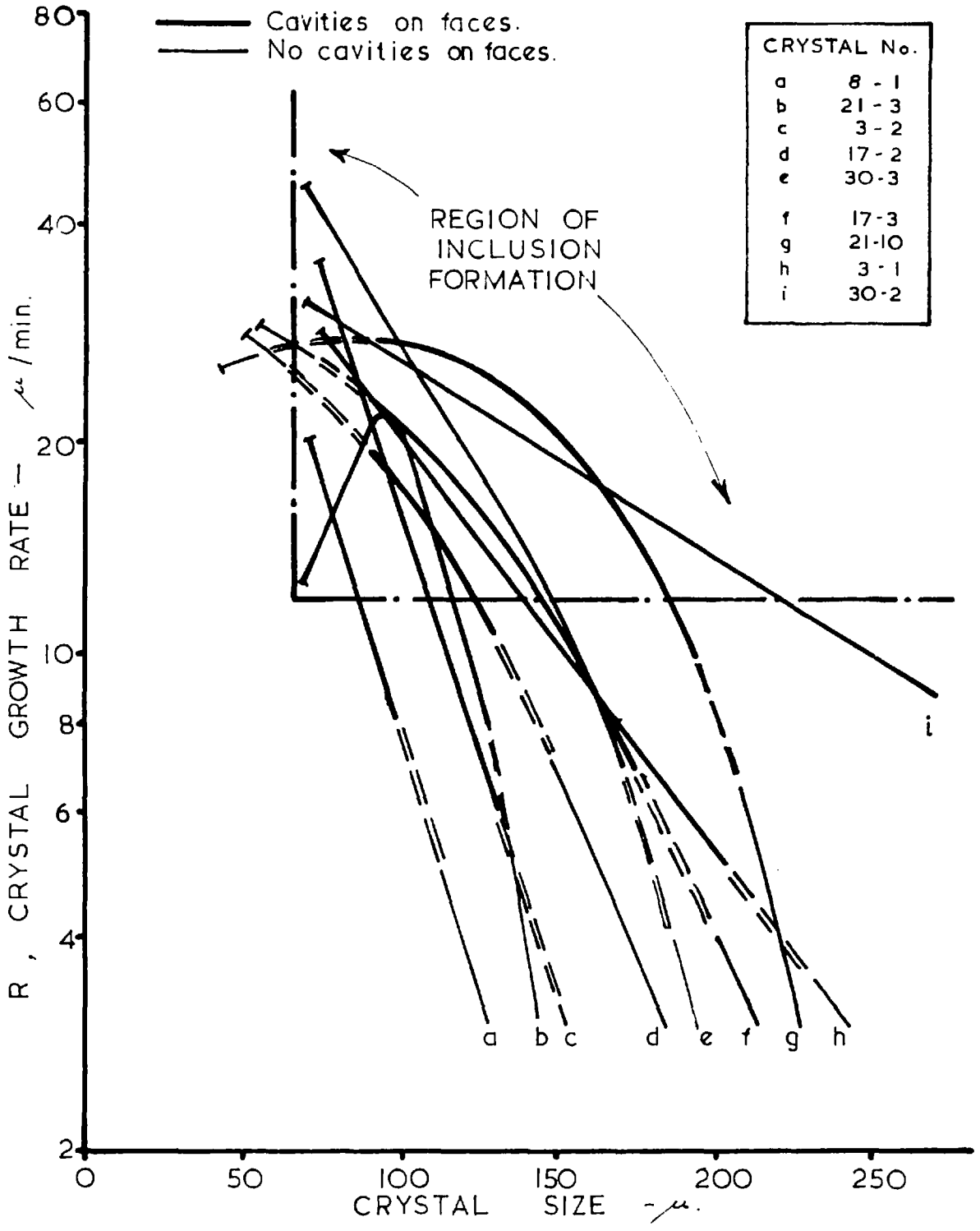

FIG. 7-38. TYPICAL GROWTH CURVES OF CRYSTALS WITH INCLUSIONS.

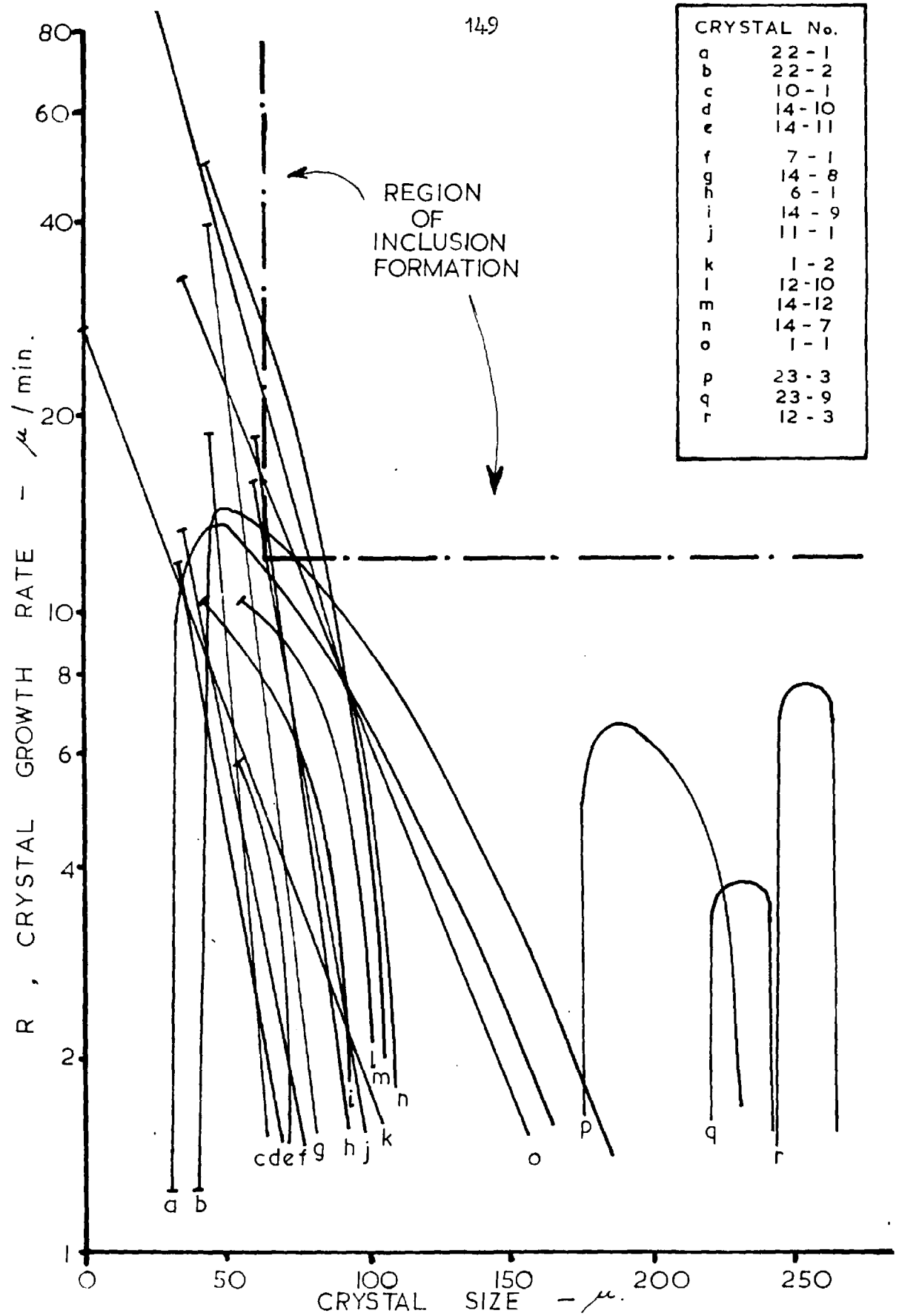

FIG. 7-39. TYPICAL GROWTH CURVES OF CRYSTALS WITH NO INCLUSIONS.

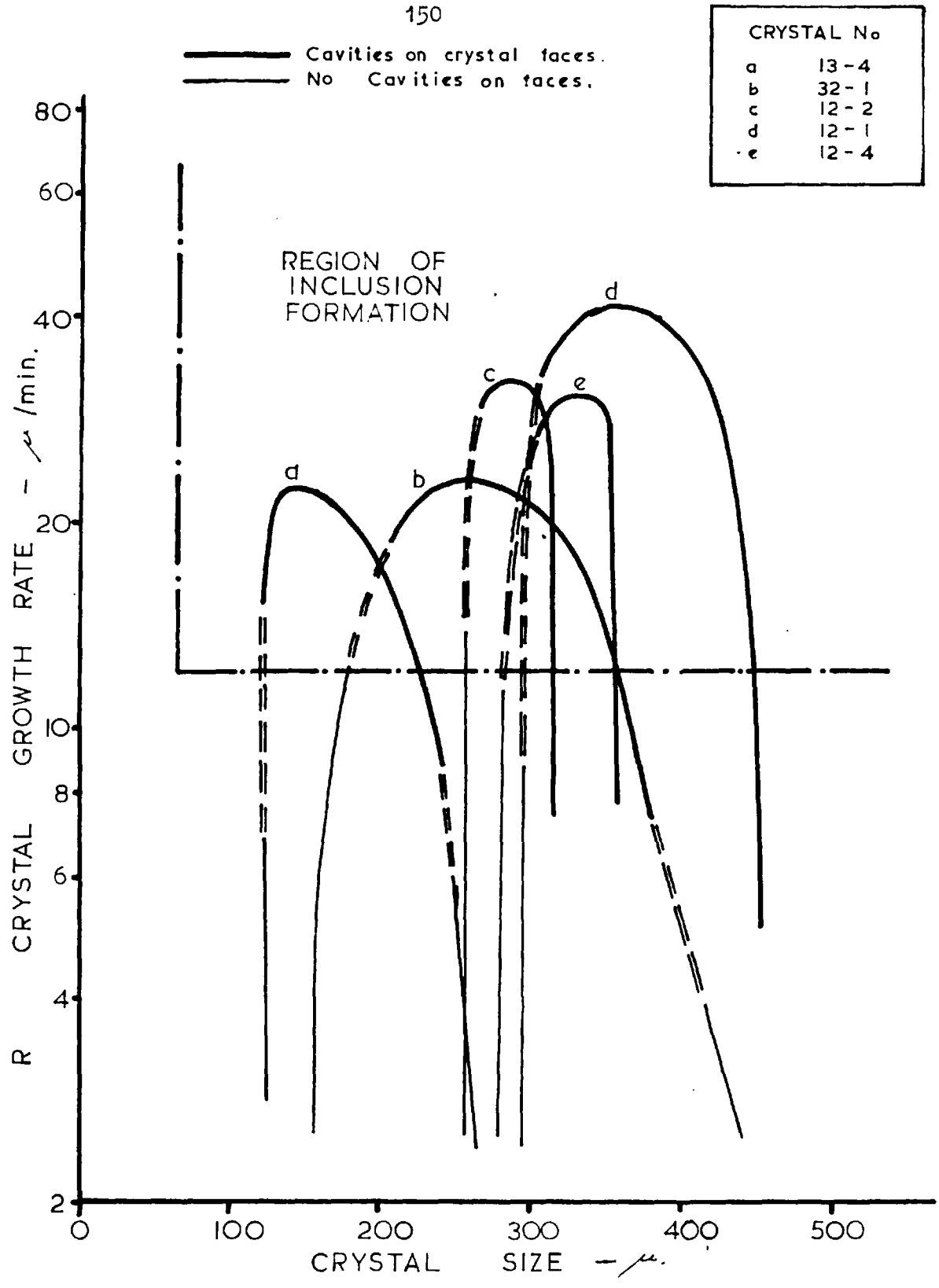

FIG. 7-40. TYPICAL GROWTH CURVES FOR CRYSTALS WITH INCLUSIONS GROWN ON SEED CRYSTALS.

the critical growth region proposed is a statistical mean quantity (see also section 7.8.6).

That the results agree with the critical growth conditions already determined, is of considerable interest. Whereas the critical conditions had been determined from experiments with highly agitated solutions, in the heated cell the solution was unstirred. The range of conditions for which an explanation by a critical growth region is applicable has thus been extended. Also, added confirmation is given that the critical growth rate is a suitable criterion of the critical growth conditions, and that having chosen a critical growth rate, agitation rate affects inclusion formation only through its effect on nucleation.

It is also of interest that the same critical values apply to the formation of inclusions on quite large seed crystals. This shows that the formation of face inclusions can be explained for all sizes of hexamine crystals up to, at least, 400μ. Thus it is possible to grow a series of concentric inclusion patterns in the one crystal by continually causing the growth curve to rise and fall through the critical growth region. A double set of inclusions formed in such a way is shown in the first of the crystals of Fig 7-35.

The effect of the number of nuclei appearing in the heated cell is similar to that observed in the evaporative crystallizer. When many nuclei appear, no inclusions are formed since the mean growth rate is low. When only a few appear, growth is rapid and large inclusions are formed.

7.11.5 Supersaturation

Solutions in the heated cell were supersaturated by increasing the temperature. Since solution temperatures were measured, it was possible to make a rough estimate of the prevailing supersaturation. For the crystal considered

in Fig 7-36 and 7-37 the supersaturation (defined as the relative change in the saturation concentration - refer Fig 5-1) was about 0.03 when the growth rate reached the critical value of 12μ/min at about 55°C. This value is of use only as a rough guide since growth conditions in the cell are quite complicated and highly non-uniform.

Several attempts were made using this cell and other apparatus to determine, under known agitation conditions, the relationship between growth rate and supersaturation. Because of excessive nuclei formation in all the supersaturated solutions used, these attempts were unsuccessful.

For the growth of hexamine from vapour, it has been shown [44] that the growth rate is proportional to the square of the supersaturation for microscopically plane surface, but only proportional to the supersaturation for the more usual flawed surface.

7.12 SHAPE CHANGES OF INCLUSIONS

The inclusions in hexamine crystals form in the shape of rhombic pyramids (or for large faces, as portions thereof). After a time the shape changes to that of a negative crystal with {011} faces. The time required for this change varies from a few minutes to a few days.

The first change in shape is the appearance of a plane face in place of the tip of the pyramid (Fig 7-41). Further changes appear as the introduction of other faces.

The internal faces of an inclusion would eventually rearrange to give a negative crystal, since this represents the conditions of minimum free energy. However, this is likely to be a very slow effect, the forces involved being so small. Much more rapid effects appear to be caused by temperature variations, as

FIG. 7-41. CHANGE OF SHAPE OF INCLUSIONS IN HEXAMINE CRYSTALS WITH TIME. [x 120]

(NOTE :- These are different crystals from consecutive samples from the same batch.)

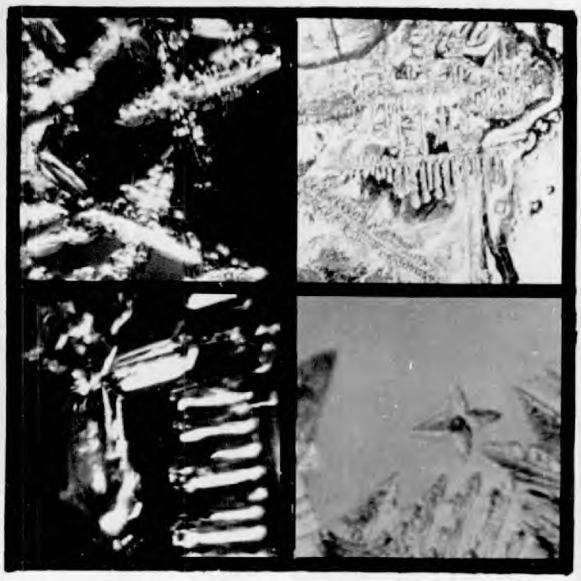

FIG. 7-42. TYPICAL APPEARANCE OF DENDRITIC HEXAMINE FORMED ON THE SURFACE OF EXPOSED SOLUTION.

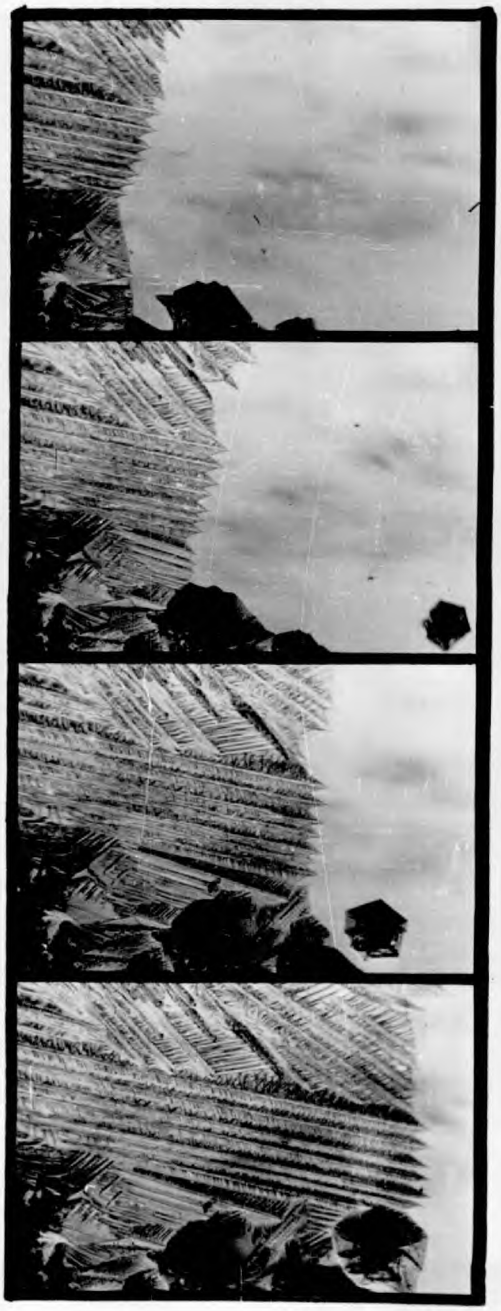

FIG. 7-43. GROWTH OF DENDRITIC SPIKES OF HEXAMINE.

(PHOTOGRAPHED AT 5 SECOND INTERVALS.)

[x 40]

follows. When a crystal of hexamine is cooled, the inclusions dissolve solute from the walls; when the crystal is reheated, the solute redeposits. The redeposition will tend to take place on the planes associated with the negative crystal, and the shape changes. The crystals shown in Fig 7-41 were treated in this way, with samples taken after successive temperature cycles.

A change in shape can also be caused by a temperature gradient across an inclusion. For hexamine, solute will dissolve from the colder edges of the inclusion and deposit on the hotter. In the transfer the inclusion will tend to change to a more regular shape. It may be noted that the position of the inclusion will change also, i.e. the inclusion will move. For hexamine, the inclusions will migrate down the direction of the temperature gradient. This effect has been discussed by Hurle [6, 7] for gallium rich inclusions in germanium crystals. In his experiments the temperature gradients are formed because a cooled rod is pulled from a hot melt.

7.13 DENDRITIC GROWTH OF HEXAMINE

Hexamine can be grown in the dendritic form (refer Supplement). From aqueous solution dendrites will form on the surface of saturation solution exposed to the air. These dendrites (Fig 7-42) are cross-shaped with spikes at right angles. In three dimensions they would be expected to appear as six-spiked dendrites with the spikes in directions mutually at right angles. It was not possible to verify this shape experimentally, since presumably, because of the inability of achieving high enough supersaturations, dendrites of hexamine could not be grown in bulk solutions. However, there is little reason to doubt that the shape would be otherwise than that described.

The directions of the dendrite points are those of the cubic $\{001\}$ axes.

These correspond to the six sharpest corners of the dodecahedron, those furthest from the centre. If the dendrite develops from the plane-faced dodecahedron, it must therefore be through the very rapid growth of these corners as columns or spikes. Each spike would be surmounted by four dodecahedral faces.

Dendrites grow very rapidly. The rate of translation of the dendrite needles shown in Fig 7-43 is of the order of 3000 to 4000 μ/min. Measurements on other examples gave growth rates usually in excess of 100 μ/min. Even allowing that for an isometric dodecahedron the corners grow at a rate $\sqrt{2}$ times that of the faces, these values are well above the growth rates measured for the polyhedral crystals.

7.14 THEORETICAL INTERPRETATION OF RESULTS

It has been shown that inclusion formation can be explained in terms of cavitite growth occurring above a critical size and a critical growth rate. It needs to be asked, what is the significance of these results in terms of basic mechanisms on the molecular level?

The most likely interpretation is one involving the effects of non-uniform diffusion around the crystal corners. Bunn [14] has explained the formation of inclusions in ammonium chloride by just such a mechanism of 'convergent diffusion'. The same mechanism could well apply to inclusions in hexamine crystals.

It is considered that the rate at which solute diffuses to the corners of a growing crystal will be greater than that to the rest of the face, because the corners are sharp angled and protrude further into the supersaturated solution. Mathematical descriptions of this behaviour, based on the diffusion equation, have been presented by Chernov [29, 30] and Seeger [31]. However, measurements

of the diffusion fields about large single crystals [32,33] indicate that conditions are not so simple as are usually assumed.

If the rate of deposition of solute is higher at the corners than at the centre of the faces then at low supersaturations there must be some compensating mechanism, because then crystals usually grow with plane faces. This mechanism may cause a buildup of supersaturation across the surface averaging out the diffusion rates, or it may cause a migration of material across the surface so that plane growth is maintained.

At higher supersaturations this mechanism must break down or be overwhelmed. The rate of deposition on the edges and corners then becomes excessive and the crystal grows as a cavitite (or 'incipient dendrite'). The critical growth rate as measured must, somehow, be linked to the breakdown conditions of the compensating mechanism. The critical crystal size is possible some measure of the limiting size of the region around the growing edges which is influenced by the convergent diffusion effect.

At higher supersaturations still, the growth at the corners becomes even more excessive and the crystal grows corner-wise as a dendrite.

The cavitite is thus considered as a stage of growth between the polyhedral ('equidimensional' or 'isometric') plane-faced crystal and the dendritic form. For hexamine, the shape of the crystal, cavitite, and dendrite are in accordance with the concept of consecutive changes from one form to the next. The same is true for ammonium chloride (Bunn [14], see also section 9.2.4).

For hexamine, limits have been found for the first transformation - polyhedr to cavitite. Perhaps similar conditions exist for the second transformation.

Mechanisms involving surface adsorption of impurity cannot be ruled out entirely, although because of the great regularity of the formation of inclusion

and because of the success of the explanation involving a constant critical growth rate, they appear very unlikely. Adsorption mechanisms may, however, be a cause of randomly distributed inclusions in hexamine crystals such as those shown in Fig 3.1. It is also possible, of course, that the cause of these inclusions may be some localised modification of the growth rate mechanism described above, occurring under non-uniform growth conditions.

7.15 CONCLUSIONS

A study of growing hexamine crystals has led to a proposed mechanism for the formation of inclusions in face patterns in these crystals. The mechanism involves a falling crystal growth rate together with a critical region of conditions in which the crystal grows with cavities on its faces.

Measurements of consecutive samples taken from a batch crystallization show that this critical region can be defined by two quantities, a critical size of 65 $\pm$ 5μ, and a critical growth rate of 12 $\pm$ 3 μ/min. These critical quantities are unaffected by the operating conditions used in crystal growth. The effect of the operating conditions can be interpreted through their effect on nucleation rates. The results are confirmed by experiments on two different types of crystallizer.

The form of growth occurring in the critical region (cavitite growth) appears to be an intermediate form of dendritic growth. It is probably caused by non-uniform diffusion processes about the corners of rapidly growing crystals.

8. THE EFFECTS OF IMPURITIES AND DIFFERENT SOLVENTS

8.1 INTRODUCTION

So far hexamine crystals have been grown only from reasonably pure aqueous solutions. It is the purpose of this chapter to consider the growth of hexamine crystals either from aqueous solutions to which impurities have been added, or from other non-aqueous solvents.

8.2 THE ADDITION OF SURFACE ACTIVE IMPURITIES

In three batches in the evaporative crystallizer (Batches No. 3, 35 and 56) quantities (respectively 5, 15 and 30 ml) of concentrated 'Lissapol' detergent were added to the batches of solution (about 1200 ml.). This introduced some difficulties with frothing in the early stages of evaporation, but provided agitation was kept below a reasonable limit, these subsided before nucleation began.

The results of these batches are given in Appendix III and in Table 8-1. The results were analysed by the method outlined in Section 7.10 (although it should be noted that the assumptions upon which this method is based need not necessarily hold when impurity is present.) The results do not differ in any significant way from the results already obtained with pure solutions. They give the same critical growth values and much the same size of inclusion in the product. It would appear, therefore, that this surface active agent has no effect on the growth conditions for inclusion formation or on the nucleation conditions in the crystallizer.

Some of the crystals from these batches showed a rather unusual haziness about the pattern of inclusions as shown in Fig 8-1a. The marks appear to be

BATCH No.	CRITICAL SIZE, $\bar{y}$ μ	CRITICAL GROWTH RATE, R* μ/min.	10^{-6} n_i	MEAN INCLUSION SIZE, $\bar{s}$ μ
3	68	8	8.5	16
35	71	13	7.2	23
56	66	11	6.4	40
57	67	10	10.4	15
75	-	>3	-	-
76	-	>3	-	-
77	62	9	8.5	39
78	56	9	7.5	48
79	65	7	14	14
80	72	6	18	15
81	-	>10	-	-
ERRORS	±10	±5	±3	± 5

TABLE 8 - 1. RESULTS FROM BATCHES OF HEXAMINE CRYSTALS GROWN FROM IMPURE SOLUTIONS.

A. PATTERN HAZINESS (WITH ADDITION OF DETERGENT).
BATCHES No. 35, 56. [x 120]

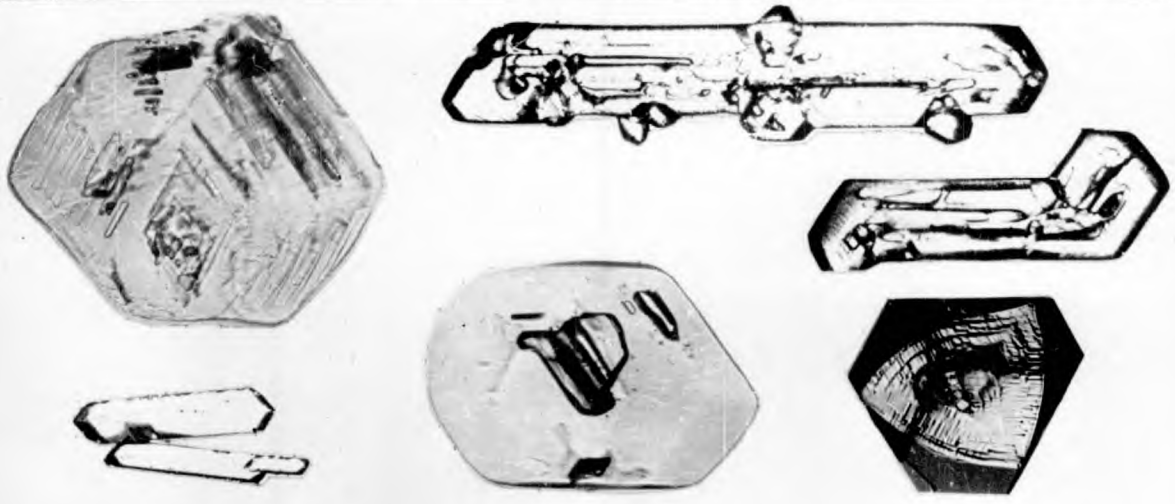

B. VARIOUS CRYSTALS GROWN FROM ETHANOL AND METHANOL SOLUTIONS, SHOWING SURFACE IRREGULARITIES OR DISTORTED SHAPES. [x 50]

C. CRYSTALS WITH DOUBLE PATTERN OF INCLUSIONS.
BATCHES No. 23, 41. [x 120]

D. HEXAMINE CRYSTAL DISSOLVED AWAY TO LEVEL OF INCLUSIONS. [x 120]

FIG. 8-1. HEXAMINE CRYSTALS OF UNUSUAL APPEARANCE.

associated with each individual inclusion, but their immediate cause is not apparent.

8.3 THE ADDITION OF OXALIC ACID

In one batch (No. 57) a quantity of oxalic acid was added to the batch. The analysis of this batch (Appendix III and Table 8-1) shows that the critical growth conditions are apparently unaffected. However the size of inclusions are somewhat smaller than would have been expected for the pure solution. Apparently the presence of the oxalic acid increased the number of nuclei, probably by the addition of foreign nuclei with the oxalic acid crystals.

8.4 THE USE OF VISCOUS ADDITIVES

It was decided to investigate the effect of the viscosity of the crystallizing solution on the formation of inclusions in hexamine crystals. The use of glycerol and sucrose as additives was considered but the quantities required to give an appreciable viscosity change appeared excessive.

It is known that certain substances such as carboxy-methyl-cellulose (C.M.C.) are powerful viscosity modifiers. Such substances were believed to be present in a readily available wallpaper adhesive ('Polycell') and a quantity of this material was used as a viscosity additive. Less than 1% of additive was required to give a forty-fold increase in viscosity.

Quantities of the adhesive were dissolved in saturated hexamine solution. Before use, the solutions were filtered and slightly diluted. After evaporation and crystallization the viscosity of the mother liquor (as measured by a U-tube viscometer) was determined at the operating temperature. This gave a measure

of the amount of additive present.

With the more viscous solutions it proved very difficult to separate the crystals from the suspension, since settling was extremely slow. This was overcome by centrifuging the samples at several hundred gravities for a few minutes.

Several batches of crystal were grown in the evaporative crystallizer using feedstocks with differing amounts of additive (Batches No. 75-81). Five of the batches (No. 77-81) were grown under identical operating conditions (40°, 60 R.P.M. and full heat). Further details of these batches are given in Appendix III. Photographs of the product are shown in Fig 8-2. It can be seen that with increasing quantities of additive, the size of the inclusions decreases, the crystal size becomes smaller, and the crystals become more irregular in shape. With an amount of additive equivalent to about a tenfold increase in viscosity, inclusion formation is completely prevented.

Although the assumptions previously used may no longer be applicable, these batches have been analysed by the method used for batches with a single sample (Section 7.10). The results are shown in Table 8-1 and Fig 8-3. It can be seen that within the accuracy of the computations, these values are in agreement with the critical values determined for the previous batches. The effect of the additive would appear to be through its effect on nucleation conditions. Increasing the quantity of additive increases the number of crystals formed per batch.

As a solution becomes more viscous, the supersaturation required to promote crystal growth tends to increase, and thus the rate of nucleation tends to increase. This may be the explanation of the results obtained. The additive

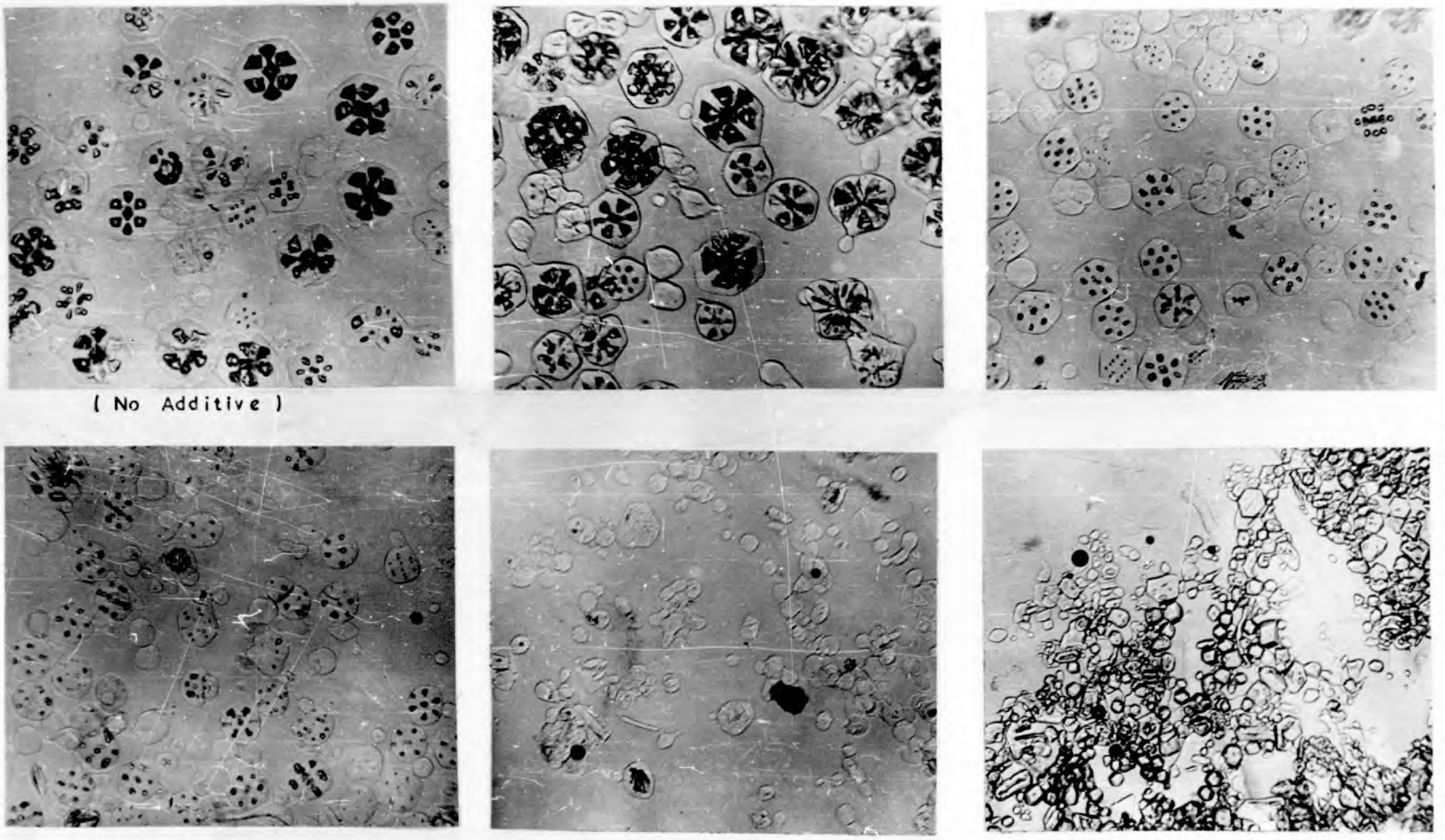

FIG. 8-2. EFFECT OF INCREASING AMOUNTS OF VISCOSITY ADDITIVE ON THE CRYSTALLIZATION OF HEXAMINE (40 °C , 60 RPM , Full heat , 5 min .)
(Batches No 77-81, 76 respectively.) [x 55]

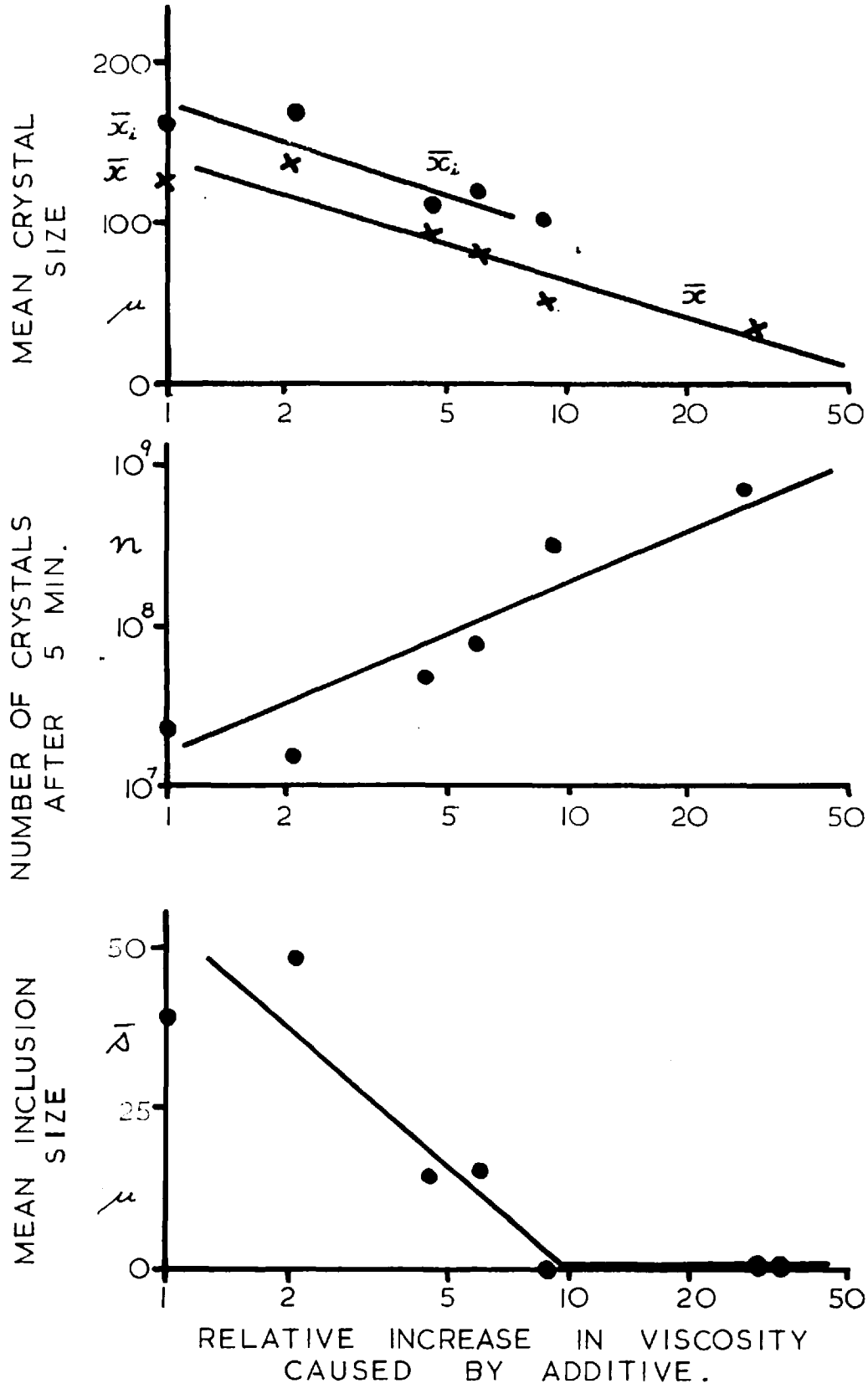

FIG. 8-3. RESULTS FOR BATCHES USING VISCOSITY ADDITIVE.

itself, a source of impurity and foreign nuclei, could also be the cause. It would be interesting to see the effects of other additives, to see if the results are due to increase in viscosity or to the additive itself.

8.5 GROWTH FROM NON-AQUEOUS SOLVENTS

Hexamine crystals were grown in the thermal crystallizer from methanol and from ethanol. Attempts were made to grow crystals from glycerol by cooling saturated solutions but crystals did not form.

Quite large crystals of hexamine could be grown readily from methanol and from ethanol. However, in not one instance were crystals with internal inclusions formed, although in many cases growth rates were much higher than the critical value determined for aqueous solutions. Typical growth curves for crystals grown from methanol are shown in Fig 8-4. Growth rates up to ten times the critical aqueous value were achieved, yet inclusions still did not form. The same results were found for ethanol.

This gives rise to the interesting conclusion that the mechanism of inclusion formation depends on the solvent from which the material is crystallized. A change in solvent would be expected to affect the diffusion field about a crystal, since the solubility is changed and probably also the diffusion coefficient. It could also affect any surface mechanisms occurring. Again the effect of changing the solvent could be due to some interaction between solvent and solute. For example, the possibility exists of some hydrated form of hexamine in aqueous solution. A more detailed investigation on a large number of solvents would perhaps lead to an explanation.

Many of the crystals of hexamine grown from methanol and ethanol often showed a series of shallow depressions on the surface (Fig 8-1b). These were

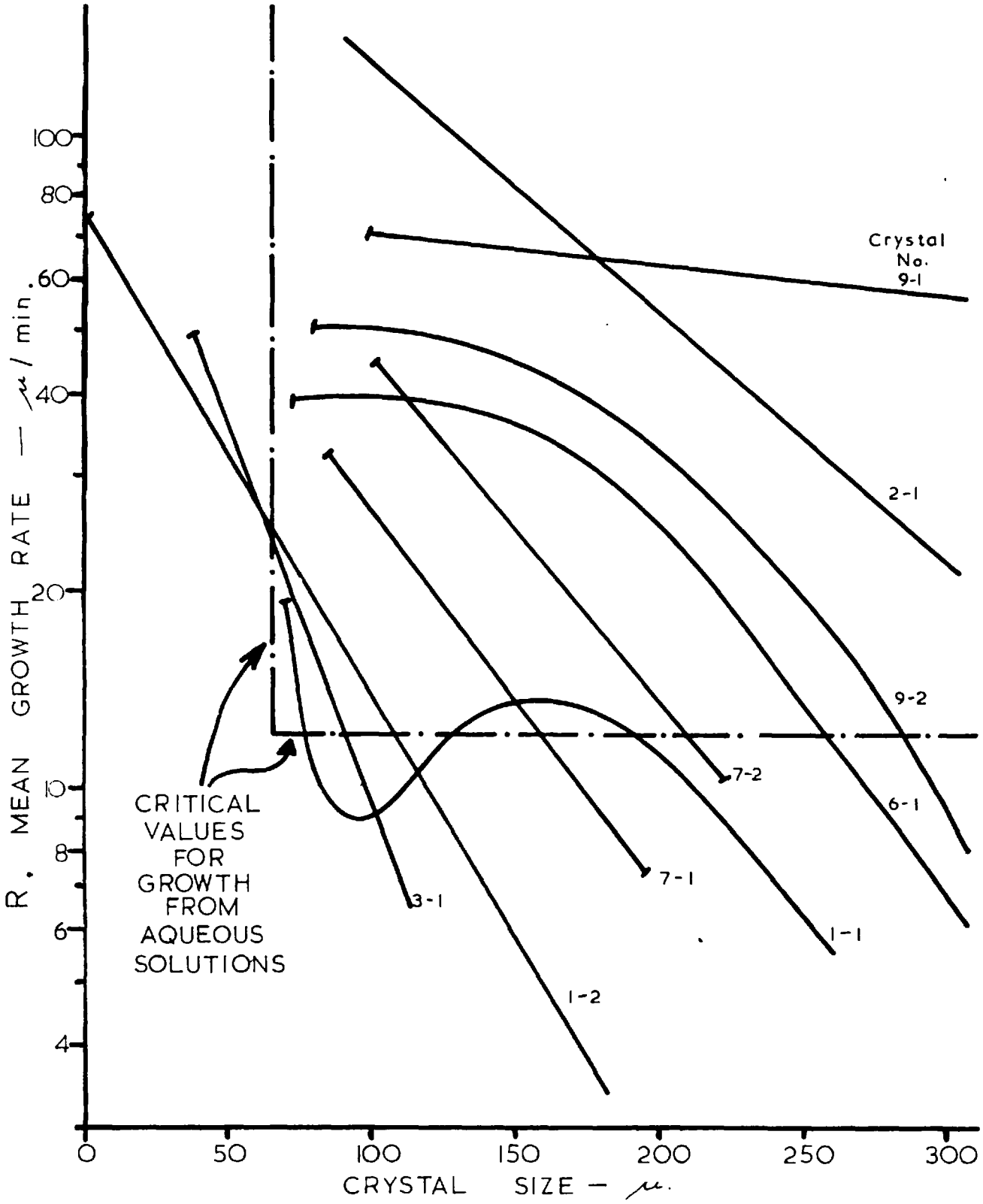

FIG. 8-4. GROWTH CURVES FOR HEXAMINE CRYSTALS GROWN FROM METHANOL.

sometimes ordered and sometimes seemingly irregular. With further growth however they did not fill in or form inclusions. On other occasions irregularly shaped crystals (Fig 8-1b) resulted.

8.6 GROWTH FROM SOLVENT MIXTURES

Hexamine crystals grown from aqueous solution form inclusions; those from methanol do not. Since methanol and water are completely miscible, it was decided to study crystals in the thermal crystallizer growing from mixtures of these two solvents. Solvent mixtures containing 70% to 90% water could not be used since the solubility does not vary sufficiently with temperature (see Supplement). However hexamine crystals with inclusions were obtained from mixed solvents with 50%, 25%, 16% and 9% water (by weight), but not from a 5% solution.

Only very rough estimates of the critical growth rate could be made from these tests. These seem to suggest that the critical growth rate increases with decreasing water content, although the results are by no means conclusive. This would be an aspect of considerable interest for further study. Perhaps the evaporative crystallizer could be modified for this purpose.

8.7 UNUSUALLY SMALL FACE INCLUSION PATTERNS

Very occasionally in the examination of samples of hexamine from the evaporative crystallizer, a crystal was observed which showed two sets of face inclusions (Fig 8-1c). One of these patterns was of the usual size (inside dimensions about 65 μ) while the other was much smaller (about half the size).

It should be emphasised immediately that such crystals are very rare. Only five such crystals were observed in the counting of about one tenth of a million

crystals. So the postulate of a critical crystal size for inclusion formation of 65 ± 5μ is still true for practical purposes.

However these smaller patterns do occur occasionally. It is not immediately obvious how they are formed. All other crystals in the batches from which these crystals were taken had the normal appearance. Perhaps there is a second set of critical conditions leading to inclusion formation with a much higher critical growth rate and a smaller critical crystal size. But why do not the other crystals in the batch show this second pattern? The crystals in which they are observed are not the largest (or by inference, the oldest) in the batch. Perhaps the inner pattern represents portion of the outer inclusion pattern that has detached and migrated inwards because of thermal effects (see section 7.12). But again why does this not occur with the other crystals? Some of the crystals in a batch may have experienced more extreme conditions than the rest, and these crystals might be those with the double patterns. It seems, then, that before a suitable explanation of this behaviour can be obtained it will be necessary to grow such crystals in greater quantities and under controlled conditions.

In some samples of hexamine, crystals with the 'dimpled' appearance shown in Fig 8-1d are observed. These are simply crystals that once contained inclusions, but now have been redissolved back to the level of the inclusions.

8.8 CONCLUSIONS

Batches of hexamine crystals were grown from aqueous solutions to which quantities of a surface active agent or an additive modifying the viscosity were added. In each case the results could still be explained in terms of the critical growth conditions determined for pure solutions. Any effects of the

additive seemed to be explained by its effects on crystal nucleation.

Hexamine crystals were grown from methanol and ethanol solutions. 'Face' inclusion patterns could not be formed. However, inclusions were formed if a moderate amount of water was mixed with the methanol solution.

9. FORMATION OF FACE INCLUSIONS IN OTHER CRYSTALS

9.1 INTRODUCTION

Face inclusion patterns were grown in two other crystalline materials, ammonium chloride and sodium chloride. The appearance of the inclusion patterns in these crystals has already been discussed in Chapter 4.

These Crystals were grown mainly to show that 'face' inclusions can be formed in other crystals. A detailed experimental study was not undertaken. Although it is possible to make rough estimates of certain quantities from the results, these quantities are not very reliable.

9.2 INCLUSIONS IN AMMONIUM CHLORIDE CRYSTALS

9.2.1 Growth of Crystals

Ammonium chloride generally crystallizes from pure aqueous solutions as six-pointed dendrites. These have the classical 'fir-tree' appearance. However, by the use of additives in the solution, cubic crystals can be obtained. A list of suitable additives is given by Buckley [17] p.535. One of the most effective is ammonium molybdate, and a small quantity ($\leq 1\%$) of this material was added to the ammonium chloride stock solution from which all batches of crystals were grown. The stock solution was given a prior crystallization to remove foreign nuclei.

Eleven batches of ammonium chloride crystals were grown in the evaporative crystallizer. Details concerning these batches (No. 95-105) are given in Appendix III. Ammonium chloride has a marked change in solubility with temperature, so the batches were grown at quite low temperatures to minimise changes when the samples were cooled to room temperature. Otherwise the

experimental procedure was the same as that used for hexamine.

Operating conditions favourable to inclusion formation, namely low stirrer speeds and full heating rate, were used at first. Large inclusions formed very readily and took an appreciable time (> 30 min.) to seal over. Later batches were grown at higher stirrer speeds or reduced heating rates in an attempt to obtain smaller inclusions.

9.2.2 The Mechanism of Inclusion Formation

The inclusions in ammonium chloride crystals form in much the same way as those in hexamine. The crystals grow as cavitites, which eventually seal over trapping mother liquor in the cavities. For ammonium chloride the cavitite has the form of a cube with an approximately pyramidal cavity in each of its six faces. Photographs of the inclusion patterns have already been given in Fig 4-1. Further photographs are shown in Fig 9-1 illustrating crystals at the cavitite stage and others just after the sealing of the inclusions. Portion of a large open cavitite is shown in Fig 9-2.

FIG. 9-2 PORTION OF CAVITITE CRYSTAL OF AMMONIUM CHLORIDE [X70]

The larger inclusions have a very unusual shape with four narrow spikes leading from the base of each inclusion towards the nearest corners of the

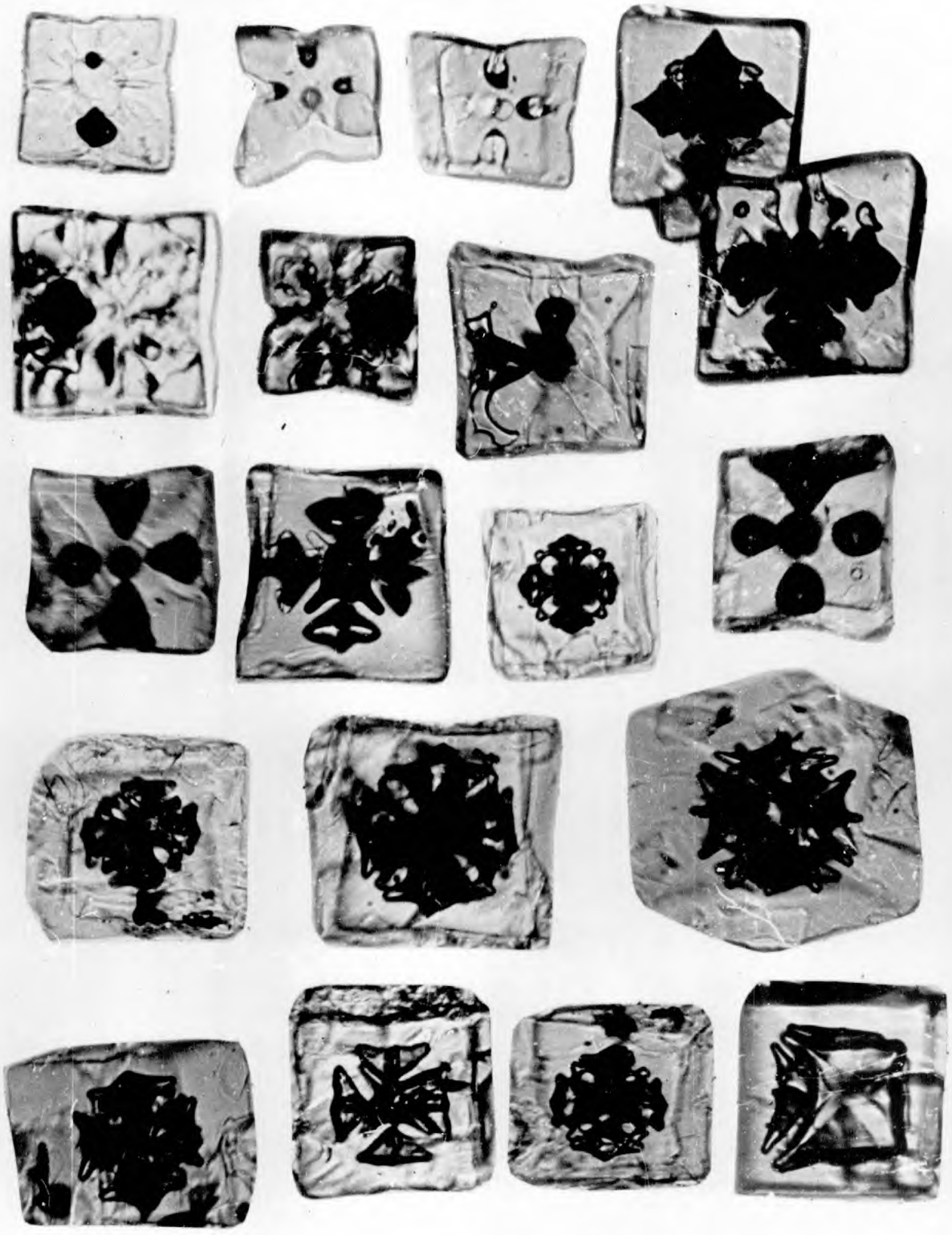

FIG. 9-1. FACE PATTERNS OF INCLUSIONS IN CRYSTALS OF AMMONIUM CHLORIDE DURING AND AFTER FORMATION.

[x150]

crystal. This probably results from the large change in solubility on cooling the included mother liquor. On cooling, crystallization will occur preferentially on those surfaces of the original pyramidal shape that cool the quickest, i.e. on those that are nearest the surface. Consequently most deposition will take place at the centre of the base of the inclusion. As the deposition progresses spikes leading to the slower cooling corners are left.

9.2.3 Quantitative Measurements

In examining the crystals of the one batch, it would seem that the general conslusions which were true for hexamine are true also for ammonium chloride. These are :-

(i) the inclusions occur only in the largest crystal;

(ii) the larger the crystal, the larger the inclusion;

(iii) inclusions do not form below a certain crystal size;

(iv) all inclusions seal over at much the same time.

This suggests that the results might be explained as for hexamine in terms of a critical growth region determined by a critical crystal size and a critical growth rate. Very rough estimates of these quantities for each batch are given in Table 9-1.

It should be emphasised again that a detailed experimental investigation was not undertaken for this material. The batches were grown only for demonstration purposes, so that the errors in these computed quantities may be quite severe. For example, the samples photographed are by no means representative since usually a crystal of attractive appearance was photographed. Also segregation of the sample occurred, since those crystals with large inclusions tended to float in the immersion fluid. Further, the single sample

SAMPLE NO.	TEMP. °C	STIRRER RPM ‡	$\bar{s}$ μ	$\bar{y}$ μ	R μ/min	10^{-6} n_i
95	31	105	@	35	< 4	> 3
96-1	30	100	50	40	1.4	6
96-2	30	100	50	35	1.7	11
♦ 97	30	230	55	32	5	3
98	30	150	40	35	2.3	10
99	32	90	@	35	< 3	> 2
100	32	95	70	35	4	3
101	32	240	-	-	> 6	-
102	33	90	55	40	5	2
♦103	28	100	60	45	1.5	6
104	43	100	70	45	1.7	3
105	43	220	-	-	> 8	-

‡ As motor RPM.
@ Inclusions not closed over.
† Speed reduced to 100 rpm after 4 min.
♦ This run at heat 6, all others full heat.

TABLE 9 - 1. RESULTS FOR GROWTH OF AMMONIUM CHLORIDE CRYSTALS.

method of analysis (see section 7.10) was used, but the assumptions upon which this is based may not be applicable to ammonium chloride. Also the numbers of crystals counted in the samples are quite insufficient for statistical purposes.

However the results (Table 9-1) do suggest that an explanation in terms of a critical size and a critical growth rate may be applicable. The critical crystal size would appear to be in the range 55 $\pm$ 10 μ with a critical growth rate, perhaps, between 2 and 6 μ/min. These values may of course depend on the quantity of additive present. The additive has a marked effect on dendrite formation so it could well effect the formation of cavitites. Furhter results on this material would be of interest.

The rate of nucleation of ammonium chloride crystals in the batch crystalliz seems to be an order of magnitude less than that for hexamine. This may be the reason for the ease with which large inclusions form.

9.2.4 Interpretation of Results

An explanation of the formation of face inclusions in terms of cavitite (incipient dendrite) formation has already been proposed by Bunn [14]. The explanation given for hexamine (section 7.14) has in fact been based on this.

For ammonium chloride, the inclusions form by the sealing over of cavitites. It is suggested that these cavitites represent a form of crystal growth intermediate between the cube and the eight-pointed dendrite. The dendrites usually observed, with ammonium chloride are six-pointed. These are formed from pure solutions and represent the breakdown of polyhedral growth on icositetrahedral crystals (i.e. crystals with twenty four faces). The icositetrahedron is the normal crystal habit for ammonium chloride grown from pure solutions. However with certain additives, the crystal habit is changed

to the cube and the corresponding dendrites which can form by the breakdown of polyhedral growth are the eight-pointed ones mentioned above. Eight-pointed dendrites have been observed

Since ammonium chloride can also crystallize as icositetrahedra, it seems that it should be possible using pure solutions to form patterns of twenty-four inclusions in crystals of ammonium chloride, if cavitites are formed intermediate between the icositetrahedron and the six-pointed dendrite.

9.3 INCLUSIONS IN SODIUM CHLORIDE CRYSTALS

9.3.1 Growth of Crystals

Sodium chloride crystallizes as cubes from aqueous solutions. Six batches of crystals were grown in the evaporative crystallizer (Batches No 106-111). Of these, only the last batch showed a reasonable quantity of 'face' inclusion patterns. This batch was grown by very rapid growth, achieved by allowing the solution to reach 100°C before suddenly applying the vacuum. The inclusions were grown on seed crystals and many of the inclusions have the flat appearance characteristic of this means of growth. Some examples have already been given as Fig 4-3; others are shown in Fig 9.3.

9.3.2 The Mechanism of Inclusion Formation

The appearance of the inclusions in sodium chloride is much the same as that in ammonium chloride and it might be expected that a similar mechanism of formation applies. The solubility of this material does not vary much with temperature, so irregularities in inclusion shape on cooling would not be expected.

FIG. 9-3 . FACE INCLUSIONS IN SODIUM CHLORIDE CRYSTALS DURING AND AFTER FORMATION.

[x 110]

9.3.3 Quantitative Measurements

From the limited number of samples it is impossible to make any really quantitative measurements or even to show that critical growth conditions might exist. However, assuming, as with hexamine, that the behaviour can be explained in terms of a critical crystal size and a critical growth rate, it would appear that the critical size is of the order of 20 to 30μ and the critical growth rate is of the order of 10μ/min.

9.3.4 Inclusions in Octahedral Crystals

With the addition of urea, sodium chloride will crystallize as octahedra instead of cubes (Buckley [17] p. 556). If 'face' inclusions can be formed with such crystals, a pattern of eight inclusions should result. Several quick attempts were made to grow such inclusions form a urea; sodium chloride solution but really definite results were not obtained.

9.4 INCLUSIONS IN NON-REGULAR CRYSTALS

All the examples of face inclusion patterns so far considered have been in crystals with cubic symmetry, which crystallize in regular forms. If the crystal grew in a non-regular habit, for example as a prism, it is possible that face inclusions could be formed in the more rapidly growing faces and not in the others, i.e. in the directions of the length of the prism. Thus a pattern appearing only in certain selected faces would be obtained.

If the barium chromate crystals of Fig 2-2 do contain mother liquor inclusions, they may be of this type, with the inclusions lying in the wake of the two most rapidly growing faces. The individual pattern members in these crystals certainly have the characteristic tapering and sealing of

face inclusions. It may also be of interest to note that barium chromate can be grown as dendrites with a shape corresponding to the crystal and its pattern [18].

9.5 CONCLUSIONS

Face inclusion patterns can be grown in other crystals. The mechanism of formation appears to be similar to that for hexamine. Further measurements are required before exact details of the conditions for growth can be given.

10. FORMATION OF EDGE INCLUSION PATTERNS

10.1 INTRODUCTION

Edge inclusion patterns have been discussed in Ch. 3 and 4. It was seen that the inclusions lie upon lines corresponding to the edges of the crystal at some prior stage of growth. In hexamine, the inclusions outline a dodecahedral form; while in ammonium and sodium chloride, a cubic one. It is the purpose of this chapter to consider the formation of these inclusions.

10.2 PREPARATION OF CRYSTALS

Edge inclusions were first noticed in a chance sample of hexamine, prepared when the solute was being recovered from the accumulated mother liquor at the end of a series of batch crystallizations. The crystals were grown, while extra batches of mother liquor were added from time to time. Unfortunately no detailed record had been kept of the conditions used in this recrystallization.

At first it was though that the important factor causing the formation of these inclusions was the impurity of the feed solution. However further crystallizations from the same mother liquor showed that this was not so. Then it was thought that the contributary factor was dissolved air, added with the later batches of feed and coming out of solution on the crystal edges. Several batches of crystals (as shown in Table IIIA3 of the Appendix) were grown to test this idea. All were unsuccessful.

It was found, then, that crystals with edge inclusions could be produced if a quantity of undersaturated feed solution were added to the crystallizer during crystal growth. It seems that somehow in the original batch a quantity of water must have added with one of the later additions of mother liquor, thus causing the inclusion patterns.

Thus the following procedure was adopted for growing batches of crystals for study. A batch of crystal was prepared in the normal way, then a quantity of water was added to dissolve some of the crystal away. This crystal was used as seed for further crystal growth to form edge inclusion patterns. Photographs of typical samples of hexamine from the initial batch, the partly dissolved seed and the resulting product are shown in Fig 10-1. Other samples formed from seed with differing amounts of initial dissolution are shown in Fig 10-2. Photographs of individual hexamine crystals with edge inclusions have already been shown in Fig 3-7 to 3-9, while similar photographs for ammonium chloride and sodium chloride crystals were given in Fig 4-2 and 4-4. Details of all the batches of crystals grown are given in Table III A4 of Appendix III.

10.3 MECHANISM OF INCLUSION FORMATION

Edge inclusions are formed by crystal growth on partly dissolved seed crystals. It is usual in dissolution for the corners and edges of a crystal to be dissolved preferentially and for the crystal to become quite rounded. It can be seen from Fig 10-1 that this rounding process has occurred on the partly dissolved hexamine seed crystals.

It is thought that edge inclusions are formed by the redevelopment of the plane surfaces on such rounded seed crystals. Planewise growth would begin from the centre of each face. As growth proceeds, the plane face would re-establish itself over the surface. However, because of the curvature of the surface, considerably more growth would be required at the edges and corners of the crystal to bring them to the level of the plane surfaces. Meanwhile the plane surfaces may be spreading, repairing themselves, at a rate faster than the edges

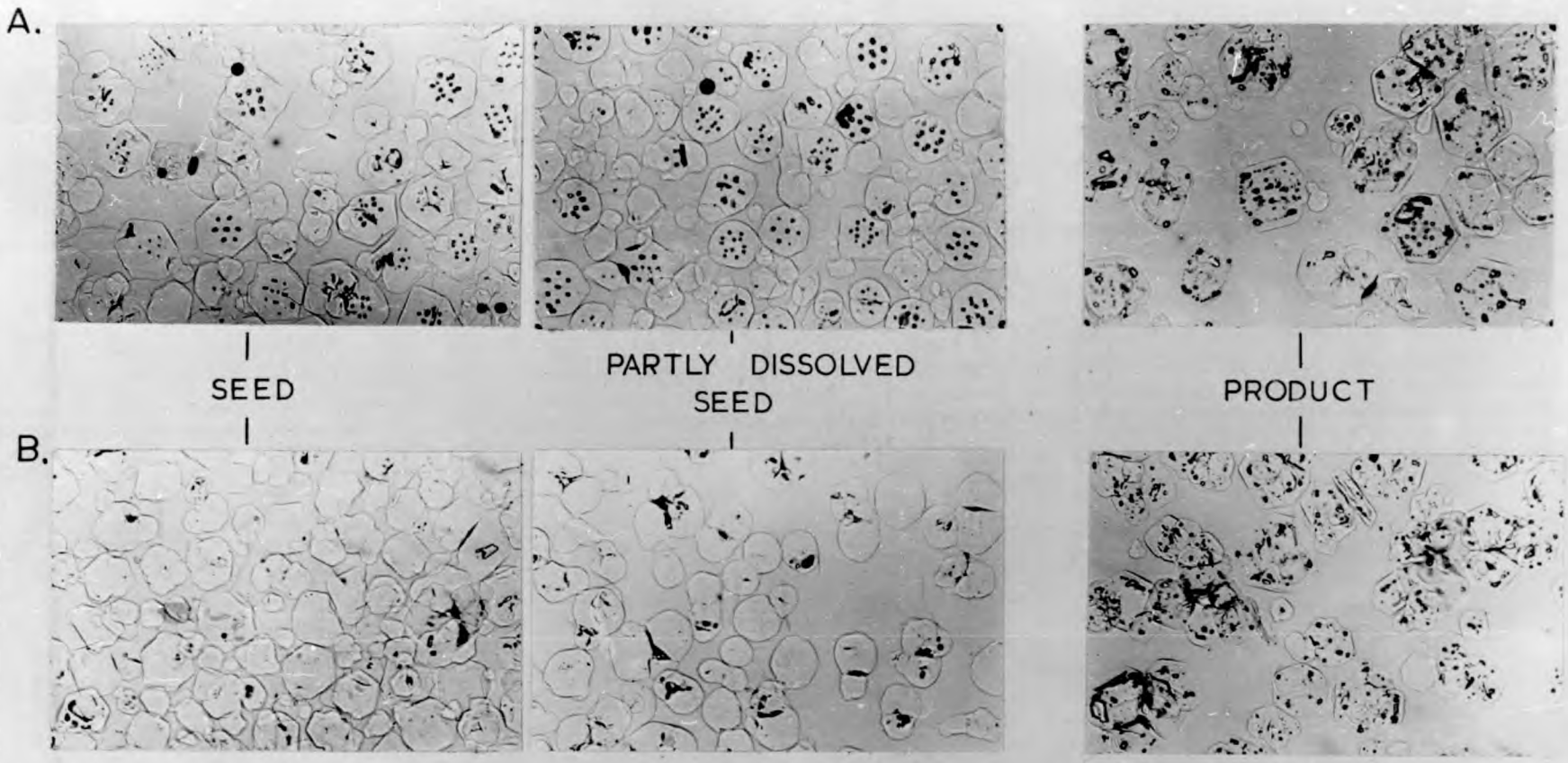

FIG.10-1. GROWTH OF HEXAMINE CRYSTALS WITH 'EDGE' INCLUSIONS

[A. Batch No. 63 ; B Batch No. 64]

[x 50]

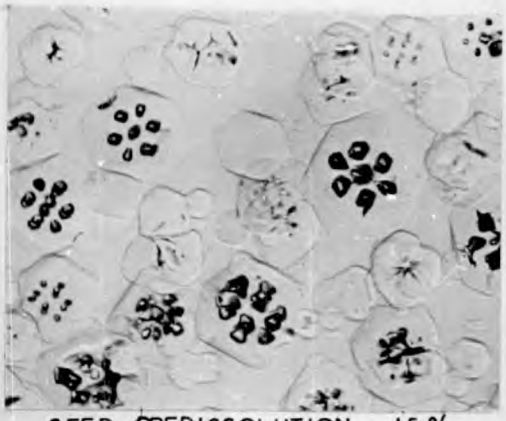

SEED PREDISSOLUTION = 15 %

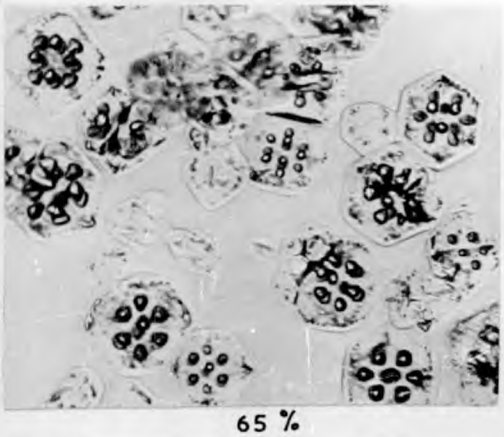

65 %

25 %

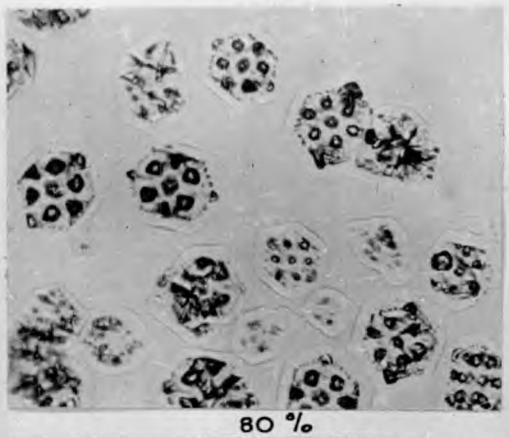

80 %

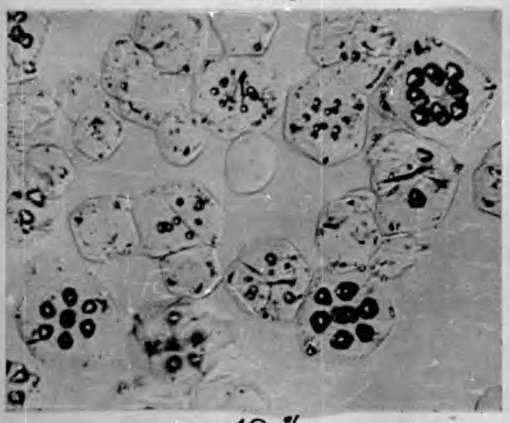

40 %

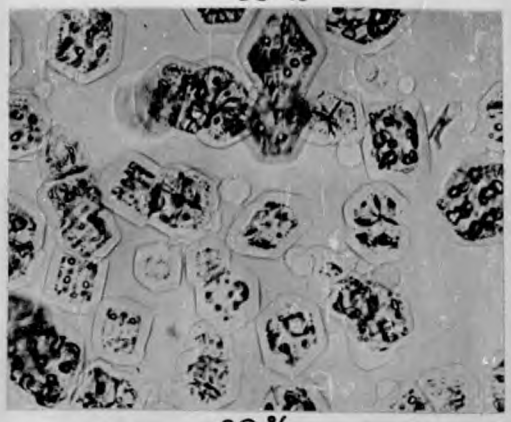

90 %

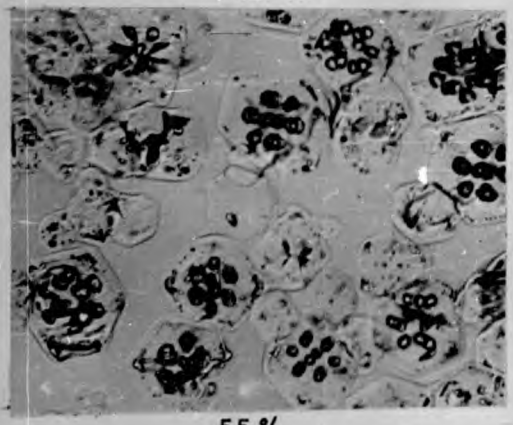

55 %

FIG. 10-2 . EDGE INCLUSION PATTERNS IN HEXAMINE — EFFECT OF THE EXTENT OF SEED PREDISSOLUTION . BATCHES No 84 – 90 (40 °C , 75 RPM .)

[x 70]

and corners can be built up. So, after a time the crystal would appear as a number of plane faces separated by an interconnected pattern of open channels running along the edges of the crystal. With further growth, neighbouring plane faces may eventually meet and thus tubes of mother liquor would be trapped in these channels. Further crystal growth would just bury the included mother liquor deeper in the crystal. This process is shown diagrammatically in Fig 10-3. The positions of the growing surfaces around one edge of a crystal at various stages are shown.

After a time the tubes of mother liquor formed in this way would break down into a series of discrete inclusions. It would be expected that larger inclusions would form at the corners since this is where the largest difference between the smoothed crystal and the plane surface occurs. This is verified by observation (see Fig 10-1).

In some instances, when the original seed crystal was not very rounded the inclusions form only at the corners and the edge patterns become just a number of isolated inclusions, one at each crystal corner. Eight such inclusions would be formed in a cubic crystal and fourteen in the dodecahedron. Six of the corners of a dodecahedron are sharper than the others and the inclusions in these corners tend to be larger than the others. Under certain circumstances the pttern of fourteen inclusions described above can degenerate into a pattern of six, one in each of these corners.

10.4 MEASUREMENTS ON CRYSTAL SAMPLES

10.4.1 Samples

Attempts were made to grow crystals with edge inclusions under the microscope

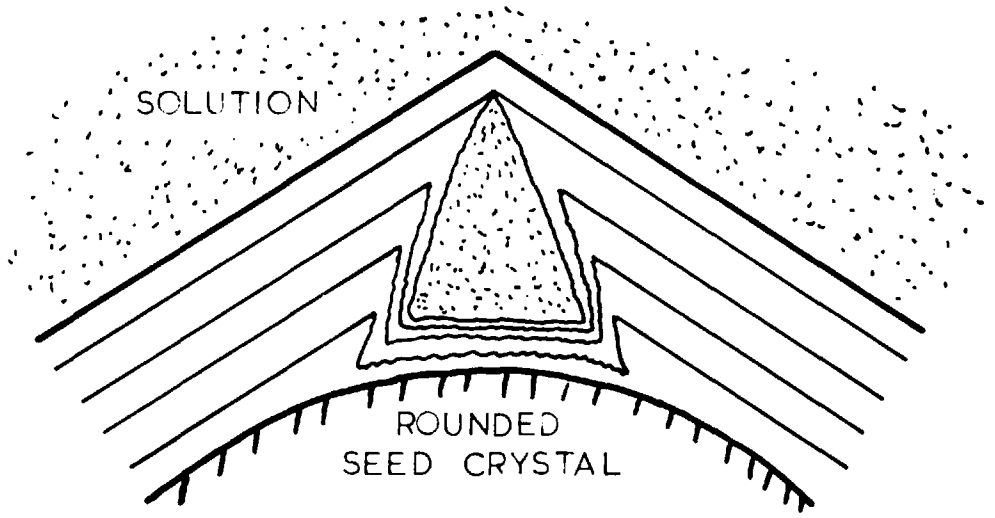

FIG. 10-3. DIAGRAMMATIC ILLUSTRATION OF PROPOSED MECHANISM FOR THE FORMATION OF EDGE INCLUSIONS, SHOWING CRYSTAL SURFACES AT VARIOUS STAGES OF GROWTH.

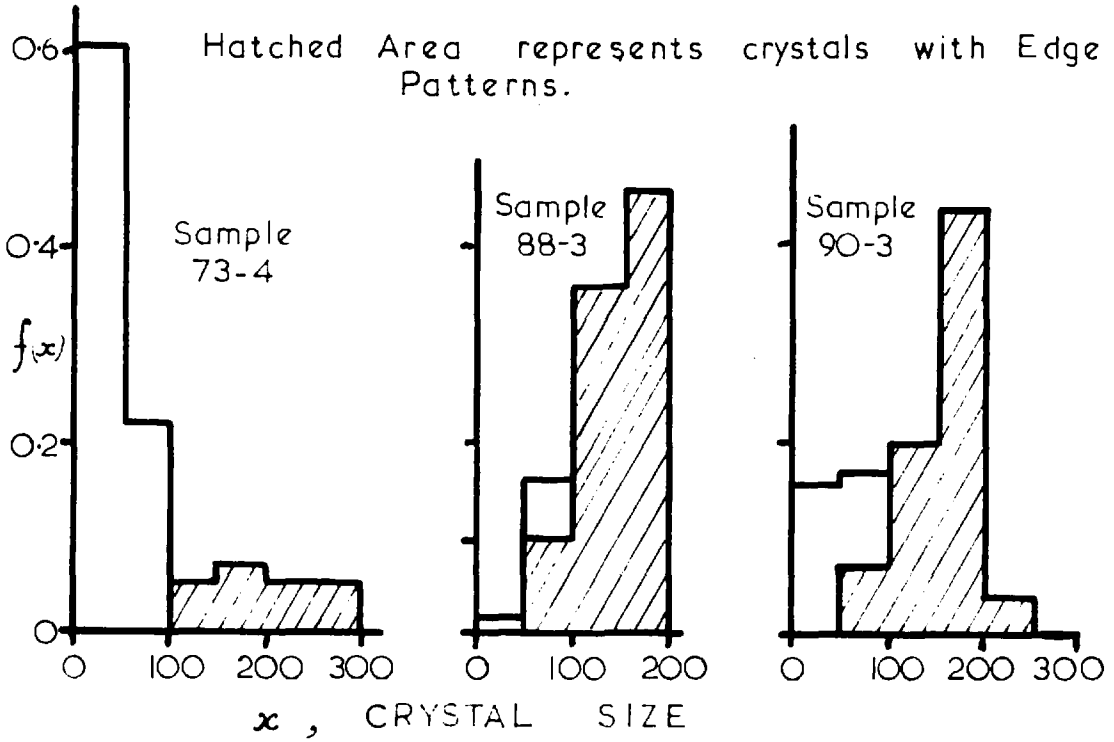

FIG. 10-4. CRYSTAL SIZE HISTOGRAMS FOR SAMPLES WITH EDGE INCLUSIONS.

using the thermal crystallizer. Inclusions were formed, but because of the difference in refractive index between crystal and solution details of the mechanism of growth could not be seen. Since the evaporative crystallizer allows greater control over the conditions of growth, this apparatus was used for the growth of all/further samples analysed in this section.

10.4.2 Generalizations From Results

Observations and measurements on the various samples (such as those in Fig 10-2) lead to the following generalizations :

(1) Inclusions occur in the largest crystals of a sample. This can be seen directly, and is also demonstrated by measurements of the crystal size histograms (Fig 10-4). This result would be expected if inclusion formation took place on all the seed crystals. Naturally, these would be larger than crystals nucleating subsequently.

(2) Inclusions form on all the seed crystals. It is immediately obvious that inclusions form at least on all those seed crystals with face inclusion patterns, since, without exception, where edge patterns were formed, those crystals showing face inclusions (present only in the seed) also showed edge inclusions. Added proof is given by measurements which show that the number of crystals with edge inclusions is approximately the same as the number of seed crystals added (Table 10-1).

(3) The size of the inclusion pattern is much the same size as the seed from which it is formed. This is shown (Table 10-1) by measurements of the mean size of the patterns, and the mean size of the seed from which they were formed. It is rather difficult to get an accurate measurement of the size of the seed, since the particles are somewhat rounded. It would be interesting to have more

Batch No.	SEED		PRODUCT				R	Comments.
	$\bar{x}$ μ	10^{-7} n	$\bar{y}'$ μ	10^{-7} n_i	x_i μ	$\bar{t}$ μ	μ /min	
84	133	2.6	-	0.7	193	10	3.0	v.few; patterns of 6
85	128	2.5	139	3.2	160	10	3.5	patterns of 6
86	125	2.3	131	3.4	151	10	4.0	patterns of 14 & others
87	122	1.9	135	3.3	151	15	5.0	full pattern
88	117	1.9	133	2.7	157	15	6.5	full pattern
89	80	1.3	92	1.6	169	26	17	highly developed
90	97	1.8	117	2.1	167	24	11	fully developed
91	106	2.1	121	2.2	143	15	2.2	medium.
92	105	2.3	128	2.1	144	12	3.0	weak patterns
93	120	1.4	142	1.4	163	10	1.6	weak patterns
94	119	1.5	127	1.8	153	12	6.5	full pattern.
5	67	1.9	89	2.4	208	55	10	-
32	280	0.08	340	0.11	420	35	25	-

TABLE 10 - 1. RESULTS FOR GROWTH OF EDGE INCLUSIONS IN HEXAMINE.

exact measurements relating the size of the inclusion pattern to the size of seed, to obtain some idea of how much growth occurs before the inclusions seal. This might be an aspect for further work.

(4) The thickness of crystal covering the inclusions is approximately constant for each batch. This can be seen directly from the photographs, and is confirmed by measurements. Assuming that all crystals in a batch grow at the same rate at the same time, this means that all the inclusions must have been sealed over at much the same time, irrespective of whether the crystal was large or small.

These generalizations are consistent with the proposed mechanism of inclusion formation.

10.4.5 Rates of Growth

Estimates of the rate at which the crystals are growing when the inclusions form, have been made for the various batches (Table 10-1). The rates of growth are quite low.

In an attempt to determine whether there is a limiting growth rate for the formation of edge inclusions, four batches of crystal (Batches No. 91-94) were grown at different heating rates, using similar amounts of seed. The resulting samples arranged in order of increasing heating rate are shown in Fig 10-5. The corresponding rates of deposition of solid, n, are given. It can be seen that inclusions are formed at all heating rates, although at lower heating rates the amount of material included seems to have decreased. Perhaps at lower rates still the inclusions would not be formed at all. If there is such a limiting growth rate it would appear to be rather low ($\ll$ 1 μ/min). This may be an aspect worthy of further study.

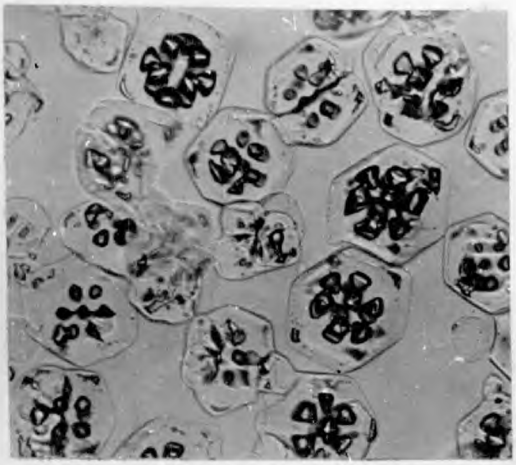

BATCH No. 93
$m = 1.8$ g/min

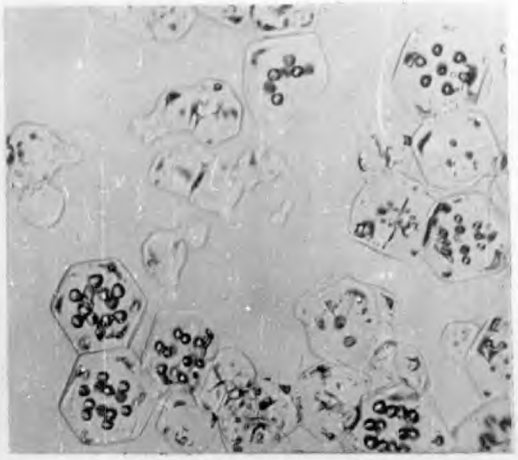

BATCH No. 91
$m = 2.1$ g/min

BATCH No. 92
$m = 3.8$ g/min

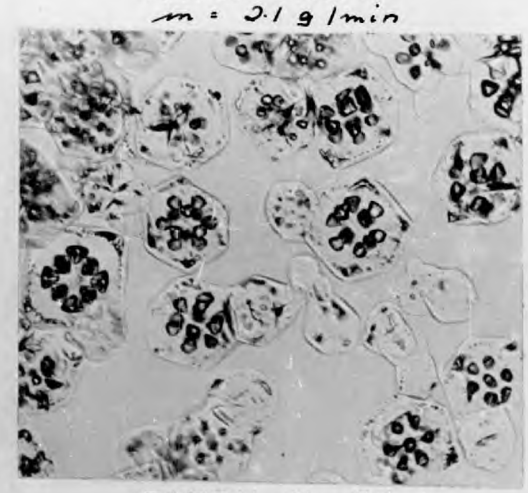

BATCH No. 94
$m = 7.5$ g/min.

FIG. 10-5. EFFECT OF EVAPORATION RATE ON 'EDGE' INCLUSION FORMATION. [x 70]
(ALL BATCHES :- 70 % PREDISSOLVED SEED , 33 °C , 70 RPM.)

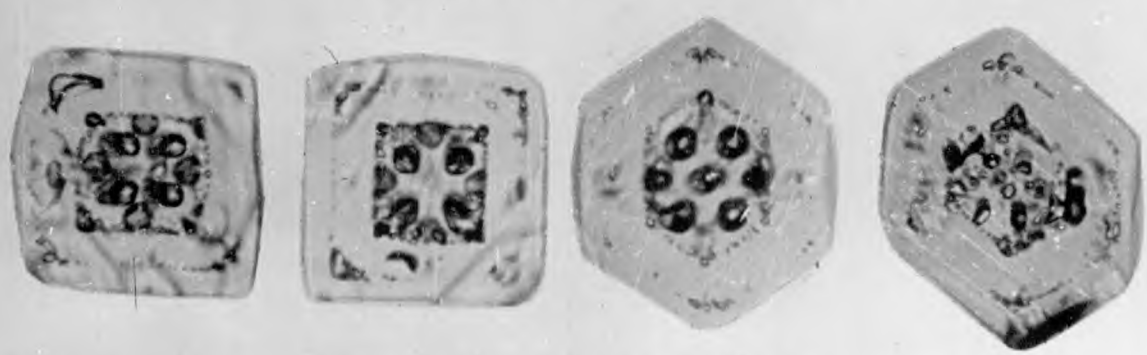

FIG. 10-6. DOUBLE PATTERN OF 'EDGE' INCLUSIONS IN HEXAMINE CRYSTALS. Sample No. 90-4. [x 120]

10.5 EFFECT OF VARIABLES ON SIZE OF INCLUSIONS

The effect of growth rate has already been noted above. Variations in growth rate do appear to have an effect on the size of the inclusions formed on a given seed, although the effect is not pronounced.

For the purposes of this project, the size of the inclusions was only estimated qualitatively. It is difficult to get a quantitative measure of the size of the inclusions since they are usually rather small, and also they vary in size at different points along the crystal edges. Measurements could have been made using the Karl Fischer apparatus (Appendix V) to determine the total amount of included moisture. From this and estimates of the number and mean size of crystals with inclusions a mean inclusion size could have been determined.

The major factor affecting the size of the inclusions formed is the amount of predissolution that has taken place on the seed. The inclusions formed on seed crystals with different extents of predissolution are shown in Fig 10-2. The amount of predissolution is taken as the fraction of the original dodecahedral volume that has been dissolved away. It can be seen that about 20% predissolution is required before any semblance of an edge pattern forms and about 40 % before the full pattern appears.

It appears that the effect of seed predissolution is simply/through the increasing roundness of the seed crystals with further dissolution. The more rounded the seed, the larger the edge inclusions that are formed.

10.6 MULTIPLE PATTERNS OF INCLUSIONS

By repeated crystal dissolution and subsequent growth, multiple patterns of edge inclusions can be built up quite readily. Crystals containing two

successive patterns of edge inclusions are shown in Fig 10-6. If the original seed crystals contained face patterns these would be visible as well. It is possible to grow further face patterns at any stage of growth (see section 7.11.4) so that patterns of great complexity could be formed in the one crystal, if one had the patience.

10.7 IRREGULARLY SHAPED SEED CRYSTALS

So far, the seed used has been uniformly rounded crystals. The edge patterns formed by subsequent growth have thus been very regular. If, however, the seed crystals were initially irregularly shaped, the inclusions which form on growth would tend to outline portions of the seed crystal and thus be somewhat irregularly arranged. For example, in the first batch illustrated in Fig 10-7, the seed crystals used were broken crystals. These irregularly shaped seeds gave the irregular inclusion patterns shown. The second batch illustrated in Fig 10-7 shows the resulting patterns when commercial crystals were used as seed.

This mechanism of regrowth over irregular surfaces may be the cause of several of the inclusion patterns illustrated in Fig 2-1. In particular, it would appear that the 'block' pattern (usually associated with growth on seeds) may have been formed by such a mechanism.

10.8 EDGE INCLUSIONS IN OTHER CRYSTALS

Edge inclusions were also grown in sodium chloride and ammonium chloride cubes. These were formed by exactly the same method as used for hexamine. A quantity of the crystal was partly redissolved (to about half its original weight) then regrown. The mechanism of formation would appear to be similar to that already described.

A.

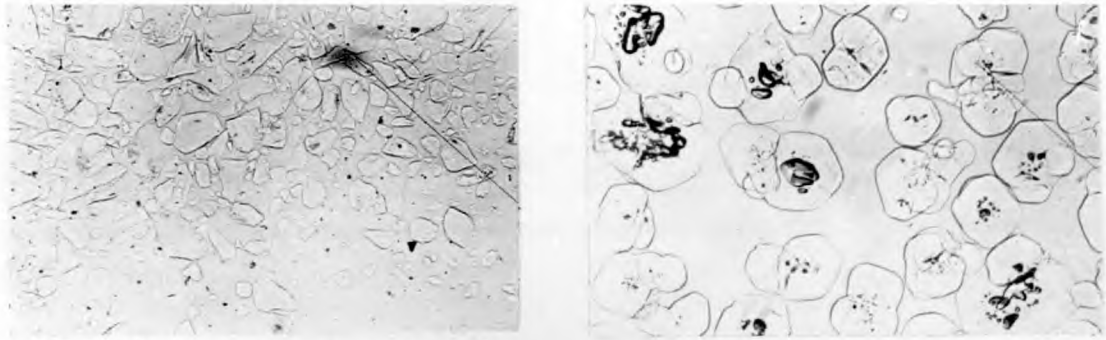

SEED (Pulverised crystal) PRODUCT

[Batch No.5 :- 40 °C , 120 RPM , Full heat , 31 min.]

B.

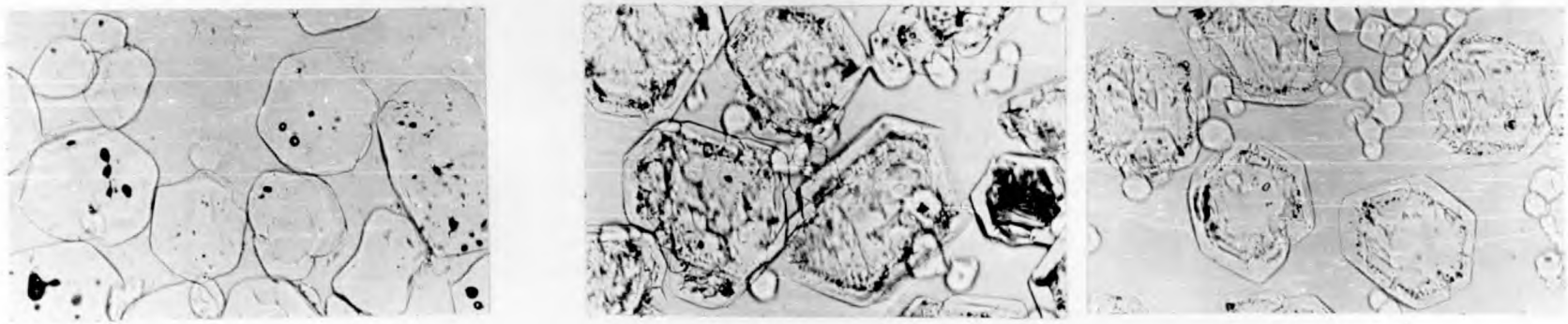

SEED (Commercial crystal) PRODUCT

[Batch No. 32 :- 42 °C , 60 RPM , Full heat , 9 min.]

FIG. 10-7. INCLUSIONS IN HEXAMINE CRYSTALS GROWN ON SEED.

[x 50]

10.9 CONCLUSIONS

Edge inclusions are formed in various crystals by subsequent regrowth on partly dissolved seed crystals. The major factor affecting this formation is the amount of dissolution that has occurred on the seed crystal. The rate of crystal growth appears to have a lesser effect. The mechanism is believed to be caused by growth on rounded crystal surfaces.

11. THE DRYING OF CRYSTALS CONTAINING INCLUDED MOTHER LIQUID

11.1 INTRODUCTION

In industrial practice it may not always be possible to avoid the formation of inclusions in crystals, and yet the presence of included mother liquor may be undesirable. Is it possible, perhaps, to remove the included liquor from the grown crystals, for example by drying? The results of experiments concerned with the drying out of inclusions will be considered in this section.

Mechanisms by which included solvent might pass from the crystal include the diffusive transfer of the solvent through the solid crystal, the seeping out of liquor through the cracks and flaws in the crystal structure, and the rupture of the crystal by the pressure generated within the inclusions. If any of these mechanisms occurs to a significant extent it should be possible to remove the included solvent by drying.

Hexamine containing aqueous inclusions was used as the test material. It was noted that hexamine samples stored in desiccators at room temperature for several months still contain appreciable amounts of included moisture. Also commercial hexamine crystals which are dried at temperatures up to 50°C in manufacture still contain moisture. By drying at higher temperatures for longer times it is possible that the included moisture may be driven out. For this purpose a small batch-operated through-dryer was constructed.

11.2 DESCRIPTION OF BATCH DRYER

Essentially the dryer (Fig 11-1 and 11-2) consists of a small bed of hexamine crystals through which hot dried air is passed. The moisture removed is recovered from the air in weighed drying tubes (8). The dryer and air heater are immersed in a constant temperature oil bath (6). The

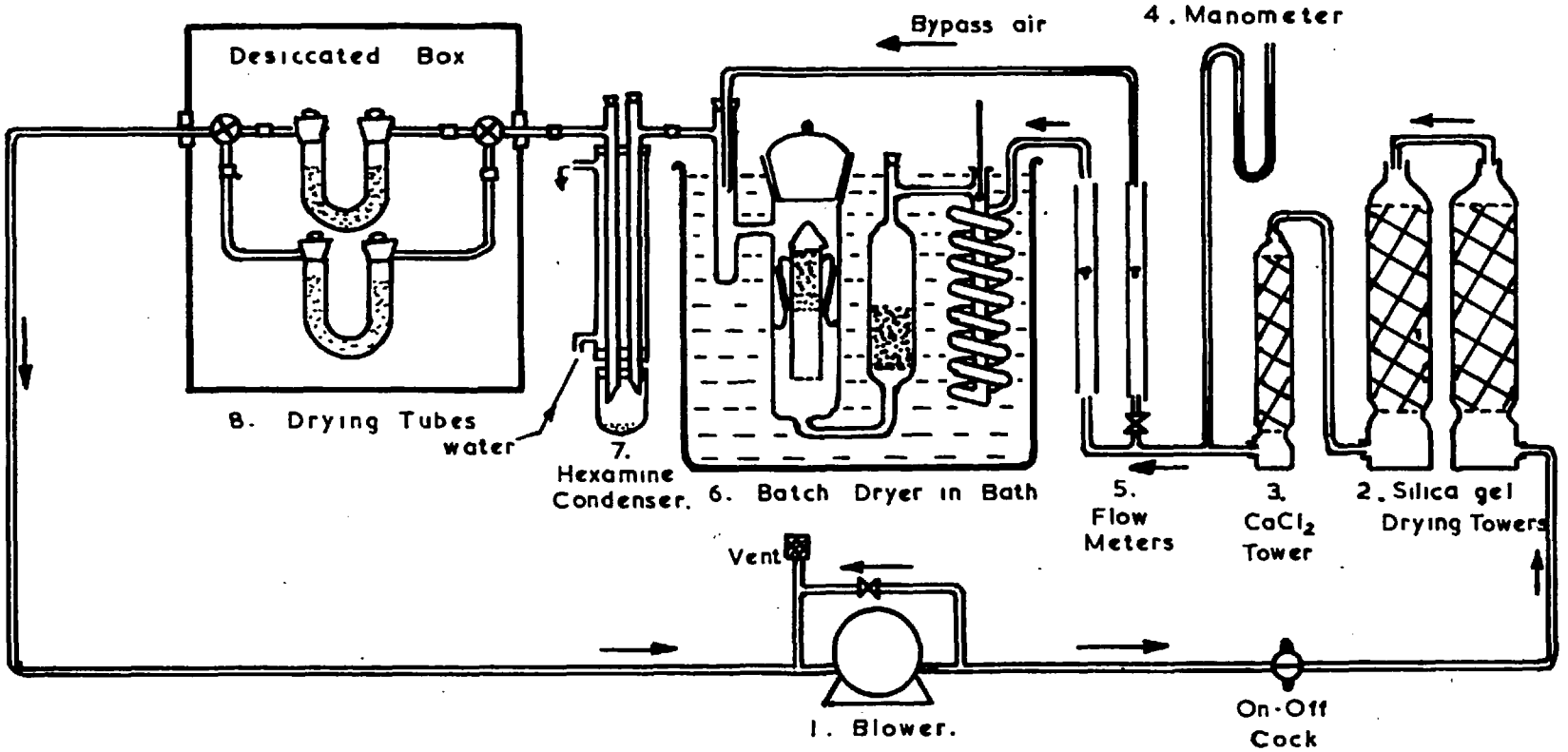

FIG. II-1. DIAGRAM OF BATCH DRYER.

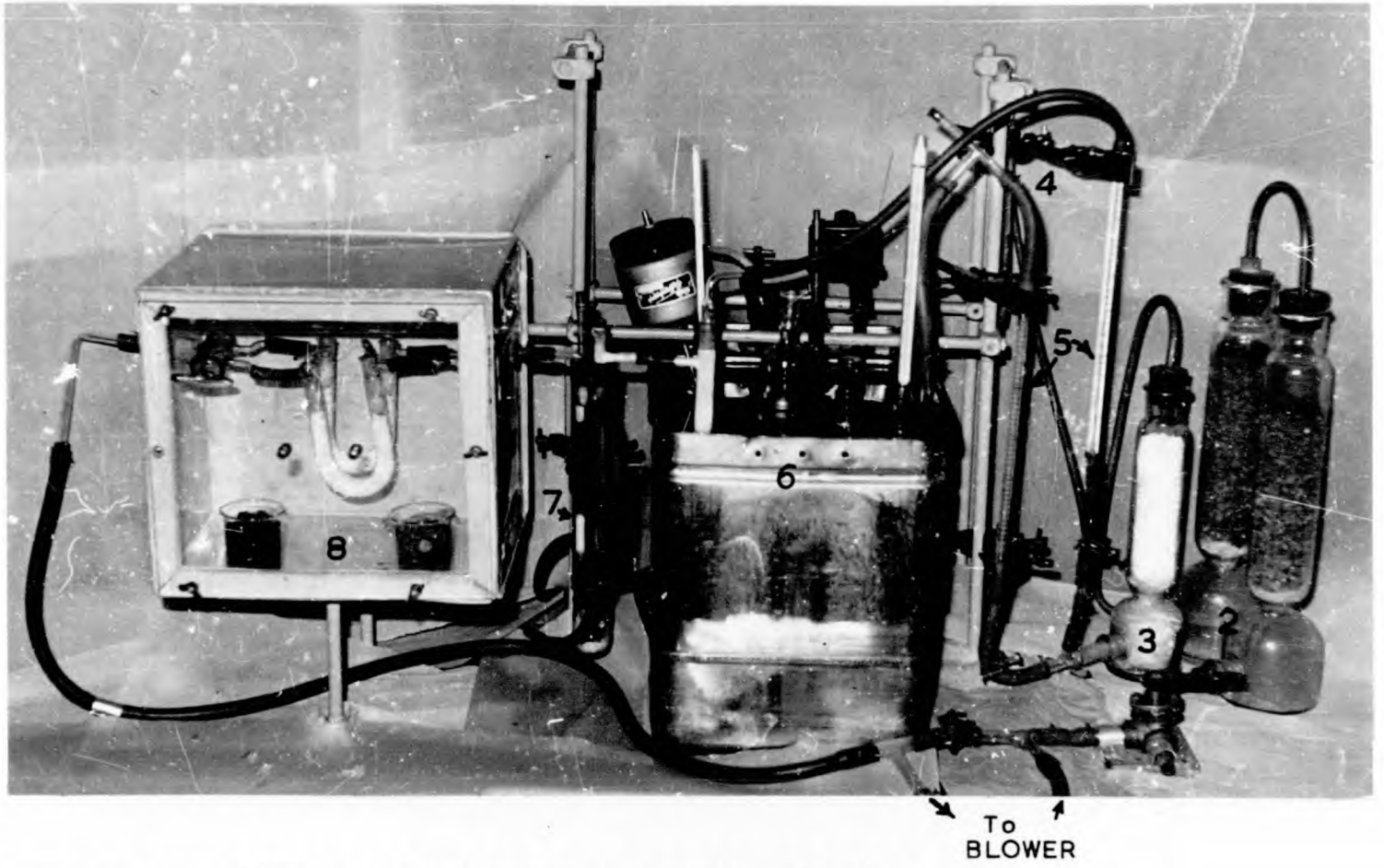

FIG. II-2. PHOTOGRAPH OF BATCH DRYER.

2 : SILICA GEL DRYING TOWERS.

3 : CALCIUM CHLORIDE TOWER.

4 : MANOMETER.

5 : FLOWMETER.

6 : BATCH DRYING VESSEL IN CONSTANT TEMPERATURE BATH.

7 : HEXAMINE CONDENSER.

8 : DRYING TUBES.

spent air is recirculated by a blower (1) through drying towers (2, 3) and a flow meter (5). To prevent the evaporation of the hexamine sample the air passes through a hexamine presaturator before entering the drying bed. Hexamine vapour is removed in a water condenser (7) ahead of the drying tubes.

11.3 DETAILS CONCERNING DESIGN AND CONSTRUCTION OF DRYER

11.3.1 Selection of Operating Conditions

A batch dryer capable of treating about 40 g. of sample was considered a convenient size. This corresponded to about a hundred mg. of included moisture, a quantity that could be detected quite accurately on a good laboratory balance. Drying temperatures up to about 100°C were to be investigated and a constant temperature oil bath could achieve this. Air flow rates up to a litre per minute were considered adequate. Too low an air flow rate would cause serious time lags in the measurement of the moisture removed.

11.3.2 Drying Vessel

The drying vessel (Fig 11.3 and 11.4) consists of a sample holder, an air preheating coil and a presaturator. The sample holder (about one inch internal diameter and six inches long) supports the sample on a coarse grade sintered disc. Air passes upwards through the disc and sample. The sample holder supported by a B40 cone joint may be readily removed for weighing or filling. Although this joint was not lubricated it proved substantially leak proof, so that little air bypassed the sample.

Originally it was intended to weigh the sample holder in situ by means of a wire passing out of the drying vessel through a rubber bung and attached directly to one arm of a balance mounted above the dryer. Lifting the arrestment would have lifted the sample holder from its cone joint. However, because of sublimation and condensation of the hexamine sample, changes in weight proved to be no measure of the moisture lost; so this proposal was discarded.

Air was preheated by a glass coil, immersed in the bath. In all tests the temperature of the air leaving the coil was substantially that of the oil bath showing that the coil provided sufficient heat transfer.

Preliminary runs showed that sublimation of hexamine from the sample and its subsequent condensation in the drying tubes were serious factors. The vapour pressures of hexamine at 20°C and 100°C are 0.0004 and 0.29 mm. Hg respectively (refer Supplement Fig SI-9). For an air flow rate of 1 litre/min under saturation conditions this corresponds to a transfer rate of about 120 mg. hexamine/hr., a quantity very large compared to the amount

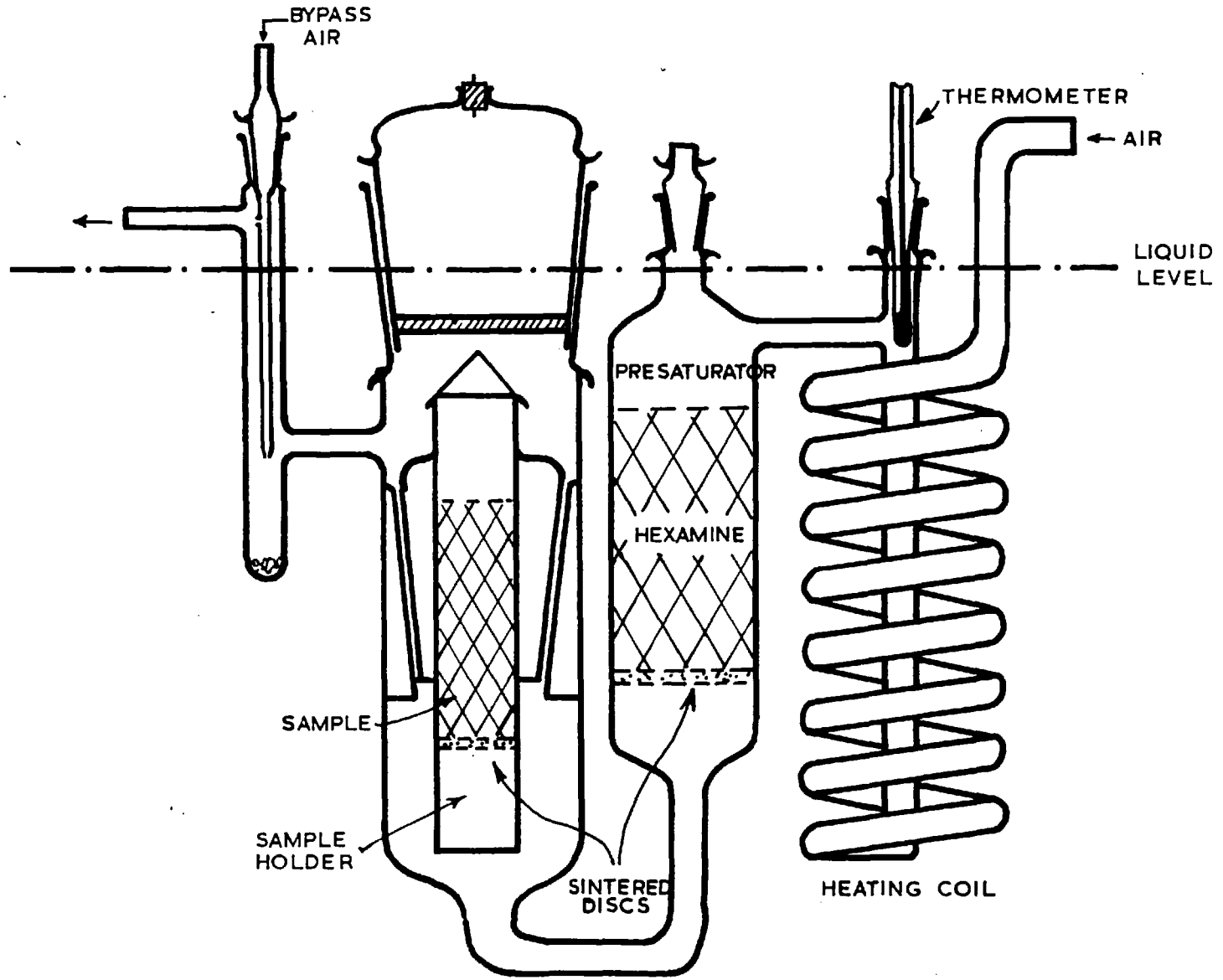

FIG. II-3. DIAGRAM SHOWING DETAILS OF DRYING VESSEL.

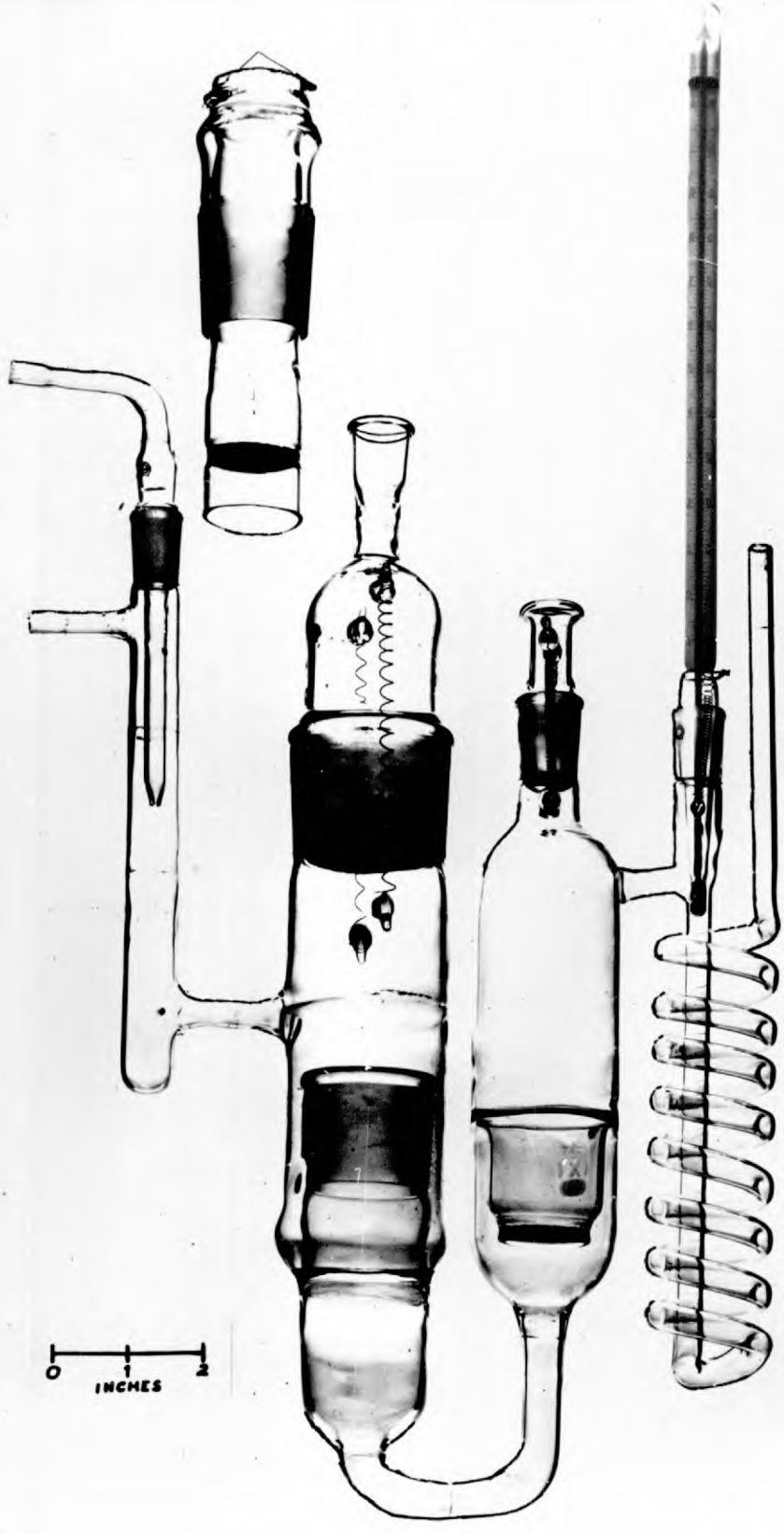

FIG. II-4. PHOTOGRAPH OF DRYING VESSEL.

of moisture present. To prevent this sublimation of the sample the hot air before passing through the sample, was presaturated with hexamine vapour by passing it through a bed of moisture free hexamine crystals. The hexamine vapour was condensed out prior to the drying tubes by a water condenser.

The small chamber at the vapour outlet was to collect any hexamine that condensed on the cooler portions of the outlet tube and to prevent it from being carried back onto the sample holder.

As much as possible of the drying vessel was below the oil level, but all joints and seals were kept above the surface to minimise contamination. All caps and joints were held tight with spring clips.

11.3.3 Constant Temperature Bath

A three gallon stainless steel tank filled with oil was used for the bath. Temperature control was achieved by a 'Sunvic' bimetallic thermostat (Model TS3) acting through a hot-wire vacuum switch on a 500W immersion heater. This gave temperature control within $\pm \frac{1}{2}^{o}$C.

11.3.4 Air Supply

Air was circulated by means of a vane blower. The flow rate was controlled by means of a bypass line around the blower. A closed air recirculation system was used, vented only through a dust filter at the blower inlet. The pressure in the drying vessel was 20 to 30 mm Hg above atmosphere. Air flow rates were measured by two Rotameters (0.1 - 0.8 l/min on the main air line and 0.2 - 2.0 l/min on the second bypass line.).

11.3.5 Drying Tubes and Towers

The rate of drying was determined from the increase in weight of a pair of drying tubes containing calcium chloride. By means of two three-way cocks air could be passed through one of the tubes while the other was removed for weighing. Both tubes were enclosed in a desiccated cabinet to avoid erroneous variation in weight caused by humidity changes or dust.

The calcium chloride in the tubes was from the same batch as that used in the drying tower before the dryer. The air entering the dryer and leaving the dryer tubes should therefore have the same moisture content (0.2 mg. H_2O/Litre [34]) and the only moisture collected in the tubes should be that from the sample.

Two silica gel drying towers were used prior to the calcium chloride tower to take most of the drying load, especially during start-up. With the recirculation of the air little drying was required once the apparatus was operating. A plug of glass wool after the drying towers, filtered out dust and entrained drying agent.

11.3.6 Condenser

To remove hexamine vapour from the air, the exit gases passed through a glass, water jacketted, two-tube condenser. Condensed hexamine was collected in a cup at the bottom of the first tube. A glass wool filter in the second tube removed entrained hexamine particles.

In preliminary tests using samples with appreciable surface moisture, water also condensed out in the tubes, and formed a pool of solution in the bottom of the cup. This eventually partially re-evaporated. To avoid this behaviour, a flow of cold dry air by-passing the sample was added to the outlet chamber. This air mixed with and undersaturated the main air flow preventing condensation. This by-pass was only used at the beginning of a run.

11.4 PRELIMINARY TESTS

11.4.1 Preparatory

Preliminary tests were undertaken in the development of the apparatus as described above. These led to the discarding of 'in situ' sample weighing and to the addition of the presaturator, condenser, and the by-pass air line.

In preparation for operation the equipment was tested and made leak-proof. To dry it out completely it was then run at a high bath temperature for several days until the drying tubes gave no increase in weight.

11.4.2 Dynamic Behaviour

To achieve some idea of how rapidly moisture could be detected, a sample comprising 57 g. of slightly damped 30 # 'Ballotini' glass beads was used with an air rate of 500 ml/min, no by-pass air, and a drying temperature of 80°C. Successive ten minute intervals gave moisture recoveries of 86. 102, 102, 111 and 108 mg. This corresponds to the value expected for saturated air at the condenser temperature. In the absence of by-pass air considerable condensation occurred in the condenser). It seems probable that even in the absence of condensation a change in the sample moisture would be fully recorded in the drying tubes in a few minutes, which is quite acceptable. The volume of air space between the sample and the drying tubes is less than 500 ml.

11.5 EXPERIMENTAL PROCEDURE

The bath was brought to the desired temperature and the apparatus run for a short time until the drying tubes reached constant weight. The sample to be dried was taken from a well mixed and sieved bulk sample, weighed into

the sample tube, and quickly put into the drying vessel through the cone joint. Several minutes were allowed for the sample to reach bath temperature, then the air was switched on. After suitable time intervals the air flow was switched to the other drying tube and the first weighed. For safety reasons the bath had to be switched off each evening so that extended drying runs consisted of a shut-down and start-up every six hours of drying. At the end of the run the sample tube was reweighed.

Samples for analysis were taken from the initial bulk sample, the dried material, and from a portion of the bulk sample stored in a desiccator until it had reached constant weight. These were analysed for moisture by the Karl Fischer Method (Appendix V).

11.6 EXPERIMENTAL RESULTS

All samples (Table 11-1) were from batches of hexamine crystals grown under vacuum at 40°C in the two litre crystallizer. All except one contained regular inclusion patterns. Sample 4 contained only random inclusions. Sample 7 contained 'edge' inclusions as well. The last three runs were carried out at some time subsequent to the others and it was possible to use hexamine samples with a much higher inclusion content.

The experimental results are presented in Table 11-1. Column A shows the moisture content (by analysis) of the sample before drying; column B, after drying. Column C shows the analysis of portion of the original sample after storage in a desiccator. The results are plotted in Fig 11-5 as the residual moisture content of the sample after various drying times.

Samples 1 and 2 are from the same batch of material. Run 1 used

Sample No.	OPERATING CONDITIONS					DRYING RESULTS							
	Description of Sample	Temp., °C.	Air Rate l./min.	Mass Sample g.	A. Sample Moisture + Content, mg/g.	Total Moisture Recovered in Drying Tubes mg./g. sample.						B. Moisture Content After Drying + mg./g.	C. Moisture of Sample Kept in Desiccator + mg./g.
						1 hr.	2 hr.	3 hr.	5 hr.	10 hr.	20 hr.		
	All crystals batch grown at 40°C and stored several weeks before use. Sieved through 18# screen before drying test a, with random inclusions b, with regular pattern c, with edge inclusions												
1	Damp crystals, b	95	0.5	34.2	12.0	7.01	9.60	9.60	9.82	9.82	9.82	1.7	2.2
2	Air dried crystals, b	80	0.5	31.8	2.9	0.45	0.47	0.49	0.51	0.55	0.63	2.7	2.3
3	Air dried crystals, b	80	0.5	23.5	2.1	0.16	0.24	0.29	0.35	0.41	0.47	-	-
4	Desiccated sample, a	94	0.6	34.6	0.9	0	0	0	0	0	0	1.1	1.0
5	Batch No.77, Air dried, b	105	0.8	34.3	13.2	0.53	0.75	1.00	1.26	-	-	11.3	12.4
6	Batch No.18, desiccated, b	105	0.8	42.5	7.5	0.04	0.08	0.16	0.24	-	-	7.2	7.5
7	Batch X, desiccated, b,c,	105	1.0	34.1	6.6	0.23	0.26	0.34	0.42	-	-	5.8	6.0

+ By Karl Fischer analysis. Errors ± 0.3 mg./g.

TABLE 11.1 : RESULTS OF DRYING RUNS ON HEXAMINE CRYSTALS.

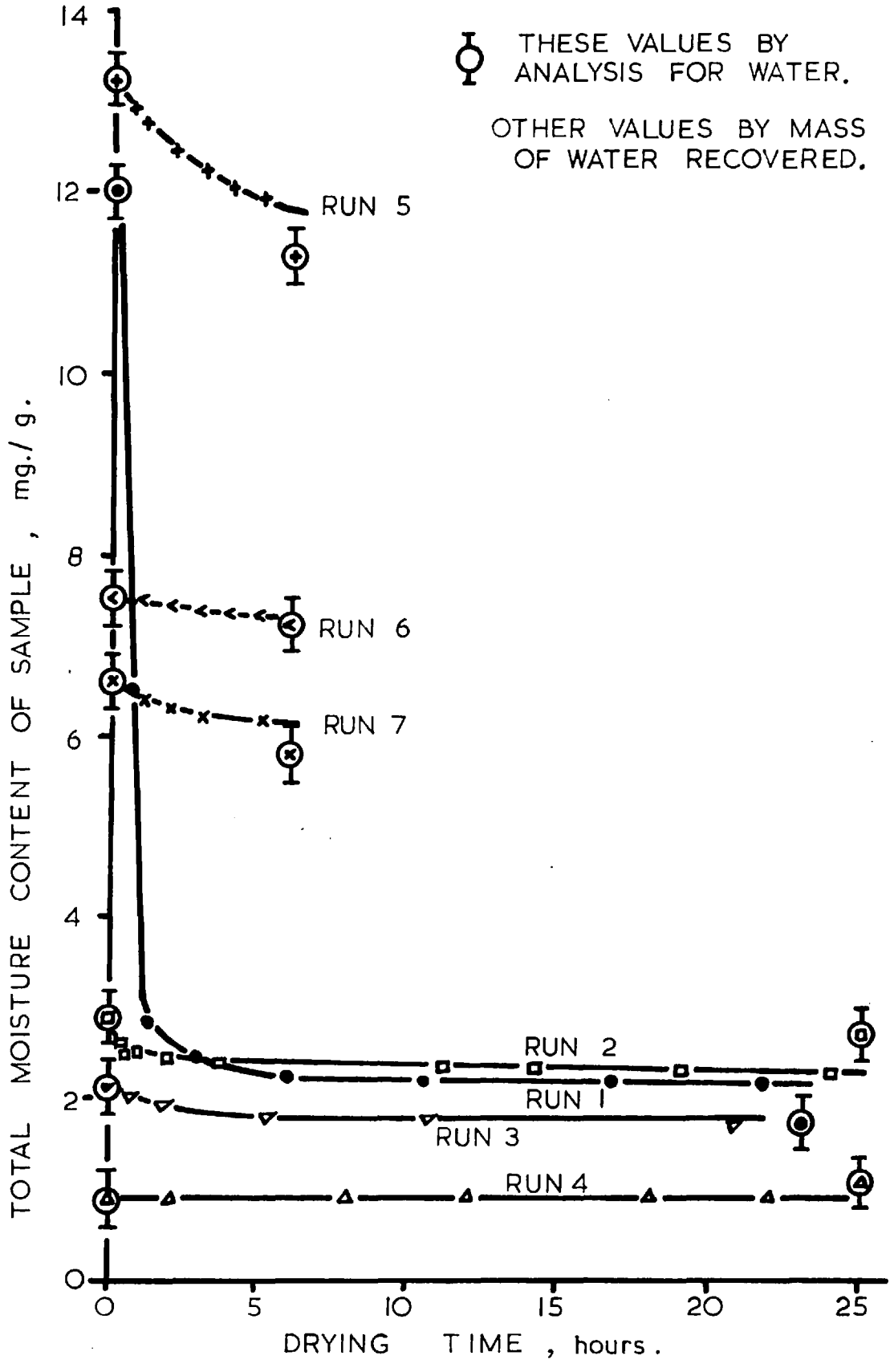

FIG.11-5 : DRYING RUNS ON HEXAMINE CRYSTALS.

a damp sample with about 1% of surface moisture, while Run 2 used air dried material. It is seen that surface moisture is very rapidly lost, but also that a certain common residual moisture remains in both cases even after lengthy drying times. Later samples were all predried either in the atmosphere or in a desiccator to substantially eliminate the surface moisture. In these cases, the rates of moisture loss were very slow or negligible.

The moisture content could be determined only to within $\pm$ 0.03 mg/g by the Karl Fischer method. Errors in determining the moisture recovered in the drying tubes are probably less than 0.1 mg/g. Within these errors, the moisture contents of the sample after drying and the desiccated sample (columns B and C) may be considered identical. Further, the moisture loss as computed from analysis is in agreement with that recovered in the drying tubes.

The change in weight found by weighing the sample before and after the drying run could not be equated to the moisture loss. In some cases the sample gained in weight. This was probably due to condensation of hexamine vapour on the initially cold sample.

11.7 DISCUSSION OF RESULTS

It seems reasonable to consider the residual moisture content as being solely included moisture, since surface moisture is so readily removed. It is impossible to say whether all the included moisture remains or whether some is lost in drying since there are no means of deciding whether the moisture recovered comes from the inclusions or from the surface (unless surface moisture has been deliberately added as in Run 1). Under the microscope there is no obvious change in the appearance of

the inclusions before and after drying. Also the residual moisture content after drying (column B) does not differ significantly from that of the bulk sample after desiccation (column C), so there are some grounds for suggesting that the included moisture remains intact.

However, it is quite clear that the major portion of the included moisture remains even after extended drying under extreme drying conditions. These conditions are considered to be beyond the limits of practical feasibility in the industrial manufacture of this material. It must therefore be concluded that drying cannot be considered a means of removing the included moisture.

The included moisture might be removed if the crystals were crushed and the liquor released but this would require extensive grinding and would give a powdery product. A likely alternative to drying would be dissolution and subsequent recrystallization under controlled conditions, or from another solvent.

11.8 EXPERIMENTS WITH HEATED CELL

One of the mechanisms by which the included liquor may be released is the rupture of the crystal by the pressure generated within the inclusions. The glass cell shown in Fig 11.6 was used to investigate the temperature at which this would occur for hexamine crystals.

The cell consisted of two optically plane faces situated about a centimetre apart. Into the cell passed a stirrer, an electric heating coil, a thermometer, and a glass sample holder. The sample holder was a flat tapering tube with two moderately plane sides. The taper was sufficiently narrow that only a single layer of crystals was held, and readily observed. The cell was mounted in place of the slide carrier of

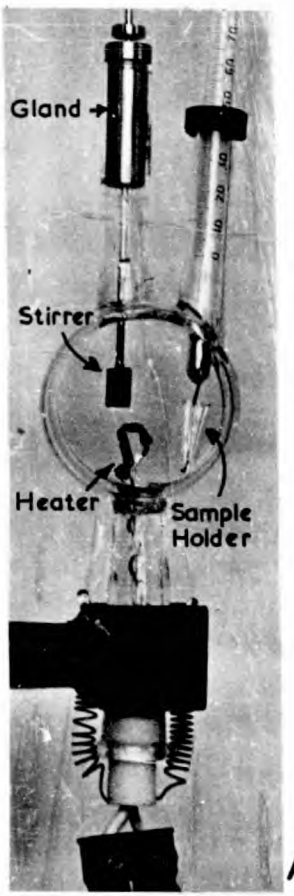

A.

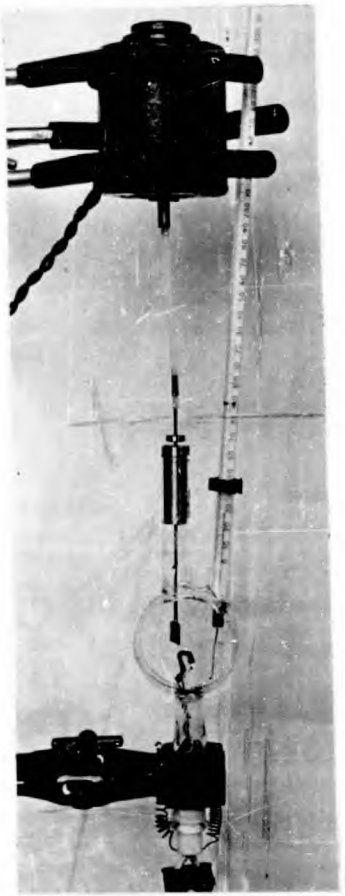

B.

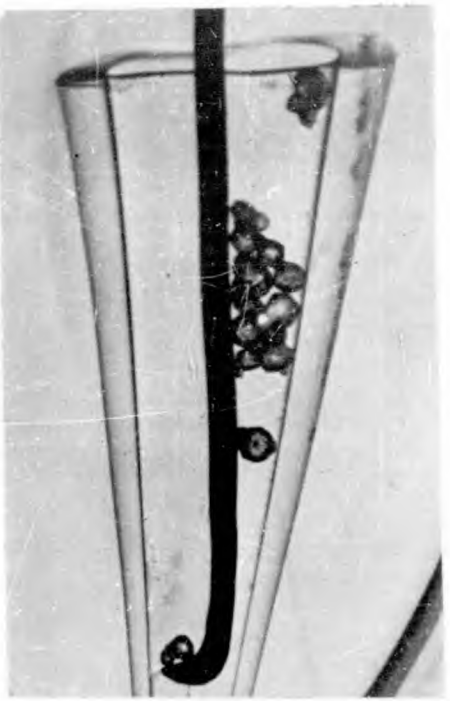

C.

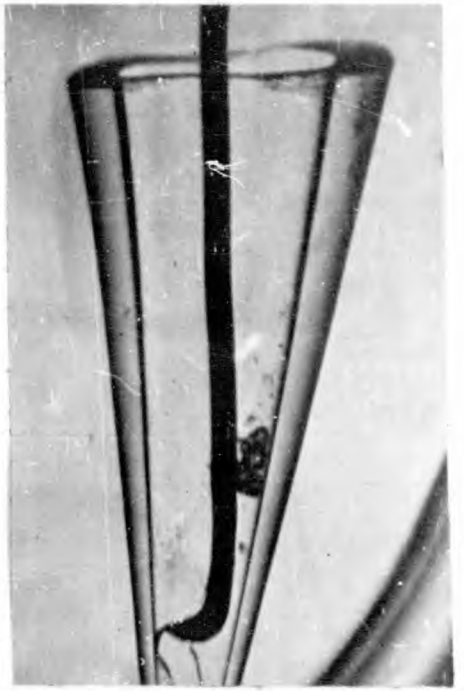

D.

FIG. II-6. PHOTOGRAPHS OF HEATED CELL.

A : CELL ; B : CELL AND MOTOR.

C : SAMPLE AT 175 °C.
D : SAMPLE AT 195 °C.

a lantern slide projector and its image projected onto a screen with sufficient magnification for the inclusion patterns in the crystals to be seen.

A suitable immersion liquid should be non-opaque, non-inflammable, have a high boiling point, and should not dissolve the sample. Glycerol and bromobenzene were tried without success; di butyl phthalate behaved satisfactorily. The sample crystals grown under vacuum at 40°C were about 300 μ in size and taken from the same batch as the crystal shown in Fig 3-2. Heating rates varied from 1 to 5°C per minute.

No evidence of crystal rupture was observed at least up to 180°C. If the volume of the inclusion and the amount of liquor in it are assumed to remain constant (though this is most unlikely) the pressure generated in the inclusion could be as much as 1000 atmos. at this temperature. Beyond 190°C the crystals dissolved rapidly. Fig 11.6c shows the sample intact at 175°C, while photograph d shows the sample dissolving at 195°C. Barely discernable on the photograph (but muchclearer on the screen) can be seen the shower of rapidly rising drops expelled at this stage. These are probably vapourised liquor released when the dissolution of the crystals reaches the inclusions.

11.9 CONCLUSIONS

Drying is not likely to be a practical means of removing the included moisture from crystals, at least from hexamine crystals.

The temperature at which hexamine crystals will rupture through pressure buildup in the inclusions is far in excess of the temperature of formation.

12. THE CAKING OF STORED CRYSTALS

12.1 INTRODUCTION

It has been argued that the presence of included solvent in crystals may be a cause of their caking in storage. The solvent might diffuse out from the inclusions and evaporate on the surface, depositing its solute in the crevices between a crystal and its neighbours, thus enabling them to bond together.

This proposal will be examined in the light of the observed storage behaviour of hexamine crystals which often cake. The type of bonding between caked crystals is clearly illustrated in Fig 12.1.

12.2 STORAGE IN DESICCATORS

Batches of damp newly-manufactured crystals when stored in a desiccator invariably caked solid, irrespective of whether the batch had inclusions or not. If the dried crystals were sieved and replaced in the desiccator no caking occurred, even after many months, although some samples contained several percent of included moisture. If the crystals were deliberately redampened they would cake again.

12.3 STORAGE IN AIR

With air of low humidity a similar behaviour to that in the desiccator was observed. In high humidity air, however, hexamine samples became most noticably damp. For air at 20°C the relative humidity at which this deliquescence occurs has been calculated as 76.3% (refer Supplement Fig SII-8). This value is in agreement with the tests shown in Table 12.1 giving the increase in weight of identical samples of hexamine stored in atmospheres of controlled relative humidity for one day. All the samples that took up moisture caked when stored in dry air.

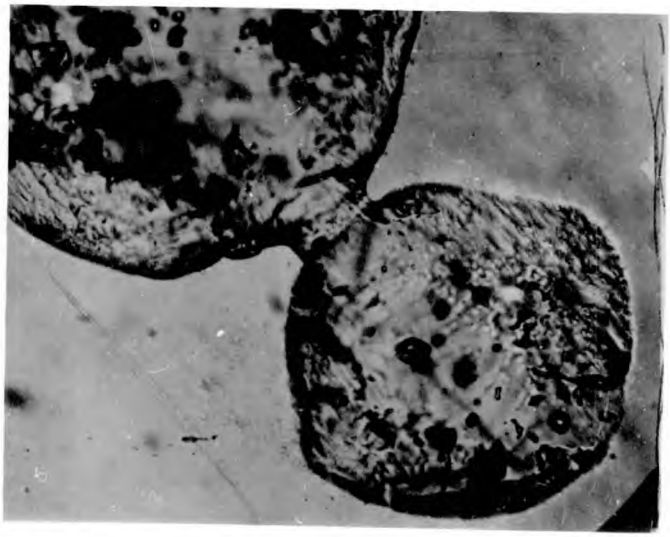

FIG. 12 .1 : CAKING BOND BETWEEN TWO HEXAMINE CRYSTALS (DENBIGH [35]).

21°C. , 3 g. of sample in 5 cm. dia. Petri dish		
Aqueous Solution.	% Relative Humidity of Air above. Solution .	% Increase in Weight after One day.
$CaCl_2$ (satd.)	ca. 30	0
$CaCl_2$ (ca. 33%)	ca. 60	0
NaCl (satd.)	75.6	0
NH_4Cl (satd.)	79.2	1½
$(NH_4)_2SO_4$ (satd.)	81.0	4
$CaCl_2$ (ca 20%)	ca. 82	8
Water	100.0	11

TABLE 12 .1 DELIQUESCENCE TESTS ON HEXAMINE SAMPLES.

12.4 DISCUSSION

Caking is a problem in the commercial production of hexamine. A recent patent [36] recommends the addition of benzoic acid derivatives as anti-caking agents.

The major cause of caking of hexamine crystals would appear to be the interplay of the deliquesent behaviour of hexamine with the varying humidity of the air. This is a common cause with many other materials [2,5]. Included moisture as a mechanism of caking seems to be of little or no importance, since samples in a desiccator do not cake. Drying tests have already indicatedthe extreme reluctance of the included moisture to be removed, so its non-effectiveness in caking is not surprising. Further it should be noted that the amount of included moisture in commercial crystals is quite small (0.1 to 0.3%).

12.5 CONCLUSION

Included moisture appears to be of little importance as a cause of caking, at least of hexamine crystals.

13. SUGGESTIONS FOR FURTHER WORK

13.1 GROWTH OF HEXAMINE CRYSTALS FROM AQUEOUS SOLUTION

The results obtained in this project can explain the formation of 'face' inclusions in terms of measured critical quantities. Little can be said of the exact significance of these quantities. The somewhat tentative ideas expressed in section 7.14 require a more thorough experimental basis, and investigations with this aim would be quite useful.

It would be interesting, for example, to grow inclusions on crystals of hexamine mounted in an interferometric cell (such as that used by other authors [32, 33]) or something similar, so that the actual concentration profiles around the crystals could be determined. A knowledge of the variation of concentration gradients about the crystal corners and cavities would be very useful in any discussion of inclusion formation. There may be certain experimental difficulties in obtaining suitably supersaturated aqueous solutions to do this. One possiblity is to use an initially cold solution and to heat the crystal internally causing the solution at the surface to become supersaturated. The non-isothermal nature of the system might however make interpretation of the interference patterns difficult.

It would also be of interest if dendrites of hexamine could be grown in bulk solutions and the existence of a change from cavitite to dendrite established. Growth conditions for the transformation could be determined.

A study of the manner in which subsequent growth seals over an open cavity could also be undertaken. Thin slices of crystal with artificial cavities could be observed growing between glass slides. Such investigations would be an aid to the understanding of the formation of edge inclusions as well.

Basic measurements linking the crystal growth rates to solution super-saturation and relative motion would also be of considerable use.

13.2 GROWTH OF HEXAMINE CRYSTALS FROM OTHER SOLVENTS

A more detailed study could be undertaken of the growth of inclusions in hexamine crystallized from other solvents, or from solvent mixtures. The conditions giving rise to inclusion formation could be determined and compared with those for aqueous solutions. The thermal crystallizer is not particularly suitable for these measurements. Perhaps the evaporative crystallizer could be modified and used to give more accurate data.

13.3 GROWTH OF OTHER CRYSTALS FORMING INCLUSIONS

A much more thorough investigation is required of the growth of ammonium chloride and sodium chloride crystals with inclusions. The technique of consecutive sampling as used in this project for hexamine should be quite suitable.

A search should be made for other crystalline materials that show 'face' inclusions to ascertain the importance of this phenomenon in crystallization practice.

13.4 GROWTH OF 'EDGE' INCLUSIONS

Tests could be carried out using well rounded (ideally, spherical) seed crystals in supersaturated solutions to ascertain if there is a limiting growth rate below which the plane crystal faces will develop without forming 'edge' inclusions. If so, this critical rate could be related to operating variables such as the seed size and relative motion of the seed crystal to the solution.

Attempts could be made to grow edge inclusions in hexamine crystals using other solvents, to see if the nature of the solvent has any effect.

13.5 MIGRATION OF INCLUSIONS

Measurements could be made of the rate of movement of inclusions in crystals subjected to a temperature gradient. This could possibly be a means of removing inclusions from crystals. The rate of migration could perhaps be linked to the rate at which the inclusions change shape under conditions of fluctuating temperatures.

13.6 INCLUSIONS AS A SOURCE OF STRAIN IN CRYSTALS

The presence of inclusions in crystals may be a cause of localized stressing within the crystal, especially with changes in temperature. For certain crystal applications this could be a serious problem. It would be interesting to measure the pressure generated in an inclusion with variations of temperature. For low temperatures the size of the vapour bubble in the inclusion could be measured. Alternatively, an artificial inclusion containing a pressure transducer could be grown, by drilling a hole through a crystal and resealing the ends by crystal regrowth. The stresses in the crystal could be seen also by optical or other methods if the crystal, as hexamine does, shows photo-elastic, electro-optical or piezo-electric properties.

13.7 APPLICATION TO LARGE SCALE EQUIPMENT

In this project most of the crystals with inclusions were produced in one crystallizer. The results were explained in terms of critical growth conditions and the nucleation behaviour. Different results, no doubt, would have been obtained in other or larger crystallizers because of the variations in nucleation behaviour. It may be of interest from a practical point of view to ascertain the nucleation behaviour in commercial batch crystallizers to see if 'scaling up' the equipment size will increase or decrease the tendency to inclusion formation.

15.8 A METHOD OF TAGGING CRYSTALS

A possible use of crystals with regular internal patterns of inclusions could be mentioned here. Such crystals could be used as 'tagged' or 'marked' crystals in crystallization studies.
The crystals are readily recognised and reasonably readily formed. An advantage over other methods of tagging is that no further impurity is introduced; however there may be a slight difference in crystal density.

14. CONCLUSIONS

Patterns of inclusions of very great regularity have been grown in crystals of hexamine, ammonium chloride, and sodium chloride. Patterns of two distinct types have been seen. In the first, termed 'Face' inclusion patterns, inclusions lie in sets with one inclusion corresponding to each face of the crystal. In dodecahedral crystals of hexamine twelve inclusions occur in the pattern; in cubes of ammonium chloride and sodium chloride, six. In the second type of pattern, termed the 'edge' pattern, a large number of small inclusions outline the edges of the crystal at some prior stage of growth. In hexamine crystals the 'edge' inclusions outline the edges of a dodecahedron; in the other two materials, the edges of a cube.

The growth of face inclusions in hexamine crystals formed from aqueous solution has been analysed in detail. It has been shown that when face inclusions form, the crystal grows first as a cavitite i.e. as a crystal with cavities on all faces. This cavitite eventually reverts to plane crystal growth and the mother liquor in the cavities is sealed in forming the inclusions. From various measurements on a large number of crystal samples it has been shown that the formation of inclusions can be described in terms of a critical crystal size and a critical growth rate. Above this critical size and at growth rates higher than the critical, hexamine crystals will grow as cavitites; below it as plane faced crystals. These critical values are the same for all batches of crystals grown, and were evaluated as 65 $\pm$ 5 μ and 12 $\pm$ 5μ/min respectively. The same results were found to apply to crystals grown in static solution.

The variation of inclusion formation with crystallizer operating conditions has been explained in terms of the variation in the batch nucleation rate. Stirring speed, for example, increases the rate of nucleation, and therefore decreases the size of the inclusions formed in the batch. The use of additives

appears to be explained also by their effect on the nucleation rate.

Hexamine crystals were grown from other solvents. From non-aqueous solvents inclusions could not be formed. From mixed solvents inclusion formation occurred provided there was a moderate amount of water in the solvent.

The growth of 'face' inclusions in other crystals appeared to follow the same general mechanism as proposed for hexamine crystals. The critical growth conditions were not measured accurately. However, they appear to be of the same order as those for hexamine

'Edge' inclusion patterns are formed by regrowth on rounded or partly dissolved seed crystals. The amount of rounding of the seed crystal is the major factor influencing the size of the edge inclusions formed.

Attempts to remove the included mother liquor from hexamine by drying were unsuccessful, even though quite severe drying conditions were used. It seems unlikely that the included moisture is a cause of crystal caking.

APPENDIX I

PHOTOMICROGRAPHIC EQUIPMENT

A standard "Spencer" transmission microscope with a 6X eyepiece and a turret objective was used. The microscope had a mechanical stage. For most work the lowest powered objective (10X, 16 mm) proved quite suitable.

A 35 mm. 'Praktica' camera body with focal plane shutter was fitted to the microscope by an adaptor tube for photographic recording (Fig.AI-1). The eyepiece was removed from the microscope and the objective acted simply as a simple lens throwing an image onto the focal plane of the camera. An object to image magnification of 16 was obtained. This was purposely kept low to give a reasonable depth of field.

Illumination was from an ordinary microscope lamp. Fine grain film ('Panatomic X') was used with shutter speeds of 1/200th of a second. The film was developed in fine grain developer. Typical micrographs showing hexamine crystals in various immersion fluids are shown in Fig. AI-1. The selection of a suitable immersion fluid was discussed in section 4.2.

Prints were made from all negatives of the evaporative crystallizer samples. An overall magnification of about 70 was achieved. The magnification was checked by photographing a piece of stainless steel wire of known dimension also immersed in these fluids. All sample measurements were made from these prints.

The negatives from the tests on the heated cell were projected across a room onto a screen, and the size of individual crystals measured. This gave an overall magnification of about 700 which was also checked against the stainless steel wire as reference. A special scale rule allowed

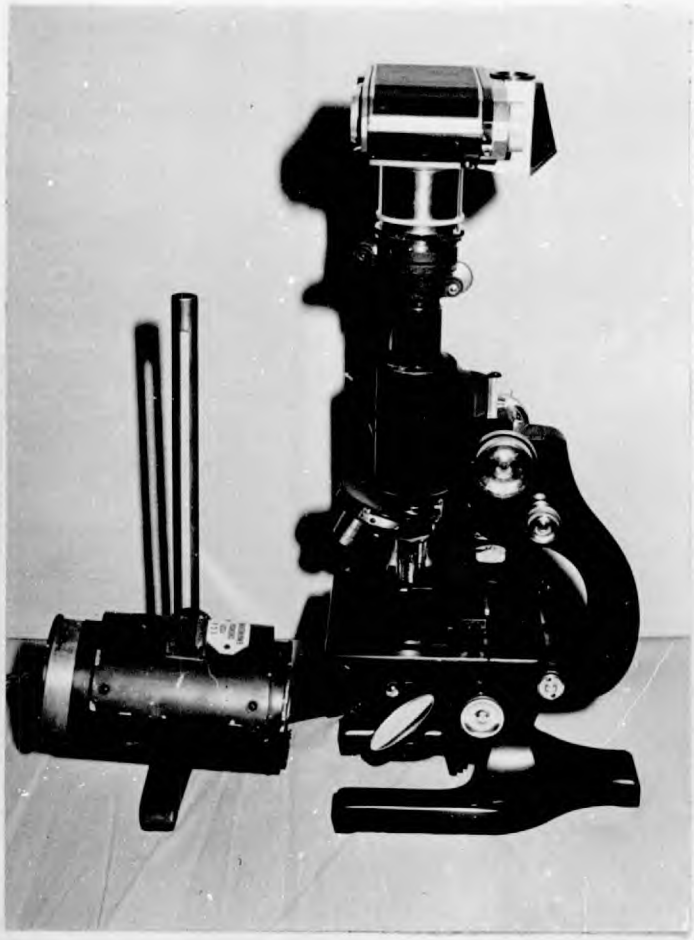

A. GLYCEROL.

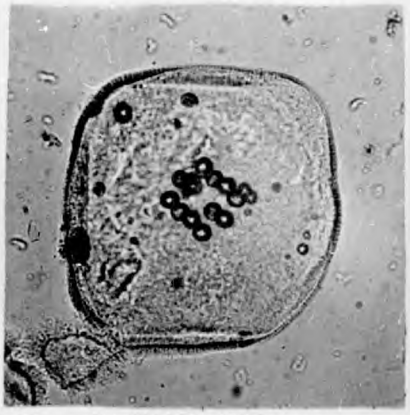

B. CLOVE OIL + BROMO-NAPHTHALENE.

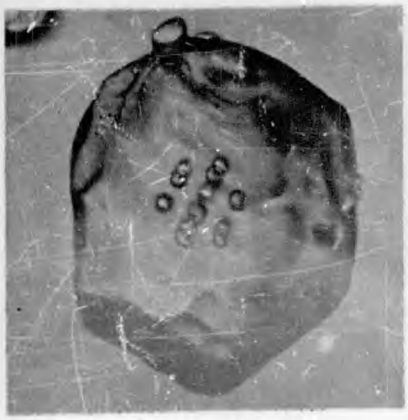

C. BROMOBENZENE.

D. ANILINE.

E. AQUEOUS SOLUTION.

FIG. AI-1. MICROSCOPE WITH CAMERA ATTACHED. TYPICAL MICROGRAPHS OF HEXAMINE CRYSTALS IMMERSED IN VARIOUS FLUIDS ARE SHOWN.

direct measurements of size to be made.

Cine photographs were taken with a 16 mm 'Bolex' reflex viewing cine camera. The camera without lenses was mounted over the microscope in place of the 35 mm camera. The microscope lamp had to be moved away to reduce the illumination to a suitable level for the filming speed used (up to 32 f.p.s.). 'Ilford' F.P.3 film was used.

APPENDIX II

SAMPLE CALCULATION

1. EVAPORATIVE CRYSTALLIZER RESULTS

(i) Measurements on Photographs.

Four different photographs of each sample were taken. On each print a rectangular frame including about 60 to 100 crystals was ruled. The crystals inside this frame were counted. At least half of a crystal had to be inside the frame for it to be included. All the crystals inside the frame were numbered consecutively and the size of each determined. The crystals were classified into various size ranges. The size range interval depended on the total size range, but usually either a 25 μ or a 50μ interval was used. The number of crystals in each range was determined and the total number for the four photographs was computed. While measuring the size of each crystal, note was also made whether the crystal showed 'face' or 'edge' inclusion patterns. The numbers and size range of such crystals was also determined.

For example for Sample No. 37-4 of Batch No. 37 a total of 556 crystals (n') from the four photographs were counted. This sample contained crystals with face patterns of inclusions. A photograph of this sample is shown in Fig 7-14. The size distributions of the crystals was as follows (see Appendix III).

Size Range, μ	Number in Range	Number with Inclusions in Range
0 - 50	82	0
50 - 75	88	0
75 - 100	62	6
100 - 125	37	33
125 - 150	52	52
150 - 175	35	35
	556	126

(ii) Direct Computations on Size Distribution

From this size distribution the fraction of the crystals with inclusions, β, can be computed. The mean crystal size, $\bar{x}$, of the distribution on a volumetric basis can also be calculated from the relation :-

$$\bar{x} = \left(\Sigma x^3 f(x)\right)^{\frac{1}{3}}$$

where x is the mean size of crystal representative of each size range, and f(x) is the fraction of the total number of crystals in that range.

The quantity α, linked to the mean surface area of crystal was computed from the definition, $\alpha = \left(\Sigma x^2 f(x)\right)/\bar{x}^2$. This quantity usually lies between 0.7 and 1.0 and this gives a useful check on the computations. The value of α depends on the shape and extent of the distribution.

For the distribution of those crystals with inclusions, similarly $\bar{x}_i$ and α_i can be computed. For the example taken,

$$\beta = 0.55$$
$$\bar{x} = 104\ \mu$$
$$\alpha = 0.87$$
$$\bar{x}_i = 141\ \mu$$
$$\alpha_i = 0.98$$

Assuming that all crystals have the same shape, the ratios of the surface area and volume associated with the crystals with inclusions to the total, γ_A and γ_V respectively, can be computed.

For the example $\gamma_A = 0.72$, $\gamma_V = 0.88$.

(iii) Further Measurements on Photographs

Those crystals in the sample with inclusions were remeasured to determine the internal and external sizes of the inclusion pattern, y and y', the size of the inclusions, s, and the thickness of crystal covering the inclusion, t. These

quantities were discussed in Section 7.6. It was shown there that y and t have substantially constant values for each batch. The various estimates of y and t were averaged (arithmetically) to give $\bar{y}$ and $\bar{t}$ for each batch. The mean values of s and y' (on a volumetric basis) were computed from the relations

$$\bar{s} = \left[\Sigma s^3 f(s)\right]^{\frac{1}{3}}$$

$$\bar{y}' = \left[\Sigma y'^3 f(y')\right]^{\frac{1}{3}}$$

where f(s) and f(y') are respectively the fraction of the total number of observations lying in the size range characterized by s and y'.

The results for the example chosen (Sample 37-4) has been shown in the text (Fig 7-10). It was shown that $\bar{y}$=64μ, $\bar{t}$=9μ, $\bar{s}$=28μ, and $\bar{y}'$=119μ.

Although $y' = y+2s = x_1-2t$ for each individual crystal, because of the way means are taken these relations are not applicable to the mean quantities.

If a flat distribution for f(s) is assumed it can be shown that $\bar{y}' = \bar{y} + \eta \bar{s}$ where η has a value between 1.59 and 2 depending on the value of s/y. This relation could be used to estimate $\bar{y}'$ fron $\bar{y}$ and $\bar{s}$ although errors would be involved if the size distribution of s were not flat. Similar corrections could be computed for the other relationship for $\bar{y}'$.

(iv) Calculation of Number and Surface Area of Crystals and Total Inclusion Volume

The number of crystals, n, can be determined from the mass of product, M, and the mean crystal size, $\bar{x}$, by the relation

$$n = M/a\rho\bar{x}^3$$

where ρ is the crystal density and a is a volume shape factor for the crystal. For dodecahedral crystals, a = 0.707.

The total surface area of crystal, A, can be evaluated by the following relation

$$A = n\alpha b\bar{x}^2$$

where α is the area-volume factor for the size distribution as discussed above and b is an area shape factor. For dodecahedra, b=4.24.

For the example considered, the sample was taken 3 min after nucleation and the rate of evaporation was 8.6 g./min, which corresponds to a hexamine deposition rate, n, of 7.5 g/min.

$$M = 22 \text{ g}$$

Hence $n = 22/0.707\ 1.33\ (104)^3\ 10^{-12}$.

$= 2.0\ .10^7$

and $A = 2.0\ 10^7\ 0.87\ 4.24\ (104)^2\ 10^{-8}\ \text{cm}^2$.

$= 8.0\ .10^3\ \text{cm}^2$.

The number of crystals with inclusions $n_i = \beta n$

$= 7.0\ .10^6$.

The total volume of included liquor may be calculated as follows :

$$v_t = n_i\ c\ \bar{x}^3$$

where c is a volume shape factor for the inclusions. If the inclusions are dodecahedral, c=0.71; if pyramidal, c=0.48.

For the example considered, the inclusions are pyramidal in shape and $v_t = 0.76$ cc.

(v) Growth Rates

Assuming all crystals grow at the same instantaneous rate, the mean growth rate per face, R, can be determined from the deposition rate, n, and the total crystal area, A.

$$R = n/\rho A = a\bar{x}/b\alpha\theta$$

For the example $R = 7.5/1.55\ \ 8.0\ \ 10^3\ 10^{-4}\ \mu/\text{min}$

$= 7.0\ \mu/\text{min}$.

An estimate of the growth rate can also be made from two consecutive samples sampled at times θ_1 and θ_2 when the mean size of those crystals with inclusion were respectively, $\bar{x}_{i_1}$ and $\bar{x}_{i_2}$. This estimate of the growth rate,

$R' = (\bar{x}_{i_2} - \bar{x}_{i_1})/2(\theta_2 - \theta_1)$.

(vi) Critical Growth Rates

For a batch where consecutive samples were taken the critical growth rate can be determined graphically. The growth rates for each sample are plotted against the corresponding value of $\bar{x}_i$ to give the $\bar{x}_i$ growth curve. The value of $\bar{x}_i$ at which the inclusions just sealed over, $\bar{x}_i^* = \bar{y}'$ is plotted and the corresponding growth rate is the critical value.

For Batch No. 37 the growth curve was shown in Fig 7-22, $\bar{y}' = 119\mu$, and the critical growth rate $R^* = 11 \pm 3$ μ/min.

From a plot of growth rate against time the moment of inclusion sealing θ_s can be determined. For the example $\theta_s =$ 1.7 min.

When only one sample is taken for each batch an estimate of the critical growth rate can be made if a linear relation between surface area and time is assumed, as follows :

Assuming $A = k\theta$

then $R = \frac{1}{2}\frac{d\bar{x}_i}{d\theta} = n/\rho k \theta$

Hence by integration, $\bar{x}_i = \frac{2n}{\rho k} \ln\theta +$ const.

i.e. $\ln R = -\frac{\rho k}{2n} \bar{x}_i +$ const.

or $\ln\left(\frac{R^*}{R}\right) = \frac{\rho A}{2n\theta} (\bar{x}_i - \bar{x}_i^*) = \frac{b\alpha}{2a\bar{x}} (\bar{x}_i - \bar{x}_i^*)$

since $k = A/\theta$, where R^* is the critical growth rate corresponding to the mean crystal size $\bar{x}_i^*$.

All the quantities R, A, , $\bar{x}_i$ and $\bar{x}_i^*$ can be determined from the single sample.

For the sample considered.

$$\ln\left(\frac{R^*}{7.0}\right) = \frac{1.33.\ 8.0.10^3}{2\ 7.5\ 3}(141-119)\quad 10^{-4}$$

and $R^* = \quad 10.7\ \mu/\text{min.}$

The assumption of a linear relation between the surface area and time means that a linear relation exists between ln R and $\bar{x}_i$ with slope of $-\ b\alpha/2a\bar{x}$. The ratio b/a is usually 6 and α is approximately constant. Hence this assumption implies that $\bar{x}$ is virtually unchanged as crystallization proceeds.

(vii) Sample with No Inclusions

Quantities which do not depend on the presence of inclusions, namely $\bar{x}$, α, n, A and R, were computed in the same way as in the previous example. In place of $\bar{x}_1$, $\bar{x}_1$ was computed. This was determined as the volumetric mean of the size of a number of the largest crystals in the sample. The number counted for this quantity was such as to correspond to about 7 million crystals in the batch, and was computed from n and n'.

For example for Sample No. 40-2 (shown in Fig 7-25) the following quantities were computed (see Appendix III).

$\bar{x} = 44\mu.$
$\alpha = 0.89$
$n = \quad 14 \quad .10^7$
$A = \quad 10.3 \quad .10^5\ \text{cm}^2$
$R = \quad 5.5 \quad \mu/\text{min.}$

The number of crystals counted in the sample was 394 and a fraction 7/140 of the largest of these (ie 20) was averaged (on volumetric basis) to give $\bar{x}_1 = 66\mu$. The largest crystal in the sample was 75μ.

For a consecutively sampled batch, comparison with other growth curves can be made if the values of R from the various samples are plotted against $\bar{x}_1$.

An estimate of R' can also be made from the relation $R' = \frac{1}{2}\frac{d\bar{x}_1}{d\theta}$.

For a batch with a single sample a growth rate of interest is that of the largest crystal when it was at the critical size of 65μ. This may be computed from the relation :-

$$\ln\left(\frac{R_{65}}{R}\right) = \frac{\rho\Lambda}{2n\theta}\ (x_{\text{largest}} - 65)$$

For the sample chosen this becomes

$$\ln\left(\frac{R_{65}}{5.5}\right) = \frac{1.53\ 10.3\ .10^5}{2\ 7.5.\ \ 1\frac{1}{2}}\ (75-65)\ 10^{-4}$$

$$R_{65} = \quad 10.1\ \mu/\text{min.}$$

(viii) Samples with Edge Inclusion Patterns

In the manner already outlined, the quantities $\bar{x}, \alpha$, n, Λ and R can be computed. Similarly the quantities β, $\bar{x}_i$ and n_i can be determined where now the quantities refer to crystals with edge inclusion patterns.

The size distribution of the inclusion patterns can be determined and the mean value on a volumetric basis $\bar{y}'$ determined. The mean thickness of crystal covering the inclusions $\bar{t}$ can also be measured. The calculations following from these data are similar to those already shown for crystals with face inclusions.

2. THERMAL CRYSTALLIZER RESULTS

For each test a set of negatives were obtained. These showed the same set of crystals at various time intervals. The negatives were projected onto a screen and the sizes of individual crystals measured. Estimates were made also of the times and crystal sizes at which inclusions began and stopped forming.

The mean growth rate in each time interval was computed from half the increase in size divided by the time interval. This was taken to be the rate at the mean crystal size during that interval. A more representative mean quantity could have been chosen but with the accuracy of measurement involved, this would not really have been warranted.

A P P E N D I X I I I

EXPERIMENTAL RESULTS FOR EVAPORATIVE CRYSTALLIZER

A. DETAILS OF OPERATING CONDITIONS

TABLE III A 1 : These batches concerned with the growth of 'face' inclusion patterns in hexamine.

TABLE III A 1

Feed Stock No.	Batch No.	Temp. °C.	Stirrer R.P.M. ±	Heat No.	Condensate g./min.	Initial Feed g.	Duration of Run, min.	Sample No.	Remarks.
	1	41	120	10	9.2	1380	25	1	
	2	40	120	10	9.0	1410	26	2-2	Sample 2-1 at 10 min.
1	4	41	120	10	9.3	1350	28	4	
	6	40	100	6	2.82	1370	93	6	
	7	40	100	8	5.0	1330	54	7	
2	8	40	100	10	8.3	1100	31	8	
	9	38	100	10	8.8	1360	20	9	
	10*	39	100	10	8.6	1350	20	10-1	
	11	38	100	10	8.6	1320	30	See Table III E 1	
	12*	44	100	10	8.8	1300	10	12-1	
3	13*	36	100	10	8.8	1340	7	13-1	
	14*	40	100	10	8.6	1350	6	14-1	
	15*	40	100	10	8.4	1350	7	15-1	
	16*	40	220	10	8.5	1310	6	16-1	
	17	44	38	10	9.0	1190	10	17	
	18	45	33	10	8.3	1160	10	18	)
	19	45	150	10	8.8	1190	10	19	)
	20	45	240	10	8.8	1140	10	20	)
	21	45	80	10	8.4	1170	10	21	) Variation
4	22	45	120	10	8.5	1160	10	22	) with
	23	45	60	10	8.5	1140	10	23	) Stirring
	24	45	44	10	8.1	1160	10	24	) Speed.
	25	45	60	10	8.3	1120	10	25	)
	26	42	60	10	8.6	1500	65	See Table III E 2	
	27	32	60	10	8.0	1530	20	27-2	Sample 27-1 at 7 min
5	28	45	60	10	8.6	1380	30	28-2	Sample 28-1 at 7 min
	29	59	60	10	8.6	1410	7	29	
	30	51	60	10	8.5	1420	30	30-2	Sample 30-1 at 7 min

/Continued....

TABLE III A 1 (Continued) (p.2)

Feed Stock No.	Batch No.	Temp. °C.	Stirrer R.P.M.†	Heat No.	Condensate Rate g./min.	Initial Feed g.	Duration of run, min.	Sample No.	Remarks
	31	41	60	10	8.6	1510	37	31-3	Samples 31-1, 31-2 at 1 min & 7 min.
6	33*	39	150	10	8.4	1490	5	33-1	
	34*	40	100	10	8.4	1460	7	34-1	
	36	40	60	10	8.6	1350	5	see Table III E 3.	
	37	40	60	10	8.6	1350	7	see Table III E 4.	
	38	40	100	10	8.6	1350	10	see Table III E 5.	
7	39	40	150	10	8.6	1350	11	see Table III E 6.	
	40	40	230	10	8.6	1350	7	see Table III E 7.	
	41	57	100	10	8.6	1350	14	see Table III E 8.	
	42*	53	100	10	8.6	1350	10	see Table III E 9.	
	44	41	90	10	8.2	600	7	44	)
	45	41	90	10	8.3	1370	7	45	) effect of
	46	41	90	10	8.7	2090	7	46	) vessel
	47	41	90	10	8.6	1520	6	47	) capacity.
	48	40	42	6	2.77	1100	22	48	)
8	49	40	42	8	4.4	1210	14	49	)
	50	40	42	10	7.9	1280	7	50	)effect of
	51	40	70	8	4.9	1280	14	51	)heating
	52	40	70	7	3.75	1250	16	52	)rate.
	53	40	70	10	8.2	1200	7	53	)
	54	40	70	9	8.2	1240	7	54	)
	55	40	70	6	3.11	1240	20	55	)
	59*	40	60	10	8.6	1250	3	59-1	
	60*	40	100	10	8.4	1210	2	60-1	
	61*	40	60	10	8.8	1230	3	61-1	
	62*	40	60	10	8.6	1230	10	62-1	
9	63*	40	65	10	8.6	1200	10	63-1	
	64*	40	150	10	8.3	1230	15	64-1	
	65	40	40	10	8.5	1280	6	65-2	Sample 65-1 at 1min
	66	39	60	10	8.6	1260	4	66	
	67	32	50	10	9.1	1290	10	see Table III E 10	
10	68	83	50	10	8.2	1270	10	see Table III E 11	
	69	58	50	10	8.5	1300	10	see Table III E 12	
	70*	42	50	10	8.4	1270	10	see Table III E 13	

/Continued...

TABLE III A 1 (Continued) (p.3.)

Feed Stock No.	Batch No.	Temp. °C.	Stirrer R.P.M.†	Heat No.	Condensate Rate g./min.	Initial Feed g.	Duration of run min.	Sample No.	Remarks
11	72*	41	50	10	8.6	1310	30	72-1	
	82*	40	33	10	8.6	1320	60	82-2	Sample 82-1 at 5 min.
	84*	40	75	10	8.6	1250	9	84-1	
	85*	40	75	10	8.6	1320	9	85-1	
	86*	40	75	10	8.6	1300	9	86-1	
12	87*	40	75	10	8.6	1280	9	87-1	
	88*	40	75	10	8.6	1290	9	88-1	
	89*	40	75	10	8.6	1210	9	89-1	
	90*	40	75	10	8.6	1280	9	90-1	
	91*	33	75	10	8.6	1250	10	91-1	
	92*	33	75	10	8.6	1300	10	92-1	
	93*	33	75	10	8.6	1250	10	93-1	
	94*	33	75	10	8.6	1270	10	94-1	

An asterisk(*) indicates that the crystals of this batch have been used for the growth of 'edge' inclusion patterns (See Table III A 3).

† Measured as motor speed (see Section 5.7).

TABLE III A 2

Those batches concerned with the growth of 'face' inclusion patterns from hexamine solutions with additives .

T A B L E I I I A 2

Batch No. & Sample No.	Feed.	Temp. °C.	Stirrer R.P.M.*	Heat No.	Condensate g./min.	Initial Feed g.	Duration of Run, min.		
3	1	39	100	10	9.0	1330	28	2 ml Lissapol added.	
35	6	40	100	10	8.7	1470	16	15 ml Lissapol added.	
56	8	40	45	10	8.7	1100	7	30 ml Lissapol added.	
57	8	40	45	10	8.6	1210	7	5½ g. onalic acid added.	
									Viscosity of soln. at 40 °C (cp)
75	-	38	110	10	9.2	1200	12	)	126
76	-	45	30	10	9.0	1200	6	) Various	116
77	-	40	60	10	9.0	1150	5	) quantities	3.8
78	-	40	60	10	8.6	1150	5	) of	7.9
79	-	40	60	10	8.2	1150	5	) viscous	17
80	-	40	60	10	8.6	1150	5	) addictive ≠	22
81	-	40	60	10	8.6	1150	5	)	34

≠ Viscous addictive - 'Polycell" wallpaper adhesive - active ingredient, carboxy - methyl-cellulose (CMC). Viscosities of the resulting solutions at 40°C. are shown.

* Measured as motor speed (see section 5.7)

TABLE III A 3

Those batches concerned with the growth of 'edge' inclusion patterns in hexamine.

(i) Those batches in which 'edge' patterns were not formed.

TABLE III A 3 (i)

Batch No.	Seed			Growth Conditions								Sample No.
		Amount g.	Seed Pretreatment	Soln.	Temp. °C.	Stirrer R.P.M.*	Heat No.	Condensate Spiral,	Temp. for Rapid Evap.	Initial soln. g.	Duration min.	
10	10-1	150	mixed with 500 ml fresh feed	3	39	100	10	8.6	-	1600	1	-
12	12-1	75	mixed 100 ml feed, cooled	3	44	100	10	8.8	-	1400	11	12-2
13	13-1	52	mixed cold feed, bubbled air thro	3	36	100	10	8.8	-	1340	10	13-2
14	14-1	45	shaken with air	3	-	100	10	-	52	1350	8	14-2
15	15-1	52	add 200 ml soln, satd with air	3	-	100	10	-	52	1350	8	15-2
16	16-1	45	cooled to room temp.	3	40	220	10	8.5	-	1310	8	16-2
33	33-1	3.5	air dried	6	39	60	10	8.7	-	1490	7	33-2
34	34-1	52	cooled and saturated with air	6	40	100	10	8.6	-	1460	40	34-2
43	48-5	7.5	air dried	7	42	30	10	8.4	-	1320	10	43
59	59-1	22	mixed with 400 ml fresh feed	9	40	60	10	8.6	-	1360	18	59-2
60	60-1	15	bubbled air through	9	40	60	10	8.6	-	1410	22	60-2
63	82-4	100	none	12	40	200	10	9.0	-	1300	10	83

* measured as motor speed (see section 5.7)

(ii) Those Batches in which Edge Patterns were formed.

TABLE III A 3 (ii)

Batch No.	Seed			Growth Conditions							Sample No.
	Seed From	Amount g.	Seed Pretreatment	Soln.	Temp. °C.	Stirrer R.P.M.*	Heat No.	Condensate Rate, g/min	Temp. for Rapid Evap.	Duration min.	
5	5-1	5.3	pulverised crystals	1	40	100	10	9.2	-	31	5-2
32	32-1	15	commercial crystal	6	42	60	10	8.5	-	9	32-2
61	61-1	23	add 12 ml water (sample 61-2)	9	-	100	10	-	55	17	61-3
62	62-1	75	add 50 ml water (sample 62-2)	9	-	60	10	-	58		62-3
63	63-1	75	add 50 ml water (sample 63-2)	9	-	65	10	-	60	12	63-3
64	64-1	108	add 75 ml water (sample 64-2)	9	-	80	10	-	60	15	64-3
71	70-7		add 35 ml water (sample 71-1)	11	45	120	10	8.6	-	10	71-2
72	72-1	25	add 10 ml water (Sample 72-2)	11	42	80	10	8.6	-	10	72-3
73	72-2	25	sampled at ½, 1, 2, 3, and 5 min.	11	39	100	10	8.5	-	10	73-6
74	72-2	100		11	40	50	10	8.6	-	10	74
82	82-2	33	add 15 ml water (sample 82-3)	12	40	33	10	8.6	-	10	82-4
83	82-4	108	none	12	40	200	10	8.6	-	10	83
84	84-1	67	add 10 ml water (sample 84-2)	12	40	75	10	8.6	-	10	84-3
85	85-1	67	add 20 ml water (sample 85-2)	12	40	75	10	8.6	-	10	85-3
86	86-1	67	add 30 ml water (sample 86-2)	12	40	75	10	8.6	-	10	86-3
87	87-1	67	add 40 ml water (sample 87-2)	12	40	75	10	8.6	-	10	87-3
88	88-1	67	add 50 ml water (sample 88-2)	12	40	75	10	8.6	-	10	88-3
89	89-1	67	add 70 ml water (sample 89-2)	12	40	75	10	8.6	-	10	89-3
90	90-1	67	add 60 ml water (sample 90-2)	12	40	75	10	8.6	-	10	90-3
91	91-1	75	add 60 ml water (sample 91-2)	12	33	75	6	2.9	-	15	91-3
92	92-1	75	add 60 ml water (sample 92-2)	12	33	75	8	4.4	-	10	92-3
93	93-1	75	add 60 ml water (sample 93-2)	12	33	75	4	2.1	-	21	93-3
94	94-1	75	add 60 ml water (sample 94-2)	12	33	75	10	8.6	-	5	94-3

All with about 1300 g. of solution initially.

* As motor speed (see section 5-7).

TABLE III A4 : Those batches concerned with the growth of ammonium chloride and sodium chloride crystals.

Material	Batch No.	Temp. °C.	Stirrer ≠ R.P.M.	Heat No.	Condensate Rate g./min.	Duration of Run, min.
Ammonium Chloride	95	31	105	10	8.6	7
	96#	30	100	10	8.6	60
	97◇	30	230	10	8.6	15
	98	30	150	10	8.6	120
	99	32	80	10	8.6	10
	100	32	95	10	8.6	20
	101*	32	240	10	8.6	20
	102	33	90	10	8.6	23
	103	28	100	6	3.45	38
	104	43	100	10	8.6	20
	105	43	220	10	8.6	20
Sodium Chloride	106	41	60	10	9.2	15
	107	44	55	10	9.0	40
	108	44	90	10	9.0	25
	109*	44	230	10	9.0	50
	110	44	50	10	8.6	60
	111	†	55	†	†	30

All batches about 1 litre of solution

≠ As motor speed.

Sampled also at 30 min.

◇ Speed altered to 100 R.P.M. after 4 min.

* Used for growth of edge inclusions. For 101, 130 ml water added and regrowth for 15 min. For 109, 400 ml. water added and regrowth for 20 min.

† Solution heated to 100°C, then vacuum applied. Equivalent time at full heat given.

B. SIZE DISTRIBUTION OF CRYSTALS

TABLE III B 1

These tables show the size analysis for samples of each batch. The number in each column in the size analysis represents the number of crystals in the sample with sizes in the micron range indicated. The upper numbers refer to all the crystal, the lower numbers to only those crystals with inclusions. Where no inclusions were formed the second size analysis is omitted. An asterisk (*) placed against the second line of size analysis figures indicates that the results apply to crystals with 'edge' inclusions; otherwise, the inclusions are in 'face' patterns.

Nomenclature :

n' : Number of crystals counted.

$\bar{x}$: Mean crystal size on volumetric basis,

$\bar{x}_i$: Mean size (on volumetric basis) of those crystals with inclusion patterns,

x_1 : Mean size of largest crystals,

α : Area-volume factor for distribution.

β : Fraction of crystals with inclusions.

TABLE III B 1

SAMPLE NO.	n'	Size Analysis							$\frac{\bar{x}}{\bar{x}_i}$	α	β
		-50	-100	-150	-200	-250	-300	-350			
1	166	9	17	37	34	35	31	3	210	0.90	0.25
		-	-	-	-	14	24	3	271		
2-1	118	7	11	41	48	11	-	-	163	0.93	0.43
		-	-	-	40	11	-	-	194		
2-2	266	53	44	80	43	33	12	1	167	0.85	0.18
		-	-	-	8	29	11	1	240		
3	204	21	25	76	53	28	1	-	163	0.90	0.16
		-	-	-	2	10	1	-	228		
4	176	11	26	45	35	45	14	-	189	0.89	0.32
		-	-	-	8	34	14	-	240		
5-1	231	103	71	38	17	2	-	-	67	0.71	-

/Cont'd.

TABLE III B.1 (Cont'd)(p.2)

SAMPLE NO.	n'	Size Analysis							$\bar{x}$ x_1	$\bar{x}$ x_2	α	β
		-50	-100	-150	-200	-250	-300	-350				
5-2	258	6	17	74	70	55	22	14	161		0.84	0.38
*			-	-	14	48	22	14	208			
6	150	7	31	43	40	18	11	-	175		0.88	-
									256			
7	223	14	53	63	50	24	18	1	175		0.94	0.04
			-	-	-	3	6	1	275			
8	213	32	87	45	27	20	2	-	149		0.71	0.08
		-	-	-	-	15	2	-	236			
9	150	39	56	37	15	3	-	-	112		0.80	0.05
		-	-	-	5	3	-	-	202			
10	150	37	60	31	18	4	-	-	118		0.81	0.06
		-	-	-	6	3	-	-	200			
11-1	251	48	104	86	13	-	-	-	107		0.86	0.33
		-	-	70	13	-	-	-	138			
11-2	241	29	78	80	53	1	-	-	130		0.90	0.30
		-	-	21	51	1	-	-	170			
11-3	225	27	83	50	39	26	-	-	145		0.84	0.24
		-	-	-	29	26	-	-	204			
11-4	294	53	107	69	33	28	4	-	141		0.80	0.19
		-	-	6	17	28	4	-	214			
11-5	260	58	103	49	24	21	5	-	136		0.77	0.12
		-	-	-	6	21	5	-	232			
12-1	305	93	108	67	37	-	-	-	112		0.79	0.12
		-	-	-	5	32	-	-	175		-	
12-2	294	86	106	57	30	15	-	-	122		0.80	0.09
		-	-	-	-	12	15	-	-	210		
13-1	322	144	104	72	2	-	-	-	87		0.81	0.18
		-	1	54	2	-	-	-	129			
13-2	328	116	116	53	43	-	-	-	119		0.70	0.11
		-	-	-	35	-	-	-	182			

/Continued.

TABLE III B.1 (Cont'd)(Page 3)

SAMPLE NO.	n'	Size Analysis							$\bar{x}$ $\bar{x}_1, \bar{x}_2$	α	β
		-50	-100	-150	-200	-250	-300	-350			
14-1	315	93	131	87	4	-	-	-	94	0.88	0.25
		-	3	74	3	-	-	-	128		
14-2	290	107	109	49	25	-	-	-	102	0.79	0.09
		-	-	3	22	-	-	-	177		
15-1	280	80	108	72	20	-	-	-	104	0.83	0.25
		-	-	51	20	-	-	-	147		
15-2	214	85	75	33	17	4	-	-	103	0.74	0.10
	-	-	-	2	15	4	-	-	90		
16-1	207	147	60	-	-	-	-	-	55	0.80	-
									80		
17	190	44	66	39	20	21	-	-	137	0.79	0.22
	-	-	-	1	20	21	-	-	207		
18	198	60	57	29	25	19	7	1	149	0.76	0.21
		-	-	-	21	19	7	1	225		
19	216	89	77	41	9	-	-	-	94	0.80	0.02
		-	-	-	4	-	-	-	170		
20	295	240	55	-	-	-	-	-	50	0.72	-
									75		
21	224	87	79	36	19	3	-	-	112	0.80	0.08
		-	-	-	14	3	-	-	192		
22	235	94	89	41	11	-	-	-	94	0.79	0.05
		-	-	4	8	-	-	-	168		
23	216	92	65	34	24	1	-	-	106	0.74	0.01
		-	-	-	2	1	-	-	200		
24	224	86	79	32	16	8	2	1	119	0.72	0.14
		-	-	5	15	8	2	1	208		
25	208	83	62	23	38	2	-	-	117	0.77	0.20
		-	-	4	36	2	-	-	181		
26-1	260	23	79	77	72	9	-	-	142	0.91	0.50
		-	-	50	72	9	-	-	170		

/Continued.

TABLE III B.1 (Continued)(Page 4)

SAMPLE NO.	n'	Size Analysis									$\bar{x}$ $\bar{x}_i \bar{x}_j$	α	β
		-50	-100	-150	-200	-250	-300	-350	-400	-450			
26-2	226	13	70	70	34	38	1	-	-	-	156	0.87	0.34
		-	-	10	29	38	1	-	-	-	205		
26-3	170	12	37	45	36	23	17	-	-	-	180	0.87	0.37
		-	-	-	23	23	17	-	-	-	232		
26-4	164	11	44	42	20	20	27	-	-	-	187	0.85	0.33
		-	-	-	8	20	27	-	-	-	254		
26-5	169	13	39	41	26	16	31	3	-	-	195	0.85	0.30
		-	-	-	4	12	31	3	-	-	268		
26-6	167	15	35	50	26	15	14	12	-	-	193	0.83	0.20
		-	-	-	-	7	14	12	-	-	293		
26-7	138	7	24	36	29	13	12	12	5	-	224	0.86	0.20
		-	-	-	-	-	11	12	5	-	318		
26-8	164	6	27	55	29	12	11	11	13	-	221	0.82	0.18
		-	-	-	-	-	6	11	13	-	346		
26-9	116	4	29	25	19	12	7	10	9	1	230	0.81	0.17
		-	-	-	-	1	1	8	9	1	355		
27-1	200	69	59	38	26	8	-	-	-	-	122	0.78	0.32
		-	-	29	26	8	-	-	-	-	170		
27-2	216	90	75	24	11	12	4	-	-	-	122	0.70	0.11
		-	-	1	6	12	4	-	-	-	228		
28-1	220	66	73	24	44	12	1	-	-	-	133	0.78	0.27
		-	-	3	44	12	1	-	-	-	193		
28-2	218	76	72	35	11	5	8	10	1	-	156	0.67	0.11
		-	-	2	3	1	7	10	1	-	302		
29	200	65	58	35	26	12	4	-	-	-	135	0.81	0.20
		-	-	-	25	12	4	-	-	-	211		
30-1	196	70	58	26	31	11	-	-	-	-	127	0.71	0.23
		-	-	4	31	11	-	-	-	-	192		
30-2	218	84	63	34	15	9	9	3	1	-	145	0.69	0.11
		-	-	-	2	9	9	3	1	-	272		

/Continued.....

TABLE III B.1 (Cont'd)(p.5)

SAMPLE NO.	n'	Size Analysis									$\bar{x}$	α	β
		-50	-100	-150	-200	-250	-300	-350	-400	-450			
31-1	252	25	103	124	-	-	-	-	-	-	107	0.93	0.63
		-	36	124	-	-	-	-	-	-	117		
31-2	101	39	23	20	20	8	-	-	-	-	138	0.82	0.34
		-	-	7	20	8	-	-	-	-	188		
31-3	103	12	21	28	17	13	10	2	-	-	183	0.91	0.10
		-	-	-	-	-	8	2	-	-	292		
32-1	42	4	6	1	3	3	13	5	7	-	280	0.89	-
32-2 *	103	37	49	7	0	0	0	0	2	8	197	0.57	0.10
		-	-	-	-	-	-	-	2	8	420		
33-1	254	124	92	38	-	-	-	-	-	-	79	0.80	0.08
		-	-	20	-	-	-	-	-	-	135		
34-1	154	59	39	27	29	-	-	-	-	-	117	0.79	0.27
		-	-	12	29	-	-	-	-	-	169		
35	179	54	56	40	14	10	5	-	-	-	133	0.76	0.13
		-	-	-	9	10	5	-	-	-	228		
43	162	75	52	28	5	2	-	-	-	-	95	0.75	-
44	178	79	63	22	14	-	-	-	-	-	97	0.77	0.17
		-	-	16	14	-	-	-	-	-	157		
45	161	62	63	29	7	-	-	-	-	-	94	0.79	0.12
		-	-	13	7	-	-	-	-	-	150		
46	149	52	49	31	17	-	-	-	-	-	108	0.80	0.21
		-	-	14	17	-	-	-	-	-	161		
47	156	55	48	28	25	-	-	-	-	-	114	0.80	0.24
		-	-	12	25	-	-	-	-	-	167		
48	151	56	61	27	7	-	-	-	-	-	95	0.80	-
											135		
49	162	61	52	23	22	4	-	-	-	-	116	0.74	0.14
		-	-	-	18	4	-	-	-	-	192		
50	146	54	45	27	19	1	-	-	-	-	112	0.78	0.24
		-	-	15	19	1	-	-	-	-	164		

/Continued....

TABLE III B.1 (Continued)(page 6)

SAMPLE NO.	n'	Size Analysis									$\bar{x}$	α	β
		-50	-100	-150	-200	-250	-300	-350	-400	-450			
51	154	48	54	30	22	-	-	-	-	-	113	0.81	0.08
		-	-	-	12	-	-	-	-	-	175		
52	168	53	64	25	25	1	-	-	-	-	113	0.78	0.05
		-	-	-	8	1	-	-	-	-	188		
53	158	61	47	25	20	5	-	-	-	-	119	0.77	0.22
		-	-	9	20	5	-	-	-	-	180		
54	164	49	63	22	29	1	-	-	-	-	117	0.80	0.20
		-	-	3	28	1	-	-	-	-	180		
55	156	46	59	26	25	-	-	-	-	-	114 170	0.80	-
56	135	31	34	26	24	20	-	-	-	-	150	0.82	0.38
		-	-	9	22	20	-	-	-	-	197		
57	225	45	96	65	19	-	-	-	-	-	109	0.85	0.24
		-	-	35	19	-	-	-	-	-	150		
75	332	285	35	12	-	-	-	-	-	-	54	0.72	-
76	318	294	24	-	-	-	-	-	-	-	40	0.82	-
77	217	41	80	51	45	-	-	-	-	-	124	0.84	0.40
		-	-	41	45	-	-	-	-	-	160		
78	128	23	39	27	34	5	-	-	-	-	139	0.84	0.50
		-	-	25	34	5	-	-	-	-	170		
79	165	44	66	55	-	-	-	-	-	-	95	0.87	0.34
		-	2	55	-	-	-	-	-	-	110		
80	114	69	43	2	-	-	-	-	-	-	82	0.86	0.25
		-	27	2	-	-	-	-	-	-	120		
81	147	126	19	2	-	-	-	-	-	-	50 100	0.75	-
84-3 *	134	29	39	36	24	6	-	-	-	-	132	0.83	0.11
		-	-	3	7	5	-	-	-	-	193		
85-3 *	142	16	33	39	44	10	-	-	-	-	150	0.88	0.80
		1	20	39	44	10	-	-	-	-	160		

/Continued....

TABLE III B.1 (Cont'd)(page 7)

SAMPLE NO.	n'	Size Analysis -50	-100	-150	-200	-250	-300	-350	-400	-450	$\bar{x}$ / x_1 $\bar{x}$ / x_2	α	β
86-3	218	4	55	81	67	11	--	--	--	--	149	0.91	0.96
*		-	51	81	67	11	--	--	--	--	151		
87-3	177	14	24	67	72	-	-	-	--	--	148	0.93	0.97
*		9	19	67	72	-	--	--	--	--	151		
88-3	177	3	27	65	82	-	-	-	--	--	153	0.94	0.92
*		-	17	65	82	-	--	--	--	--	157		
89-3	160	37	33	63	27	-	-	-	--	--	152	0.90	0.67
*		--	16	63	27	--	--	--	--	--	169		
90-3	157	26	26	32	67	6	-	-	--	-	149	0.82	0.75
*		--	12	32	67	6	--	--	--	--	167		
91-3	216	31	62	64	59	-	-	-	-	-	133	0.88	0.81
*		3	48	64	59	-	-	--	-	-	143		
92-3	208	20	50	92	46	-	--	--	-	--	133	0.90	0.76
*		-	20	92	46	-	--	--	--	--	144		
93-3	151	13	21	50	42	25	--	--	--	-	150	0.92	0.74
*		-	4	41	42	25	--	-	-	-	163		
94-3	132	7	21	60	39	5	-	-	-	-	148	0.89	0.89
*		-	14	60	39	5	-	-	-	-	153		
95	21	2	9	4	5	1	-	-	-	-	138	0.85	0.5
		-	3	2	5	1	-	-	-	-	163		
96-1	58	4	7	18	22	7	-	-	-	-	164	0.87	0.43
		-	-	7	11	7	-	-	-	-	187		
96-2	20	0	1	2	7	9	1	--	-	-	206	0.96	0.75
		-	-	1	4	9	1	--	-	-	218		
97	119	6	26	32	42	9	5	-	-	-	166	0.89	0.50
		-	-	12	33	9	5	-	-	--	196		
98	16	-	-	3	0	4	6	3	-	-	256	0.94	0.75
		-	-	-	-	3	6	3	-	-	285		
99	11	-	-	4	3	4	-	-	-	-	188	0.94	0.6
		-	-	-	3	4	-	-	-	-	210		
100	29	-	1	4	7	6	11	-	-	-	230	0.93	0.54
		-	-	-	4	6	11	-	--	-	254		

/Continued.....

TABLE III B.1 (Cont'd)(page 8)

SAMPLE NO.	n'	Size Analysis									$\bar{x}$ / $\bar{x}_1$ $\bar{x}_2$	α	β
		-50	-100	-150	-200	-250	-300	-350	-400	-450			
101	41	-	8	17	16	-	-	-	-	-	149	0.95	-
102	24	3	6	6	7	2	-	-	-	-	195	0.92	0.33
		-	-	2	4	2	-	-	-	-	236		
103	19	2	6	7	1	3	-	-	-	-	145	0.84	0.63
		1	1	6	1	3	-	-	-	-	166		
104	24	-	5	9	5	3	2	-	-	-	176	0.87	0.42
		-	-	-	3	3	2	-	-	-	215		
105	47	3	15	16	12	1	-	-	-	-	139	0.90	-
106	107	17	76	14	-	-	-	-	-	-	81	0.85	-
107	19	1	3	10	5	-	-	-	-	-	139	0.91	-
108	84	9	69	6	-	-	-	-	-	-	82	0.91	-
109	198	15	159	22	2	-	-	-	-	-	88	0.91	-
110	27	-	7	12	6	2	-	-	-	-	148	0.75	-
111	26	1	8	6	6	5	-	-	-	-	162	0.88	0.34
		-	-	-	6	4	-	-	-	-	200		

T A B L E I I I B. 2.

SAMPLE NO.	n'	Size Analysis						
		-50	-75	-100	-125	-150	-175	-200
36 - 1	354	210	91	39	14	-	-	-
		-	44	34	14	-	-	-
36 - 2	607	335	156	60	44	12	-	-
		-	26	58	44	12	-	-
36 - 3	385	155	85	54	56	33	2	-
		-	9	50	56	33	2	-
36 - 4	471	179	130	67	50	44	1	-
		-	9	64	50	44	1	-
36 - 5	235	86	51	37	34	26	1	-
		-	13	37	34	26	1	-
36 - 6	202	81	53	31	16	18	2	1
		-	5	17	15	17	2	1
36 - 7	269	62	71	61	17	24	20	14
		-	-	-	10	20	20	14
37 - 1	375	101	207	58	9	-	-	-
		-	27	45	7	-	-	-
37 - 2	432	148	153	55	49	27	-	-
		-	1	39	49	27	-	-
37 - 3	356	95	107	47	48	49	9	-
		-	1	22	47	49	9	-
37 - 4	356	82	88	62	37	52	35	-
		-	-	6	33	52	35	-
37 - 5	363	98	76	78	35	40	29	7
		-	-	1	16	40	29	7
37 - 6	365	82	85	83	35	28	36	16
		-	-	-	9	25	36	16
37 - 7	74	8	8	14	13	18	7	6
		-	-	-	8	18	7	6

/Continued.....

TABLE III B.2. (Continued)(p.2.)

SAMPLE NO.	n'	Size Analysis						
		+50	-75	-100	-125	-150	-175	-200
38-1	234	88	98	48	-	-	-	-
		-	-	19	-	-	-	-
38-2	304	77	81	77	61	8	-	-
		-	-	42	61	8	-	-
38-3	405	99	103	86	73	44	-	-
		-	-	4	63	44	-	-
38-4	452	106	100	99	82	65	-	-
		-	-	3	49	65	-	-
38-5	365	106	84	52	47	63	13	-
		-	-	-	9	60	13	-
38-6	402	173	69	50	31	41	34	4
		-	-	-	-	27	34	4
38-7	447	150	102	59	24	37	38	37
		1	-	-	-	11	33	37
39-1	451	267	177	7	-	-	-	-
		1	-	-	-	-	-	-
39-2	488	164	176	146	2	-	-	-
		1	-	56	2	-	-	-
39-3	433	140	152	126	15	-	-	-
		1	-	30	13	-	-	-
39-4	497	184	147	99	62	5	-	-
		1	-	3	32	5	-	-
39-5	324	118	96	68	30	12	-	-
		1	-	-	10	12	-	-
39-6	327	96	72	71	51	37	-	-
		1	-	-	1	18	-	-
39-7	298	67	76	56	42	39	17	1
		1	-	-	-	9	11	1

/Continued....

TABLE III B.2.(Continued)(p.3)

SAMPLE NO.	n'	Size Analysis					
		-25	-50	-75	-100	-125	
40-1	292	39	182	71	-	-	no inclusions
40-2	394	110	207	77	-	-	
40-3	390	79	158	137	16	-	
40-4	375	67	149	115	44	-	
40-5	203	38	46	75	36	8	

SAMPLE NO.	n'	Size Analysis								
		-50	-75	-100	-125	-150	-175	-200	-225	-250
41-1	456	120	133	107	78	18	-	-	-	
		-	-	42	78	18	-	-	-	
41-2	312	75	82	66	55	34	-	-	-	
		-	-	4	48	34	-	-	-	
41-3	307	80	75	43	44	51	14	-	-	
		-	-	-	23	51	14	-	-	
41-4	344	103	87	52	31	41	27	3	-	
		-	-	-	1	29	27	3	-	
41-5	246	62	51	51	32	19	18	13	-	
		-	-	-	-	7	17	13	-	
41-6	254	51	62	43	24	18	13	22	15	6
		-	-	-	-	-	[illegible]	16	15	6

SAMPLE NO.	n'	Size Analysis					
		-50	-75	-100	-125	-150	
42-1	685	251	434	-	-	-	No inclusions
42-2	536	161	255	120	-	-	
42-3	484	137	201	146	-	-	
42-4	547	212	129	108	98	-	
42-5	353	131	93	53	40	36	

/Cont'd.

TABLE III B.2. (Cont'd)(p.4.)

SAMPLE NO.	n'	Size Analysis							
		<50	-75	-100	-125	-150	-175	-200	-225
67-1									
67-2									
67-3									
67-4									
67-5									
67-6									
68-1									
68-2									
68-3									
68-4									
68-5									
68-6									
68-7									

/Continued....

TABLE III B.2.(Continued)(p.5)

SAMPLE NO.	n'	Size Analysis							
		-50	-75	-100	-125	-150	-175	-200	-225
69-1									
69-2									
69-3									
69-4									
69-5									
69-6									
70-1									
70-2									
70-3									
70-4									
70-5									
70-6									
70-7									

C. SIZE DISTRIBUTION OF INCLUSIONS

These tables show the size distribution of the face inclusions in each sample. Only one inclusion from each pattern was measured.

Nomenclature :

n_1' : Number of crystals with inclusions counted.
$\bar{s}$: Mean inclusion size(on volumetric basis)
s_1 : Size of largest inclusion
$\bar{t}$: Mean thickness of crystal covering inclusion
$\bar{y}$: Mean internal size of pattern
$\bar{y}'$: Mean external size of pattern

TABLE JII C 1

SAMPLE NO.	n_1'	Size Analysis -10	-20	-30	-40	-50	$\bar{y}$	$\bar{t}$	$\bar{s}$	s_1	$\bar{y}'$
1	17	8	9	-	-	-	74	63	15	20	99
2-1	19	6	7	6	-	-	65	34	19	30	98
2-2	10	3	3	4	-	-	65	49	21	30	102
3	6	2	4	-	-	-	68	46	16	20	96
4	26	10	13	3	-	-	67	50	18	25	98
7	9	9	-	-	-	-	70	68	7	10	81
8	11	7	4	-	-	-	65	65	13	15	87
9	8	6	2	-	-	-	61	59	12	15	82
10	8	5	3	-	-	-	69	67	14	15	93
11-1	26	7	12	7	-	-	59	17	22	30	99
12-1	19	13	6	-	-	-	63	40	13	15	85
12-2	8	4	4	-	-	-	66	61	14	15	90
13-1	16	11	5	-	-	-	54	25	13	15	76
13-2	11	5	6	-	-	-	56	49	15	15	82
14-1	21	17	4	-	-	-	55	26	12	15	75
14-2	9	6	3	-	-	-	56	39	13	15	78
15-1	18	8	10	-	-	-	57	27	15	20	83
15-2	15	9	6	-	-	-	58	45	14	20	82
17	23	2	4	6	9	2	69	34	33	45	137
19	7	7	-	-	-	-	66	45	6	10	76
21	10	6	4	-	-	-	74	45	14	20	98
22	10	9	1	-	-	-	63	34	10	15	80
23	6	6	-	-	-	-	72	48	7	10	83
25	14	2	5	5	1	1	70	44	28	45	116
26-1	42	3	9	13	10	7	65	18	34	50	127

/Continued.

TABLE III C 1. (Continued) (p.2)

SAMPLE NO.	n_1'	Size Analysis					$\bar{y}$ μ	$\bar{t}$ μ	$\bar{s}$ μ	s_2 μ	$\bar{y}'$ μ
		-10	-20	-30	-40	-50					
30-1	22	0	1	8	11	2	68	28	35	45	133
31-2	25	1	6	9	8	1	65	32	31	45	124
33-1	24	18	6	-	-	-	67	23	12	15	87
34-1	13	2	8	3	-	-	71	26	20	30	109
35	17	1	9	7	-	-	71	62	23	30	111
36-6	31	4	11	4	8	4	64	5	32	50	122
37-4	32	7	6	10	9	-	64	9	28	40	119
38-3	21	7	12	2	-	-	70	13	18	30	100
39-2	15	15	-	-	-	-	65	6	6	10	78
41-1	29	11	18	-	-	-	69	8	16	20	98
44	17	4	4	6	3	-	55	24	26	35	106
45	18	5	10	3	-	-	65	26	19	25	111
46	31	12	15	4	-	-	74	26	18	25	106
47	32	9	5	13	5	-	69	26	26	40	115
49	16	2	7	7	-	-	79	33	23	30	123
50	25	4	2	6	9	4	65	22	33	50	122
51	10	9	1	-	-	-	74	44	10	15	84
52	8	6	2	-	-	-	79	48	12	15	96
53	15	2	1	3	4	5	61	28	38	50	127
54	13	1	6	5	1	-	73	33	25	35	114
57	28	11	17	-	-	-	67	25	15	20	101
67-4	30	4	4	7	9	6	60	11	35	50	126
68-2	10	10	-	-	-	-	63	8	6	10	75
69-2	12	12	-	-	-	-	72	7	8	10	87
70-4	34	6	4	9	13	2	69	13	32	45	128
79	15	9	6	-	-	-	65	14	14	20	108
80	14	6	8	-	-	-	72	10	15	20	100

TABLE III C 2a

SAMPLE NO.	n'	Size Analysis					$\bar{y}$ μ	$\bar{t}$ μ	$\bar{s}$ μ	s_1 μ	$\bar{y}'$ μ
		-20	-40	-60	-80	-100					
18	20	2	11	4	3	-	74	40	48	80	154
24	22	7	3	11	1	-	67	38	43	70	140
27-1	18	3	9	6	-	-	59	20	41	60	132
27-2	18	5	8	5	-	-	61	49	36	55	129
28-1	25	9	10	6	-	-	63	27	38	60	136
28-2	10	2	6	2	-	-	72	66	38	55	140
29	23	4	6	13	-	-	70	33	42	60	146
56	23	7	9	7	-	-	66	34	40	60	146
77	51	15	19	17	-	-	62	15	39	60	132
78	34	3	9	20	2	-	56	12	48	65	140
95	5	2	2	1	-	-	35	0	30	-	160
96-1	4	1	1	1	1	-	40	10	50	90	160
96-2	9	2	4	1	2	-	40	37	48	70	130
97	24	2	12	5	3	2	32	30	54	90	135
98	5	-	1	3	1	-	35	80	40	60	125
100	7	0	2	0	4	1	35	30	70	100	170
102	7	0	2	3	2	-	40	30	55	70	105
103	12	2	2	4	3	1	45	22	60	90	130
104	7	-	-	3	3	1	45	0	70	90	210

D. SIZE OF EDGE INCLUSION PATTERNS

This table shows the size distribution of the edge inclusion patterns in hexamine crystals. The size of the pattern is taken as the outside dimension of the crystal just enclosing the pattern.

Nomenclature :

n' : Number of crystals counted.

$\bar{t}$: Mean thickness of crystal covering inclusion.

$\bar{y}'$: Volumetric mean size of pattern.

SAMPLE NO.	n'	Size Analysis						$\bar{t}$	$\bar{y}'$
		-50	-100	-150	-200	-250	-300	μ	μ
85	110	9	28	39	33	1	-	10	139
86	167	17	52	60	38	-	-	10	131
87	120	10	31	49	30	-	-	10	135
88	105	4	26	53	22	-	-	15	133
89	115	20	67	28	-	-	-	26	92
90	128	13	35	73	7	-	-	24	117
91	169	27	57	61	24	-	-	15	121
92	109	9	35	41	24	-	-	12	128
93	112	5	21	44	42	-	-	10	142
94	107	9	35	44	19	-	-	12	127

E. DETAILED CALCULATIONS OF THOSE BATCHES FOR WHICH SEVERAL CONSECUTIVE SAMPLES WERE TAKEN

Nomenclature.

A : Total surface area of crystal, cm^2.

n : Rate of hexamine production, g/min.

M : Total mass of product in batch, g.

n : Total number of crystals in batch.

n_i : Number with inclusions.

n' : Number counted in sample.

R : Crystal growth rate per face (calculated from $\bar{x}$), μ/min.

R' : Crystal growth rate (computed from $\bar{x}_i$), μ/min

R^* : Critical growth rate, μ/min.

$\bar{s}$: Volumetric mean size of inclusion,

v_t : Volume of included liquor in whole batch, cc.

$\bar{x}$: Volumetric mean crystal size,

$\bar{x}_i$: Volumetric mean size of those crystals with inclusions,

$\bar{x}_l$: Volumetric mean size of largest crystals,

$\bar{y}$: Critical crystal size.

α : Area -volume factor for total crystal distribution.

α_i : Area-volume factor for the distribution of crystals with inclusions.

β : Fraction of crystals with inclusion pattern.

γ_A : Fraction of surface area associated with those crystals with inclusions.

γ_v : Fraction of crystal volume associated with those crystals with inclusions.

θ : Period of time after nucleation, min.

θ_s : Time of inclusion sealing, min.

Batch No.11. Feed 3, Temp. 38°C, 100 RPM, Heat No.10
Condensate Rate 8.6 g/min, Initial solution 1320 g, m = 7.5 g/min.

SAMPLE NO.	Θ min	MEASUREMENTS FROM PHOTOGRAPHS: n'	$\bar{x}$ μ	α	β	$\bar{x}_i$ μ	α_i	γ_A	γ_V	M g.	COMPUTED QUANTITIES: $10^{-7} n$	$10^{-6} n_i$	$10^{-3} A$ cm²	R μ/min.	R' μ/min.
-1	6	251	107	0.86	0.33	138	0.98	0.63	0.72	45	3.9	13	16.7	3.4	2.7
-2	12	241	130	0.90	0.30	170	0.98	0.58	0.68	90	4.4	13	28	2.0	
-3	19	225	145	0.84	0.24	204	0.99	0.58	0.70	142	4.9	12	37	1.54	2.3
-4	24	294	141	0.80	0.19	214	0.97	0.52	0.66	180	6.9	12	47	1.21	1.3
-5	30	260	136	0.77	0.12	232	0.98	0.45	0.61	225	9.4	12	57	0.99	

$\bar{y}$ = 59 μ, $\bar{x}_i^*$ = 99 μ, R^* = 8 ± 5 μ/min, Θ_s = 1.1 min

$\bar{s}$ = 22 μ, shape, pyr., v_t = 0.61 cc.

TABLE III E 1 : Results for Batch No.11.

Batch No.26, Feed 5, Temp. 42°C., 60 R.P.M., Heat No. 10.
Condensate Rate 8.6 g./min, Initial solution 1500 g., n = 7.5 g/min.

SAMPLE NO.	Θ min	Analysis of Photographs								Computed Quantities					
		n'	$\bar{x}$ μ	α	β	$\bar{x}_i$ u	$\mathcal{L}_i$	γ_A	γ_v	M gc	10^{-7} n	10^{-6} n_i	A $\times 10^{-4}$ cm²	R μ/min	R' μ/min
-1	5	260	142	0.91	0.50	170	0.99	0.78	0.86	37	1.4	6.9	1.1	5.1	3.5
-2	10	226	156	0.87	0.34	205	0.97	0.66	0.78	75	2.1	7.1	1.9	3.0	
-3	15	170	180	0.87	0.37	232	0.97	0.70	0.81	112	1.9	7.1	2.3	2.4	2.7
-4	20	164	187	0.85	0.33	254	0.98	0.71	0.83	150	2.4	7.9	3.0	1.9	2.2
-5	25	169	195	0.85	0.30	268	0.98	0.65	0.77	187	2.6	7.9	3.6	1.55	1.4
-6	35	167	193	0.83	0.20	293	0.98	0.54	0.69	262	3.8	7.7	5.0	1.12	1.25
-7	45	138	213	0.86	0.20	318	0.98	0.54	0.67	337	3.8	7.5	6.3	0.90	1.03
-8	55	164	221	0.82	0.18	346	0.99	0.54	0.70	412	4.0	7.2	6.8	0.83	
-9	65	116	230	0.81	0.17	355	0.99	0.51	0.63	487	4.2	7.2	7.6	0.74	

$\bar{y}$ = 65 μ, $\bar{x}_i^*$ = 127 μ, R^* = 10 ± 5 μ/min, Θ_s = 1.4 min.

$\bar{s}$ = 34 μ, shape - β_{yx}, v_t = 1.38 cc.

TABLE III E 2 : RESULTS FOR BATCH NO.26.

Batch No. 36. Feed 7, Temp. 40°C, 60 R.P.M. Heat No.10
Condensate Rate 8.6 g./min, Initial solution 1350 g, m = 7.5g/min.

Sample No.	θ min	Measurements from Photographs								Computed Quantities					
		n'	$\bar{x}$ μ	α	β	$\bar{x}_i$ μ	α_i	γ_A	γ_v	M g	10^{-7} n	10^{-6} n_i	10^{-3} A cm^2	R μ/min	R' μ/min.
-1	$\frac{1}{3}$	354	60	0.82	0.26	85	0.96	0.60	0.72	2.5	1.2	3.2	1.5	37	26
-2	$\frac{2}{3}$	607	68	0.80	0.23	102	0.95	0.61	0.77	5.0	1.7	3.9	2.7	21	
-3	1	385	87	0.82	0.39	114	0.94	0.80	0.90	7.5	1.2	4.8	3.2	17.5	
-4	$1\frac{1}{3}$	471	85	0.82	0.36	115	0.96	0.75	0.87	10	1.7	6.2	4.3	13.1	10
-5	$1\frac{2}{3}$	235	90	0.84	0.46	113	0.97	0.85	0.92	12.5	1.8	8.4	5.2	10.7	3.5
-6	2	202	86	0.81	0.29	120	0.95	0.65	0.78	15	2.5	7.3	6.3	8.9	
-7	5	269	108	0.82	0.24	158	0.98	0.61	0.75	38	3.2	7.7	12.8	4.4	6

$\bar{y}$ = 64 μ , x_1^* = 122 μ , R* = 12 ± 3 μ/min , θ_s = 2.1 min

$\bar{s}$ = 32 μ , shape , pyr. v_t = 1.19 cc.

TABLE III E 3 : Results for Batch No.36.

Batch No. 37 Feed, 7., Temp. 40°C., 60 R.P.M. Heat No.10.
Condensate Rate 8.6 g./min, Initial solution 1350 g., m = 7.5 g/min.

SAMPLE NO.	Θ min	MEASUREMENTS FROM PHOTOGRAPHS								COMPUTED QUANTITIES					
		n'	$\bar{x}$ μ	α	ρ	$\bar{x}_i$ μ	α_i	γ_A	γ_v	M g.	10^{-7} n_v	10^{-6} n_i	10^{3} A cm^2	R μ/min	R' u/min
-1	½	375	66	0.92	0.21	85	0.97	0.37	0.45	3.8	1.4	3.0	2.4	23.5	} 15
-2	1	432	81	0.81	0.27	115	0.97	0.63	0.77	7.5	1.5	4.0	3.4	16.5	} 6
-3	2	356	95	0.85	0.36	127	0.97	0.73	0.86	15	1.8	6.5	5.9	9.5	} 7
-4	3	356	104	0.87	0.35	141	0.98	0.72	0.88	22	2.0	7.0	8.0	7.0	} 4.5
-5	4	363	105	0.83	0.26	150	0.98	0.62	0.75	30	2.7	7.0	10.5	5.4	} 5
-6	5	365	109	0.83	0.23	160	0.98	0.59	0.74	38	2.9	7.8	12.0	4.7	
-7	7	74	127†	-	0.53†	150†	-	-	-	53	-	-	-	-	

$\bar{y}$ = 64 μ , $\bar{x}_i^*$ = 119 μ, R^* = 11 ± 3 μ/min , Θ_s = 1.7 min

$\bar{s}$ = 28 μ, shape, *pyr.*, v_t = 0.76 cc.

† Crystals partly redissolved.

TABLE III E 4 : RESULTS FOR BATCH NO.37.

Batch No. 38, Feed 7, Temp. 40°C., 100 R.P.M. Heat No.10,
Condensate Rate 8.6 g./min, Initial solution 1350 g., m = 7.5 g./min.

SAMPLE NO.	θ min	Measurements from Photographs								Computed Quantities					
		n'	$\bar{x}$ μ	α	β	$\bar{x}_i$ μ	α_i	γ_A	γ_v	M g.	10^{-7} n	10^{-6} n_i	10^{-3} A cm^2	R μ/min	R' μ/min
- 1	½	234	62	0.88	0.08	89	1.00	0.18	0.22	3.8	1.7	1.3	2.4	23.4	10
- 2	1½	304	85	0.89	0.36	109	0.99	0.65	0.75	11.3	1.9	6.9	5.2	10.8	8.5
- 3	2½	405	93	0.87	0.27	126	0.99	0.57	0.69	19	2.5	6.8	8.0	7.0	2.0
- 4	3½	452	96	0.88	0.26	130	0.99	0.54	0.64	26	3.1	7.8	10.7	5.3	4.3
- 5	5	365	100	0.85	0.22	143	0.99	0.54	0.66	38	4.0	8.8	14.5	3.9	3.7
-6	7	402	100	0.73	0.16	158	1.00	0.54	0.64	52	5.5	8.8	17	3.3	2.5
- 7	10	447	112	0.79	0.18	173	1.00	0.55	0.68	75	5.7	10.2	24	2.3	

$\bar{y}$ = 70 μ, $\bar{x}_i^*$ = 100 μ, R^* = 14 ± 3 μ/min. θ_s = 1.2 min.

$\bar{s}$ = 16 μ, shape , pyr., v_t = 0.22 cc.

TABLE III E5 : RESULTS FOR BATCH NO.38.

Batch No. 39, Feed 7, Temp. 40°C., 150 R.P.M. Heat No.10.
Condensate Rate 8.6 g./min., Initial Solution 1350 g., m = 7.5 g./min.

SAMPLE NO.	θ min	Measurements from Photographs								Computed Quantities					
		n'	$\bar{x}$ μ	α	β	$\bar{x}_i$ μ	α_A	γ_A	γ_V	M g.	10^{-7} n_v	10^{-6} n_i	10^{-3} A cm^2	R μ/min	R' μ/min
-1	½	451	51	0.87	0	60≠	-	-	-	3.8	3.1	-	3.0	18.7	
-2	1½	488	68	0.91	0.12	90	1.00	0.23	0.27	11.3	3.8	4.6	6.8	8.3	-
-3	2½	433	70	0.92	0.10	97	0.99	0.21	0.27	19	5.8	5.8	11	5.6	3.5
-4	4	497	76	0.85	0.08	117	0.99	0.22	0.29	30	7.2	5.8	15	3.8	6.7
-5	6	324	78	0.80	0.07	130	0.99	0.22	0.32	45	10.0	6.8	21	2.7	3.3
-6	8	327	92	0.86	0.06	140	1.00	0.16	0.21	60	10.6	6.1	33	1.7	2.5
-7	11	298	102	0.85	0.07	157	0.99	0.20	0.26	82	8.2	5.8	31	1.8	2.8

$\bar{y}$ = 65 μ, $\bar{x}_i^*$ = 78 μ, R^* = 11 ± 2 μ/min, θ_s = 1.1 min.

$\bar{s}$ = 6 μ, shape, μ_{y^*}, v_t = 0.01 cc.

≠ No inclusions visible. This value estimated from largest 17% of crystals.

TABLE III E6 : RESULTS FOR BATCH NO.39.

Batch No. 40, Feed 7, Temp. 40°C., 230 R.P.M. Heat No.10
Condensate Rate 8.6 g./min, Initial solution 1350 g, m = 7.5 g./min

SAMPLE NO.	θ min	Measurements from Photographs					Computed Quantities				
		n'	$\bar{x}$ μ	α	β	$\bar{x}_\ell$	M g.	$10^{-7}n$	$10^{3}A$ cm^2	R μ/min	R'_ℓ μ/min.
- 1	$\frac{1}{2}$	292	47	0.92	0	47	3.8	4	3.5	16.0	9.5
- 2	$1\frac{1}{2}$	394	44	0.89	0	66	11.3	14	10.3	5.5	2.3
- 3	3	390	52	0.90	0	73	22	16	17	3.4	3.5
- 4	5	375	57	0.88	0	87	36	20	25	2.3	3.5
- 5	7	203	63	0.93	0	101	52	22	34	1.67	

NO INCLUSIONS

TABLE III E 7 : RESULTS FOR BATCH NO. 40.

Batch No. 41, Feed 7, Temp. 57°C., 100 R.P.M. Heat No.10
Condensate Rate 8.6 g./min., Initial Solution 1350 g, m = 7.5 g./min.

SAMPLE No.	θ min	Measurements from Photographs								Computed Quantities					
		n'	$\bar{x}$ μ	α	β	$\bar{x}_i$ μ	α_i	γ_A	γ_V	M g	10^{-7} n	10^{-4} n_i	10^{3}A cm^2	R μ/min.	R' μ/min
- 1	$1\frac{1}{2}$	456	85	0.88	0.30	113	0.99	0.60	0.70	11	1.91	5.7	5.1	11.0	6.5
- 2	$2\frac{1}{2}$	312	92	0.88	0.28	126	0.99	0.58	0.69	19	2.6	7.3	8.2	6.9	4.7
- 3	4	307	102	0.84	0.29	140	0.98	0.63	0.74	30	2.9	8.1	10.8	5.2	5.0
- 4	$5\frac{1}{2}$	344	104	0.88	0.17	155	0.99	0.48	0.58	41	3.9	6.6	15.8	3.6	4.7
- 5	7	246	109	0.83	0.15	169	1.00	0.44	0.57	53	4.4	6.5	18.4	3.1	3.0
- 6	$13\frac{1}{2}$	254	131	0.80	0.15	208	1.00	0.47	0.60	101	4.8	7.1	28	2.0	

$\bar{y}$ = 69 μ, $\bar{x}_i^*$ = 98 μ, R^* = 14 ± 4 μ./min, θ_s = 1.1 min.

$\bar{s}$ = 16 μ, shape, *pyr.*, v_t = 0.20 cc.

TABLE III E 8 : RESULTS FOR BATCH NO.41.

Batch No.42, Feed 7, Temp. 33°C, 100 R.P.M., Heat No.10
Condensate Rate 8.6 g/min, Initial Solution 1350 g, $\dot{m}$ = 7.5g/min.

SAMPLE NO.	θ min.	Measurements from photographs. n'	$\bar{x}$ μ	α	β	$\bar{x}_\ell$ μ	Computed Quantities M g.	$10^{-7}m$	10^{-3} A cm^2	R μ/min	R'_ℓ μ/min
-1	1	685	57	0.90	0	63	7.5	4.4	5.4	12.8	
-2	$1\frac{1}{2}$	536	66	0.92	0	81		4.2	7.2	7.8	8.3
-3	$2\frac{1}{2}$	484	68	0.90	0	88	1	6.2	11.1	5.0	
-4	7	547	78	0.86	0	121	52	11.5	26	2.2	3.3
-5	10	353	86	0.83	0	128	75	12.5	33	1.7	1.2
NO INCLUSIONS											

TABLE III E 9 : RESULTS FOR BATCH NO.42.

Batch No. 67. Feed 10, Temp. 32°C, 50 R.P.M. Heat 10.
Condensate Rate 9.1 g./min. Initial solution 1290 g., m = 7.9 g./min.

Sample No.	θ min	Measurements from Photographs								Computed Quantities					
		n'	$\bar{x}$ μ	α	β	$\bar{x}_i$ μ	α_i	γ_A	γ_V	M g.	$10^{-7}n$	$10^{-6}n_i$	10^{-3} A cm^2	R μ/min	R' μ/min
-1	½									4					
-2	1									8					
-3	2									16					
-4	4									31					
-5	6									47					
-6	10									79					

$\bar{y}$ = 60 μ, $\bar{x}_i^*$ = 126 μ, R* = μ/min, θ_s = min.

$\bar{s}$ = 35 μ; shape, pyr. ; v_t = cc.

TABLE III E.10 : RESULTS FOR BATCH NO.67.

Batch No. 68. Feed 10, Temp. 83°C. 50 R.P.M. Heat 10

Condensate Rate 8.2 g./min, Initial solution 1270 g. m = 7.2 g./min.

Sample No.	min	Measurements from Photographs								Computed Quantities					
		n'	$\bar{x}$ μ	α	β	$\bar{x}_i$ μ	α_i	γ_A	γ_V	M g.	$10^{-7} n$	$10^{-6} n_i$	10^{-3} A cm^2	R μ/min	R' μ/min
-1	½									3.6					
-2	1									7					
-3	2									14					
-4	3									22					
-5	4									29					
-6	6									43					
-7	10									72					

y = 63 μ, $\bar{x}_i^*$ = 75 μ, R* = μ/min., θ_s = min.

s = 6 μ, shape, dodec., v_g = cc.

TABLE III E 11 : RESULTS FOR BATCH NO. 68.

Batch No. 69, Feed 10, Temp. 58°C. 50 R.P.M. Heat 10.

Condensate Rate 8.5 g./min., Initial solution 1300 g. m = 7.4 g./min.

Sample No.	min	Measured from Photographs								Computed Quantities					
		n'	$\bar{x}$ μ	α	β	$\bar{x}_i$ μ	α_i	γ_A	γ_v	M g	$10^{-7} n$	$10^{-6} n_s$	10^{-3} A cm^2	R μ/min	R' μ/min.
1	1									7.4					
2	2									15					
3	3									22					
4	4									30					
5	6									44					
6	10									14					

$\bar{y}$ = 72 μ, $\bar{x}_i^*$ = 87 μ, R* = μ/min, θ_s = min.

s = 8 μ, shape , dodec. , v_e = cc.

TABLE III E 12 : Result for Batch No. 69.

Batch No.70, Feed 10, Temp. 42°C., 50 R.P.M., Heat 10

Condensate Rate 8.4 g./min., Initial solution 1270, g., m = 7.3 g./min

Sample No	θ min	Measurements from Photographs: n'	$\frac{1}{N}$ μ	α	β	$\bar{x}_i$ μ	α_i	γ_A	γ_V	Computed Quantities: M g	$10^{-7} n$	$10^{-6} n_i$	$10^{-3} A$ cm^2	R μ/min	R' μ/min
-1	½									3.6					
-2	1									7.3					
-3	2									15					
-4	3									22					
-5	4									29					
-6	6									44					
-7	10									73					

$\bar{y}$ = 69 μ, $\bar{x}_i^*$ = 128 μ, R* = μ/min., θ_s = min.

$\bar{s}$ = 32 μ, shape, pyr. , v_c = cc.

TABLE LLL E 13 : RESULTS FOR BATCH NO.70

F. COMPUTED QUANTITIES

These tables show values computed from the previous data.

Nomenclature :

A : Total surface area of crystals.
M : Total mass of crystal
n : Total number of crystals.
n_i : Number of crystals with inclusions.
R : Mean growth rate
R*: Critical growth rate for inclusion formation.
R_{65}: Maximum growth rate at crystal size 65 μ.

TABLE III F 1 : Batches with inclusions

SAMPLE NO.	M g	10^{-7} n	$10^{-6} n_i$	10^{-3}A cm^2	R μ/min	R* μ/min
1	198	2.3	5.7	39	1.52	14
2-1	78	1.9	8.1	21	2,8	16
2-2	200	4.6	7.7	46	1.27	17
3	218	5.3	8.5	54	1.08	10
4	226	3.6	11.4	48	1.27	9
7	235	4.7	2.1	57	0.57	13
8	223	7.2	5.7	48	1.12	11
9	153	10.6	5.6	48	1,20	14
10	150	9.6	5.8	46	1.22	11
12-1	75	5.7	6.8	24	2.4	15
12-2	160	9.5	8.7	48	1.20	13
13-1	52	8.7?	15?	23	2.5	12
13-2	130	8.6	9.2	36	1.59	11
14-1	45	5.8	14?	19	3.0	13
14-2	105	10.6	9.1	37	1.52	16
15-1	52	4.8	12?	18	3.0	13
15-2	109	10.4	10.5	35	1.56	14
17	78	3.2	7.2	20	2.9	10
18	72	2.3	4.9	17	3.2	10
19	77	10.0	1.8	30	1.92	18
21	73	6.6	5.0	24	2.3	17
22	74	9.5	4.8	28	1.98	18
23	74	6.5	0.6	23	2.4	-
24	71	4.4	6.1	19	2.9	9
25	72	4.8	9.6	21	2.5	9

/Continued....

TABLE III F 1 (Continued)(p.2.)

SAMPLE NO.	M S	10^{-7} n	10^{-6} n_1	10^{-3} A cm^2	R μ/min	R* μ/min
27-1	49	2.9	9.1	14	3.7	8
27-2	140	8.2	8.6	36	1.45	8
28-1	52	2.2	6.0	13	4.3	11
28-2	225	6.3	6.9	44	1.28	8
29	52	2.2	4.6	14	4.0	13
30-1	52	2.7	6.3	13	4.3	11
30-2	222	7.7	8.5	47	1.17	11
31-2	52	2.0	7.0	13	4.0	14
33-1	36	7.2	5.7	15	3.6	14
34-1	51	3.3	8.9	15	3.6	11
35	121	5.4	7.2	31	1.84	13
44	50	5.8	9.8	18	2.9	10
45	50	6.4	8.0	19	2.8	8
46	53	4.4	9.1	17	3.2	11
47	45	3.2	7.6	14	4.0	12
49	54	3.6	4.9	15	1.87	7
50	48	3.6	8.7	15	3.4	8
51	59	4.4	3.4	19	1.7	12
52	52	3.8	2.0	16	1.51	11
53	50	3.2	6.8	15	3.7	10
54	50	3.3	6.5	15	3.5	13
56	53	1.7	6.4	13	4.3	11
57	53	4.3	10.4	18	3.0	10
77	39	2.2	8.5	12	4.7	9
78	38	1.5	7.5	10	5.5	9
79	36	4.4	14	15	3.7	-
80	38	7.3	18	18	3.2	1

TABLE III F.2. Batches Without

SAMPLE NO.	M S	10^{-7} n	10^{-3} A cm^2	R μ/min	R_{65} μ/min
6	256	5.0	52	0.35	3
16	44	28	29	2.0	4
20	77	69	53	1.09	1.8
48	53	6.2	19	0.90	5
55	54	3.8	17	1.19	10
75	96	66	58	1.03	3
76	47	75	42	1.39	3
81	38	32	25	2.2	

APPENDIX IV

THE ANALYSIS OF HEXAMINE SOLUTIONS

The usual chemical method was used for the analysis of hexamine. In this method, the hexamine is reacted with an excess of acid. This promotes the decomposition of hexamine into ammonia and formaldehyde. The ammonia reacts with the acid and the formaldehyde is driven off by boiling the solution. The excess acid is back-titrated with alkali.

A gravimetric method of analysis was used for increased accuracy. [illegible] Accuracies to within ± 0.1% could be expected.

Details of Analytical Procedure

A quantity of the sample is weighed directly into a stoppered 100 ml flask. An excess of 4N sulphuric acid is added from a weight burette. Distilled water and tile chips are added and the solution is boiled for about 7 hours. Further distilled water is added as required. After this time (when the odour of formaldehyde has entirely dissappeared) the solution is cooled, and boiled, distilled water and a few drops of methyl orange are added. The solution is then titrated to a slight excess with 1N caustic soda from a weight burette. The final end point is obtained by volumetric titration with 0.1N HCl.

The acids were standardised against sodium bicarbonate and the caustic against potassium hydrogen phthalate. Also the solutions were intercalibrated one against the other.

APPENDIX V

THE DETERMINATION OF INCLUDED MOISTURE

1. Possible Methods

A means is required of determining the amount of mother liquor included in various batches of crystals. Several methods could be used.

1. By direct measurement. A sample of each batch could be taken, examined under the microscope and the size and number of inclusions (and crystals) measured. Simple calculations would then give the percentage of included volume directly. This method was used for samples which contained only regular patterns of face inclusions. However it is very time consuming and not very accurate.

2. By analysis for solute. Quite accurate gravimetric methods of analysis are available for the solute materials used in this project - hexamine, ammonium chloride and sodium chloride. The quantity of included liquor is generally small. Since it would be computed in these cases by a difference method involving two large quantities, the resultant estimate is not likely to be too accurate.

3. By variations in physical properties. The presence of included mother liquor would change the physical properties (e.g. density) of the crystal. These properties could be measured reasonably accurately, but again a difference method is involved, and the resulting accuracy may be low.

4. By analysis for solvent. Since the solvent is present only in small quantities, a method which analysed directly for the solvent should have certain advantages. However, it would measure the total amount of solvent, including that adsorbed or adhering to the crystal surface. The solvent was usually water, so the Karl Fischer method of analysis for water could be used.

2. Karl Fischer Apparatus

The application of the Karl Fischer method to the analysis of water in hexamine has been described by Mitchell and Smith [37]. Other descriptions of the method are available [38, 39].

The apparatus (Fig AV-1) was based on that described in Vogel [38]. The solvent used was methanol with a low moisture content, prepared by the repeated fractional distillation of commercial methanol. The desiccated hexamine sample was dissolved in a quantity of this methanol and the moisture content of the resulting solution was determined. The solubility of hexamine in methanol gives a limit to the amount of sample that can be used. The dissolved hexamine does not interfere with the reaction, although it tends to precipitate out of the titrated solution on standing. The usual 'dead stop' electrometric method of determining end points was used. A catalyst involving n-ethyl-piperidine [40] was added to the solutions to give a more rapid reaction.

3. Procedure

The methanol solvent (for moisture content) and the Karl Fischer reagent (for reactant strength) were calibrated initially by titration against each other and against methanol containing known amounts of water. Before a series of titrations was begun, catalyst was added to the reaction vessel and titrated with the Karl Fischer reagent to the end point. The reaction vessel was agitated by shaking.

In analysing the hexamine samples, a weighed quantity of the dried sample (about 5g.) was dissolved in 50 ml. of methanol and used to titrate quantities of the Karl Fischer reagent. With corrections for the moisture content of the methanol and the volume of the sample the moisture content of the sample could be determined.

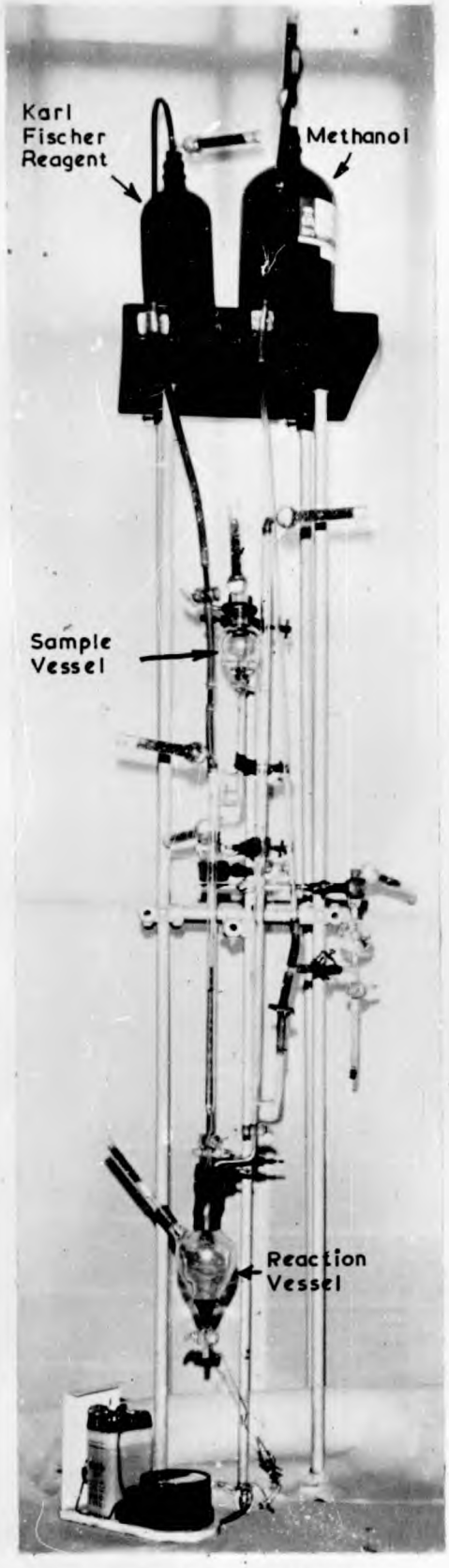

A. OVERALL VIEW.

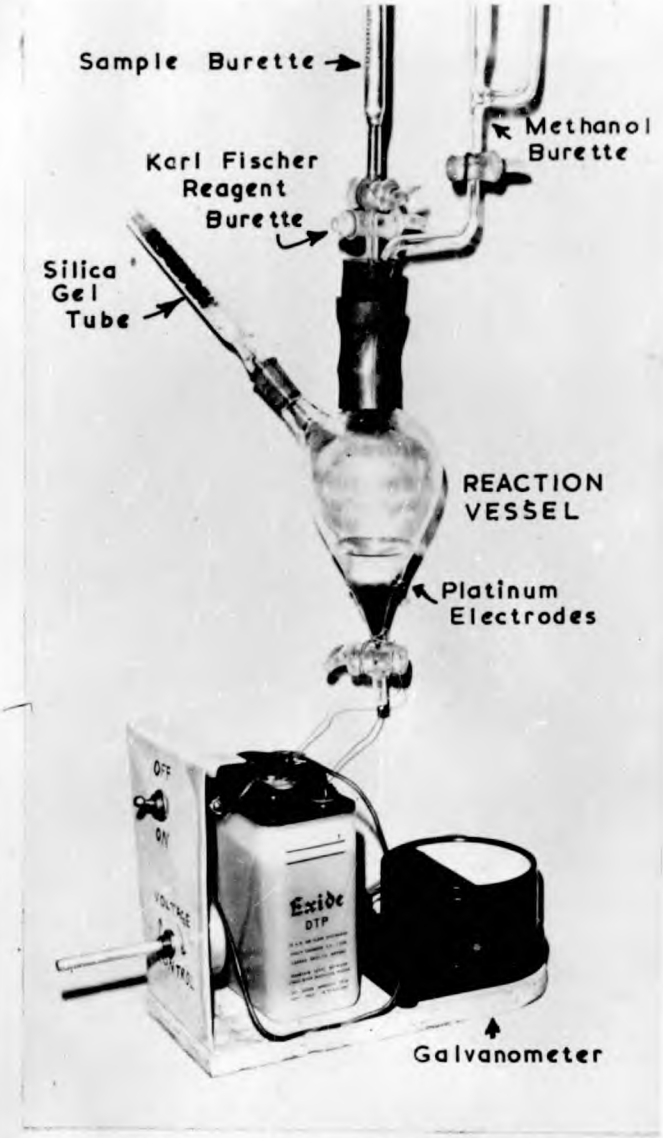

B. DETAIL OF REACTION VESSEL AND DEAD-STOP END-POINT APPARATUS.

FIG.AV-1. KARL FISCHER APPARATUS.

APPENDIX VI

APPARATUS USED IN THE MEASUREMENT OF PROPERTIES

Introduction

A brief description will be given of the equipment used in measuring the properties of hexamine and its solutions. The techniques of measurement were for the most part, based on those described by Weissberger [41]. The data have been given directly in the attached Supplement of Properties.

Hexamine solutions were prepared from the solvent and from dried hexamine specially recrystallized from the solvent. Crystals prepared for aqueous solution were analysed for included moisture by the Karl Fischer method (Appendix V). The compositions of certain of the solutions were checked by the analytical method (Appendix IV).

(i) Density

Solution densities were measured with 25 ml. specific gravity bottles, used in constant temperature baths. The bottles were calibrated with boiled distilled water. All weighings were done on an accurate analytical balance, with corrections for buoyancy. Crystal densities were measured while immersed in a petroleum fraction.

(ii) Refractive Index

Refractive indices were measured on an Abbé refractometer maintained at 25.0°C. The instrument was calibrated against distilled water. Supersaturated hexamine solutions could not be used, since they tended to crystallize out on the prism surfaces.

(iii) Analysis of Hexamine Hydrate

Crystals of the hydrate were prepared by freezing saturated hexamine solutions. Samples of the filtered crystals (maintained $< 15^{\circ}C$) were taken, weighed, and dissolved in a known quantity of water. The composition of the resulting solution was determined by the refractometer to give the hydrate composition.

(iv) Viscosity

Solution viscosities were measured with standard U-tube viscometers maintained in constant temperature baths. The procedure is described in British Standard B.S. 188-1929.

(v) Surface Tensions

Surface tensions were measured by the rise of liquid in a capillary tube tensioneter. The tube was calibrated with distilled water. The height of the liquid column was measured with a travelling microscope.

(vi) Solubility

Several methods were used to measure the solubility of hexamine in water.

The solubility was determined directly by the analysis of solution stored over excess crystal for prolonged periods of time in constant temperature baths.

The solubility was also measured in the reverse way by evaluating the saturation temperature at which solutions of known composition became saturated. This was done at first using the light slit method [42,43] in the apparatus shown in Fig AVI-1c. The change in appearance of a thin light beam on passing through the film about a crystal surface allows the saturation temperature to be determined. A Schlieren method (Fig AVI-1a) was also used. Here the Schlieren patterns about an immersed crystal (Fig AVI-1b) change as the solution approaches saturation, so allowing the saturation temperature to be determined.

The solubilities of hexamine in non-aqueous solvents and prepared solvent mixtures were determined directly by chemical analysis. In the case of saturated solutions of hexamine in aqueous ammonia, the chemical analysis gave the hexamine plus ammonia content. The quantity of ammonia was estimated separately by the Nessler method.

(vii) Freezing Points

The melting points of aqueous hexamine solutions were determined as the temperatures at which frozen solution first started and finally completed melting. The solutions were contained in thin sample tubes attached to a thermometer in a brine bath of slowly varying temperature.

The melting point of the hydrate was determined in a similar manner.

(viii) Boiling Points

Elevations of boiling point were measured using two standard ebullioneters, one containing the solution, the other distilled water. Both were interconnected and connected to the same vacuum system. The elevation of boiling point was determined as the differences in reading of two standard thermometers and also as the reading from a thermocouple.

(ix) Conductivity

Conductivities were measured using a pair of platinized electrodes and a standard conductivity bridge. The electrodes were calibrated against standard KCl solutions.

(x) Thermal Properties

All measurements of thermal properties were made in a water jacketted copper calorimeter, with manual stirrer.

A.

B.

C.

FIG. A VI-1. APPARATUS USED TO MEASURE THE SOLUBILITY OF HEXAMINE IN AQUEOUS SOLUTION.

A. SOLUBILITY CELL USED IN SCHLIEREN APPARATUS.

B. PHOTOGRAPH OF PROJECTED IMAGE OF CRYSTAL SHOWING SCHLIEREN PATTERNS ABOUT A CRYSTAL IN UNDERSATURATED SOLUTION.

C. LIGHT SLIT APPARATUS.

The temperature rise on solution was determined by adding weighed quantities of hexamine to weighed quantities of distilled water all initially at 25.0°C, and measuring the resulting temperatures. Corrections were applied for the calorimeter and stirrer, and for heat losses.

Heat capacities of solutions were measured by electrically heating the solutions and measuring the temperature rise. The quantity of electrical energy added was measured by an accurate wattmeter and a stop-watch. The heat capacity of the crystalline material was measured using a slurry of crystals in saturated solution. Corrections were applied for the solution and the change in solubility.

The heat of decomposition of hydrate crystals was determined in a similar way.

REFERENCES

1. Buckley H.E., "Crystal Growth", Wiley, New York (1951).

2. van Hook, A., "Crystallization: Theory and Practice," Chapman Hall, London (1961).

3. Mullin J.W., "Crystallization", Butterworths, London (1961).

4. Perry J.H., "Chemical Engineers Handbook", 4th ed., p. 17-7, McGraw Hill, New York (1963).

5. Coulson J.M. and Richardson J.F., "Chemical Engineering", Ch. 22, Pergamon, London (1955).

6. Hurle D.T.J., Solid State Electronics, 5, 37, 142 (1961).

7. Bardsley W., Boulton J.S., and Hurle D.T.J., Solid State Electronics 5, 395 (1962).

8. Powers H.E.C., Internat. Sugar J., 61, 17, 41 (1959).

9. Powers H.E.C., Nature, 182, 715 (1958).

10. Powers H.E.C., Indus. Chem., 39, 351, 421, 485 (1963).

11. Smith F.G., "Historical Development of Inclusion Thermometry", Univ. Toronto Press (1955).

12. Roedder E., Scientific American, Oct., 38 (1962).

13. Denbigh K.G., Dis. Faraday Soc., No. 5, "Crystal Growth", 188, (1949).

14. Bunn, C.W., "Crystals: Their Role in Nature and in Science", Academic Press (1964).

15. Birchall, J.D., I.C.I. Ltd., Mond. Division, Winnington, Cheshire, private communication (1964).

16. Ayerst R.P., Ministry of Defence, Waltham Abbey, private communication (19

17. Adamski T., and Trojanowski L., Nature, 197, 894, 1005 (1963).

18. Adamski T., Polish Acad. Sc. Inst. Nucl. Res., Report 362/IV (1962).

19. Walker J.F., "Formaldehyde", A.C.S. Monograph No. 120, 2nd ed. Ch. 19, Reinhold, New York (1953).

20. Lange N.A. "Handbook of Chemistry", 9th ed., p. 1277, Handbook Publishers Inc., Ohio (1956).

21. Denbigh K.G., and White E.T.., Nature, 199, 799 (1963).

22. Sherwood P.W., Petroleum Refiner, 37, No. 9, 551 (1958).

23. Branson S.H., Dunning W.J., and Millard B., Dis. Faraday Soc., No. 5, "Crystal Growth", 83 (1949).

24. Saeman W.C., A.I.Ch.E. Journal, 2, 107 (1956).

25. Randolph A.D. and Larson M.A., A.I.Ch.E. Journal, 8, 639 (1962).

26. Branson S.H., and Dunning W.J., Dis. Faraday Soc., No. 5,"Crystal Growth", 96 (1949).

27. Phillips F.C., "An Introduction to Crystallography", 2nd ed., Fig. 310, Longmans, London (1956).

28. McCabe W.L., Ind. Eng. Chem., 21, 30, 112 (1929).

29. Belyaev L.M. and Chernov A.A., Soviet Physics-Crystallography, 7, 535 (196

30. Chernov A.A., Soviet Physics-Crystallography, 8, 63, 401 (1964).

31. Seegar A., Phil. Mag. 44, 1 (1953).

32. Bunn C.W., Dis. Faraday Soc., No. 5, "Crystal Growth", 132 (1949).

33. Humphreys-Owen S.P.F., Dis. Faraday Soc., No. 5, "Crystal Growth" 144 (194

34. Lange N.A., "Handbook of Chemistry" 9th ed., Handbook Publishers Inc., Ohio (1956). (p.1420).

35. Denbigh K.G., Private communication (1963).

36. Patent, Badische Anilin & Soda Fabrik, U.S. 2,912, 435 ;Brit.810, 765.

37. Mitchell J. and Smith D.M., "Aquametry", Interscience, New York (1948).

38. Vogel A.I., " Quantitative Inorganic Analysis" 2nd ed., p. 698. Longmans Green, London (1951).

39. BDH pamphlet, "Moisture Determination by the Karl Fischer Reagent", Poole, England (1961).

40. Hopkins and Williams pamphlet, "Karl Fischer Catalyst", Chadwell Heath, Essex (1960).

41. Weissberger A. "Techniques of Organic Chemistry" 3rd. ed. Vol. I. (1959).

42. Dauncey, L.A., and Still J.E., J. Appd. Chem., 2, 399 (1952).

43. Wise, W.S., and Nicholson E.B., J. Chem. Soc. 2714 (1955).

44. Honigmann B., and Heyer H., Z. Electrochem, 61, 74 (1957).

Supplement to Thesis

SUPPLEMENT

PROPERTIES OF HEXAMINE AND HEXAMINE MIXTURES

Compiled by
E.T. WHITE,
Chem. Eng. Dept.,
Imperial College.

December, 1963.

TABLE OF CONTENTS

LIST OF TABLES

LIST OF FIGURES

SI. PROPERTIES OF PURE HEXAMINE

INTRODUCTION

Excellent sourcebooks for the available data on the properties of hexamine are Beilstein [1] (in German) and Walker [2]. Less comprehensive surveys are given in Kirk-Othmer [3] and Heilbron & Bunbury [4]. Additional data may be found in Landolt-Börnstein [5].

SI-1 DESCRIPTION

(i) Name: Hexamethylene tetramine.

(ii) Other Names: Hexamine, "Urotropin", Methenamine, "Formin", Formamine, "Hexa", Hexamethylenamine, "Aminoform".

(iii) Formula: $(CH_2)_6N_4$

(iv) Molecular Weight: 140.19

(v) Appearance:

Hexamine is a colourless crystallire solid. It crystallizes from the vapour and from solvents as regular rhombic dodecahedra (Fig. SI-1). The commercial product (Fig. SI-2) appears as an opaque mass of small rounded crystals about 1mm. in size. Under certain conditions, both from the vapour and from solution, hexamine can grow dendritically giving the usual fir-tree appearance (Figs. SI-3 and SI-4).

(vi) Odour

The pure material is practically odourless. The commercial product often has a strong amide odour due to the presence of impurities.

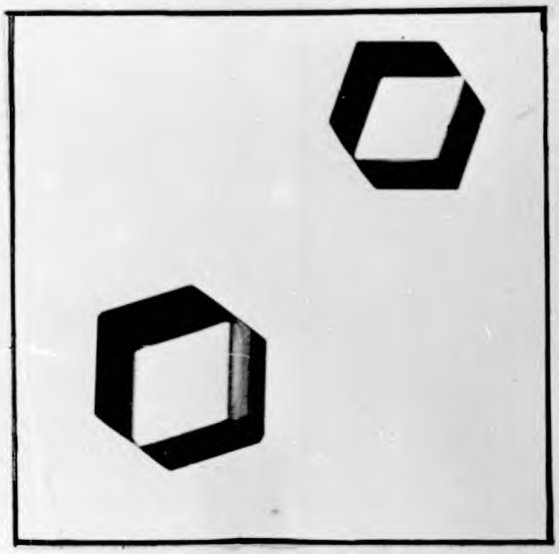

FIG. SI-1. CRYSTALS OF HEXAMINE.

[x 50]

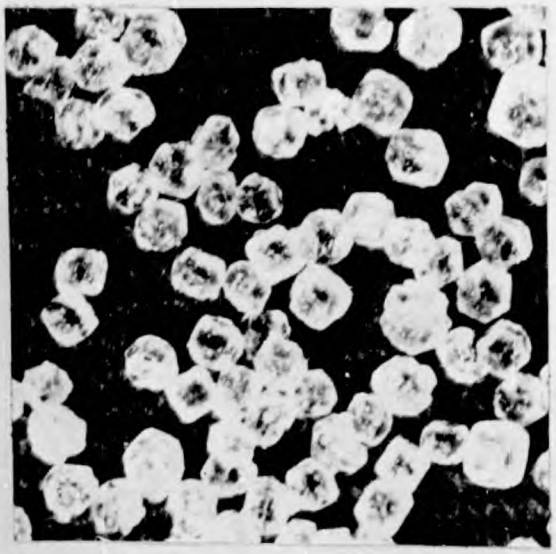

FIG. SI-2. COMMERCIAL HEXAMINE CRYSTALS.

[x 6]

FIG. SI-3. DENDRITIC HEXAMINE GROWN FROM VAPOUR.

[x 6]

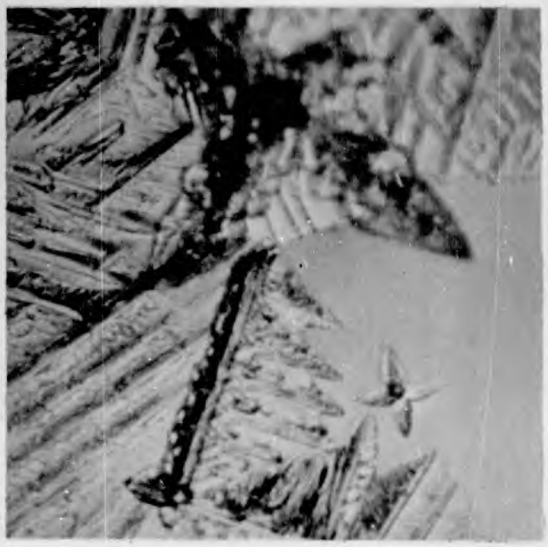

FIG. SI-4. DENDRITIC HEXAMINE GROWN ON SURFACE OF AQUEOUS SOLUTION EXPOSED TO AIR.

[x 100]

(vii) Taste and Toxicity:

Hexamine has a sweet metallic taste. In small amounts it is often prescribed for internal use as a urinary antiseptic drug. However in some instances toxic action has been reported [2, 6]. With certain people it may also be a cause of skin rash [7, 8].

SI-2 MOLECULAR AND CRYSTAL STRUCTURE

Various chemical structures have been proposed for hexamine. These are reviewed by Walker [2]. The structure generally accepted is that of Duden and Scharff [9] shown in Fig. SI-5. In this structure all the nitrogen atoms in the molecule are equivalent as are all the carbon atoms. An alternative structure of some interest (Fig. SI-7) in which the nitrogen atoms are not all equivalent is given by Lösekann [10]. This structure explains the monobasic behaviour of hexamine in solution. However it does not agree with the X-ray and spectra results on the solid and vapour, nor apparently with dipole moment and Raman measurements [11] of hexamine in chloroform and aqueous solution. The atom numbering convention shown in Fig. SI-6 is taken from the Ring Index [12].

The spatial arrangement of the atoms in the hexamine molecule has been determined by X-ray, nuetron diffraction, electron diffraction and other techniques [11, 13-49]. The structure so found is very regular. The nitrogen atoms occupy the corners of a tetrahedron while the carbon atoms lie on the corners of an octahedron. This structure is shown in Fig SI-8. Bond lengths and bond angles as computed by

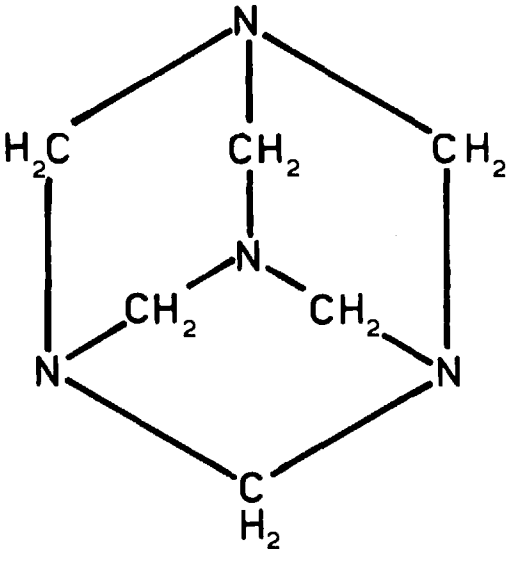

FIG.SI-5. CHEMICAL STRUCTURE OF HEXAMINE (Proposed by DUDEN and SCHARFF [9]).

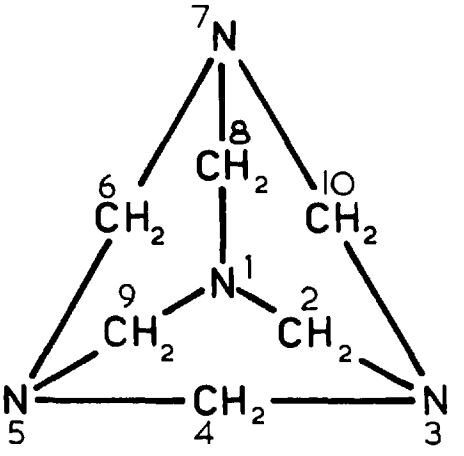

FIG. SI-6. RING NUMBERING SYSTEM FOR HEXAMINE. (RING INDEX [12].)

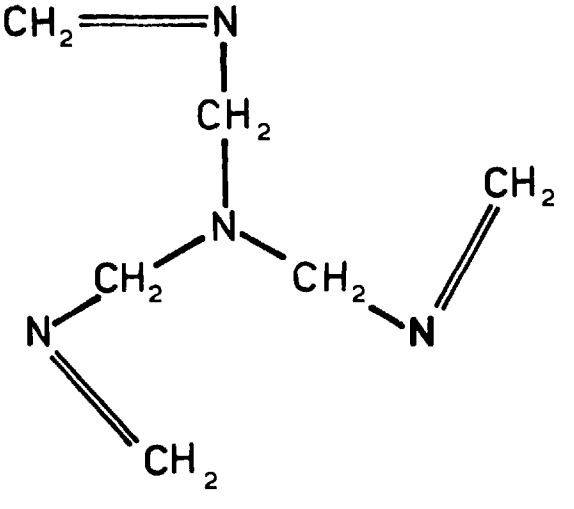

FIG.SI-7. THE CHEMICAL STRUCTURE OF HEXAMINE PROPOSED BY LÖSEKANN [10].

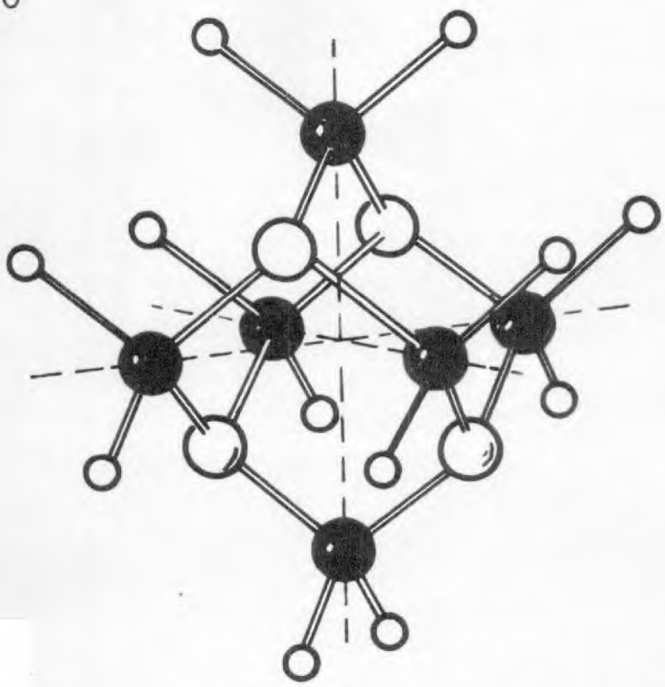

FIG. S I-8. STRUCTURE OF HEXAMINE. (From Dickinson and Raymond [14]).

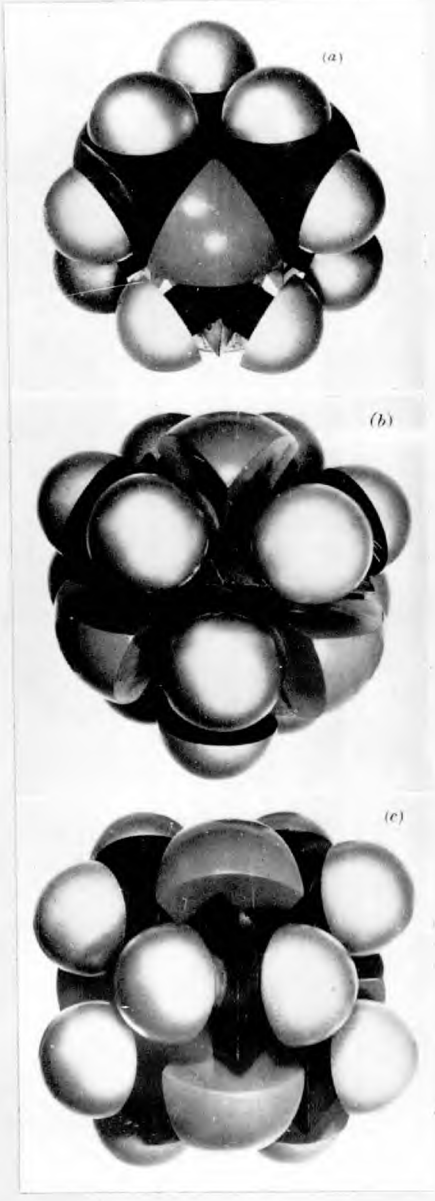

FIG. SI-9. PHOTOGRAPH OF SCALE MODEL OF HEXAMINE MOLECULE. (Becka and Cruickshank [13]).

Becka and Cruickshank [13] are shown in Table SI-1. Bond lengths measured for hexamine vapour [24, 25] are in substantial agreement with these values [13]. Fig. SI-9 shows a scale model of the hexamine molecule. The molecule is almost spherical except for the slight protrusion of the CH_2 groups.

Crystalline hexamine has a body centred cubic lattice of the space group T_d^3 $I\bar{4}3m$. The molecular lattice is equivalent to the space lattice. The unit cell is a cube of length 7.02Å at 298°K and contains two molecules. Each molecule is surrounded by eight others along <111> at 6.08Å between centres and by six others along <100> at 7.02Å [13]. A nitrogen atom of one molecule fits neatly into the recess formed by three hydrogen atoms of a neighbouring molecule. The CH_2 group at the top of one molecule nestles at 90° across the CH_2 group at the bottom of the next molecule. The positioning of the molecule in the unit cell is also shown in Landolt-Börnstein [5].

This structure is retained over the full temperature range 5 to 300°K [13, 26]. Increasing temperature merely expands the unit cell and increases the magnitude of the lattice vibrations [13]. It has been suggested that the cause of the high stability and low volatility of hexamine may be the hydrogen bonding between neighbourning molecules. This view is not accepted by Becka and Cruickshank [13] who consider the cause to be simply the shape and packing of molecules in the lattice.

A lattice model of hexamine has been proposed [13] capable of predicting many of the observed optical, elastic, and thermodynamic properties.

Bond Lengths.

C - N	1.476 ± 0.002 Å
C - H	1.088 ± 0.011 Å

Bond Angles.

C - N - C	107.2 ± 0.1°
N - C - N	113.6 ± 0.2°
H - C - H	108.5 ± 1.2°

Length of Unit Cell.

298° K	7.02 ± 0.01 Å
100° K	6.93 ± 0.01 Å
34° K	6.91 ± 0.01 Å

TABLE SI - 1. Structural Parameters For Hexamine. (Becka & Cruickshank [13])

SI-3 PHASE RELATIONSHIPS

(i) Number of Phases

Under normal experimental conditions (atmospheric and sub-atmospheric pressures) only two hexamine phases are known - the vapour and the crystalline solid. Liquid hexamine is unknown, since hexamine sublimes at these pressures. Only the one solid phase is known, at least for the temperature range 5°K to 500°K [26, 50].

(ii) Solid-Vapour Behaviour: Vapour Pressure of Hexamine

The vapour pressure of solid hexamine (corrected for decomposition) has been determined [51, 52]. Data between 20°C and 280°C (10^{-4} to 800 mm Hg.) may be correlated [53] by

$$\log_{10} p = -\frac{2940}{T} + 10.0$$

where p is the true vapour pressure in m.m of Hg. at an absolute temperature T°K. This correlation is shown in Fig. SI-10.

From this relation the vaporisation temperature at atmospheric pressure was computed as 255°C. At temperatures above about 230°C charring and decomposition of the hexamine may occur. Charring is quite rapid above 280°C. The decomposition of hexamine is considered further in Section SI-8.

(iii) Phase Diagram

Since there are only the two phases, the known phase diagram is solely the vapour pressure curve given above.

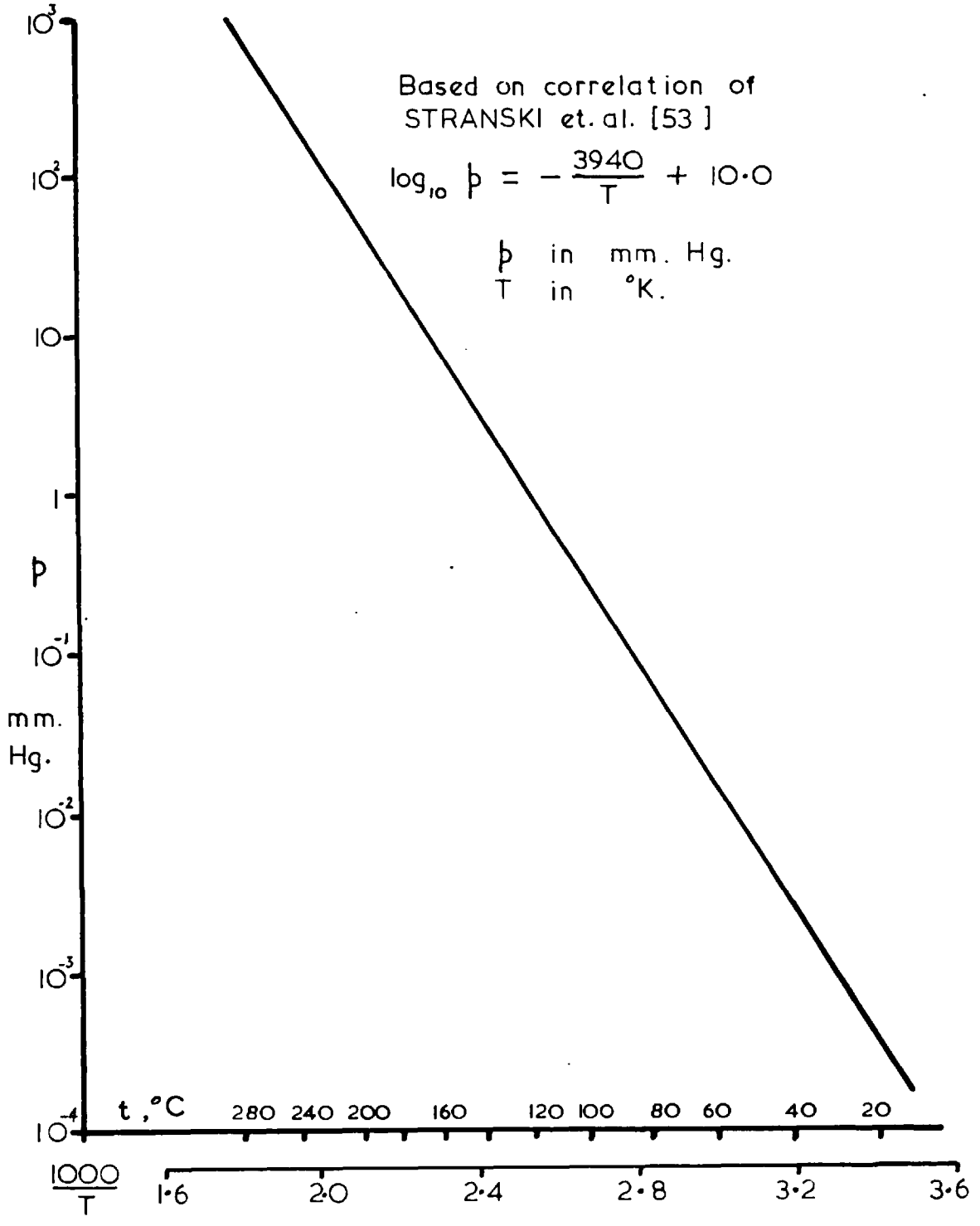

FIG. SI-10. VAPOUR PRESSURE OF SOLID HEXAMINE.

SI-4 PROPERTIES OF HEXAMINE VAPOUR

Published data could not be located. If required, values might be predicted from generalised equations of state.

SI-5 PHYSICAL PROPERTIES OF SOLID HEXAMINE

(i) Density

Available density data are given in Table SI-2. At room temperature the density of solid hexamine might be taken as 1.335 ± 0.002 g/ml. with a coefficient of variation with temperature of $-(1.85 \pm 0.01).10^{-4}/^{\circ}K$. The effect of pressure has been measured [59]. At low pressures the compressibility is approximately 9×10^{-6} atmos^{-1}.

(ii) Flash Point

The flash point is given [56] as 482°F (250°C), a value close to the normal vaporisation temperature.

(iii) Refractive Index

The refractive index of solid hexamine at room temperature was determined by an immersion method as 1.590 ± 0.003. Much more accurate data are available [60] and are given in Table SI-3.

(iv) Other Optical Properties

Extensive measurements have been made of the Raman [11, 39-43, 45, 48] and infra red spectra [40, 46-49] for crystals, vapour and solutions.

A recent reference [61] claims that hexamine shows a large electro-optical effect, comparable to CuCl and ZnS.

(v) Magnetic Properties

Magnetic resonance studies have been published [23, 26-29].

Hexamine is reported [62] as having a surprisingly high positive

a. Values at Room Temperature.

TEMP. °C	DENSITY g./ml.	REFERENCE
- 5	1.331	Beck [54]
Room	1.333	Jessop [55]
Room	1.337	L.-B. [57] 2/3 p. 422.
25	1.270	Faith et. al. [56]
25	1.345	Chang & Westrum [50]
20	1.339	Mosebach [111]
25.0 (± 0.02)	1.335 (± 0.01)	Author

b. Variation With Temperature.

TEMP. RANGE °C	$\frac{1}{\rho}\cdot\frac{d\rho}{dT}$ x 10^4	REFERENCE
- 183 to 20	- 1.36	Lonsdale [57]
- 259 to -173	- 1.38	Becka and Cruickshank [13]
- 173 to 25	- 1.98	
- 150 to -100	- 1.3	Mirskaya [58]
- 100 to 25	- 1.8	

FIG SI - 2. DENSITY OF SOLID METHANE

a. Values at room temperature.
b. Variation with temperature.

WAVELENGTH mμ	REFRACTIVE INDEX
436.1	1.5984
501.6	1.5953
546.1	1.5917
578.0	1.5899
587.6	1.5893
667.6	1.5856

n_D = 1.5892 (by interpolation).

TABLE SI - 3. REFRACTIVE INDEX OF SOLID HEXAMINE [607]

PROPERTY	VALUE	
ΔH_f°	28.8	k.cal/g. mole
ΔF_f°	102.7	k.cal/g. mole
ΔS_f°	-247.911	cal/(g. mole)(°C)

C_p	36.397	cal/(g.mole)(°C)
S°	39.048	cal/(g.mole)(°C)
$H^\circ - H_o^\circ$	5452.2	cal/g. mole
$-(F^\circ - H_o^\circ)/T$	20.761	cal/(g.mole)(°C)

TABLE SI - 4. THERMODYNAMIC PROPERTIES OF CRYSTALLINE HEXAMINE AT 25.0°C. [507]

diamagnetic behaviour.

(vi) Electrical Properties

The dipole moments of hexamine have been measured [11].

Hexamine exhibits piezo-electric behaviour [63 - 66] and the electromechanical constant has been measured ([5], 2/3, p.434).

(vii) Elastic Constants

The elastic properties of hexamine have been measured by X-ray methods [5, 31-33, 36] and ultrasonics [31, 38].

(viii) Diffusion Through Hexamine Crystals

The diffusion coefficient of water through solid hexamine is given by Smith [23].

SI-6 THERMODYNAMIC PROPERTIES OF HEXAMINE

(i) Heat of Combustion

Values reported for the molal heat of combustion at constant pressure, in k-cal/g.mole are

ΔH_c = -1003.6 [67], ΔH_c = -1006.7 [68], and ΔH_c = -1037.1 [69]

(ii) Standard Heat of Formation

The standard heat of formation at 25°C of hexamine has been computed from the above data as

$$\Delta H_f^{\circ} = 28.8 \text{ k-cal/g.mole [50].}$$

(iii) Entropy and Free Energy of Formation

The values at 25°C have been calculated [50] and are shown in Table SI-4.

(iv) Heat Capacity of Solid Hexamine

The heat capacity of hexamine between 5°K and 350°K has been

determined by Chang and Westrum [50]. Their tables should be consulted for accurate data. Their results are shown in Fig. SI-11, and also on Fig. SI-12, where they are compared with rough data obtained by the author. Over the range 0° to 50°C the linear relation

$$c = 0.2535 + 0.00105\ t$$

may be used without undue error, where c is the heat capacity in cal/(g)(°C) and t the temperature in °C.

(v) Other Thermodynamic Properties

Table SI-4 lists other properties at 25°C computed by Chang and Westrum [50].

Values of the Debye and Einstein temperatures have been calculated [13, 70, 71]. Estimates of (Cp - Cv) have been made [58, 71] and range from 0.7 to 1.1 cal/(g.mole)(°C).

A theoretical model capable of predicting many of the properties of hexamine has been proposed by Becka and Cruickshank [13].

(vi) Latent Heat of Sublimation

The latent heat of sublimation computed from the vapour pressure data of Section SI-3(ii) is ΔH_v = 18.0 k-cal/g. mole. This is in good agreement with values of 17.5 and 17.9 k-cal/g.mole at 8°C and 25°C measured by Buderov [52] and the value of 18.1 k-cal/g.mole proposed by Smith [23].

SI-7 RATES OF EVAPORATION AND GROWTH

(i) Evaporation of Hexamine Crystals

Rates of evaporation of solid hexamine have been measured [72, 73]. From -12°C to 20°C the evaporation coefficient is constant at 0.27, ..

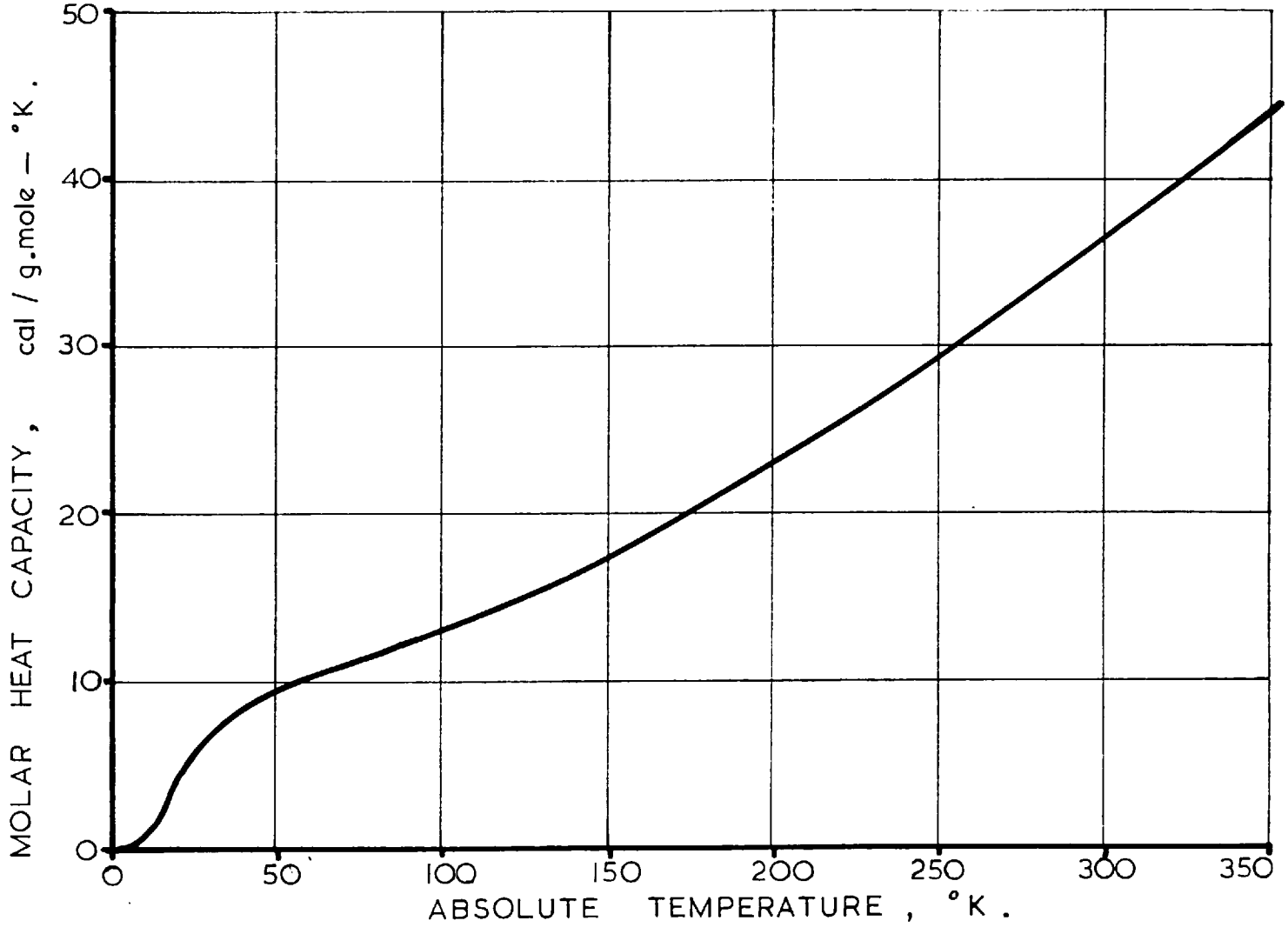

FIG. SI-11. MOLAR HEAT CAPACITY OF SOLID HEXAMINE.
(Data of Chang and Westrum [50].)

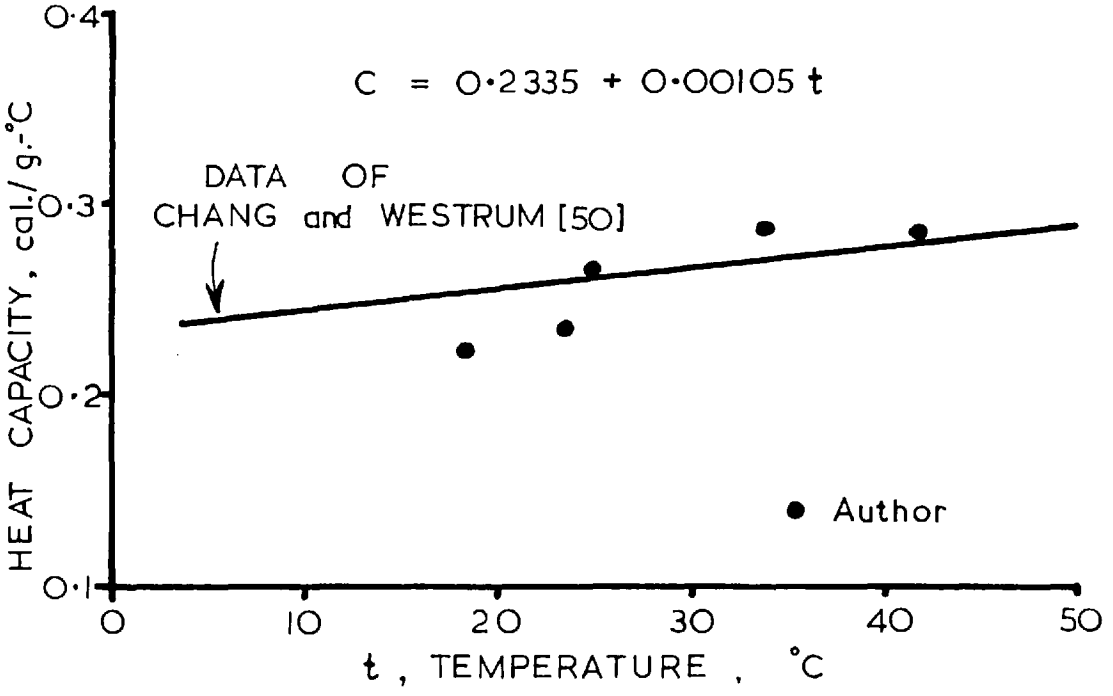

FIG. SI-12. HEAT CAPACITY OF SOLID HEXAMINE.

and the apparent activation energy equals the heat of sublimation. Limited data are also given by Buderov [52].

(ii) Growth of Crystals

The growth of hexamine from its vapour has been extensively studied by Stranski, Honigman, and others [74 - 82] over a wide range of temperatures. Early work was concerned with the morphology of the crystals formed. As well as the usual {011} faces, {001} and {112} planes were also obtained. Later work was concerned with the rates of crystal growth. Honigmann and Heyer [78] found that the rates of growth on {011} faces was proportional to the square of the supersaturation for microscopically plane surfaces, but only proportional to the supersaturation for flawed surfaces.

High purity hexamine crystals suitable for testing purposes have been prepared by sublimation, or by recrystallization from methanol, ethanol, chloroform, acetone, or water [13, 22, 23 50]. Very small crystals may be prepared by adding gaseous ammonia to a saturated aqueous solution [83, 84]. The growth of large crystals for piezo-electric purposes has been considered by Chumakov and Koptsik [85].

The presence of inclusions in crystals grown from aqueous solution has been reported [86, 87]. Hexamine crystals have been grown from benzene solution on the face of gypsum crystals [88].

SI-8 CHEMICAL PROPERTIES

Further details concerning the chemical behaviour of hexamine can be found in the texts quoted [1-4].

(i) Effect of Heat

Hexamine is readily ignited and burns with a bluish yellow flame. In the absence of oxygen charring becomes noticeable above 250°C. The products and rates of decomposition under heating have been investigated. [51, 53, 89-91]

(ii) Reaction with Acids

With acids hexamine decomposes to give formaldehyde. The kinetics of these reactions have been investigated [92, 93]. This reaction is the basis of the method of analysis usually used for hexamine solutions.

(iii) Decomposition by Radiation and Ultrasonics

Decomposition of hexamine can be caused by irradiation [94] and ultrasonics [95].

(iv) Compound Salt Formation

Hexamine readily reacts to form salts with a variety of acids and other materials. An extensive list is given in Beilstein [1].

(v) Nitration

Hexamine may be nitrated to give the explosive cyclonite (R.D.X.). Further details are given by Walker [2] and Simmonds et.al. [96]. The mechanism of this reaction has been studied. [2, 97]

SII. PROPERTIES OF HEXAMINE-WATER SYSTEM

INTRODUCTION

Hexamine is prepared industrially by crystallization from aqueous solution. Yet the amount of published data on the hexamine-water system is limited.

Much of the data given here was determined by the author. Details of the experimental methods used are described in Appendix VI of the author's thesis [101]. Estimates have been given of the errors associated with the experimental values. The errors are expressed as the 95% confidence limits about the experimental values with respect to the true values. In most instances it was possible only to give a very rough estimate of these errors since errors of method are involved as well as errors of measurement.

SII-1 PHASE RELATIONSHIPS

(i) Possible Phases

At pressures up to one atmosphere, at least five phases are possible in the hexamine-water system: the vapour, the liquid, and at least three solid phases. Only one liquid phase occurs, since at these pressures hexamine itself does not exist as a liquid (solid hexamine sublimes). Neglecting the various different forms of solid water, the three solid phases are hexamine, ice, and the hexamine hydrate $C_6H_{12}N_4 \cdot 7H_2O$.

(ii) Composition of Hydrate

If a near saturated solution of hexamine in water is cooled to

well below 0°C the hydrate may crystallize out. Such solutions can become highly supersaturated with respect to the hydrate without nucleation occuring, even in the presence of dust or hexamine crystals. The seeding with hydrate crystals however will cause rapid crystal growth as clusters of long needles radiating from the seed point (refer Fig. SII-1). Individual crystals of the hydrate are shown to larger magnification in Fig. SII-2.

The composition of the hydrate corresponds to hexamine heptahydrate $C_6H_{12}N_4.7H_2O$ (mass fraction of hexamine = 0.526). This was determined by measuring the composition of the solution formed by dissolving a known quantity of the filtered and dried crystals in a known amount of water (Table SII-1). The presence of a hydrate has been reported previously [99-109] although it was termed a hexahydrate.

The hydrate is stable below 13.5 ± 0.2 °C (Table SII-1). Above this temperature it decomposes immediately into hexamine crystals and solution. The heat of decomposition of the heptahydrate at 13.5°C into hexamine and saturated solution at 13.5°C was determined with an electrically heated calorimeter [101] as $\Delta H = 6.3 \pm 0.2$ k.cal/g.mole of hydrate.

(iii) Solid - Liquid Behaviour:- Solubility of Hexamine in Water

Hexamine will dissolve readily at all temperatures in a little over its own weight of water. Aqueous hexamine solutions show an inverse solubility-temperature behaviour up to 80°C, however the variation with temperature is small. With prolonged heating at temperatures above 50°C decomposition of the hexamine will occur [102]. The heptahydrate is the stable form of hexamine below 13.5°C (± 0.2°C) but metastable

FIG. SII-1. HEXAMINE HEPTAHYDRATE CRYSTALS GROWING IN SHALLOW DISH. [X2]

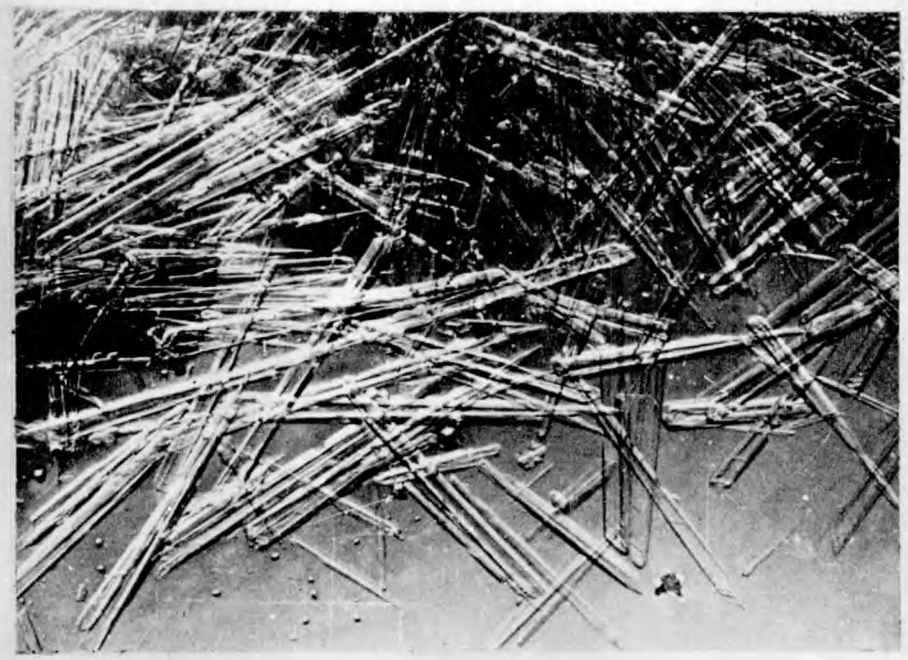

FIG. S II-2. HEXAMINE HEPTAHYDRATE CRYSTALS. [X 8]

Composition of hydrate.

Mass of hydrate g.	Mass of Water g.	Composition of solution †	Composition of Hydrate †	Moles H_2C / Mole Hx. ≠≠
5.001	1.906	0.382	0.526	7.00
8.759	9.598	0.251	0.527	6.98
7.870	4.133	0.343	0.524	7.06
7.859	3.394	0.369	0.527	6.98
10.695	4.343	0.375	0.527	6.98

† As mass fraction of hexamine. Error in solution composition ± 0.001; in hydrate ± 0.002.

≠≠ Error ± 0.05.

Decomposition Temperature of Hydrate

Reference	Hydrate Decomposition Temp., °C.
Evrard [100]	13 °C
Walker [27]	13.5 °C
Author	13.5 ± 0.2 °C

TABLE SII- 1. COMPOSITION AND DECOMPOSITION TEMPERATURE OF HYDRATE.

solutions of hexamine can be prepared and maintained without difficulty.

Published solubility data are given in Table SII-2 and Figures SII-3 and SII-4. These include the much neglected data of Evrard [100] for temperatures between -4°C and 165°C. An abnormally high solubility value of 167g hexamine per 100g water at room temperature was reported by Utz [104]. This may refer to the solubility of the hydrate since at 13.5°C its solubility is 167.1g of heptahydrate per 100g of total water. The author's values obtained by several different methods [101] are given in Table SII-3 and are also plotted on Fig. SII-3. These data are in excellent agreement with those of Evrard.

(iv) Solid-Liquid Behaviour: Freezing Points of Solutions

The solubility of hexamine heptahydrate can be determined from freezing point data. The temperatures at which frozen hexamine solutions of known composition finally melt when slowly warmed are given in Table SII-4 and Fig. SII-5. Literature values including the comprehensive data of Evrard [100] are given in Table SII-5.

It can be seen that hexamine in water exhibits eutectic behaviour at a mass fraction of hexamine of 0.292 ± 0.003 (Evrard, 0.298). This corresponds to a mole ratio of water to hexamine of 18.6 to 19.1 (Evrard 18.3). The freezing point of this eutectic is -10.2 ± 0.5°C (Evrard -9.0°C). Theory for dilute solutions overestimates the depression of the freezing point by about 15% [105].

There appears to be a volume increase on solidification, for on freezing a number of the solutions the glass sample tubes shattered.

Temperature, °C.	Solubility *	Reference
12	0.448	(Delepine [99], (Perry [103] p.141
0	0.473	)
25	0.465	)
50	0.450	) Walker [27]
70	0.434	)
- 4 ≠	0.473	)
- 1 ≠	0.472	)
7 ≠	0.470	)
		)
		)
13	0.468	)
16	0.465	)
20	0.465	)
30	0.463	)
40	0.462	)
		)
49	0.460	)
65	0.457	) Evrard [100]
85	0.456	)
95	0.460	)
100	0.463	)
		)
110	0.468	)
115	0.474	)
130	0.486	)
145	0.500	)
150	0.510	)
165	0.525	)

* As mass fraction hexamine in solution.

≠ Metastable.

TABLE SII - 2. PUBLISHED SOLUBILITY DATA FOR HEXAMINE IN WATER.

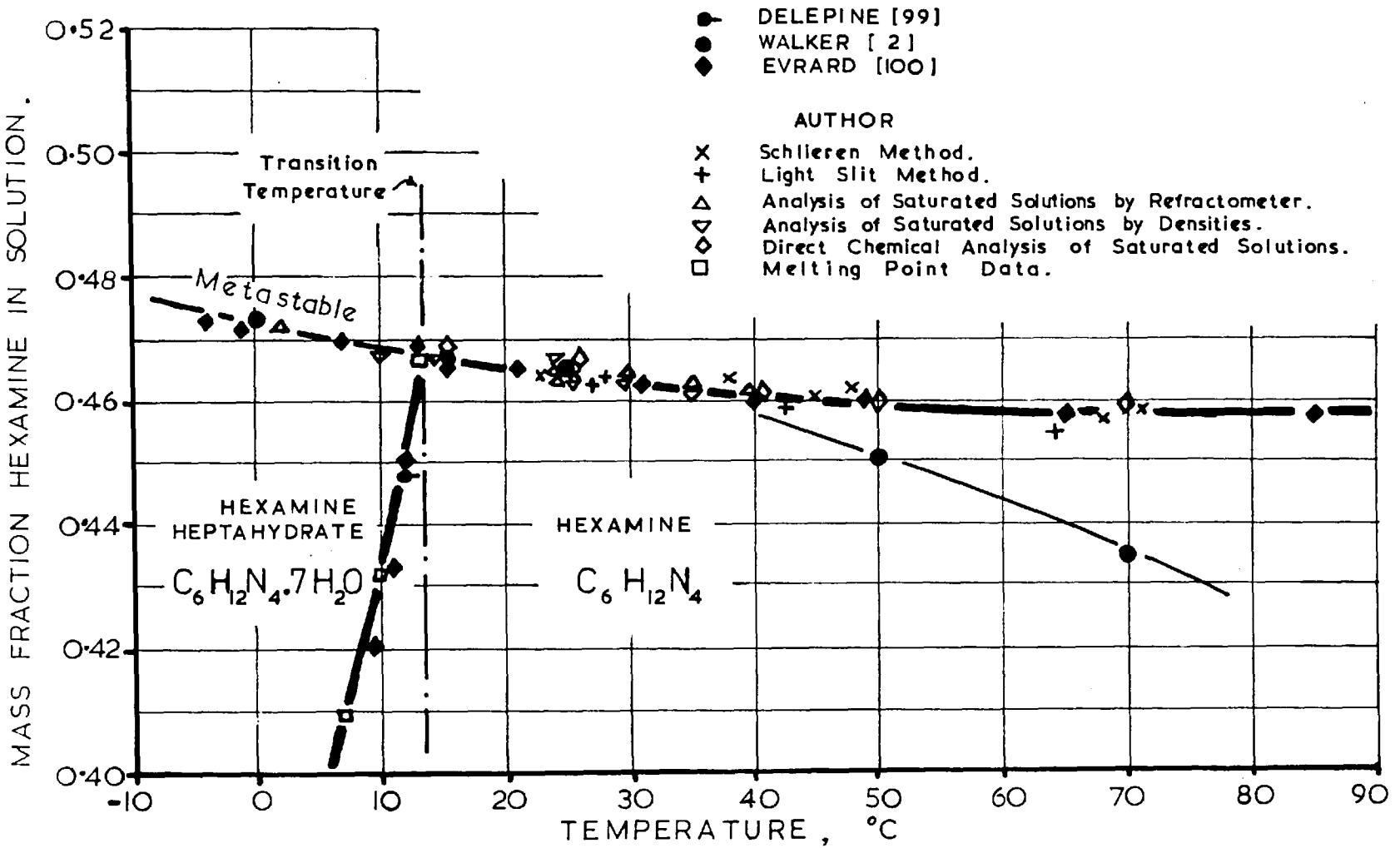

FIG SII-3. SOLUBILITY OF HEXAMINE IN WATER, −10 °C to 90 °C.

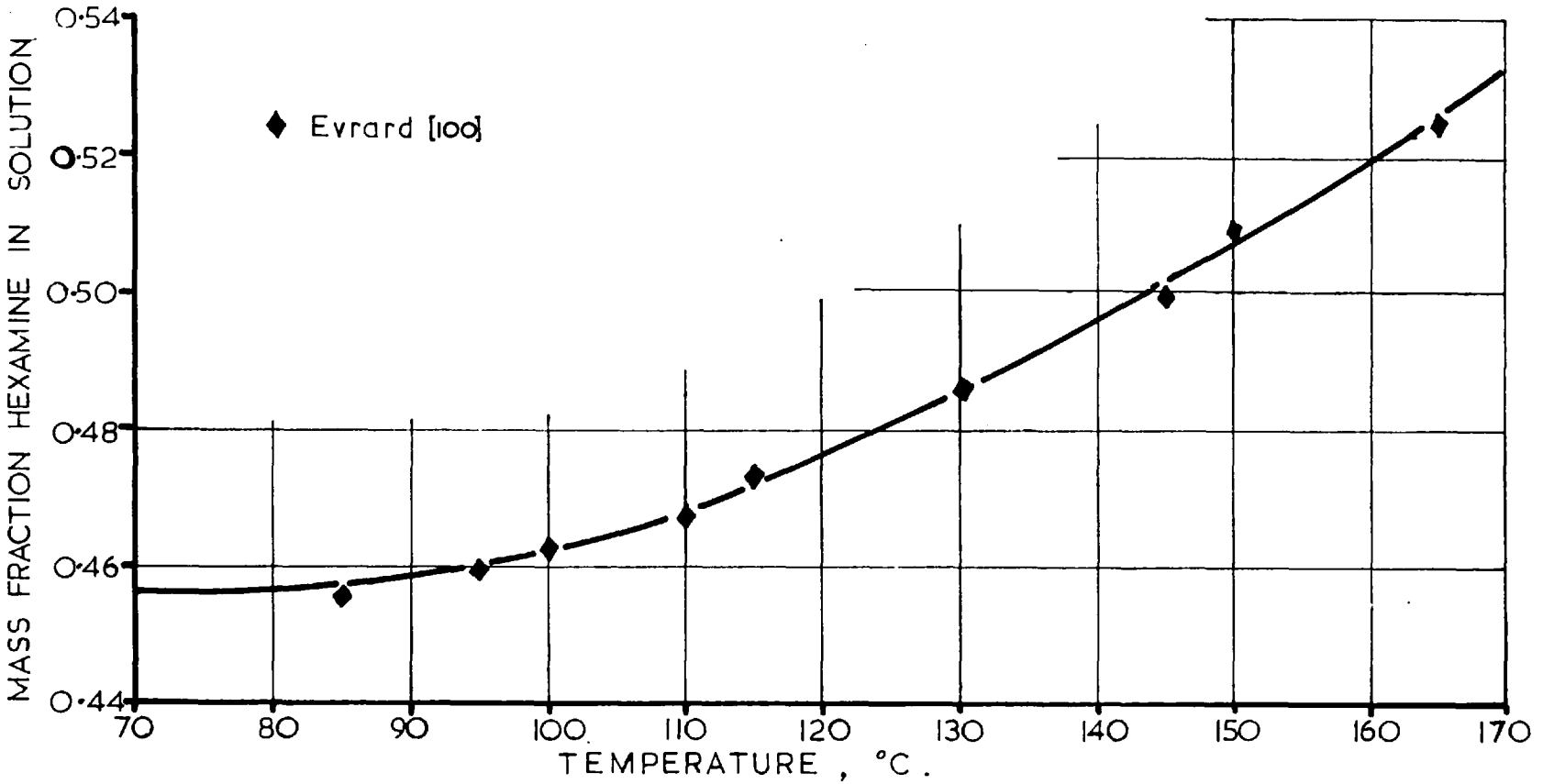

FIG. S II-4 . SOLUBILITY OF HEXAMINE IN WATER , 70°C to 170 °C .

ANALYSIS OF SOLUTIONS MAINTAINED AT CONSTANT TEMPERATURE			
Temperature °C.	SOLUBILITY *		
	By direct chemical analysis †	By refractive index measurements †	By density measurements ≠
3 ± 1	-	0.472	-
10.0 ± 0.1	-	-	0.467
14.5 ± 0.05	-	-	0.464
15.50 ± 0.02	0.469	-	-
25.00 ± 0.02	0.466	0.466	0.466
25.00 ± 0.02	-	0.465	0.463
25.00 ± 0.02	-	0.466	-
30.00 ± 0.02	-	0.464	0.462
35.00 ± 0.02	-	0.462	0.460
40.00 ± 0.02	0.462	0.461	0.460
50.0 ± 0.05	0.459	-	-
70.0 ± 0.05	0.459	-	-

DETERMINATION OF SATURATION TEMPERATURES			
LIGHT SLIT METHOD		SCHLIEREN METHOD	
Temperature, °C	Solubility * †	Temperature, °C	Solubility * †
28 ± 2	0.463	23 ± 2	0.464
28 ± 2	0.462	26 ± 2	0.464
43 ± 3	0.458	38 ± 2	0.463
64 ± 5	0.454	45 ± 2	0.460
		48 ± 2	0.461
		68 ± 3	0.457
		70 ± 4	0.458
		> 95	0.452

* Solubility as mass fraction hexamine in solution.
† Error in analysis ± 0.001.
≠ Error in analysis ± 0.002.

TABLE SII - 3. MEASURED SOLUBILITIES OF HEXAMINE IN WATER.

MASS FRACTION HEXAMINE IN SOLUTION†	FINAL MELTING TEMPERATURE, °C ≠
0.0	0.0
0.053	- 1.5
0.129	- 2.2
0.170	- 3.5
0.212	- 5.4
0.237	- 6.5
0.280	- 9.2
0.282	- 9.4
0.294	- 9.4
0.302	- 8.9
0.312	- 7.1
0.339	- 2.9
0.356	- 0.3
0.379	3.1
0.409	6.9
0.432	9.7
0.466	13.3

† Error in analysis ± 0.001

≠ Error in temperature ± 0.2°C.

TABLE SII - 4. MEASURED MELTING POINTS OF AQUEOUS HEXAMINE SOLUTIONS.

MASS FRACTION HEXAMINE IN SOLUTION	FREEZING POINT, °C.	REFERENCE.
0.0371	- 0.56	
0.0580	- 0.90	
0.105	- 1.80	
0.198	- 4.0	
0.230	- 5.7	
0.276	- 8.0	
0.288	- 8.3	
0.298	- 9.0	Evrard [109]
0.305	- 6.0	
0.308	- 5.0	
0.348	0.0	
0.405	7.0	
0.420	9.2	
0.433	10.8	
0.450	12.0	
0.468	13.0	
0.0081	- 0.121	
0.0176	- 0.276	Pummerer & Hofmann [105]
0.0283	- 0.459	
0.0543	- 0.814	
0.0725	- 1.087	
0.010	- 0.14	Husa & Rossi [106]
0.0361	- 0.52	Hammarlund et. al. [107]

TABLE SII - 5. PUBLISHED FREEZING POINT DATA FOR AQUEOUS HEXAMINE SOLUTIONS.

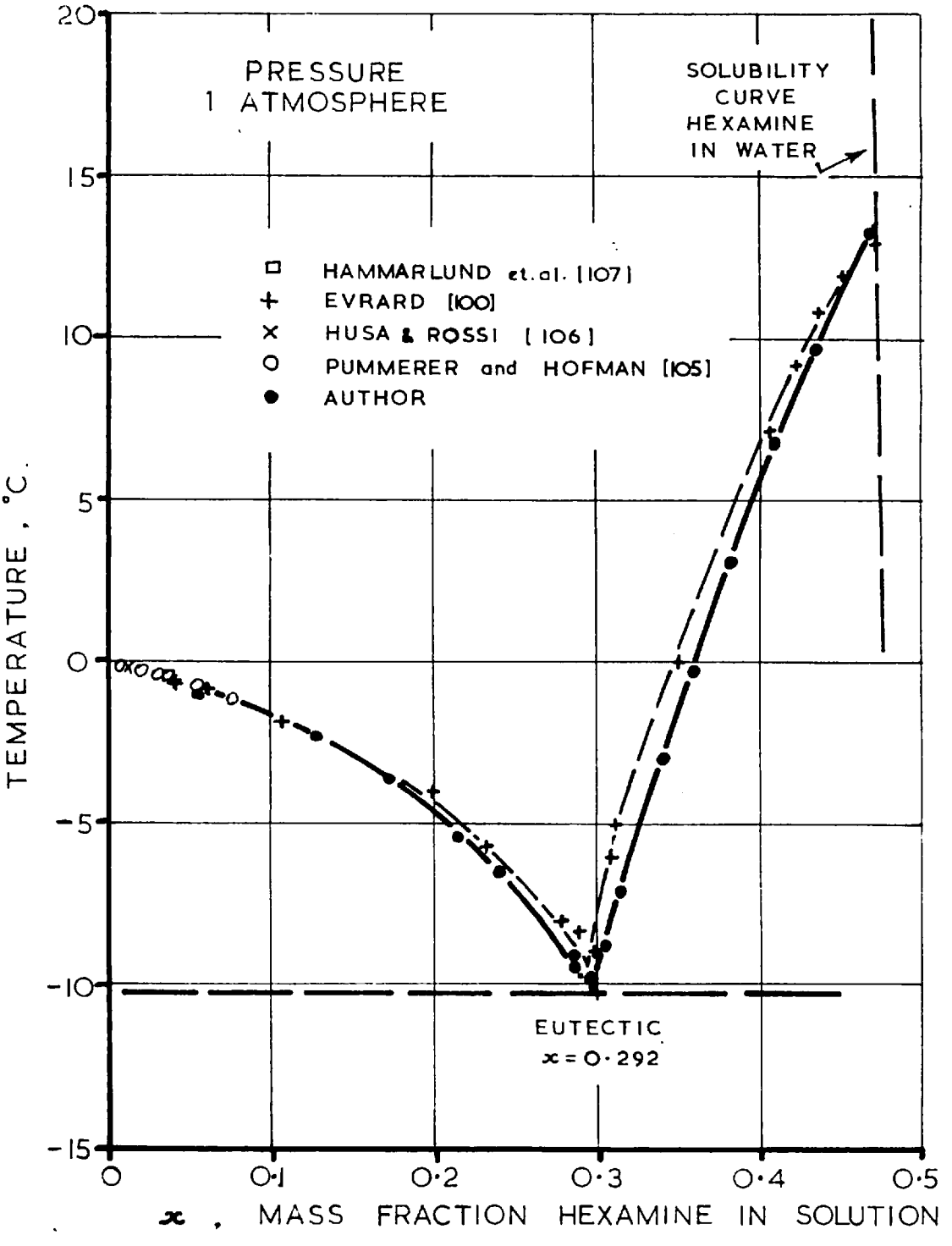

FIG. S II-5. FREEZING POINT DIAGRAM FOR AQUEOUS HEXAMINE SOLUTIONS.

(v) Liquid-Vapour Behaviour: Boiling Points of Solutions

The boiling point of a hexamine solution of known composition was determined as the difference in temperature between the solution and water both boiling under the same pressure. Details are given elsewhere [101]. The data obtained are given in Table SII-6 and Fig. SII-6. Smoothed and interpolated values are given on Fig. SII-7.

The elevations of boiling point of saturated hexamine solutions lie between 4.3°C and 4.9°C. Using the above data the boiling point curve for saturated solution was prepared (Fig. SII-8). This curve is in reasonable agreement with approximate values supplied to the author from Bridgewater [108].

The ratio of the partial pressure of saturated solution to that of water is also shown in Fig. SII-8. If an inert third component (e.g. air) is present in the vapour this ratio corresponds to the relative humidity at which deliquescence occurs.

(vi) Phase Diagram

With the use of the preceding data the phase diagram for the hexamine-water system was prepared (Fig. SII-9).

SII - 2 PHYSICAL PROPERTIES OF AQUEOUS HEXAMINE SOLUTIONS

Of the regions shown by the phase diagram by far the most important is that of the aqueous solution. Solubilities, boiling points and freezing points of aqueous solutions have been given in the previous section. Further properties of aqueous solutions are considered in this section.

x											
0.261	To	20.8	29.1	35.9	43.8	47.6	53.7	64.9	78.1	86.4	–
	ΔT	1.16	1.19	1.30	1.35	1.38	1.3	1.5	1.55	1.55	–
	ΔT'	1.20	1.22	1.31	1.38	1.42	1.44	1.58	1.61	1.65	–
0.340	To	24.7	28.2	37.3	41.1	47.6	48.0	55.0	64.0	77.3	92.0
	ΔT	2.03	2.07	2.24	2.27	2.32	2.3	2.5	2.6	2.6	2.6
	ΔT'	2.10	2.14	2.27	2.29	2.36	2.35	2.45	2.56	2.68	2.72
0.428	To	22.6	32.8	37.8	43.5	44.0	56.4	64.7	76.0	90.1	–
	ΔT	3.67	3.66	3.41	3.88	3.85	4.2	4.2	4.5	4.6	–
SATURATED	To	19.4	20.6	25.5	26.2	28.2	33.8	35.2	37.5	39.4	40.3
	ΔT	4.30	4.30	4.34	4.27	4.36	4.39	4.38	4.33	4.34	4.30
	ΔT'	4.21	4.24	4.28	4.16	–	4.32	–	4.31	–	–
	To	43.8	45.6	52.2	54.0	58.5	63.7	74.3	81.4	87.7	–
	ΔT	4.36	4.4	4.5	4.5	4.5	4.5	4.7	4.8	4.7	–
	ΔT'	4.40	4.38	4.46	4.39	4.48	4.52	4.65	4.72	4.82	–

Preliminary run; x = 0.363, To = 38.5°C, ΔT = 2.53°C.

Nomenclature. x = Composition, as mass fraction of hexamine in solution. To = Boiling point of water, °C.
ΔT, ΔT' = Difference in boiling points between solution and water in °C as measured respectively by thermometers and thermocouple.

Errors, in x, ± 0.001; in To, ± 0.1°C; in ΔT, for To <45°C, ± 0.07; for To > 45°C, ± 0.15°C; in ΔT', ± 0.07°C.

TABLE SII - 6. ELEVATION OF BOILING POINTS FOR AQUEOUS HEXAMINE SOLUTIONS.

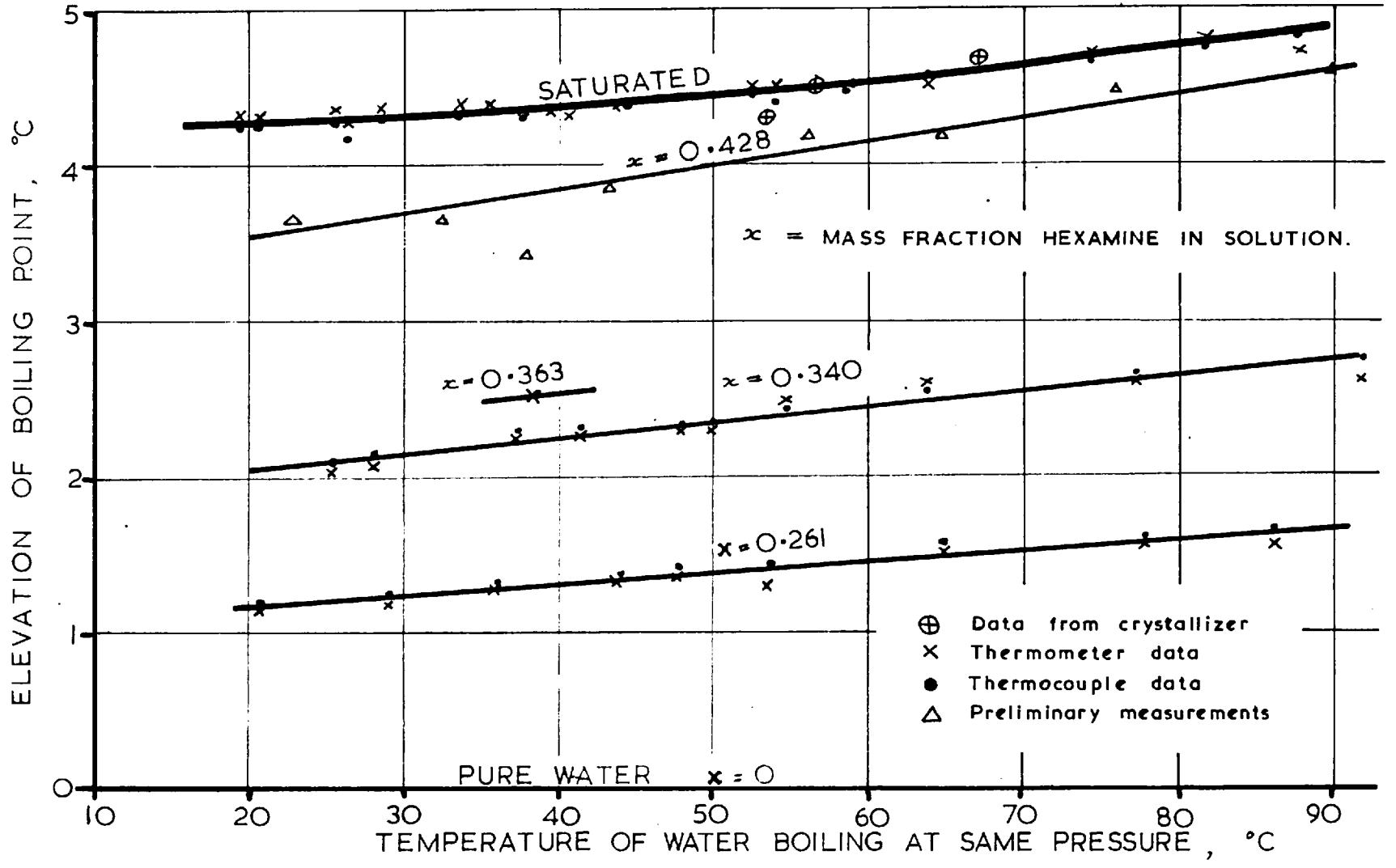

FIG. S II-6. ELEVATION OF BOILING POINT FOR AQUEOUS HEXAMINE SOLUTIONS.
(Experimental Results)

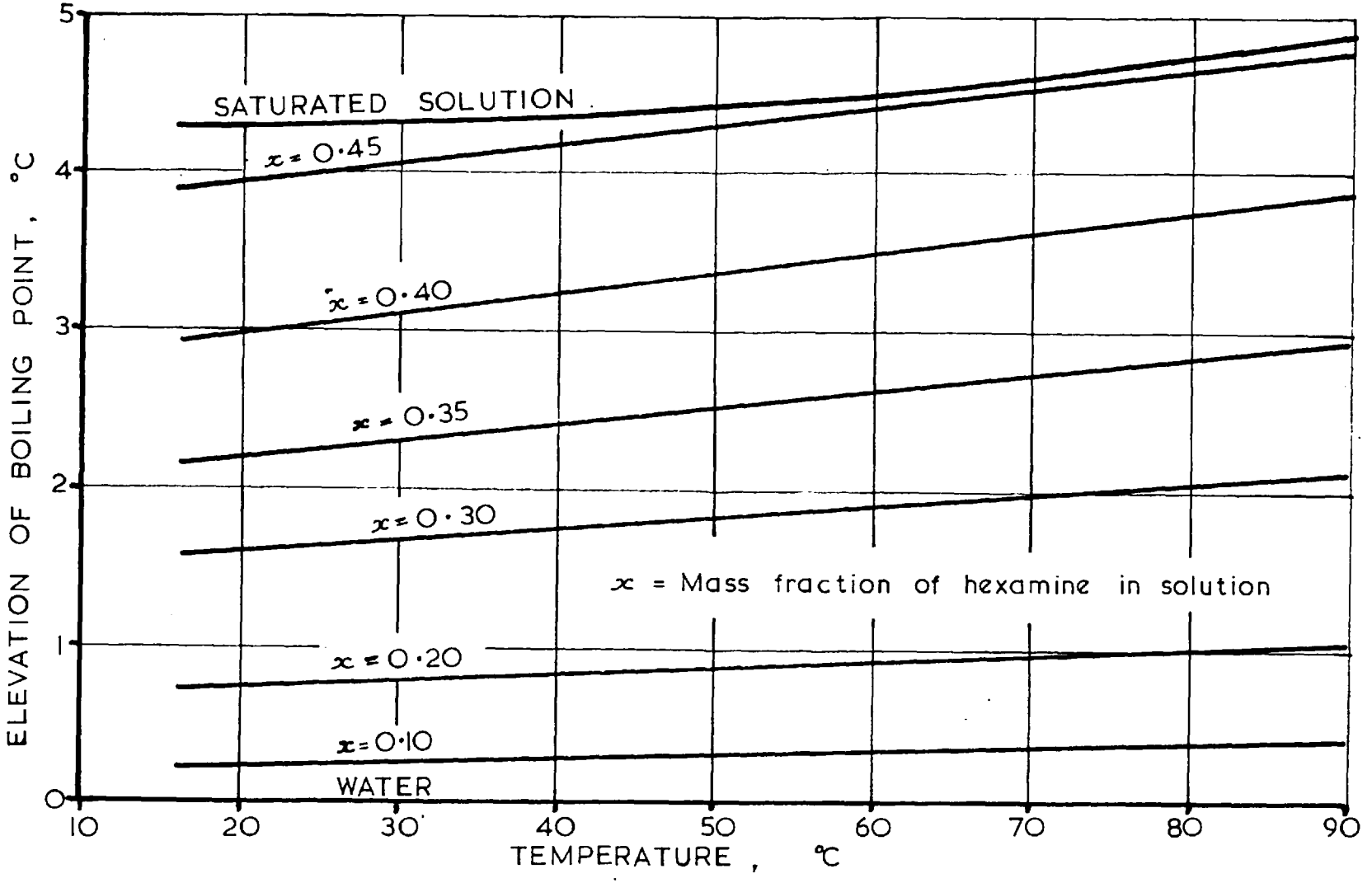

FIG. S II-7. ELEVATION OF BOILING POINT FOR AQUEOUS HEXAMINE SOLUTIONS. (SMOOTHED DATA)

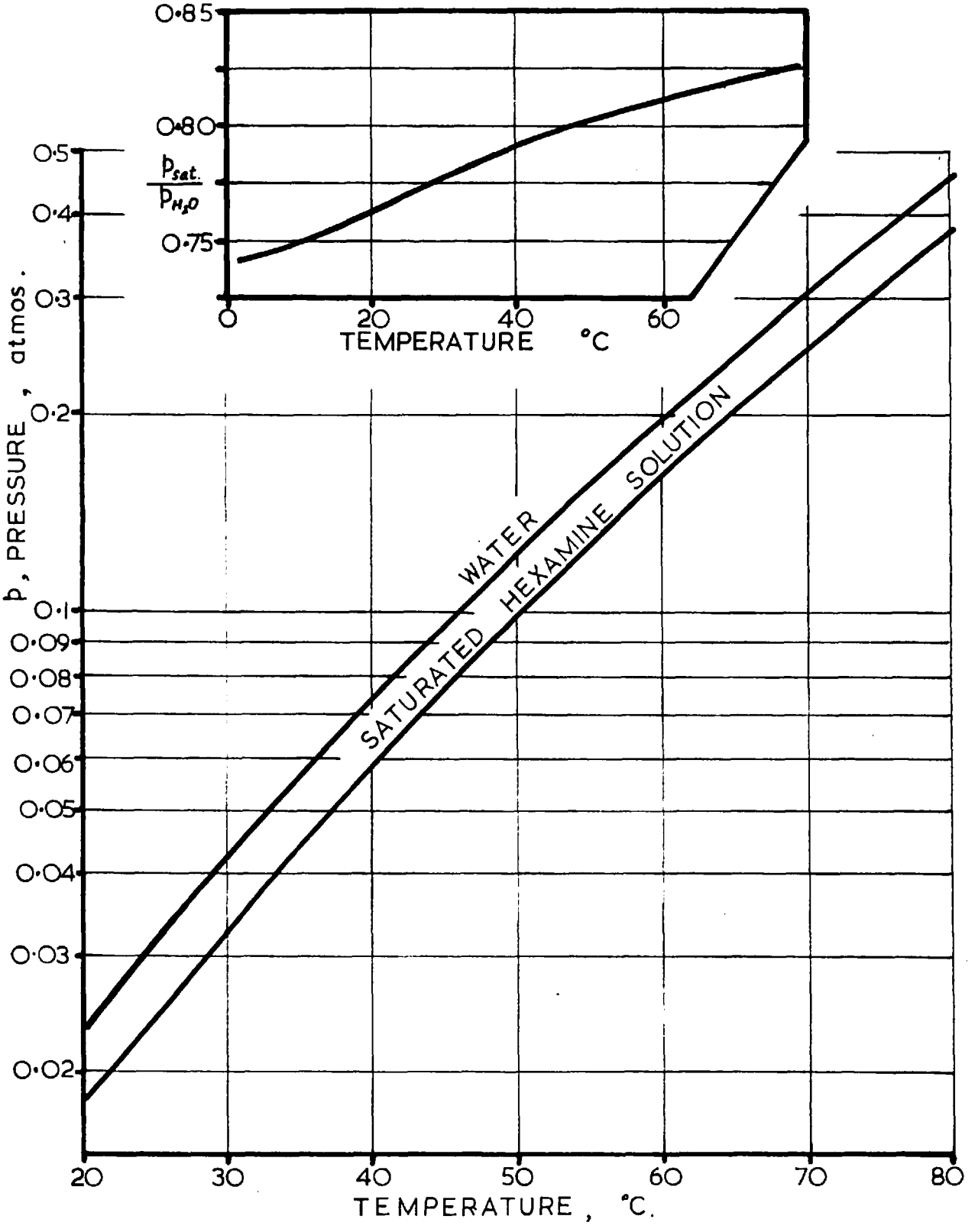

FIG. SII-8. BOILING POINT – TOTAL PRESSURE CURVE FOR SATURATED AQUEOUS HEXAMINE SOLUTIONS.

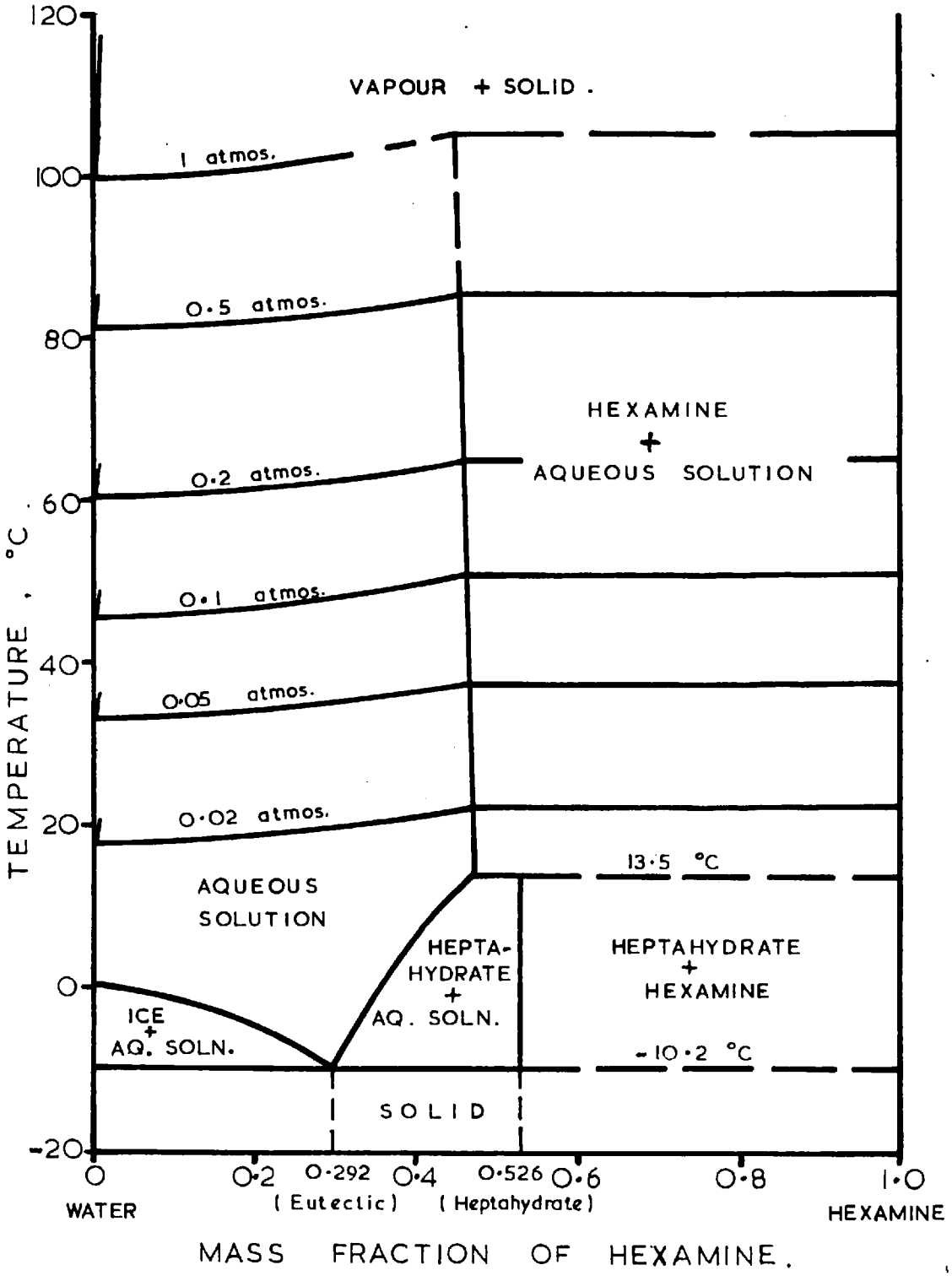

FIG. S II-9. PHASE DIAGRAM, HEXAMINE – WATER.

(i) Refractive Index

Measurement of the refractive index of an aqueous hexamine solution is a very convenient method of evaluating its composition. An accuracy of $\pm$ 0.001 mass fraction units can be readily achieved.

Data at 25.0°C measured by the author are given in Table SII-7 and Figs. SII-10 and SII-11. Both the refraction angle as determined directly from the Abbe refractometer and the computed refractive indices are given. Experimental details are given elsewhere [101]. Published data [11, 100, 109-111] are given in Table SII-7 and Fig SII-11.

The refraction angle data may be correlated within $\pm$ 1.0 minutes by the relation

$$\theta = \theta_o + 965x + 354x^2$$

where θ represents the refraction angle of an aqueous solution of hexamine of mass fraction x. Alternatively the refractive index at 25.0°C relative to air, n_D, may be correlated within $\pm$ 0.0002 refractive index units by

$$n_D = n_{D_o} + 0.169x + 0.048x^2$$

Figures SII-12 and SII-13 show the test of these correlations to the experimental data. In a similar manner the data of Fialkov and Egerskaya [109] at 20°C may be correlated by

$$n_D = n_{D_o} + 0.171x + 0.048x^2$$

(ii) Density

Measurement of the density is another convenient means of determining the composition of an aqueous hexamine solution.

DATA OF AUTHOR : TEMPERATURE 25.00 ± 0.02°C.

CONCENTRATION † x	REFRACTION ANGLE ≠ $\theta - \theta_0$ (Minutes)	REFRACTIVE INDEX ϕ n_D
pure water (x = 0)	0.0	1.33250
0.1021	104.0	1.3505
0.1207	121.5	1.3535
0.1322	133.9	1.3556
0.1868	193.5	1.3658
0.1938	199.7	1.3669
0.1950	200.3	1.3670
0.2356	246.7	1.3749
0.2534	267.0	1.3784
0.2535	267.8	1.3785
0.2778	294.0	1.3830
0.3086	330.9	1.3892
0.3144	337.0	1.3902
0.3297	355.3	1.3932
0.3333	360.2	1.3941
0.3868	426.8	1.4052
0.3881	427.8	1.4054
0.3962	437.2	1.4070
0.4139	460.0	1.4108
0.4473	502.5	1.4178
0.4630	522.8	1.4212
0.4658 *	526.4	1.4218
0.4661 *	526.7	1.4218

† Concentration as mass fraction hexamine in solution Error ± 0.0002.

* Composition by chemical analysis. Error ± 0.0010

≠ Difference in refraction angle between solution and distilled water, Error in angle difference ± 1.0 minutes

ϕ Relative to dry air at 25.0 and atmospheric pressure; computed from charts provided with Abbe refractometer. Error in refractive index ± 0.0002.

TABLE SII - 7 REFRACTIVE INDEX DATA FOR AQUEOUS HEXAMINE SOLUTIONS.

MASS FRACTION HEXAMINE IN SOLUTION	REFRACTIVE INDEX $n_{\sim}$ †	REFERENCE
0.0100	1.3342	)
0.0200	1.3359	)
0.0299	1.3376	)
0.0398	1.3393	)
0.0496	1.3409	) Evrard
		) [10]
		)
0.0594	1.3426	)
0.0692	1.3443	) 25°C.
0.0789	1.3461	)
0.0886	1.3478	)
0.0982	1.3495	)
0.0444	1.3406	)
0.0562	1.3424	) Le Fèvre &
0.0710	1.3450	) Rayner
0.0819	1.3469	) [11]
		) 25°C.
0.0100	1.3347	)
0.0201	1.3365	)
0.0298	1.3381	)
0.0395	1.3398	)
0.0496	1.3416	)
		)
0.0690	1.3450	) Fialkov &
0.0882	1.3484	) Egerskaya
0.0975	1.3501	) [10]
0.1076	1.3519	)
0.1465	1.3591	) 20°C.
		)
0.1938	1.3679	)
0.2391	1.3766	)
0.2845	1.3857	)
0.4014	1.4093	)
Saturated.	1.4242	Mosebach [11]

† Based on values for water [10],
$n_D^{25} = 1.33250$, $n_D^{20} = 1.33299$.

TABLE SII - 8. PUBLISHED REFRACTIVE INDICES FOR AQUEOUS HEXAMINE SOLUTIONS.

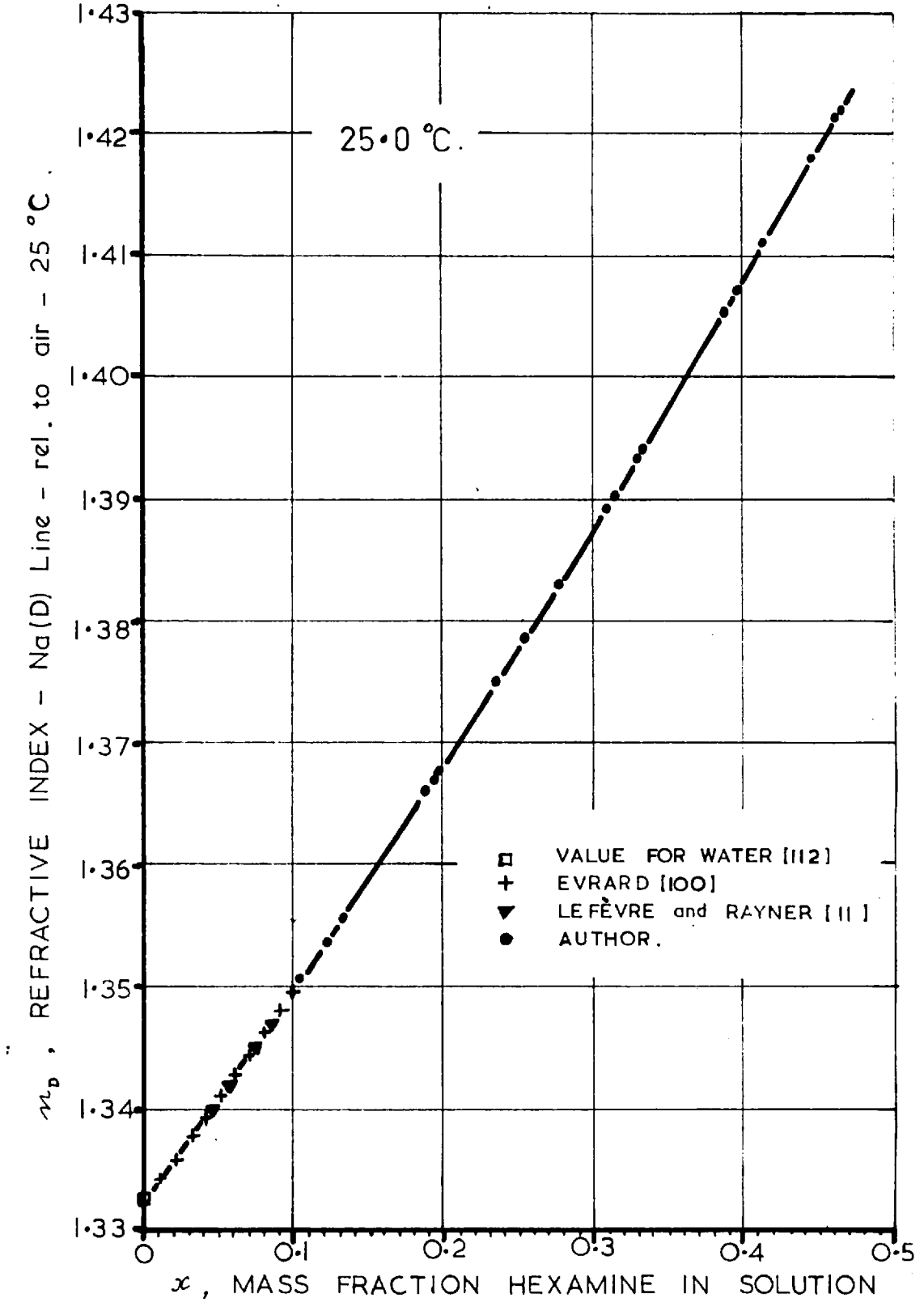

FIG. S II-10. REFRACTIVE INDICES OF AQUEOUS HEXAMINE SOLUTIONS AT 25·0 °C.

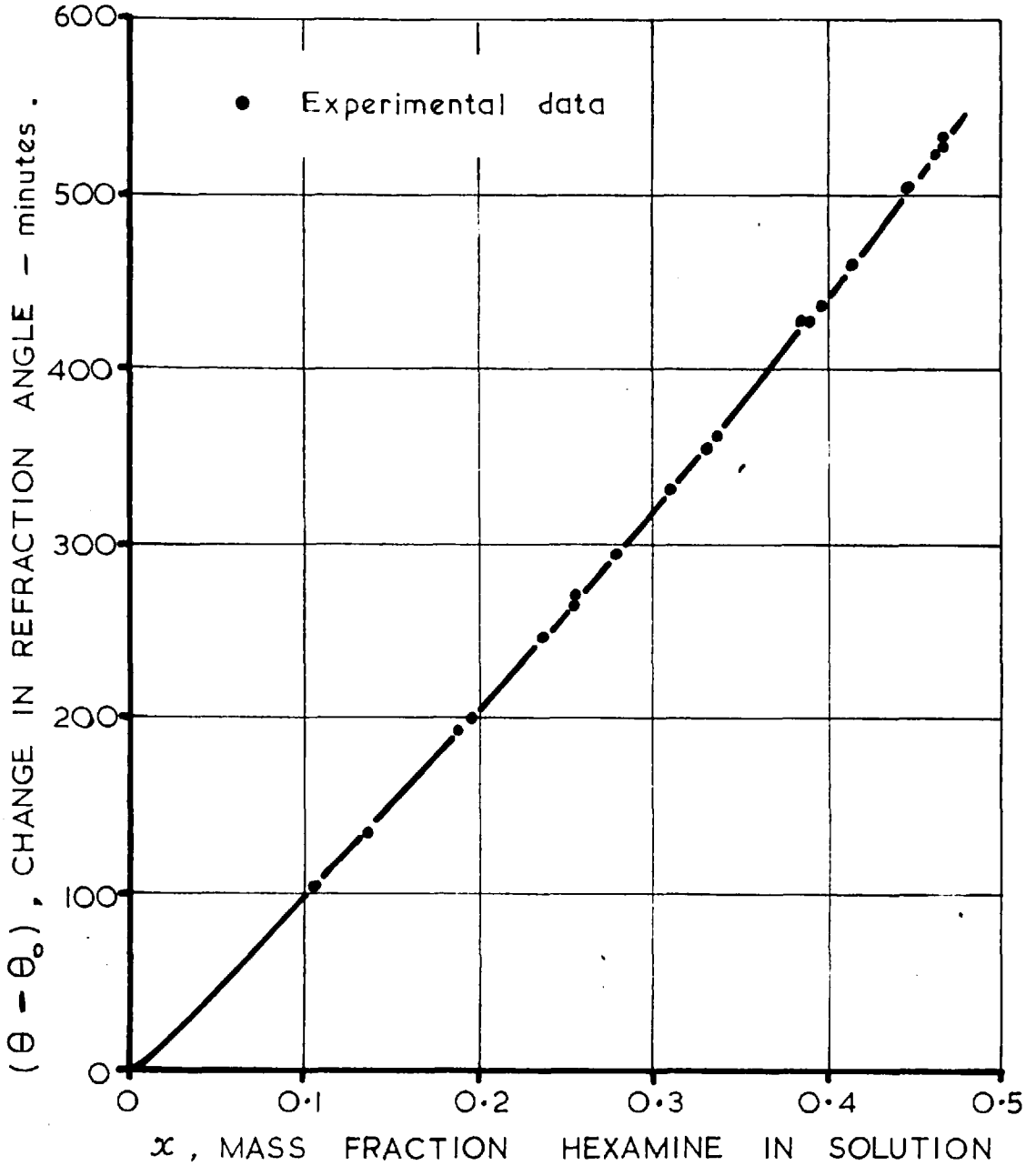

FIG. SII-11. REFRACTION ANGLE FOR AQUEOUS HEXAMINE SOLUTIONS AT 25·0 °C.

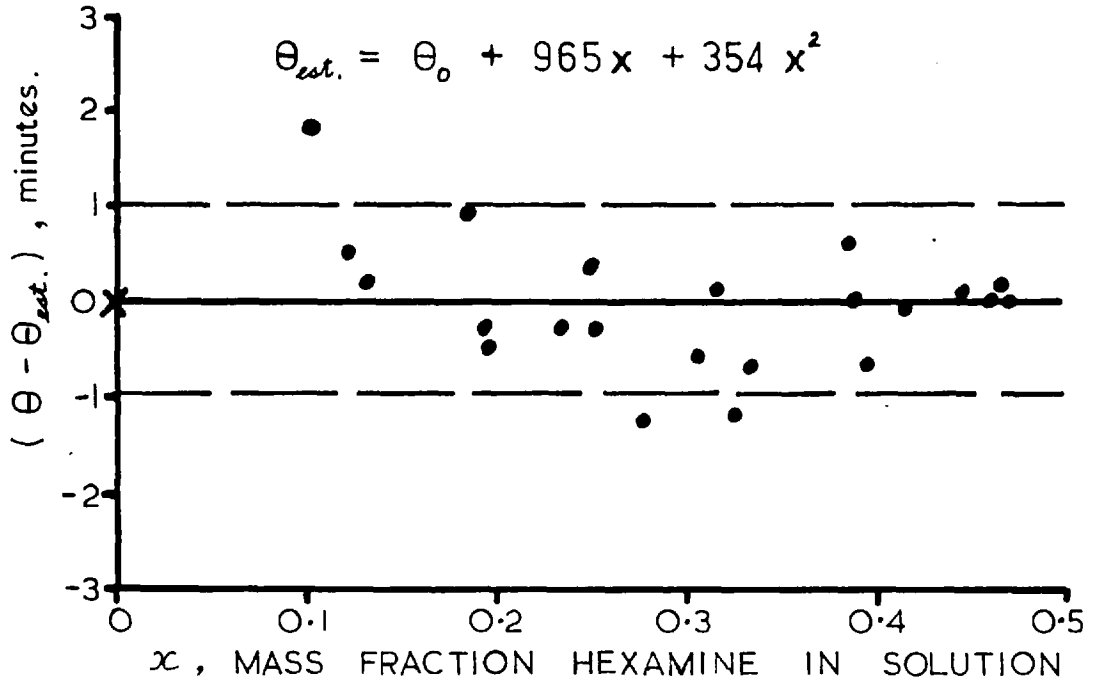

FIG. S II-12. TEST OF CORRELATION OF REFRACTION ANGLE DATA FOR AQUEOUS HEXAMINE SOLUTIONS AT 25·0 °C.

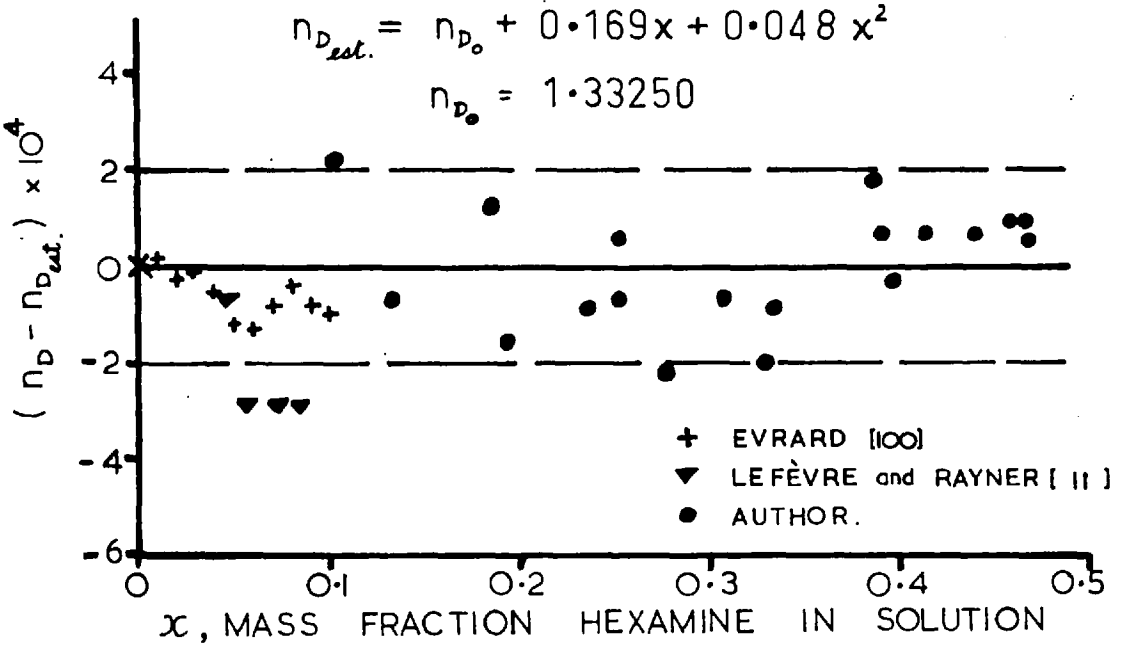

FIG. SII-13. TEST OF CORRELATION OF REFRACTIVE INDEX DATA FOR AQUEOUS HEXAMINE SOLUTIONS AT 25·0 °C.

Data at 25.0°C measured by the author and published data [113, 114] are given in Table SII-9 and Fig SII-14. Most of the experimental data may be correlated within ± 0.0001 g/ml by

$$\rho = \rho_o + 0.2135x + 0.066x^2$$

where ρ_o is the density at 25.0°C of an aqueous hexamine solution of hexamine mass fraction x. Figure SII-15 shows the test of this correlation to the experimental data.

Densities at temperatures other than 25.0°C are given in Table SII-10 and Fig . SII-16 and SII-17.

(iii) Viscosity

Viscosities of aqueous hexamine solutions at various temperatures are given in Table SII-11 and Fig. SII-18. Experimental details are given elsewhere [101]. Smoothed and interpolated viscosity values are given in Fig. SII-19. Viscosities of saturated hexamine solutions are five to ten times that of water.

(iv) Surface Tension

Surface tensions of aqueous hexamine solutions in contact with air at room temperature were measured by a capillary tube method [101]. These values and the published data of Huang et. al. [113] are given in Table SII-12 and Fig. SII-20. The variation of surface tension with composition is quite small.

(v) Diffusion Coefficient

Diffusion coefficients for hexamine in aqueous solution are given in Table SII-13. Values for dilute solutions at other temperatures may be predicted by the Stoke-Einstein relation.

TEMPERATURE: 25.00°C ± 0.02°C.

CONCENTRATION x †	DENSITY g./ml.	PROBABLE ERROR IN DENSITY g./ml.
Water (x=0)	0.99707 ℘	-
0.1021	1.01965	)
0.1668	1.03922	)
0.2535	1.05537	) ± 0.00005
0.3868	1.08935	)
0.4661 ≠	1.11050	)
0.1322	1.0264	)
0.1938	1.0408	)
0.3086	1.0692	) ± 0.0001
0.3962	1.0919	)
0.4473	1.1054	)
0.1208	1.02372	)
0.1950	1.04107	) ± 0.00005
0.3144	1.07058	)
* 0.1721	1.0353	
* 0.2559	1.0557	

† Concentration as mass fraction of hexamine in solution. Solutions prepared by weight with recrystallized hexamine and distilled water; corrected for included moisture. Error in concentration ± 0.0002.

≠ Composition by chemical analysis. Error ± 0.0010.

℘ Value from Perry [103] p.175.

* Data of Huang et. al. [113]

TABLE SII - 9. DENSITY OF HEXAMINE SOLUTIONS AT 25.0°C.

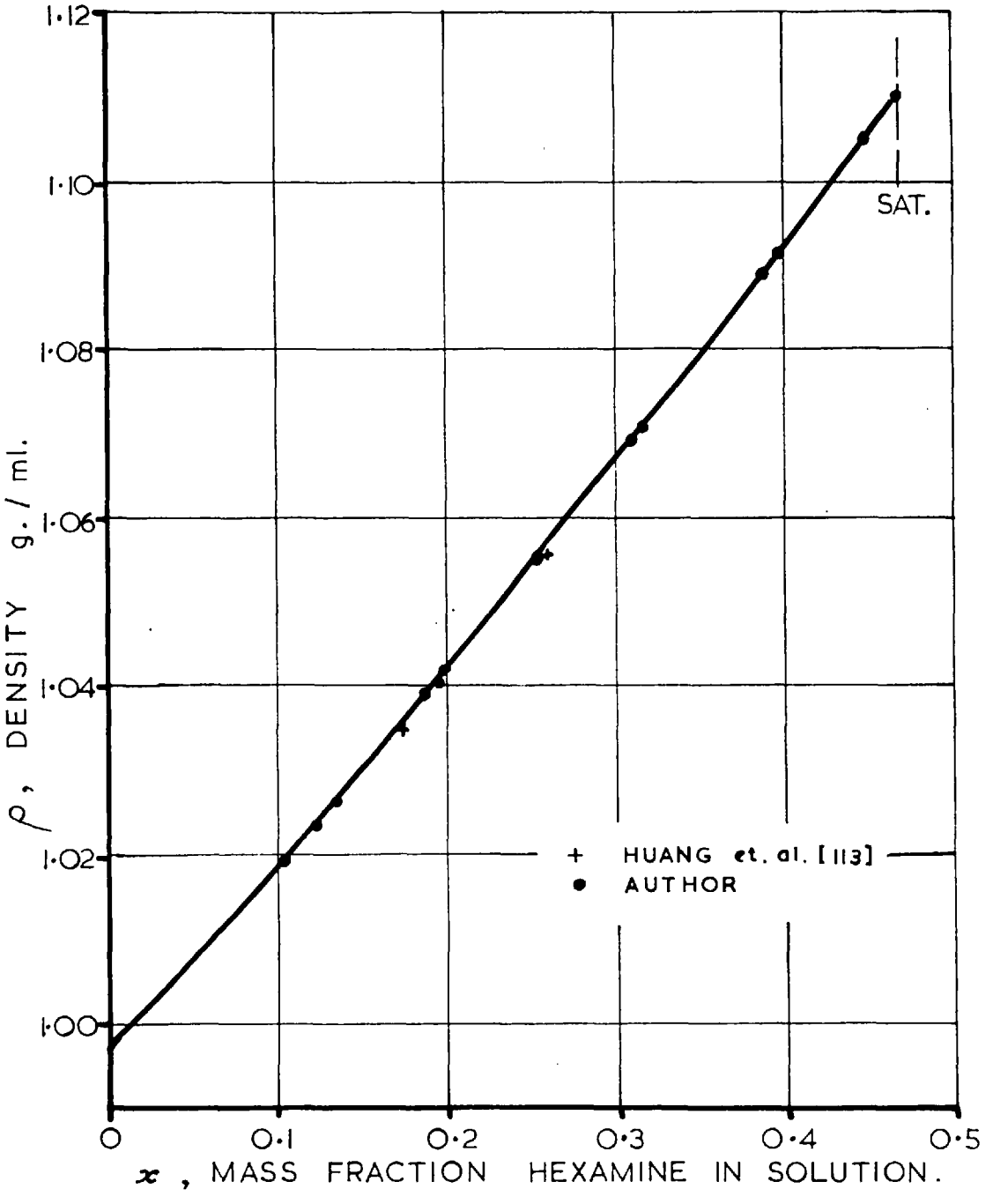

FIG. S II-14. DENSITIES OF AQUEOUS HEXAMINE SOLUTIONS AT 25·0 °C.

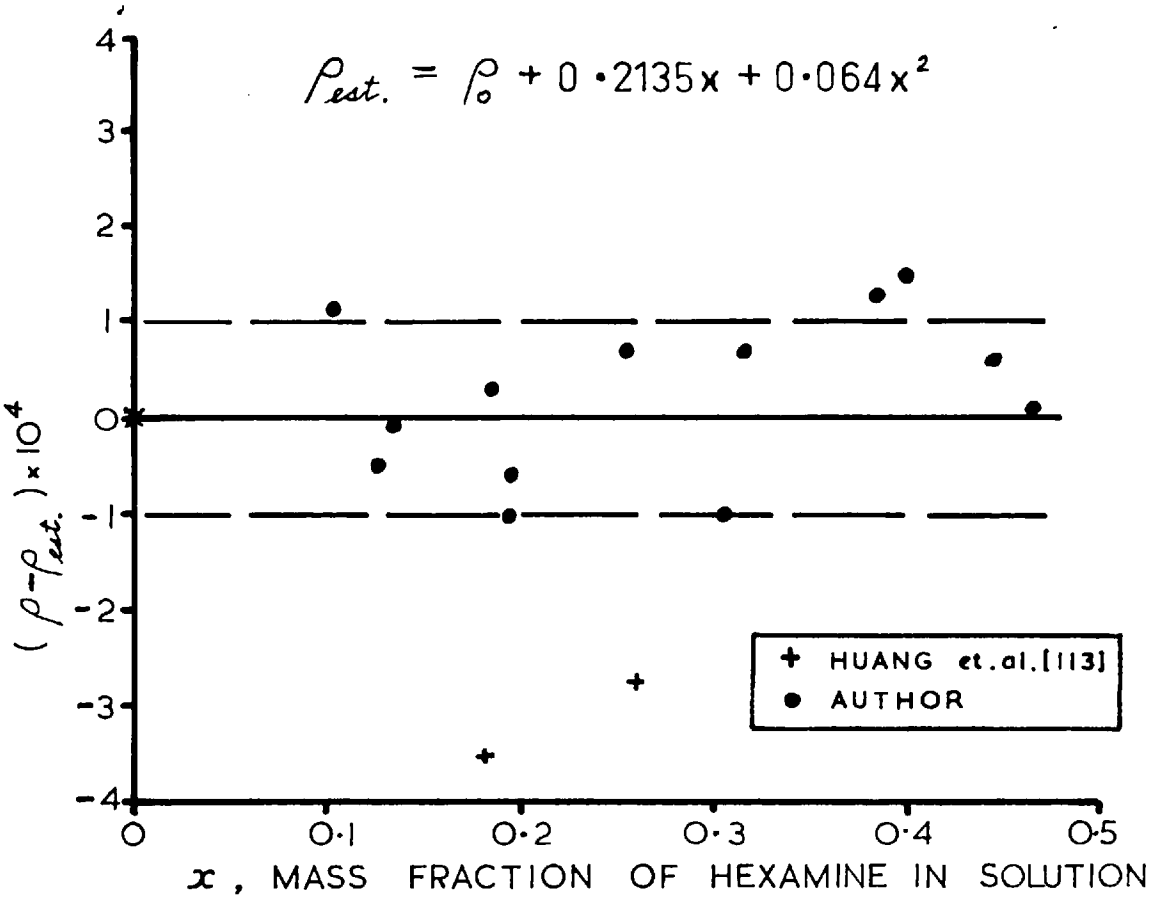

FIG. S II-15. TEST OF CORRELATION FOR DENSITIES OF AQUEOUS HEXAMINE SOLUTIONS AT 25·0 °C.

TEMPERATURE °C.	MASS FRACTION HEXAMINE	DENSITY g./ml.	REFERENCE
20.0 ± 0.1	0.1900	1.0422	)
20.0 ± 0.1	0.2125	1.0482	) Huang et.al.
35.0 ± 0.1	0.0603	1.0070	)
35.0 ± 0.1	0.1455	1.0261	) [113]
45.0 ± 0.1	0.0983	1.0115	)
45.0 ± 0.1	0.1919	1.0324	)
18°C	0.0444	1.00825	)
18°C	0.0562	1.01081	) Le Fèvre &
18°C	0.0710	1.01405	) Rayner [11]
18°C	0.0819	1.01652	)
room	satd.	1.0985	Utz [104]

Data of author.

TEMPERATURE °C.	DENSITY OF SOLUTION g/ml ≠				
	x† = 0.1322	0.1938	0.3086	0.3962	0.4473
10.0 ± 0.2	1.0297	1.0447	1.0744	1.0979	1.1126
15.0 ± 0.2	1.0288	1.0436	1.0728	1.0960	1.1103
20.0 ± 0.1	1.0277	1.0423	1.0711	1.0940	1.1079
30.0 ± 0.1	1.0249	1.0391	1.0672	1.0897	1.1029
35.0 ± 0.1	1.0232	1.0372	1.0651	1.0874	1.1003
40.0 ± 0.1	-	1.0352	1.0629	1.0849	1.0976
45.0 ± 0.1	-	-	1.0606	1.0823	1.0949
52.5 ± 0.2	-	-	-	1.0780	1.0906

† Composition of solution as mass fraction of hexamine. Probable error in composition ± 0.0005.

≠ Error in density ± 0.0002 g./ml.

TABLE SII - 1C. DENSITIES OF HEXAMINE SOLUTION AT TEMPERATURES OTHER THAN 25°C.

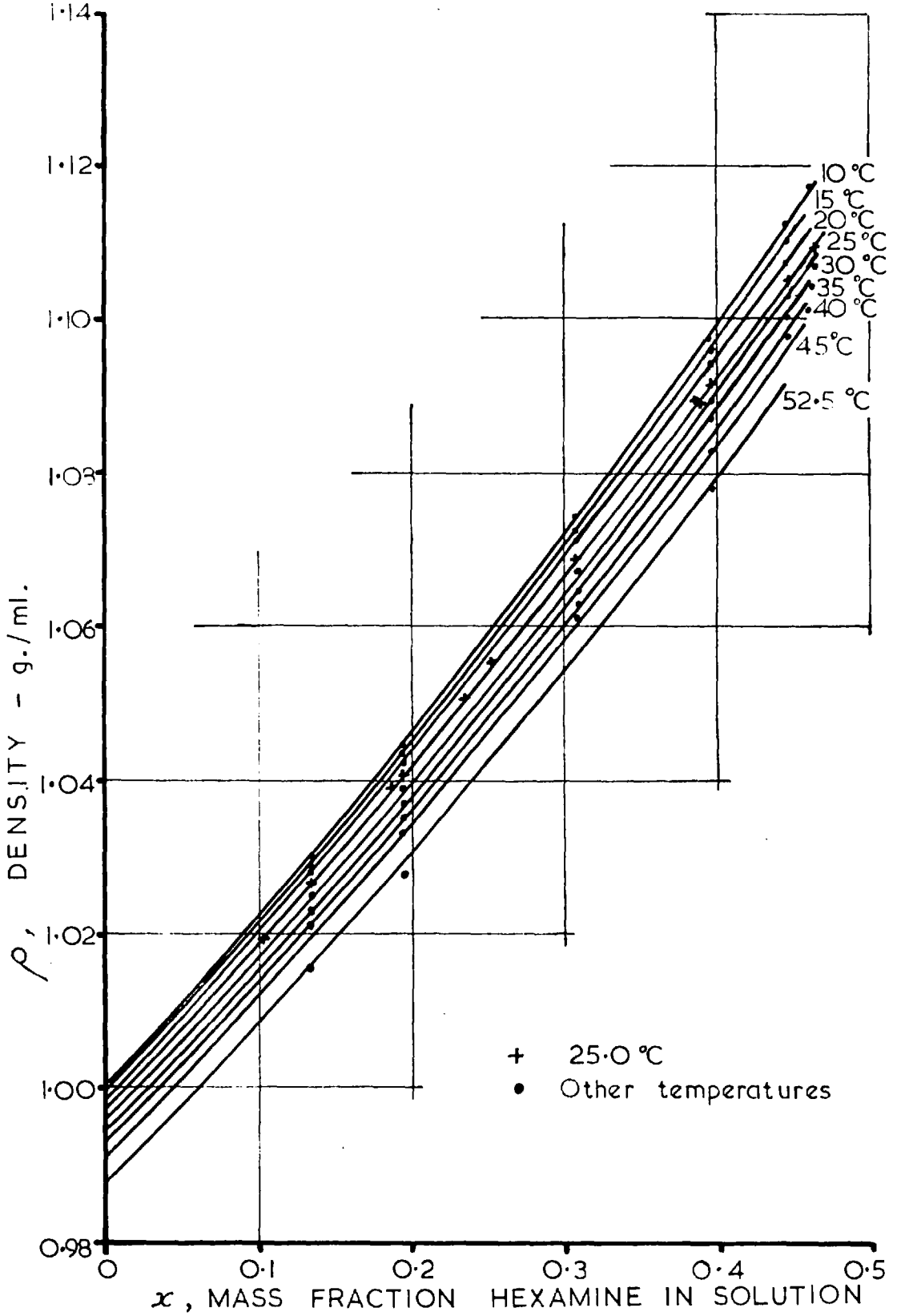

FIG. SII-16. DENSITIES OF AQUEOUS HEXAMINE SOLUTIONS.

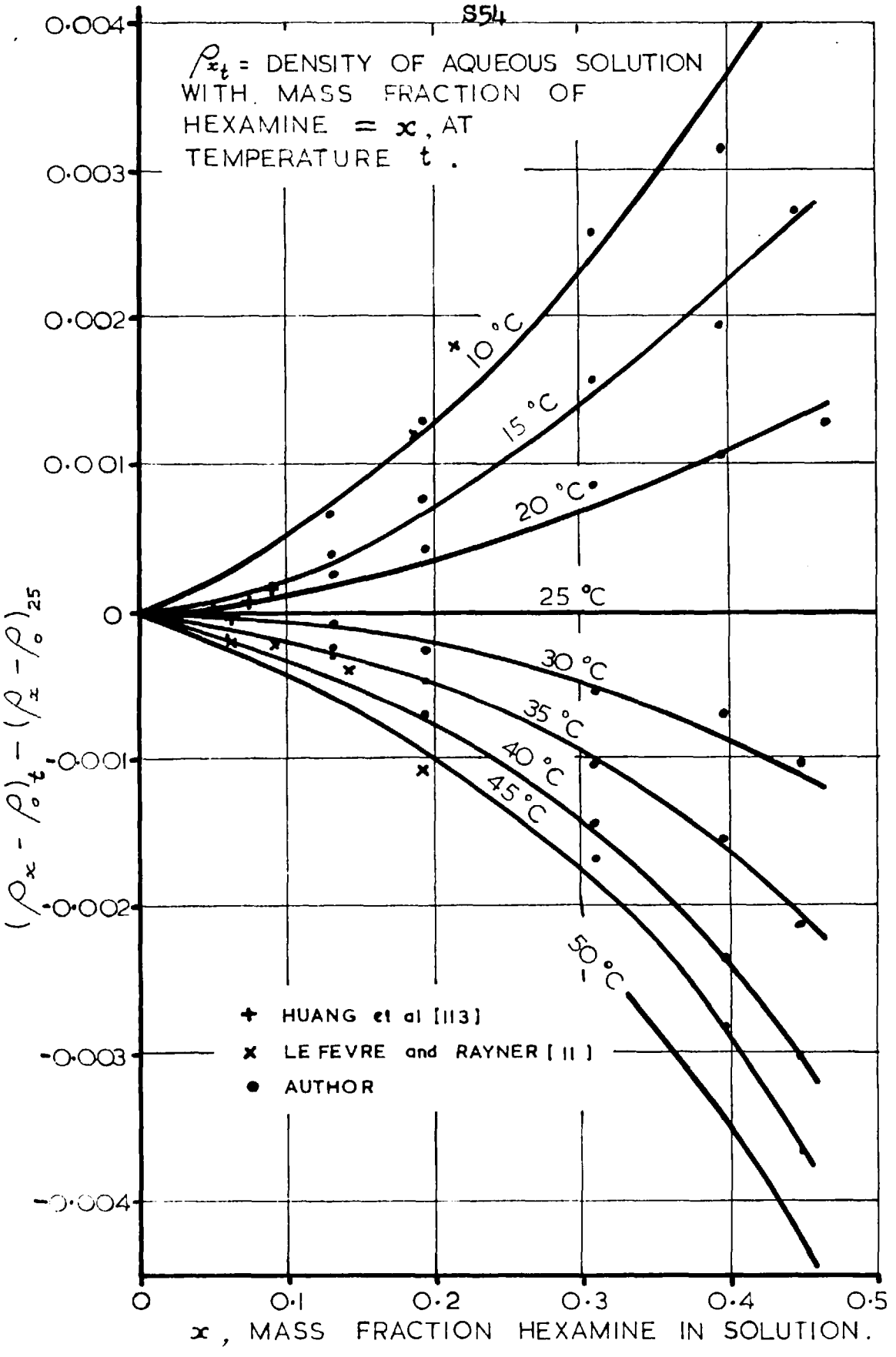

FIG. S II-17. DENSITIES OF AQUEOUS HEXAMINE SOLUTIONS 10 to 50 °C.

MASS FRACTION HEXAMINE IN SOLUTION † x = 0.134								
TEMPERATURE,≠°C	8.2	18.6	25.4	31.1	36.0	40.6	45.5	49.8
VISCOSITY cp*	2.23	1.613	1.356	1.186	1.087	0.959	0.871	0.809

MASS FRACTION HEXAMINE IN SOLUTION x = 0.236								
TEMPERATURE,°C	19.3	25.2	30.6	35.5	40.8	45.8	49.6	59.8
VISCOSITY cp.	2.36	1.993	1.719	1.522	1.366	1.223	1.120	0.925

MASS FRACTION HEXAMINE IN SOLUTION x = 0.282								
TEMPERATURE,°C	8.2	18.6	25.4	31.1	36.0	40.6	45.5	49.8
VISCOSITY,cp	4.14	2.94	2.38	2.04	1.795	1.606	1.436	1.306

MASS FRACTION HEXAMINE IN SOLUTION x = 0.388										
TEMPERATURE,°C	7.1	15.2	19.3	25.2	30.6	35.5	40.8	45.8	49.6	59.8
VISCOSITY,cp	8.39	5.67	4.95	4.05	3.42	2.96	2.54	2.23	2.04	1.625

MASS FRACTION HEXAMINE IN SOLUTION x = 0.460								
TEMPERATURE,°C	9.3	15.4	19.4	25.0	30.2	35.9	40.5	47.1
VISCOSITY,cp	11.62	9.05	7.91	6.25	5.18	4.35	3.77	3.11

SATURATED SOLUTION					
TEMPERATURE,°C	10.0	25.0	30.0	35.0	40.0
VISCOSITY,cp	12.82	6.36	5.39	4.47	3.80

† Error in composition ± 0.001

≠ Error in temperature ± 0.1 °C.

* Error in viscosity ± ½%.

TABLE SII - 11, VISCOSITIES OF AQUEOUS HEXAMINE SOLUTIONS.

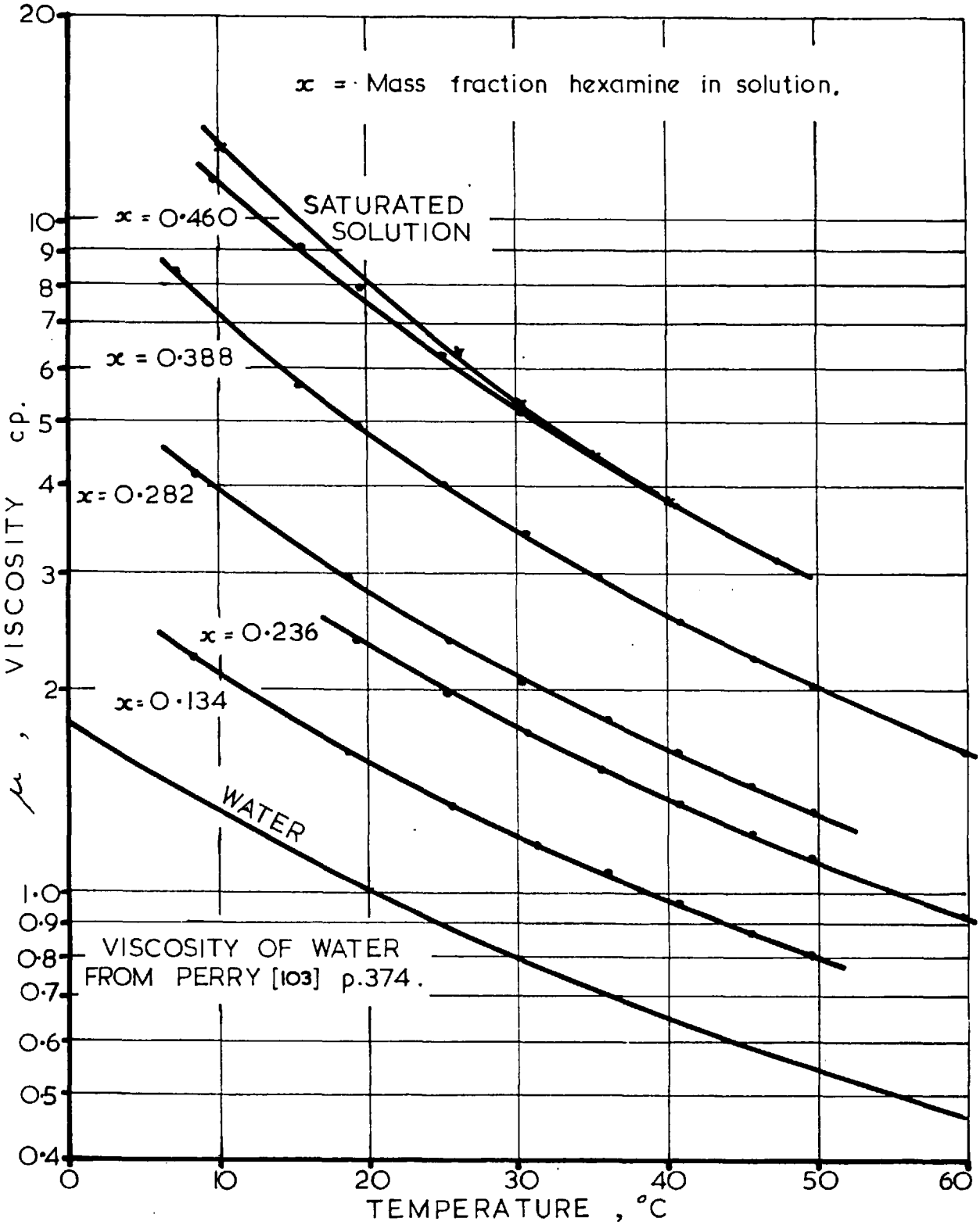

FIG. SII-18. VISCOSITIES OF AQUEOUS HEXAMINE SOLUTIONS — MEASURED VALUES.

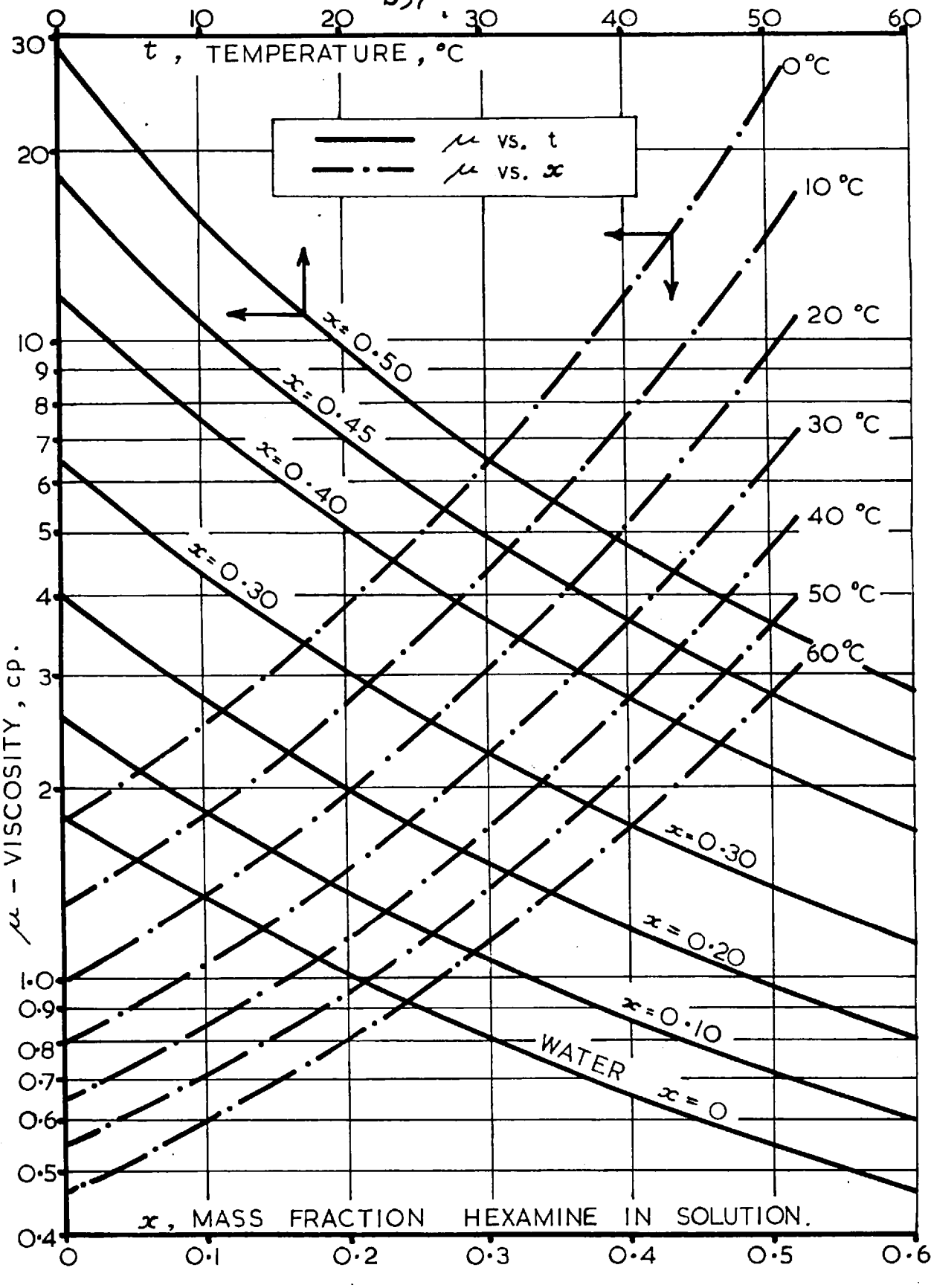

FIG. SII-19. VISCOSITIES OF AQUEOUS HEXAMINE SOLUTIONS — SMOOTHED AND EXTRAPOLATED DATA.

Pure water : International Critical Tables [115]	
TEMPERATURE, °C.	SURFACE TENSION ϕ dynes/cm.
18.0	73.05
20.0	72.75
25.0	71.97
35.0	70.38
45.0	68.74

ϕ ± 0.05.

Huang et. al. [113]		
TEMP. †, °C.	x ≠	SURFACE TENSION dynes/cm.
20.0	0.1900	72.19
20.0	0.2125	72.11
25.0	0.1721	71.22
25.0	0.2559	70.77
35.0	0.0603	70.07
35.0	0.1455	69.98
45.0	0.0983	68.40
45.0	0.1919	67.97

TEMP. †, °C.	x ≠	SURFACE TENSION* dynes/cm.
18.0	0.131	72.2
18.3	0.254	71.6
18.1	0.334	70.7
18.0	0.369	70.3
18.4	0.460	68.8

† Error ± 0.1 °C.

≠ Composition of solution as mass fraction hexamine. Authors data, error ± 0.001.

* Error ± 0.2 dynes/cm.

TABLE SII - 12 : SURFACE TENSIONS OF AQUEOUS HEXAMINE SOLUTIONS.

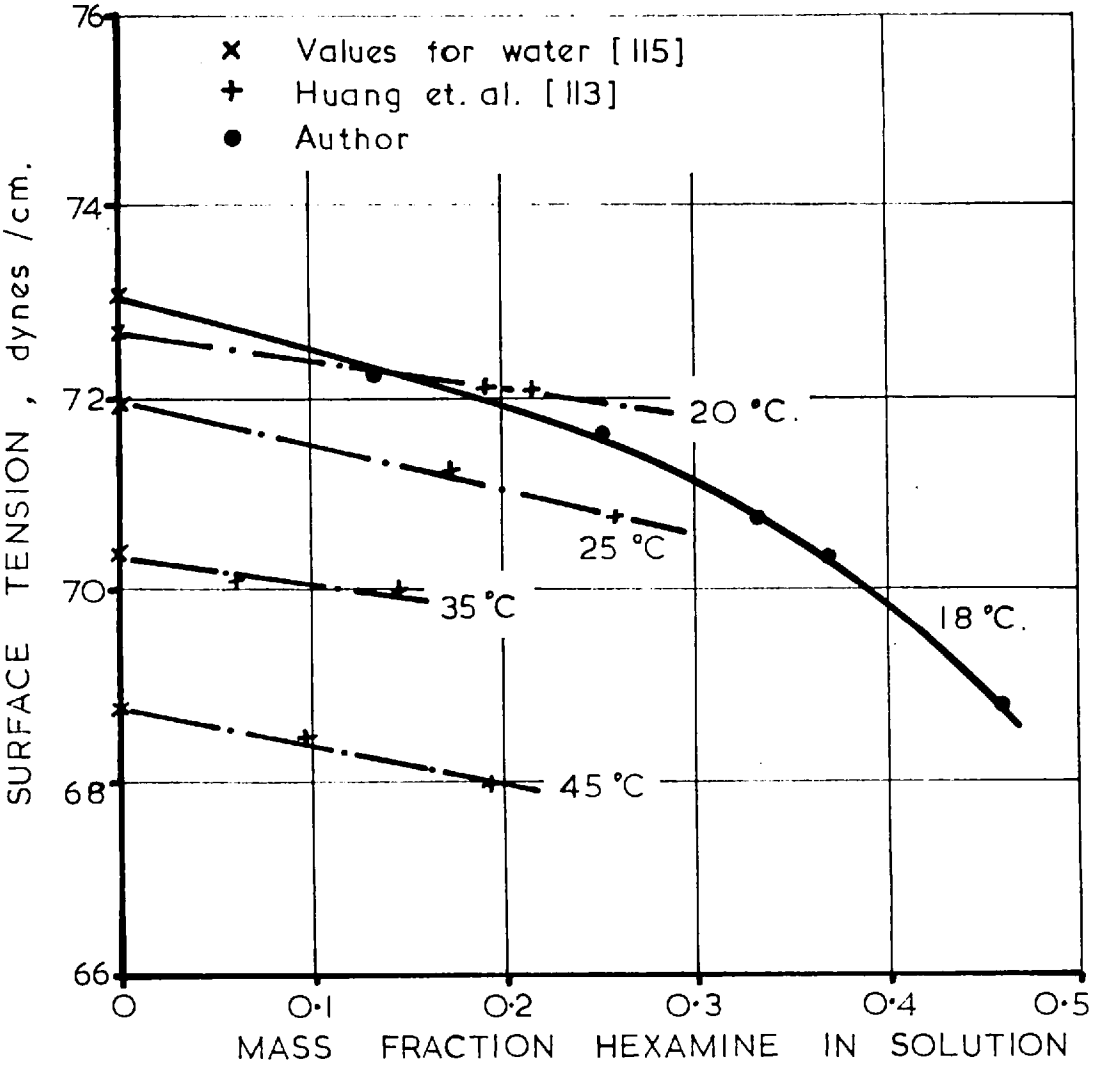

FIG. S II-20. SURFACE TENSIONS OF AQUEOUS HEXAMINE SOLUTIONS.

Temp. °C.	Mean concn.*	$D \times 10^6$ cm²/sec.	Reference
21	0.04	6	I.C.T. /1157
(	0.0025	8.99	)
(	0.005	9.34	)
18(	0.01	8.92	)Sullman
(	0.04	7.97	) /1167
(	0.08	6.80	)

* as mass fraction of hexamine in solution.

TABLE SII - 13. DIFFUSION COEFFICIENTS FOR AQUEOUS HEXAMINE SOLUTIONS.

---

x = 0.211 †		x = 0.341		x = 0.436	
Temp. °C ℘	C ≠	Temp. °C.	C	Temp. °C	C
21.0	0.848	14.2	0.755	17.6	0.693
26.8	0.856	20.7	0.770	20.3	0.709
33.2	0.868	28.1	0.782	25.2	0.713
37.3	0.867	33.5	0.788	26.3	0.709
44.6	0.877	39.0	0.796	26.4	0.702
		45.4	0.801	30.6	0.729
				32.6	0.730
				38.1	0.732
				43.8	0.729
				71.8	0.78 *

† Mass fraction of hexamine in solution; Error ± 0.001

℘ Mean Temperature, Error ± 0.1° C.

≠ Mean heat capacity as cal/(g.) (°C.) Error ± 0.015 cal/(g) (°C.)

* Error ± 0.03 cal/(g) (°C.).

TABLE SII - 14 : HEAT CAPACITIES OF AQUEOUS HEXAMINE SOLUTIONS.

(vi) Conductivity

Hexamine solutions have a very low electrical conductivity [2, 105]. Hexamine in aqueous solution behaves as a very weak base (about the strength of aniline) having a pH in the range 8 to 8.5. Values of the dissociation constant have been reported [105, 117-120]. In water hexamine hydrolyses to a very slight extent to give formaldehyde and ammonia.

Conductivities of solutions of commercial hexamine in distilled water are shown in Fig. SII-21. These values cannot be considered to be in any way absolutely accurate, since the nature of the impurities in the hexamine greatly affects the measured conductivity. However the figure serves as an indication of the variation of conductivity with concentration and temperature.

SII-3 THERMAL PROPERTIES OF AQUEOUS HEXAMINE SOLUTIONS

(i) Heat Capacity

Heat capacities of aqueous hexamine solutions were determined by means of an electrically heated calorimeter [101]. The data obtained are presented in Table SII-14 and Fig. SII-22. Values for water are taken from Perry [103], p225.

The available heat capacity data may be correlated within ±0.015 cal/(g)(°C) by the relation

$$C = 1 - 0.77x + 0.004xt$$

where C is the heat capacity at constant pressure in cal/(g)(°C)

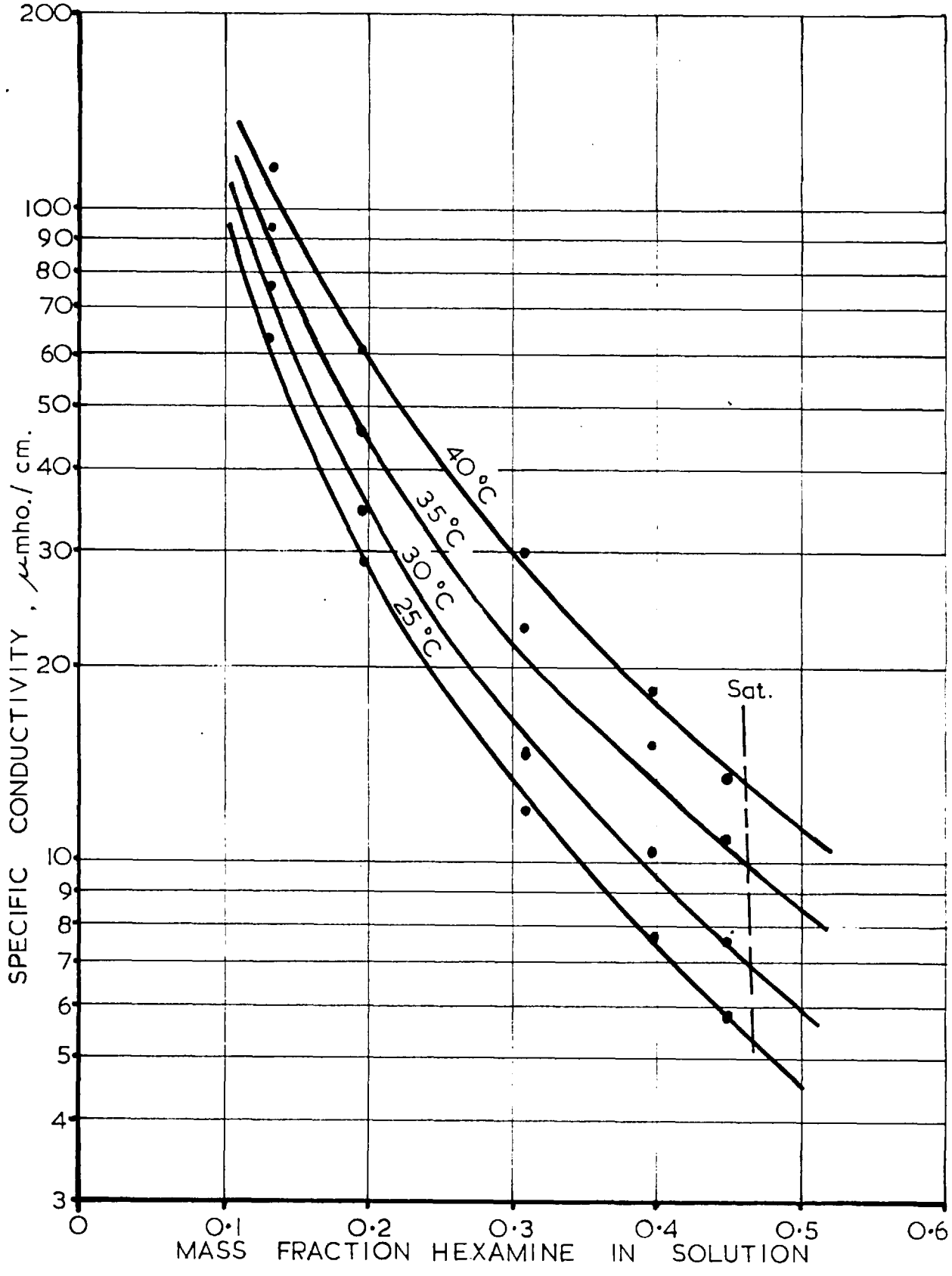

FIG. S II-21. CONDUCTIVITIES OF SOLUTIONS OF COMMERCIAL GRADE HEXAMINE IN DISTILLED WATER.

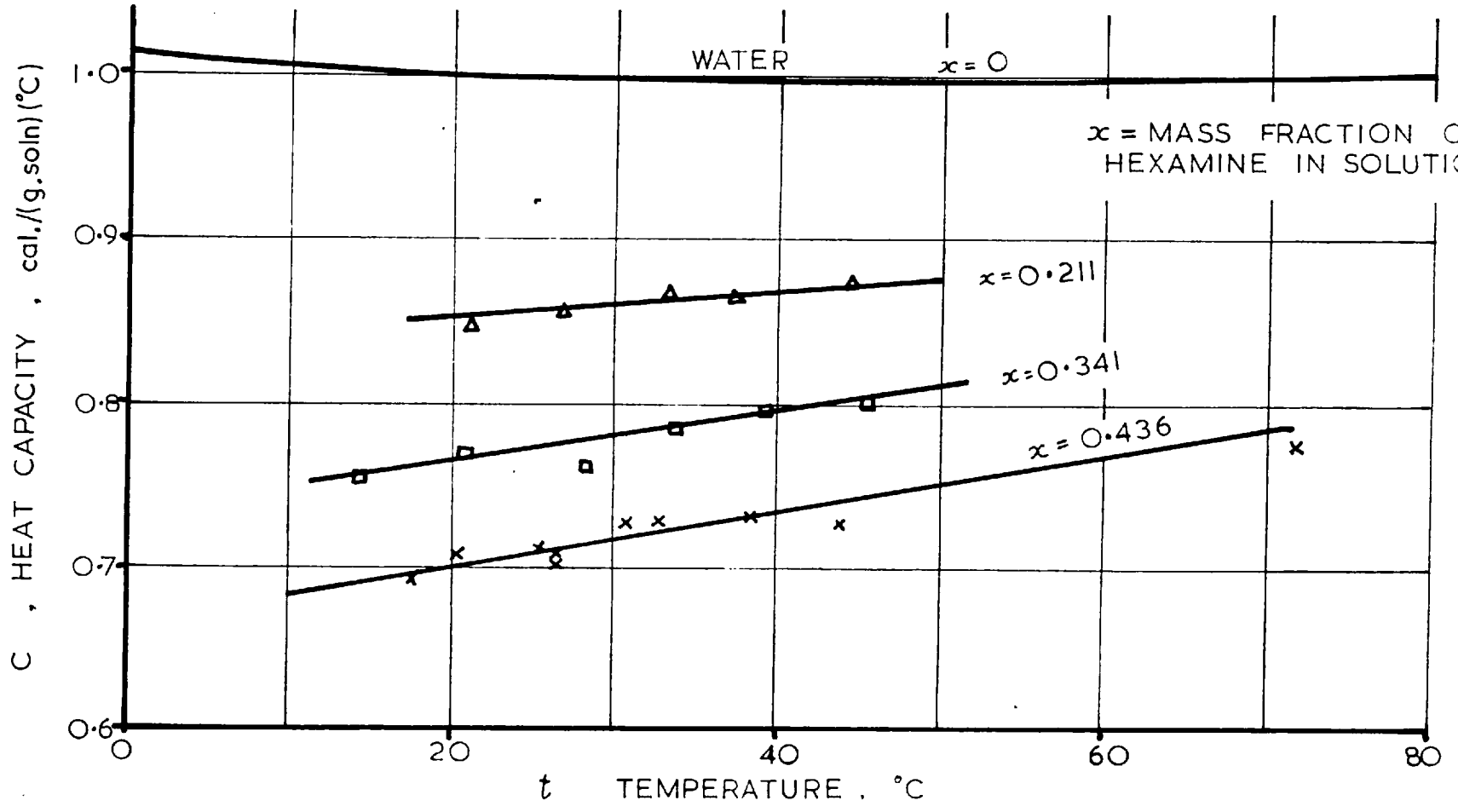

FIG. SII-22. HEAT CAPACITIES OF AQUEOUS HEXAMINE SOLUTIONS.

of an aqueous hexamine solution of mass fraction hexamine x, at a temperature t°C. The test of this correlation to the experimental data is shown in Fig. SII-23.

(ii) Heat of Solution

Hexamine dissolves readily in water with an appreciable evolution of heat. The adiabatic temperature rise on mixing crystalline hexamine and distilled water, both at 25.0°C was determined in a calorimeter [101]. The experimental values are given in Table SII-15 and Fig. SII-24. Using the heat capacity data given above integral heats of solution at 25.0°C were computed (Table SII-15 and Fig. SII-25). Published values for the heat of solution at infinite dilution [69, 99] are also given.

(iii) Enthalpy-Composition Chart

Using the phase and thermal data given above the enthalpy-composition chart for the hexamine-water system (Fig. SII-26) was prepared. The chart is for engineering use and is given in engineering units. Enthalpies are relative to a datum of zero enthalpy for liquid water at 32°F (the steam table datum), and an enthalpy of 100 Btu/lb chosen for solid hexamine at 77°F. The enthalpies of water were taken from steam tables.

The liquid region of the chart is shown to larger scale in Fig SII-27 and numerical values are given in Table SII-16. The data given is probably accurate to ± 2 Btu/lb.

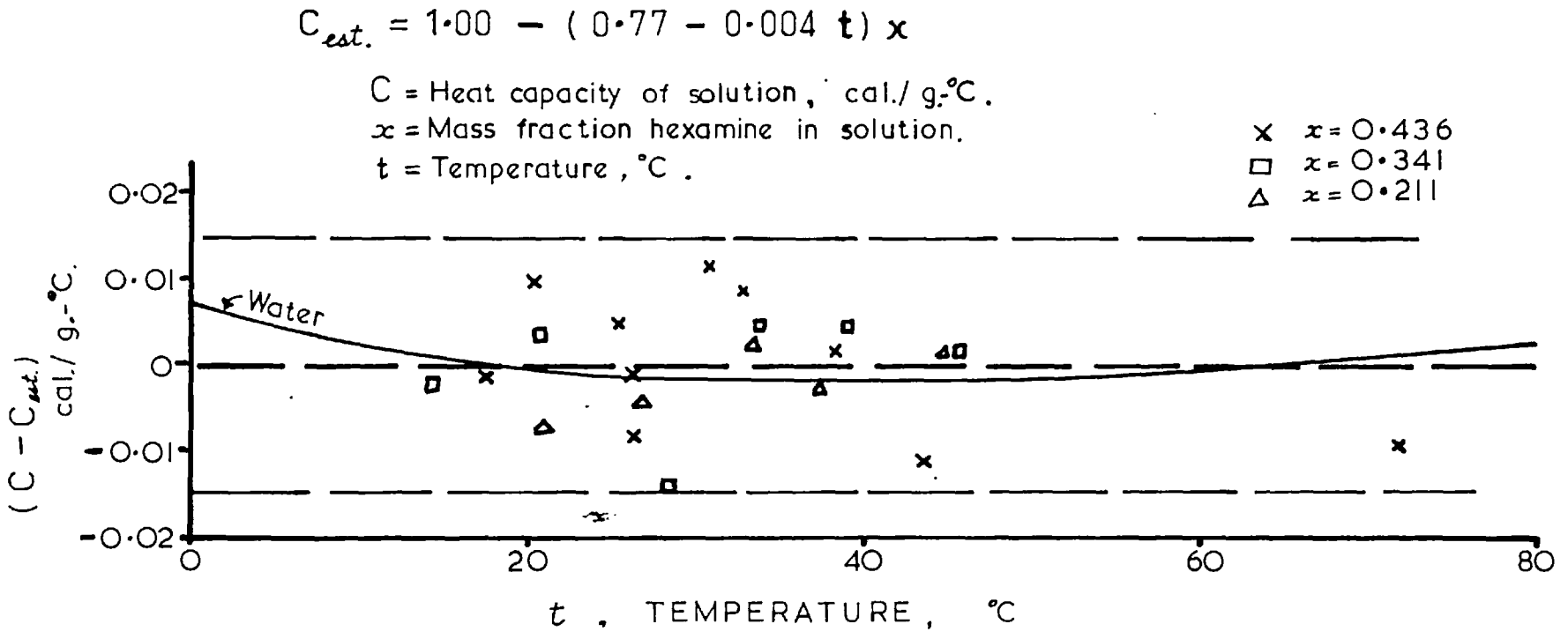

FIG. SII-23. TEST OF CORRELATION FOR HEAT CAPACITIES OF AQUEOUS HEXAMINE SOLUTIONS.

Composition of final solution. ℘	Adiabatic Temperature Rise on Solution in Water at 25°C, °C.	Integral Heat of Solution at 25.0°C $\Delta H_{s_{298}}$, K.cal/g. mole Hx.
infinite dilution	-	- 4.8 *
"	-	- 4.9 †
0.097	3.43 ± 0.15	- 4.6 ± 0.3
0.131	4.6 ± 0.5	- 4.5 ± 0.5
0.221	8.25 ± 0.15	- 4.41 ± 0.15
0.226	8.34 ± 0.15	- 4.38 ± 0.15
0.285	10.30 ± 0.15	- 4.12 ± 0.08
0.321	11.2 ± 0.5	- 3.85 ± 0.2
0.413	13.2 ± 0.5	- 3.30 ± 0.15
0.436	13.76 ± 0.15	- 3.19 ± 0.07

℘ As mass fraction hexamine in solution. Error ± 0.001.

* Value from I.C.T. /1157 p.150; data of Delépine /997

† Value from Harvey & Baekeland /697

TABLE SII - 15. HEAT OF SOLUTION OF HEXAMINE IN WATER AT 25.0°C.

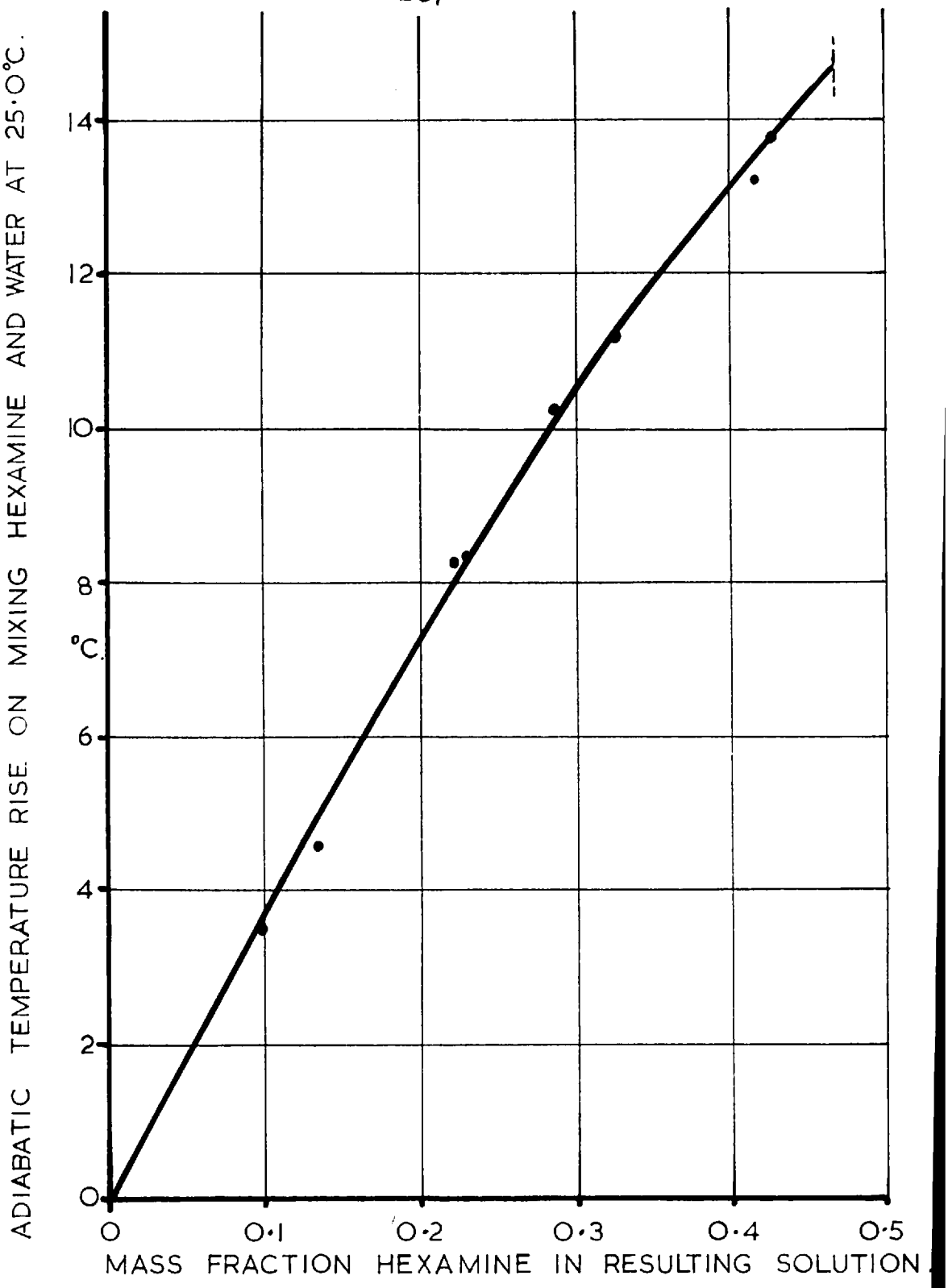

FIG. SII-24. ADIABATIC TEMPERATURE RISE ON SOLUTION OF HEXAMINE IN WATER AT 25·0 °C

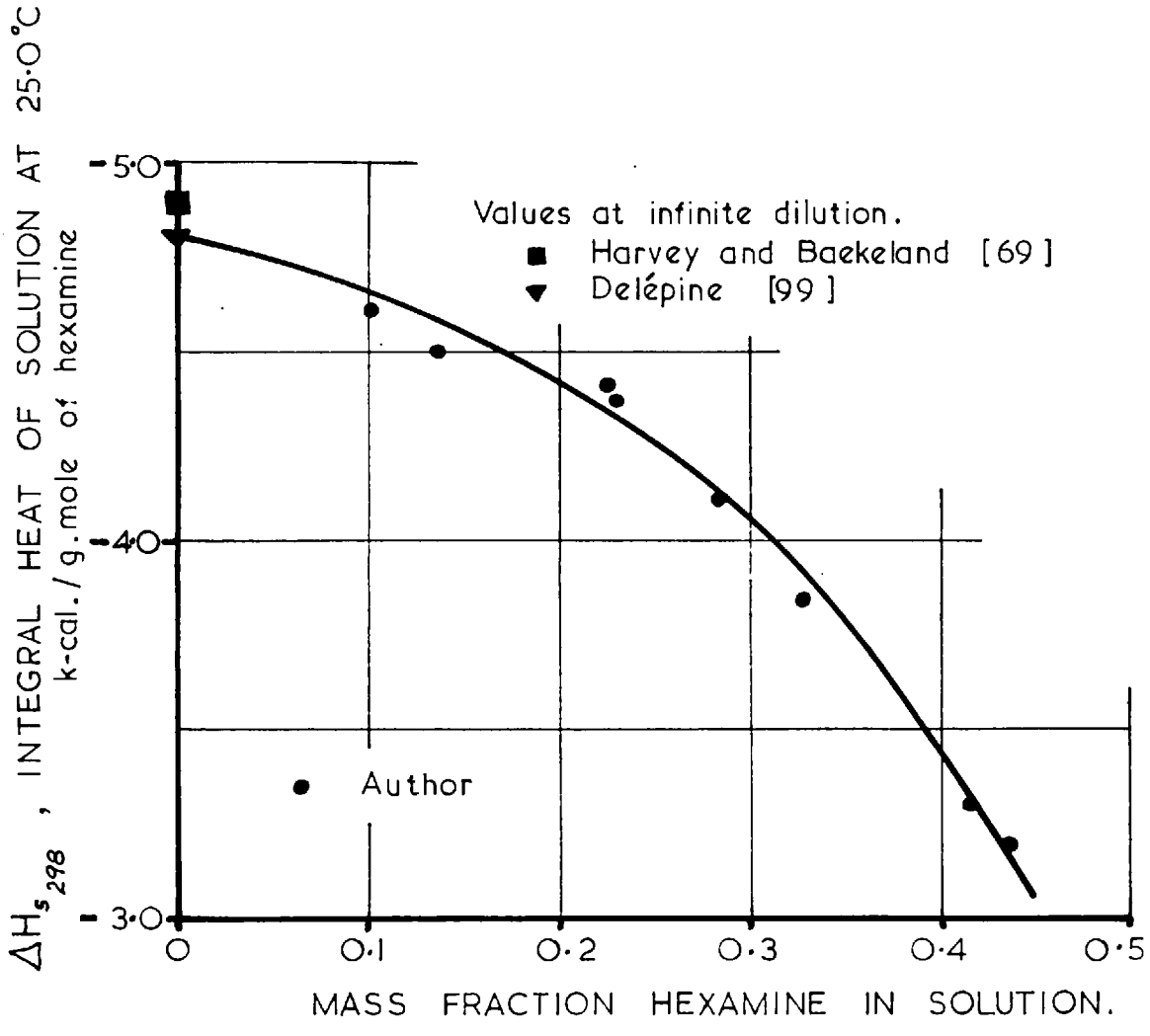

FIG. S II-25. INTEGRAL HEATS OF SOLUTION OF HEXAMINE IN WATER AT 25·0°C.

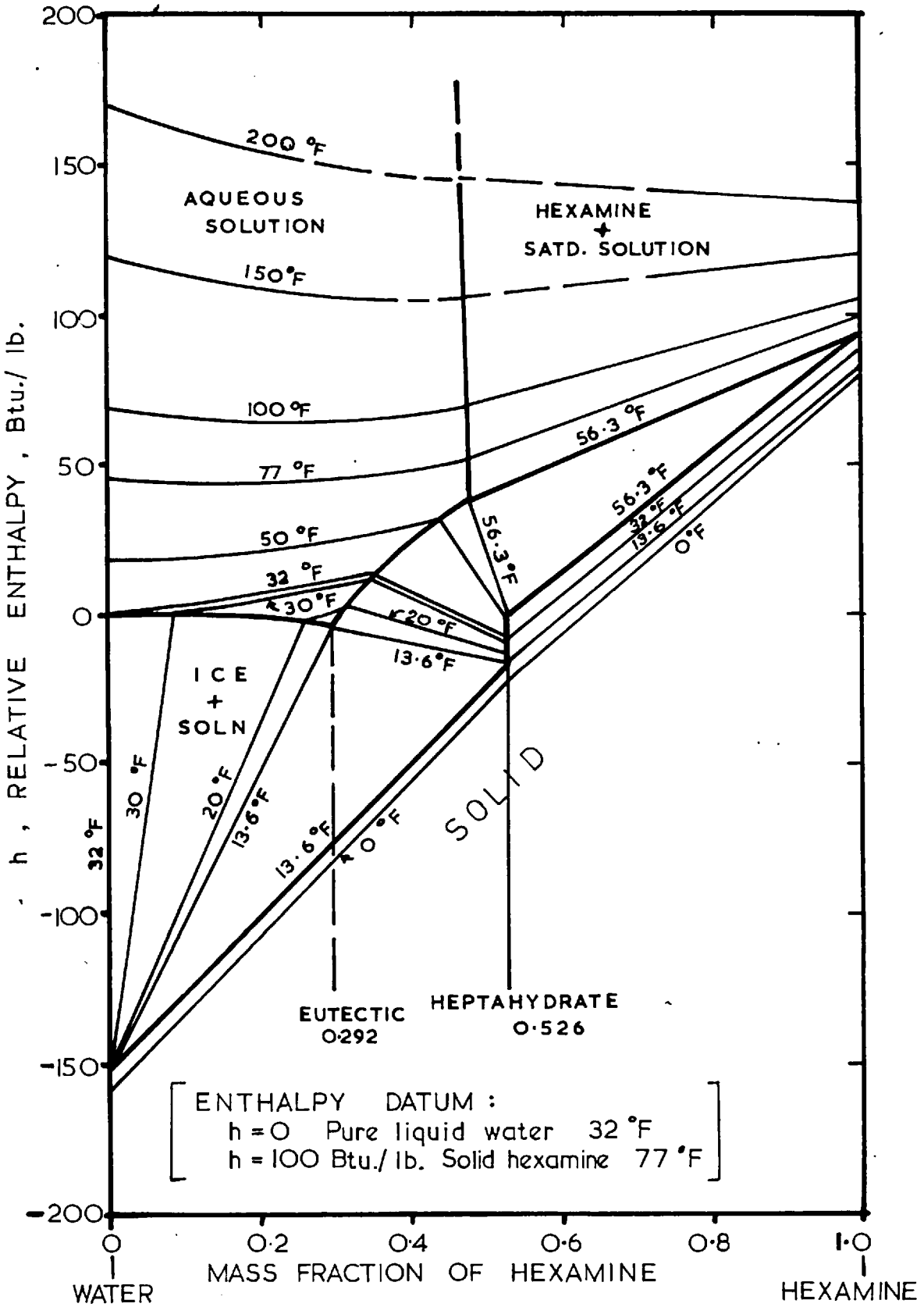

FIG. SII-26. ENTHALPY COMPOSITION CHART : HEXAMINE - WATER .

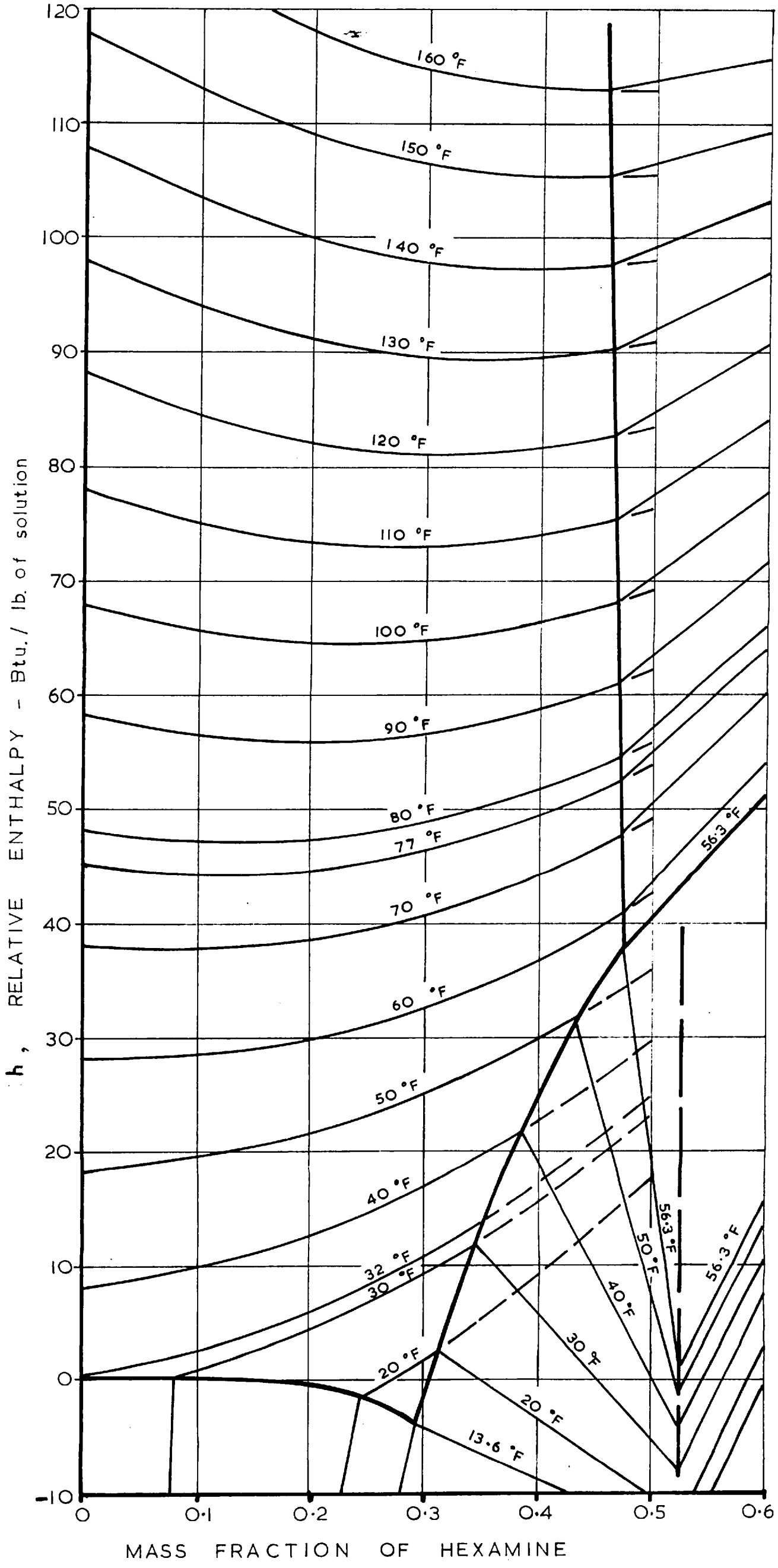

FIG. SII-27. ENTHALPY - COMPOSITION CHART FOR AQUEOUS HEXAMINE SOLUTIONS – LIQUID REGION.

TABLE S II - 16. RELATIVE ENTHALPIES OF HEXAMINE - WATER SYSTEM.

Enthalpy datum:- h=0 for liquid water at 32°F, h = 100 Btu /lb. for solid hexamino at 77°F.

TEMP. °F.	ENTHALPY OF LIQUID, Btu/lb.							ENTHALPY OF SOLID PHASE		
	x=0.0	x=0.1	x=0.2	x=0.3	x=0.4	SATN.	x=0.5	x=1.0	x=0	x=0.526
200	168.0	160.7	154.4	149.3	146.2	144.6	144.1*	136.3		
170	137.9	132.1	127.0	123.2	121.5	120.6	120.5*	126.6		
160	127.9	122.5	118.0	114.5	113.4	112.9	112.8*	123.6		
150	117.9	113.0	109.0	106.1	105.4	105.3	105.3*	120.5		
140	107.9	103.5	100.1	97.6	97.4	97.7	97.9*	117.5		
130	97.9	94.1	91.1	89.2	89.6	90.2	90.6*	114.6		
120	87.9	84.6	82.3	80.9	81.9	82.7	83.4*	111.7		
110	77.9	75.2	73.4	72.3	74.1	75.3	76.4*	108.9		
100	68.0	65.8	64.7	64.5	66.5	68.1	69.3*	106.1		
90	58.0	56.4	55.9	56.4	59.1	61.0	62.5*	103.4		
80	48.0	47.1	47.2	48.4	51.8	54.7	55.8*	100.8		
77	45.0	44.3	44.6	46.0	49.5	52.6	53.8*	100.0≠		
70	38.0	37.7	38.6	40.4	44.5	47.9	49.2*	98.2		
60	28.1	28.5	29.9	32.5	37.1	41.0	42.7*	95.7		
56.3	-	-	-	-	-	38.1	-	94.8		1.0
50	18.1	19.2	21.4	24.7	30.1	32.0	36.3*	93.2		-1.2†
40	8.1	9.9	12.9	16.9	23.0*	20.9	29.9*	90.8		-4.7†
32	0.0≠	2.5	6.1	10.6	17.4*	14.0	25.0*	88.9	-143.4	-7.5†
30	- 2.0*	0.7	4.4	9.2	16.1*	12.1	23.8*	88.4	-144.4	-8.2†
20			-4.0*	1.6	9.2*	2.5	17.8*	86.1	-149.3	-11.7†
13.6						-4.0		84.7		-15.2†
10								83.9	-154.2	
0								81.7	-158.9	-18.7†

x = Mass fraction of hexamine. * Hypothetical values. ≠ Datum values.

† Based on assumed hydrate heat capacity = 0.35 Btu/(lb °F.)

SIII. PROPERTIES OF MIXTURES OF HEXAMINE AND OTHER COMPONENTS

Introduction

This section will be concerned only with solutions of hexamine in other materials of common use. Reference has already been made (Section SI-8) to the large number of compounds formed by hexamine, and details of these substances may be found in the reference quoted.

SIII-1 SINGLE COMPONENT

(i) Solubility in pure solvents

Reported solubilities in various solvents at room temperature are given in Table SIII-1. The solubilities in absolute methanol, absolute ethanol, and commercial chloroform at various temperatures are shown in Table SIII-2 and Fig. SIII-1.

(ii) Refractive Indices of Solutions

The refractive indices of non-aqueous solutions at 25.0°C are given in Table SIII-3 and Fig SIII-2. The curve shown for water on Fig. SIII-2 has been plotted from the correlation given in Section SII-2i.

(iii) Densities of Hexamine-Chloroform Solutions

These data of Le Fèvre and Rayner [11] are given in Table SIII-4.

SIII-2 SEVERAL COMPONENTS

(i) Solubility in aqueous mixtures

The solubility of hexamine at several temperatures in aqueous methanol and aqueous ethanol solutions was determined [101]. The data are given in Table SIII-5 and Fig. SIII-3. The plot of the data

Data of Utz. [1047]

Solvent	Solubility, g.Hx. per 100 ml solvent	
	Room temp.	Hot solvent
Chloroform	13.40	14.84
Methanol	7.25	11.93
Ethanol	2.89	-
Iso-amyl alcohol	1.04	-
Carbon tetrachloride	0.85	-
Acetone	0.65	-
Tetrachlorethane	0.50	-
Benzene	0.23	-
Carbon disulphide	0.17	-
Xylene	0.14	-
Trichlorethylene	0.11	-
Ether	0.06	0.38
Petrol ether	0.0	0.0

Solvent	Temp., °C.	Solubility *	Reference
liq.ammonia	-	0.016	Carter [1217]
ethanol	12	0.0312	)Delépine [997]
chloroform	12	0.0743	)Seidell [1257]
glycerol	20	0.20	Holm [1227]
ethylene glycol 400	20	0.01	)Wahlgren
" 40	60	0.02	) [1237])

* as mass fraction of hexamine.

TABLE SIII - 1 SOLUBILITY OF HEXAMINE IN VARIOUS SOLVENTS.

Temperature †, °C.	Solubility, as mass fraction hexamine in Solution ≠		
	in methanol	in ethanol	in chloroform ※
15.5	0.0861	0.0279	-
25.0	0.0958	0.0340	0.0907
39.5	0.1148	0.0487	0.0912
55.5	0.1368	0.0661	0.0937
70.0	-	0.0864	-

† Error ± 0.1°C.

≠ Error ± 0.0010

※ Commercial Chloroform: 99% $CHCl_3$, 1% Ethanol.

TABLE SIII - 2. SOLUBILITY OF HEXAMINE IN METHANOL, ETHANOL, AND CHLOROFORM.

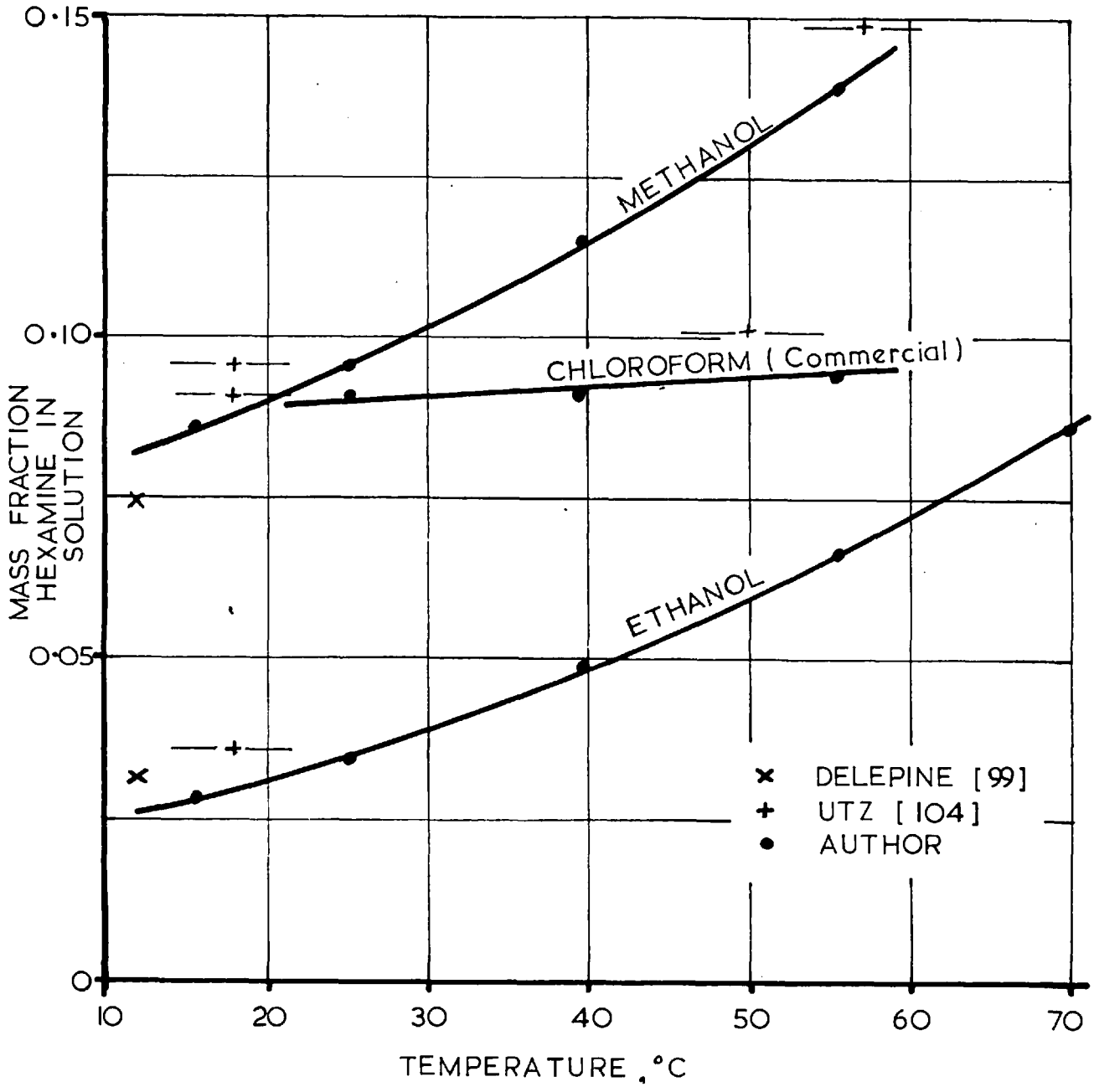

FIG. S III-1. SOLUBILITY OF HEXAMINE IN ORGANIC SOLVENTS.

SOLVENT	MASS FRACTION HEXAMINE IN SOLUTION	$n_D^{25.}$ *
ETHANOL	0.0	1.3596 †
	0.0093	1.3607
	0.0224	1.3620
	0.0340 ≠	1.3638
METHANOL	0.0	1.3268 †
	0.0196	1.3298
	0.0287	1.3316
	0.0376	1.3324
	0.0577	1.3355
	0.0815	1.3403
	0.0860	1.3405
	0.0958	1.3421
CHLOROFORM ‡	0.0	1.4427 †
	0.0095	1.4442
	0.0172	1.4454
	0.0256	1.4468
	0.0398	1.4489
	0.0688	1.4531
	0.0907 ≠	1.4558
CHLOROFORM Le Fèvre & Rayner [117]	0.0	1.44310
	0.0128	1.44582
	0.0223	1.44723
	0.0250	1.44757
	0.0434	1.45012

* With respect to dry air at 25.0°C; error ± 0.0002

† Data for pure solvents from Weissberger [112]

≠ Saturated solution at 25.0°C.

‡ Commercial : 99% $CHCl_3$ 1% Ethanol.

TABLE SIII - 3. REFRACTIVE INDICES OF HEXAMINE SOLUTIONS.

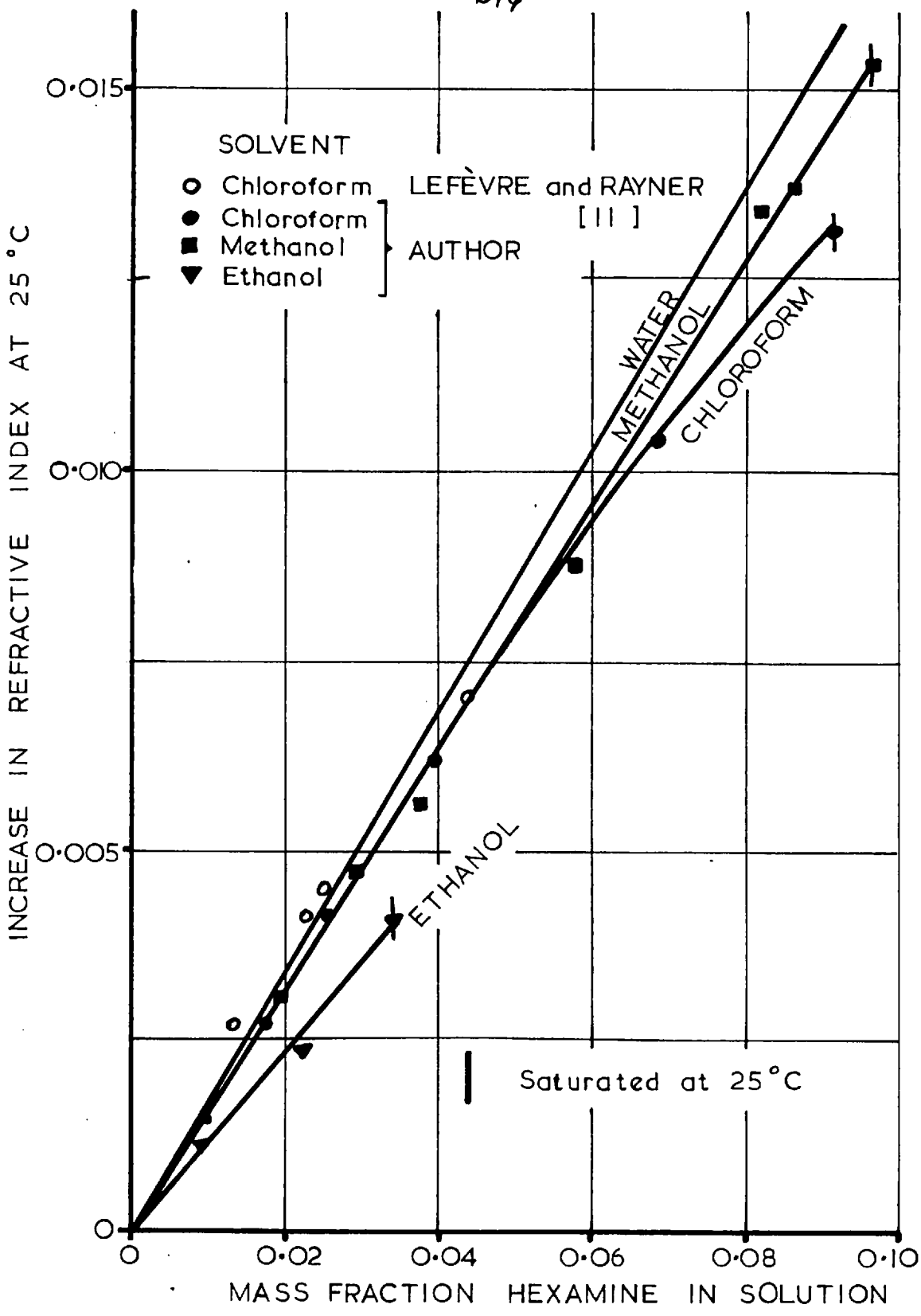

FIG. S III-2. INCREASE IN REFRACTIVE INDEX AT 25·0°C WITH HEXAMINE CONCENTRATION.

MASS FRACTION HELLEBORE IN CHLOROFORM SOLUTION	DENSITY OF SOLUTION, g/ml.		
	25°C.	35°C.	45°C.
0.0	1.47099	1.46060	1.44190
0.01880	1.47663	-	-
0.02867	1.47493	-	-
0.03501	1.47440	-	-
0.02855	1.47360	1.45610	1.43010
0.03852	1.47325	1.45606	1.43744
0.04937	1.47107	-	-
0.04680	1.47010	1.45290	-

TABLE SIII - 4. DENSITIES OF HELLEBORE CHLOROFORM SOLUTIONS (Le Fèvre & Rayner [117])

Author

SOLVENT *	Solubility† as mass fraction of hexamine				
	≠15.5°C	25.0°C	39.5°C	55.5°C	70.0°C
0.730 MeOH:0.270 H_2O	0.246	0.255	0.279	0.314	-
0.493 MeOH:0.507 H_2O	0.343	0.348	0.357	0.369	0.386
0.249 MeOH:0.751 H_2O	0.410	0.413	0.415	0.419	0.425
0.702 EtOH:0.298 H_2O	0.237	0.250	0.280	0.319	-
0.479 EtOH:0.521 H_2O	0.339	0.344	0.353	0.362	-
0.248 EtOH:0.752 H_2O	0.412	-	0.414	0.416	0.423

* Compositions as mass fractions. Error in composition for 15.5, 25.0 and 39.5°C, ± 0.002. Error in solvent composition at higher temperatures unknown through possible differential evaporation of solvent.

† Error in analysis ± 0.002.

≠ Error in temperature ± 0.1°C.

Solvent	Temp. °C.	Solubility Mass Fraction Hex.	Reference
90% aq.ethanol	15-20°C.	0.133	Squire & Caines /124/
90% aq.ethanol	room	0.0558	Utz /104/
86.5% aq.glycerol	20°C.	0.209)	Holm /122/
98.5% aq.glycerol	20°C.	0.173)	

TABLE SIII - 5 SOLUBILITY OF HEXAMINE IN AQUEOUS SOLVENT MIXTURES.

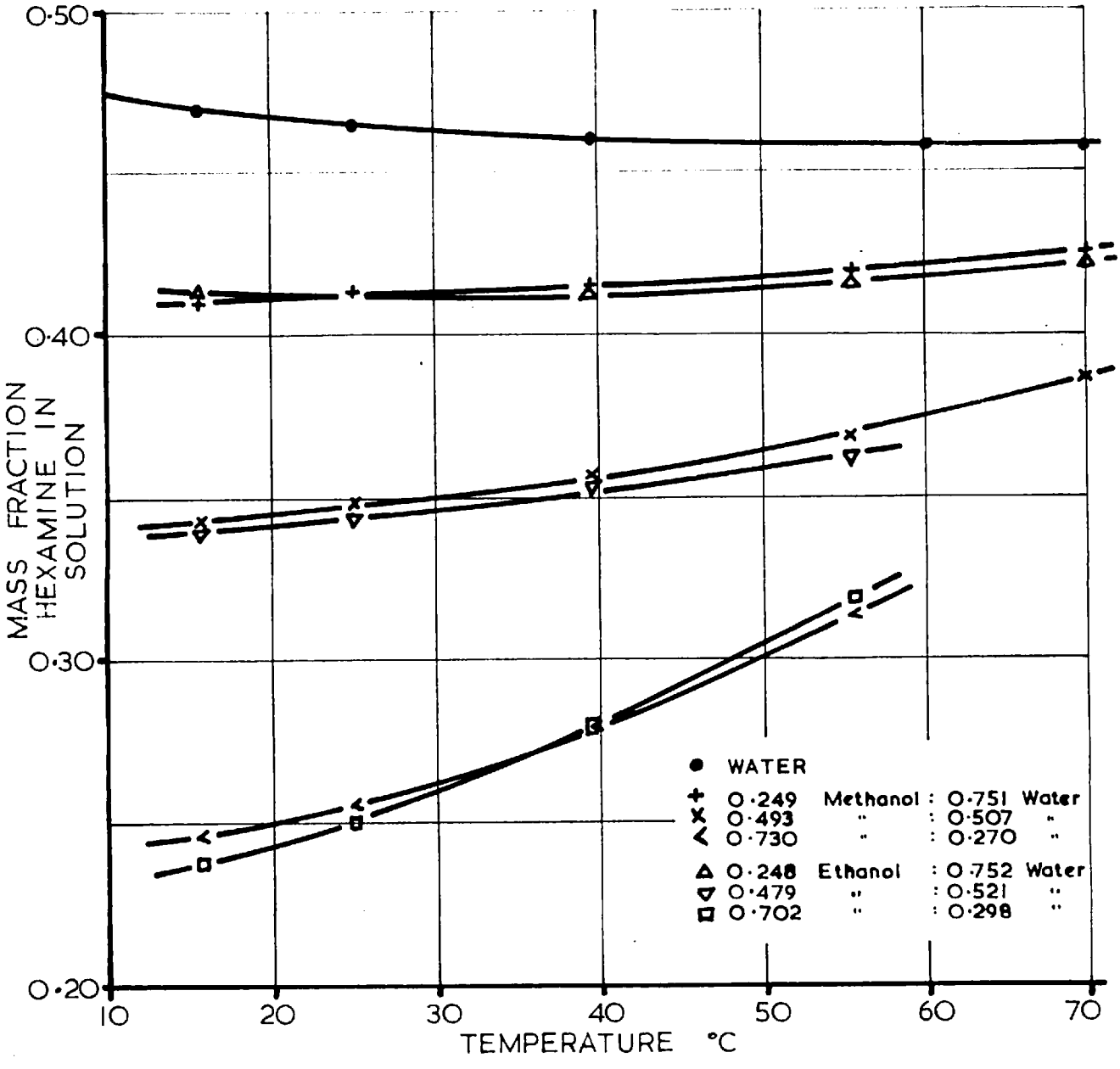

FIG. S III-3. SOLUBILITY OF HEXAMINE IN AQUEOUS METHANOL AND AQUEOUS ETHANOL.

on triangular diagrams (Fig . SIII-4 and SIII-5) show that supersaturated hexamine solutions cannot be prepared by mixing ethanol or methanol solutions with aqueous solutions. The data of Holm [122] for glycerol are given in Table SIII-5 and shown on Fig. SIII-6.

Adding gaseous ammonia to aqueous solutions will cause a high degree of supersaturation. This effect is used in the commercial manufacture of hexamine [105]. The data of Carter [121] and of the author are given in Table SIII-6 and Fig. SIII-6. Temperature has no great effect on the solubility curve. The amount of hexamine 'salted out' by adding gaseous ammonia has been computed from the above data and is presented in Fig . SIII-7 and SIII-8.

(ii) Solubility in Non-aqueous Mixtures

Utz [104] states that hexamine can be precipitated out of chloroform solution by adding ether. This was confirmed by the author but quantative measurements were not made. Petrol ether will behave similarly on chloroform solutions.

(iii) Solubility in non-miscible solvents

Collander [126] has measured the distribution coefficient of hexamine between ether and water and butanol and water at 13°C. For a hexamine concentration in the aqueous phase of 0.252 g.moles/l. the coefficient (hexamine concentration in organic to that in the aqueous phase) was found to be 0.067 for butamol-water and 0.00026 for ether-water.

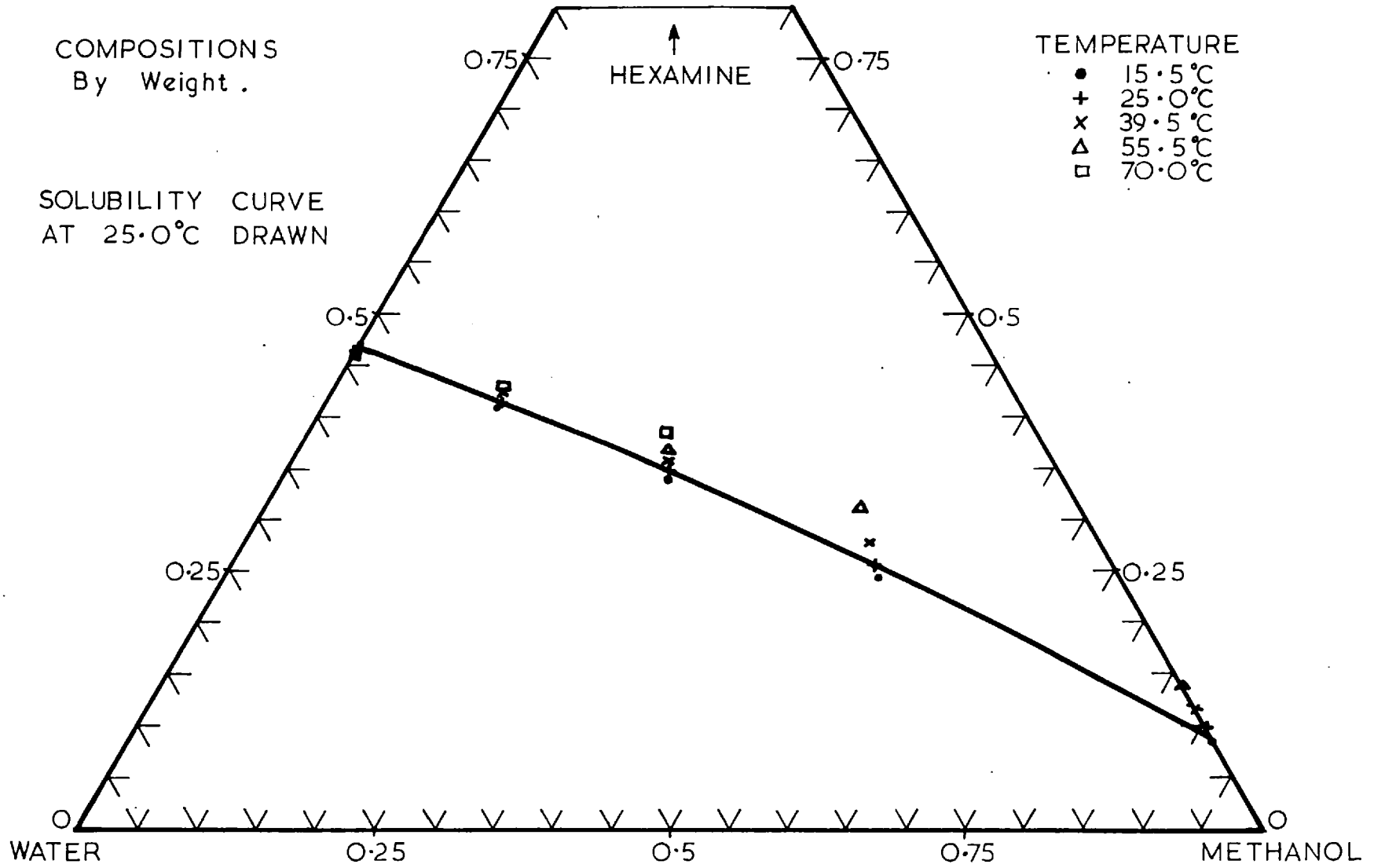

FIG. SIII-4. SOLUBILITY OF HEXAMINE IN AQUEOUS METHANOL.

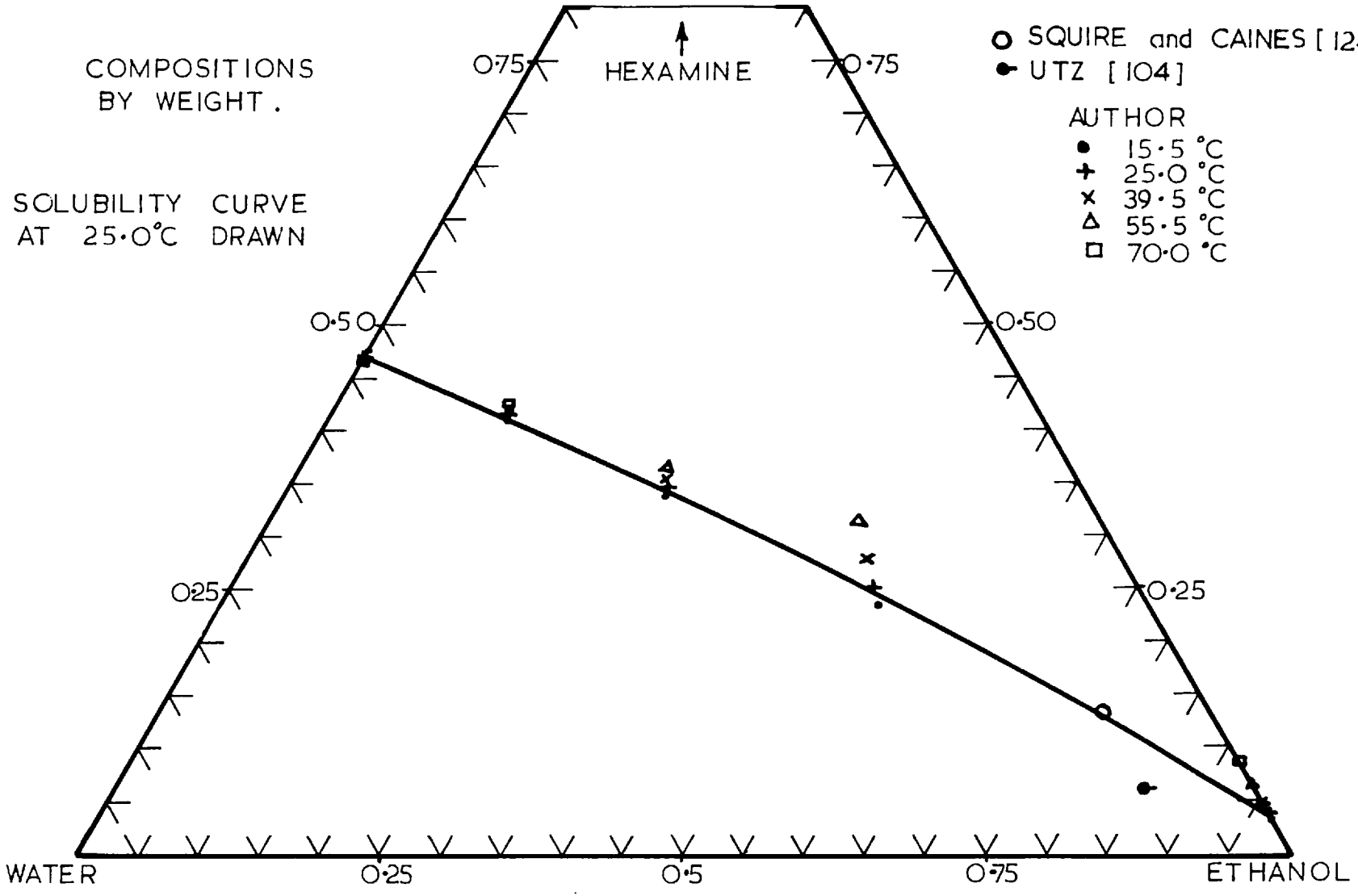

FIG. S III-5. SOLUBILITY OF HEXAMINE IN AQUEOUS ETHANOL.

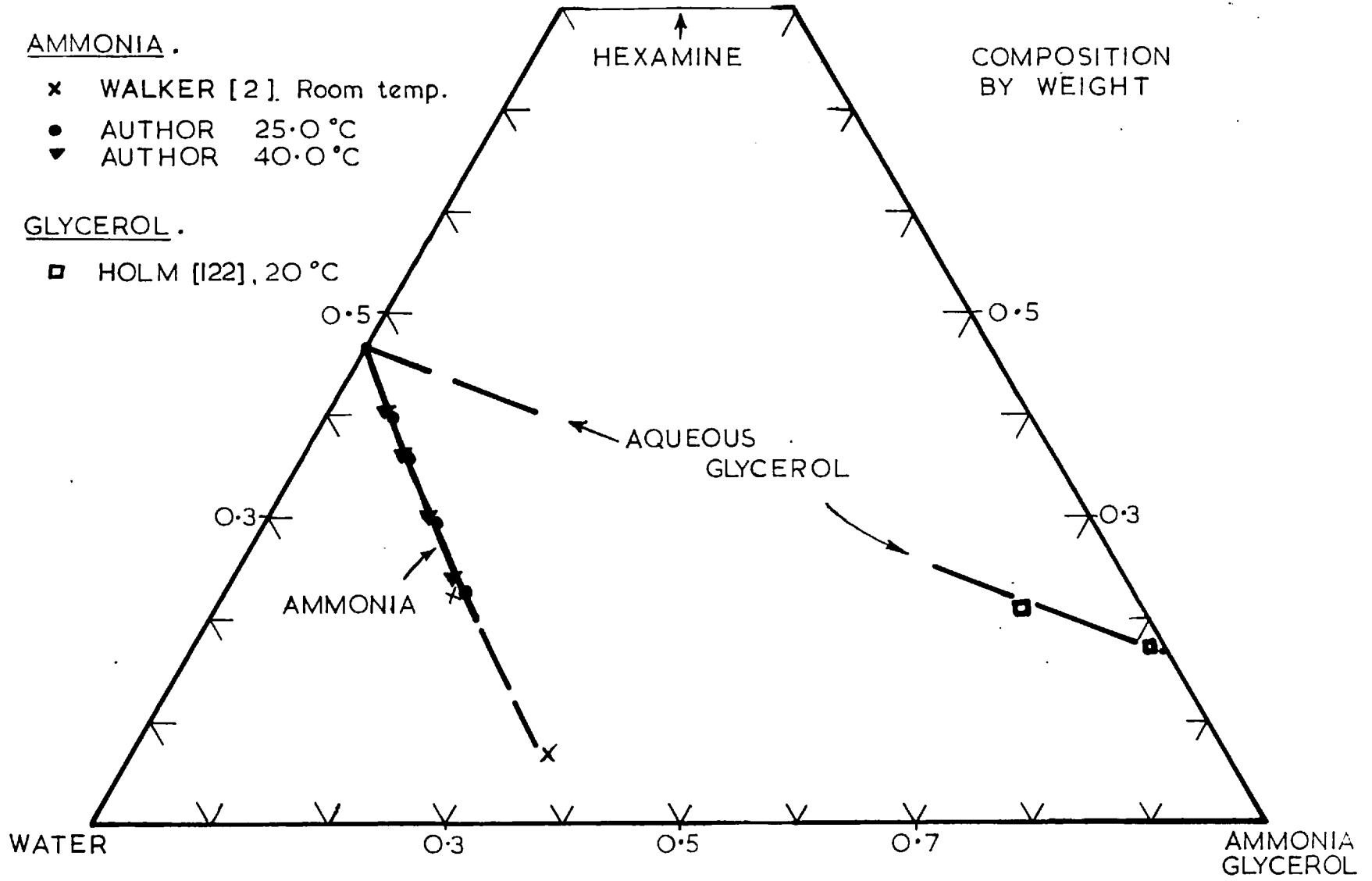

FIG. S III-6. SOLUBILITY OF HEXAMINE IN AQUEOUS AMMONIA AND AQUEOUS GLYCEROL.

Carter [12] (Walker [2]). Room Temperature.

Ammonia Content		Hexamine Content	
as g/100 cc soln	as mass fraction ≠	as g/100 cc soln	as mass fraction ≠
18.4	0.19	22.2	0.23
35.7	0.40	6.4	0.07

≠ Computed on assumed densities.

Author : 25.0°C.

Mass fraction ammonia in soln.	Mass fraction hexamine in soln.	Mass fraction Water.(by diff.)
0.0	0.466	0.534
0.055	0.396	0.549
0.087	0.356	0.557
0.140	0.293	0.567
0.192	0.230	0.578
0.198	0.229	0.573

Author : 40.0°C.

Mass fraction ammonia in soln.	Mass fraction hexamine in soln.	Mass fraction Water (by diff.)
0.0	0.462	0.538
0.048	0.402	0.550
0.081	0.359	0.560
0.134	0.298	0.568
0.181	0.242	0.577

TABLE SIII - 6. SOLUBILITY OF HEXAMINE IN AQUEOUS AMMONIA SOLUTIONS.

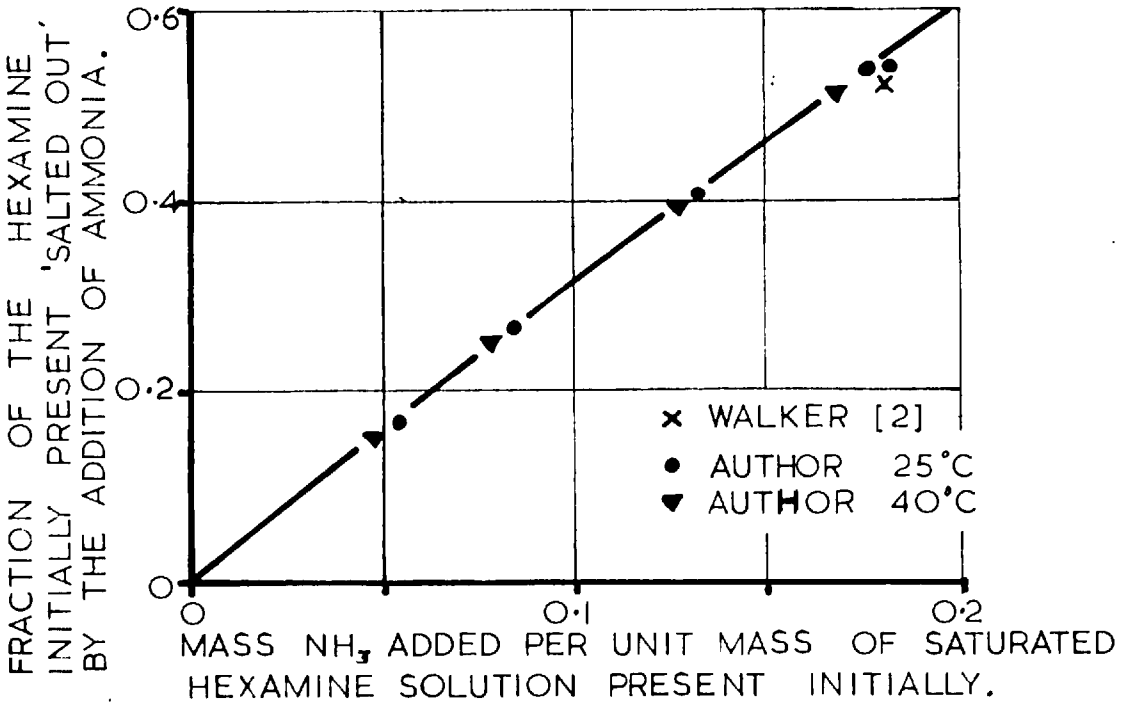

FIG. SIII-7. THE ADDITION OF GASEOUS AMMONIA TO A SATURATED SOLUTION OF HEXAMINE.

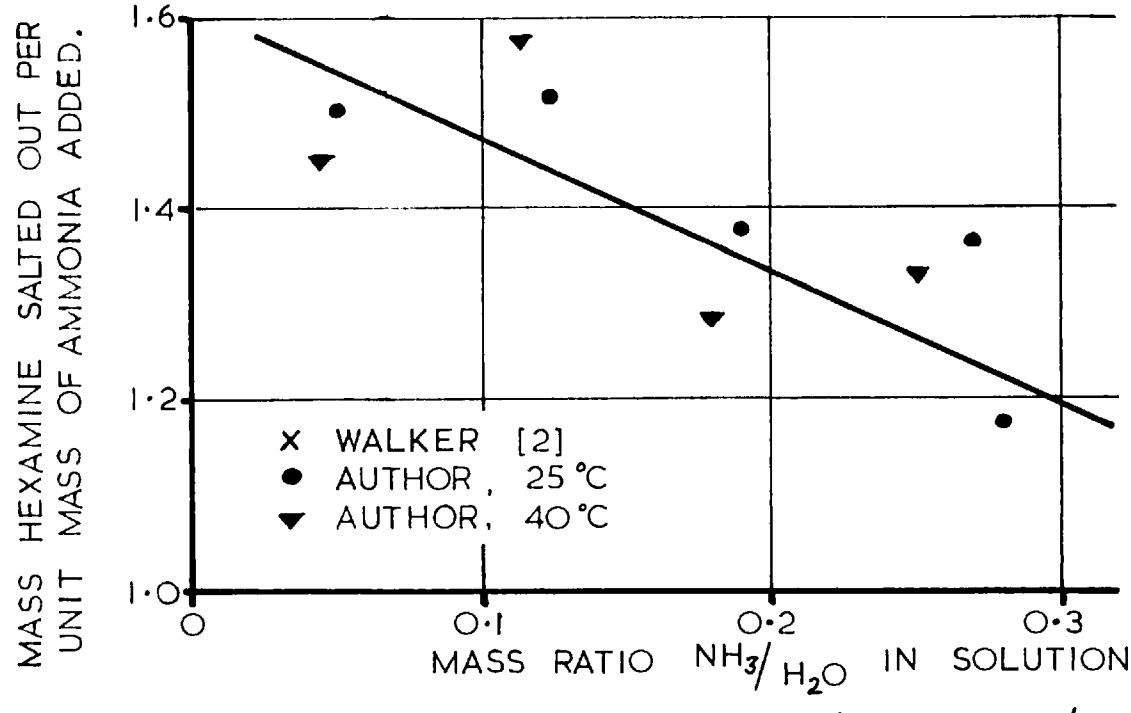

FIG. S III-8. MASS RATIO OF HEXAMINE 'SALTED OUT' TO AMMONIA ADDED TO HEXAMINE SOLUTION OF THE SHOWN AMMONIA CONTENT.

SIV. OTHER INFORMATION CONCERNING HEXAMINE

(i) Manufacture

Hexamine is usually prepared industrially by the exothermic reaction between ammonia and formaldehyde.

$$6HCHO + 4NH_3 \rightarrow C_6H_{12}N_4 + 6H_2O$$

The hexamine is recovered from the resulting solution by evaporation and crystallization. Further details of this process are given in the literature [2, 3, 56, 96, 102, 127-129]. Other methods of manufacture are possible and many patents on hexamine manufacture are on file.

(ii) Kinetics of Formation of Hexamine

The mechanics of the formation of hexamine have been studied [2, 130-134].

(iii) Materials of Construction

Aluminium has found considerable use as a material of construction for hexamine solutions. Brass and other copper containing alloys cannot be used.

(iv) Analysis for Hexamine

The usual method of analysis for hexamine when the sample is reasonably pure involves the consumption of acid in the hydrolytic decomposition of hexamine. Details of this and other methods are given in Walker [2].

SV. REFERENCES

(C.A. refers to Chemical Abstracts)

1. Beilstein "Handbuch der Organischer Chemie", Vierte Auflage, Band XXVI, EII 26-200, Springer, Berlin (1954).

2. Walker, J.F., "Formaldehyde", 2nd. ed., Ch. 19, A.C.S. Monograph No. 120, Reinhold, New York (1953).

3. Kirk R.E., and Othmer D.F., "Encyclopedia of Chemical Technology" Vol. 7, p. 466, Interscience, New York (1951).

4. Heilbron I, and Bunbury H.M., "Dictionary of Organic Compounds", Vol. 2, p. 670, Eyre and Spottiswoode, London (1953).

5. Landolt-Börnstein, "Zahlenwerte und Funktionen", 6 Auflage, Springer-Verlag, Berlin.

6. Böhmer, K, and Hartman, A., Deut. Z. ges. gerichtl. med., 32, 281 (1940) /C.A. 38 : 2392[8]/.

7. Sax, N.I., "Dangerous Properties of Industrial Materials", p.754, Reinhold, New York (1957).

8. Patty, F.A., "Industrial Hygiene and Toxicology", 2nd. ed., Vol. II, p. 2206, Interscience, New York (1962).

9. Duden, P. and Scharff, M., Ann., 288, 218 (1895).

10. Lösekann, G., Chem. Ztg., 14, 1409 (1890).

11. Le Fèvre, R.J.W. and Rayner, G.J., J. Chem. Soc., 1921 (1938).

12. Patterson, A.M., Capell, L.T. and Walker D.F., "The Ring Index" 2nd ed. Ring Index No. 3237, Am. Chem. Society, Washington (1960).

13. Becka L.N. and Cruickshank D.W.J., Proc. Roy. Soc. A273, 435 (1963).

14. Dickinson, R.G., and Raymond A.L., J. Am. Chem. Soc. 45, 22 (1923).

15. Gonell W. and Mark H., Z. Physik Chem. 107, 181 (1923).

16. Wyckoff R.W.G. and Corey R.B., Z. Krist, 89, 462 (1934).

17. Brill R., Grimm H.G., Hermann C. and Peters A., Ann. Phys. Lpz. 34, 393 (1939).

18. Shaffer P.A., J. Am. Chem. Soc. 69, 1557 (1947).

19. Wells A.F., "Structural Inorganic Chemistry" 3rd ed. p. 609, Claredon Press, Oxford (1962).

20. Hampson G.C. and Stosick A.J., J. Am. Chem. Soc. 60, 1814 (1938).

21. Labatchev A.N., Trudy. Inst. Krist. Akad. Nauk. U.S.S.R., 10, 71, (1954).

22. Andresen A.F., Acta Cryst. 10, 107 (1957).

23. Smith G.W., J. Chem. Phys. 36, 3081 (1962).

24. Schomaker V. and Shaffar P.A., J. Am. Chem. Soc. 69, 1555 (1947).

25. Traetteberg and Bastiansen, quoted in reference 13.

26. Yagi M., Sci. Repts. Tohoku Univ. First Ser. 42, 182 (1958).

27. Watkins G.D. and Pound R.V., Phys. Rev. 85, 1062 (1951).

28. Weber K.E. and Todd J.E., Rev. Sci. Instr., 33, 390 (1962).

29. Ayant Y., Compt. rend. 236, 2232 (1953).

30. Becka L.N., J. Chem. Phys. 37, 431 (1962).

31. Haussühl S., Acta Cryst. 11, 58 (1958).

32. Ramachandran G.N. and Wooster W.A., Acta Cryst., 4, 431 (1951).

33. Wooster W.A., Proc. Natl. Acad. Sci. India, A25, 58 (1956).

34. Ahmed M.S., Acta Cryst., 5, 587 (1952).

35. Krishnamurti P., Indian J. Phys., 3, 507 (1929).

36. Amoros Partoles J.L. and Canut M.L., Bolivian Acad. Nacl. Cienc., 42, 205 (1961).

37. Chandrasekhar S. and Phillips D.C., Nature, 190, 1164 (1961).

38. Miyahara Y., Bull. Chem. Soc. Japan, 26, 390 (1953).

39. Couture-Mathieu L. Mathieu J.P., Cremer J and Poulet H., J. Chim. Phys., 48, 1 (1951).

40. Zijp D.H., Proc. Internat. Meeting Mol. Spectry., 4th, Bologn 1959, 1, 345 (1962).

41. Kahovec L., Kohrausch K.W.F., Reitz A.W. and Wagner J., Z.phys. Chem. B39, 431 (1938).

42. Bai S., Proc. Indian Acad. Sci., 20A, 71 (1944).

43. Canals E. and Peyrot P., Compt. rend., 206, 1179 (1938).

44. Venkateswaran C.S., Proc. Indian Ac d Sci., 14A, 415 (1941).

45. Krishnamurti P., Indian J. Phys., 6, 309 (1931).

46. Price W.C. and Tetlow K.S., J. Chem. Phys., 16, 1157 (1948).

47. Cheutin A. and Mathieu J.P., J. chim. phys., 53, 106 (1956).

48. Mecke R. and Spiesecke H., Spectrochim. Acta., 7, 387 (1956).

49. Baker A.W., J. Phys. Chem., 61, 451 (1957).

50. Chang S.S. and Westrum E.F., J. Phys. Chem., 64, 1547 (1960).

51. Klipping I.G., and Stranski I.N., Z. anorg. u. allgem. chem., 297, 23 (1958); 299, 69 (1959).

52. Buder ov S.T., Izvest. Khim. Bulgar. Akad. Nauk., 7, 281 (1960) /C.A. 55: 17138a/.

53. Stranski I.N., Klipping G., Bogenschultz A.F., Heinrich H.J. and Maennig H., "Advances in Catalysis", 9, 406 (1957).

54. Beck G., Wien. Chem. Ztg., 46, 18 (1943) /C.A. 39: 4593[8]/

55. Jessop J.A., Brothertons Ltd., Wakefield, private communication (1962).

56. Faith W.L., Keyes D.B. and Clark R.L., "Industrial Chemicals", 2nd ed., Wiley, New York (1957).

57. Lonsdale K, Z. Kristallogr., 112, 188 (1959).

58. Mirskaya K.V., Sov. Phys. Crystallography, 8, 167 (1963).

59. Bridgman P.W., Proc. Am. Acad. Arts Sci., 76, 71 (1948).

60. Hendricks S.B., and Jefferson M.E., J. Optical Soc. Am., 23, 299 (1933).

61. Belyaev L.M., Blokh O.G., Gil'varg A.B., Dobrzhanski G.F., Netesov G.B., Shamburov V.A. and Shuvalov L.A., Sov. Phys. Crystallogrophy, 8, 383 (1963).

62. Havemann R., Haberditzl W. and Koeppel H., Z. Physik. Chem., 219, 402 (1962).

63. Elings S.B. and Terpstra P., Z. Krist. Mineral., 67, 279 (1928). /C.A. 23: 2863/.

64. Hettich A., and Schleede A., Z. Phys., 50, 252 (1928).

65. Koptsik V.A., Izvest. Akad, Nauk. SSSR, Ser. Fiz., 20, 219 (1956).

66. Koptsik V.A., et. al., Vestnik Moskov. Univ. Ser. Mat. Mekh. Astron. Fiz. Khim., 13, No. 6, 91 (1958) /C.A. 53: 15673e/

67. Delépine M. and Badoche M., Compt. rend., 214, 777 (1942).

68. Kharasch M.S. and Sher B., J. Phys. Chem., 29, 625 (1925).

69. Harvey M. and Backeland L.H., Ind., Eng. Chem., 13, 135 (1921).

70. Joshi S.K. and Mitra S.S., Proc. Phys. Soc., 76, 295 (1960).

71. Kitaigorodskii A.I., Sov. Phys. Crystallography, 7, 152 (1962).

72. Klipping L., Stranski I.N. and Wandelburg K., Z. Physik Chem., 34, 238 (1962).

73. Becker K.A., Niesler R.A. and Stranski I.N., Z. Physik.Chem, 27, 372 (1961

74. Stranski I.N. Disc. Faraday Soc., 5, 13 (1949)

75. Stranski I.N. and Honigmann B., Naturwiss, 35, 156 (1948).

76. Honigmann B., Z. Electrochem, 58, 322 (1954).

77. Honigmann B., Z. Kryst., 106, 199 (1955).

78. Honigmann B., and Heyer H., Z. Electrochem 61, 74 (1957).

79. Stranski I.N. and Honigmann B., Z. Physik. Chem. 194, 180 (1950)

80. Honigmann B. and Stranski I.N., Z. Elektrochem. 56, 338 (1952).

81. Kaishev R., Annuaire Univ. Sofia, Faculté phys.-maths. 43, 99 (1946) (C.A. 43: 8228h).

82. Lemmlein G.G., Doklady Akad. Nauk. SSSR, 98, 973 (1954) (C.A. 49: 5061e)

83. Ohara T., J. Soc. Rubber Ind. Japan., 10, 438 (1937) (C.A. 31: 7395^{3}).

84. Egorov A.M., Te L.J., Liven A.V., Patent USSR 150,111 (1962) (C.A. 58: 12420b).

85. Chumakov A.A., and Koptsik V.A., Sov. Phys. Crystallography, 4, 212 (1959).

86. Denbigh K.G., Disc. Farad. Soc., 5, 188 (1949).

87. Denbigh K.G. and White E.T., Nature, 199, 799 (1963).

88. Willems J., Naturewissenschaften, 31, 146 (1943): Z. Krist., 105, 149 (1943). (C.A. 38: 8^{4}).

89. Stranski I.N., Klipping G. and Maennig H., Z. Elektrochem., 63, 135 (1959).

90. Hoene D., Klipping I. and Stranski I.N., Chem. Ber., 93, 2782 (1960).

91. Plischke H., Z. Chem., 1, 25 (1960) (C.A. 55, 10301g).

92. Tada H. et. al., J. Chem. Soc. Japan., 58, 10 (1955). (C.A. 49, 12096h)

93. Rattu A., Ann. Chim. Applicata, 29, 221 (1939). (C.A. 34, 413)

94. Stech B., Z. Naturforsch., 7A, 175 (1952). (C.A. 46, 7902h)

95. Szalay. A., Z. Physik. Chem., 164A, 234 (1933). (C.A. 27: 3379[9]).

96. Simmonds W.H., Forster A. and Bowden R.C., Ind. Chem., 24, 429, 550, 595 (1948

97. Dunning W.J., Millard B. and Nott C., J. Chem. Soc., 1264 (1962).

98. Cambier R. and Brochet A., Bull. soc. Chim. France, (3), 13, 394.

99. Delépine M., Bull. soc. chim. France (3), 13, 353 (1895); ibid. (3) 17, 110 (1897).

100. Evrard V., Naturw. Tijdschr., 11, 99 (1929) (C.A. 23:4875).

101. White E.T., Ph.D. thesis, Appendix VI, University of London (1964).

102. Sherwood P.W., Petroleum Refiner, 37, No. 9, 351 (1958).

103. Perry J.H., "Chemical Engineers Handbook", 3rd ed. McGraw Hill, New York, (1950).

104. Utz F., Suddeut. Apoth, Ztg. 59, 832 (1919). (C.A. 14, 3345)

105. Pummerer R. and Hofman J., Berichte Deut. Chemis. Gesellschaft., 56B 1255 (1923) (C.A. 17, 3159)

106. Husa W.J., and Rossi O.A., J. Am. Pharm. Assoc., 31, 270 (1942).

107. Hammarlund E.R., Larsen J. and Pedersen - Bjergaard K., Pharm. Acta. Helv., 35, 593 (1960).

108. Ministry of Supply, Royal Ordnance Factory, Bridgwater, Somerset, private communication (1962).

109. Fialkov Y.A. and Egerskaya V.A., Farmatsiya, 6, No. 2, 14 (1943).

110. Sol'ts L.M. and Sol'ts F.M., Aptechnoe Delo. 2, 1, 22 (1953) (C.A. 47:5859c).

111. Mosebach R., Z. Naturforsch., 16B, 614 (1961).

112. Weissberger A., "Techniques of Organic Chemistry", 3rd. ed. Vol I., Interscience, New York (1959).

113. Huang T.C., Peng M.Y., Hu K.S. and Sah P.P.T., J. Am. Chem. Soc., 60, 489, (1938).

114. Tsisina G.V. and Al'shits M.I., Farm. Zhur., 1, 45, (1957). (C.A. 32:5090[1]).

115. "International Critical Tables", Vol. V, McGraw Hill, New York (1925).

116. Süllman H., Protoplasma, 13, 546 (1931).

117. Russo C., Gazz. chim. ital., 44, I, 18 (1914) (C.A. 8:2155).

118. Osaka Y., Z. Physik Chem., 13, 237.

119. Philippi E. and Löbering J., Biochem Z., 277, 365 (1935). (C.A. 29,4655[9])

120. Gillespie R.J. and Wasif S., J. Chem. Soc., 204 (1953).

121. Carter C.B., Patent U.S. 1,566,820 (1935). Data given in Walker [2].

122. Holm. K., Am. J. Pharm., 94, 138 (1922): Pharm. J., 107, 538 (1921).

123. Wahlgren S., Svensk Farm. Tidsk., 66, 585 (1962).

124. Squire P.W. and Caines C.M., Pharm. J., 74, 720, 784 (1905).

125. Seidell A., "Solubilities of Organic Compounds". 3rd. ed. Vol II, p. 434, Van Nostrand, New York (1941).

126. Collander R., Acta Chem. Scand., 4, 1085 (1950).

127. Latapié F., Ion, 3, 338 (1943).

128. Kent J.A., "Riegels Industrial Chemistry", 6th ed., Reinhold, New York, (1962).

129. Chemical Engineering Practice School, Bridgwater Report No. G282 (1960).

130. Baur E., and Ruetschi W., Helv. Chim. Acta, 24, 754 (1941).

131. Boyd M.L., and Winkler C.A., Can. J. Research, 25B, 387 (1947).

132. Polley J.R., Winkler, C.A. and Nicholls, R.V.V., Can. J. Research, 25B, 525 (1947).

133. Richmond H.H., Myers G.S., and Wright G.F., J. Am. Chem. Soc., 70, 3659 (1948).

134. Ingraham T.R., and Winkler C.A., Can. J. Research, 30, 687 (1952).